REPORT DOCUMENTATION PAGE

READ INSTRUCTIONS BEFORE COMPLETING FORM

1. REPORT NUMBER: WT-1317 (EX)
2. GOVT ACCESSION NO.:
3. RECIPIENT'S CATALOG NUMBER:

4. TITLE (and Subtitle): Operation REDWING - Project 2.63, Characterization of Fallout

5. TYPE OF REPORT & PERIOD COVERED:

6. PERFORMING ORG. REPORT NUMBER: WT-1317 (EX)

7. AUTHOR(s): T. Triffet, Project Officer; P. D. LaRiviere

8. CONTRACT OR GRANT NUMBER(s):

9. PERFORMING ORGANIZATION NAME AND ADDRESS: US Naval Radiological Defense Laboratory, San Francisco, California

10. PROGRAM ELEMENT, PROJECT, TASK AREA & WORK UNIT NUMBERS:

11. CONTROLLING OFFICE NAME AND ADDRESS: Headquarters, Field Command, Defense Atomic Support Agency, Sandia Base, Albuquerque, New Mexico

12. REPORT DATE: March 15, 1961

13. NUMBER OF PAGES:

14. MONITORING AGENCY NAME & ADDRESS (if different from Controlling Office):

15. SECURITY CLASS. (of this report): UNCLASSIFIED

15a. DECLASSIFICATION/DOWNGRADING SCHEDULE:

16. DISTRIBUTION STATEMENT (of this Report): Approved for public release; unlimited distribution.

17. DISTRIBUTION STATEMENT (of the abstract entered in Block 20, if different from Report):

18. SUPPLEMENTARY NOTES: This report has had the classified information removed and has been republished in unclassified form for public release. This work was performed by Kaman Tempo under contract DNA001-79-C-0455 with the close cooperation of the Classification Management Division of the Defense Nuclear Agency.

19. KEY WORDS (Continue on reverse side if necessary and identify by block number):
Operation REDWING
Fallout
Surface Radiation

20. ABSTRACT (Continue on reverse side if necessary and identify by block number): The general objective was to obtain data sufficient to characterize the fallout, interpret the aerial and oceanographic survey results, and check fallout-model theory for Shots Cherokee, Zuni, Flathead, Navajo, and Tewa during Operation REDWING. Detailed measurements of fallout buildup were planned. Measurements of radiation characteristics and physical, chemical, and radiochemical properties of individual solid and slurry particles and total cloud and fallout samples were also planned, along with determinations of the surface densities of activity and environmental components in the fallout at each major station.

ABSTRACT

The general objective was to obtain data sufficient to characterize the fallout, interpret the aerial and oceanographic survey results, and check fallout-model theory for Shots Cherokee, Zuni, Flathead, Navajo, and Tewa during Operation Redwing. Detailed measurements of fallout buildup were planned. Measurements of the radiation characteristics and physical, chemical, and radiochemical properties of individual solid and slurry particles and total cloud and fallout samples were also planned, along with determinations of the surface densities of activity and environmental components in the fallout at each major station.

Standardized instruments and instrument arrays were used at a variety of stations which included three ships, two barges, three rafts, thirteen to seventeen deep-anchored skiffs, and four islands at Bikini Atoll. Total and incremental fallout collectors and gamma time-intensity recorders were featured in the field instrumentation. Special laboratory facilities for early-time studies were established aboard one ship. A number of buried trays with related survey markers were located in a cleared area at one of the island stations. Instrument failures were few, and a large amount of data was obtained.

This report summarizes the times and rates of arrival, times of peak and cessation, mass-arrival rates, particle-size variation with time, ocean-penetration rates, solid- and slurry-particle characteristics, activity and fraction of device deposited per unit area, surface densities of chemical components, radionuclide compositions with corrections for fractionation and induced activities, and photon and air-ionization decay rates. A number of pertinent correlations are also presented: predicted and observed fallout patterns are compared, sampling bias is analyzed, gross-product decay is discussed in relation to the $t^{-1.2}$ rule, fraction-of-device calculations based on chemical and radiochemical analyses are given, the relationship of film-dosimeter dose to gamma time-intensity integral is considered, a comparison is made between effects computed from radiochemistry and gamma spectrometry, air-sampling measurements are interpreted, and the fallout effects are studied in relation to variations in the ratio of fission yield to total yield.

Some of the more-important general conclusions are summarized below:

The air burst of Shot Cherokee produced no fallout of military significance.

Fallout-pattern locations and times of arrival were adequately predicted by model theory.

Activity-arrival-rate curves for water-surface and land-surface shots were similar, and were well correlated in time with local-field ionization rates.

Particle-size distributions from land-surface shots varied continuously with time at each station, with the concentration and average size appearing to peak near time-of-peak radiation rate; the diameters of barge-shot fallout droplets, on the other hand, remained remarkably constant in diameter at the ship stations.

Gross physical and chemical characteristics of the solid fallout particles proved much the same as those for Shot Mike during Operation Ivy and Shot Bravo during Operation Castle. New information was obtained, however, relating the radiochemical and physical characteristics of individual particles. Activity was found to vary roughly as the square of the diameter for irregular particles, and as some power greater than the cube of the diameter for spheroidal particles.

Fallout from barge shots consisted of slurry droplets, which were composed of water, sea salts, and radioactive solid particles. The latter were spherical, generally less than 1 micron in diameter, and consisted mainly of oxides of calcium and iron. At the ship locations, the solid particles contained most of the activity associated with the slurry droplets; close in, however, most of the activity was in soluble form.

Bulk rate of penetration of fallout in the ocean was, under several restrictions, similar for both solid and slurry particles. Estimates are given of the amount of activity which may have

been lost below the thermocline for the fast-settling fraction of solid-particle fallout.

Fractionation of radionuclides from Shot Zuni was severe while that from Shot Tewa was moderate; Shots Flathead and Navajo were nearly unfractionated. Tables are provided, incorporating fractionation corrections where necessary, which allow the ready calculation of infinite-field ionization rates, and the contribution of individual induced activities to the total ionization rate.

Best estimates are given of the amount of activity deposited per unit area at all sampling stations. Estimates of accuracy are included for the major stations.

Chapter 1
INTRODUCTION

1.1 OBJECTIVES

The general objective was to collect and correlate the data needed to characterize the fallout, interpret the observed surface-radiation contours, and check the models used to make predictions, for Shots Cherokee, Zuni, Flathead, Navajo, and Tewa during Operation Redwing.

The specific objectives of the project were: (1) to determine the time of arrival, rate of arrival, and cessation of fallout, as well as the variation in particle-size distribution and gamma-radiation field intensity with time, at several points close to and distant from ground zero; (2) to collect undisturbed samples of fallout from appropriate land- and water-surface detonations for the purpose of describing certain physical properties of the particles and droplets, including their shape, size, density and associated radioactivity; measuring the activity and mass deposited per unit area; establishing the chemical and radiochemical composition of the fallout material; and determining the sizes of particles and droplets arriving at given times at several important points in the fallout area; (3) to make early-time studies of selected particles and samples in order to establish their radioactive-decay rates and gamma-energy spectra; (4) to measure the rate of penetration of activity in the ocean during fallout, the variation of activity with depth during and after fallout, and the variation of the gamma-radiation field with time a short distance above the water surface; and (5) to obtain supplementary radiation-contour data at short and intermediate distances from ground zero by total-fallout collections and time-of-arrival measurements.

It was not an objective of the project to obtain data sufficient for the determination of complete fallout contours. Instead, emphasis was placed on: (1) complete and controlled documentation of the fallout event at certain key points throughout the pattern, also intended to serve as correlation points with the surveys of other projects; (2) precise measurements of time-dependent phenomena, which could be utilized to establish which of the conflicting assumptions of various fallout prediction theories were correct; (3) analysis of the fallout material for the primary purpose of obtaining a better understanding of the contaminant produced by water-surface detonations; and (4) gross documentation of the fallout at a large number of points in and near the lagoon.

1.2 BACKGROUND

A few collections of fallout from tower shots were made in open pans during Operation Greenhouse (Reference 1). More extensive measurements were made for the surface and underground shots of Operation Jangle (Reference 2). Specialized collectors were designed to sample incrementally with time and to exclude extraneous material by sampling only during the fallout period. The studies during Operation Jangle indicated that fallout could be of military importance in areas beyond the zones of severe blast and thermal damage (Reference 3).

During Operation Ivy, a limited effort was made to determine the important fallout areas for a device of megaton yield (Reference 4). Because of operational difficulties, no information on

fallout in the downwind direction was obtained. Contours were established in the upwind and crosswind directions by collections on raft stations located in the lagoon.

Elaborate plans to measure the fallout in all directions around the shot point were made for Operation Castle (Reference 5). These plans involved the use of collectors mounted on free-floating buoys placed in four concentric circles around the shot point shortly before detonation. Raft stations were also used in the lagoon and land stations were located on a number of the islands. Because of poor predictability of detonation times and operational difficulties caused by high seas, only fragmentary data was obtained from these stations.

The measurement of activity levels on several neighboring atolls that were unexpectedly contaminated by debris from Shot 1 of Operation Castle provided the most useful data concerning the magnitude of the fallout areas from multimegaton weapons (Reference 6). Later in the operation, aerial and oceanographic surveys of the ocean areas were conducted and water samples were collected (References 7 and 8). These measurements, made with crude equipment constructed in the forward area, were used to calculate approximate fallout contours. The aerial-survey data and the activity levels of the water samples served to check the contours derived from the oceanographic survey for Shot 5. No oceanographic survey was made on Shot 6; however, the contours for this shot were constructed from aerial-survey and water-sample data.

In spite of the uncertainty of the contours calculated for these shots, the possibility of determining the relative concentration of radioactivity in the ocean following a water-surface detonation was demonstrated. During Operation Wigwam (Reference 9), the aerial and oceanographic survey methods were again successfully tested.

During Operation Castle, the question arose of just how efficiently the fallout was sampled by the instruments used on that and previous operations. Studies were made at Operation Teapot (Reference 10) to estimate this efficiency for various types of collectors located at different heights above the ground. The results demonstrated the difficulties of obtaining reliable samples and defined certain factors affecting collector efficiency. These factors were then applied in the design of the collectors and stations for Operation Redwing.

1.3 THEORY

1.3.1 General Requirements. Estimates of the area contaminated by Shot 1 during Operation Castle indicated that several thousand square miles had received significant levels of fallout (References 5, 11 and 12), but these estimates were based on very-meager data. It was considered essential, therefore, to achieve adequate documentation during Operation Redwing. Participation in a joint program designed to obtain the necessary data (Reference 13) was one of the responsibilities of this project.

The program included aerial and oceanographic surveys, as well as lagoon and island surveys, whose mission was to make surface-radiation readings over large areas and collect surface-water samples (References 14, 15 and 16). Such readings and samples cannot be used directly, however, to provide a description of the contaminated material or radiation-contour values. Corrections must be made for the characteristics of the radiation and the settling and dissolving of the fallout in the ocean. It was these corrections which were of primary interest to this project.

1.3.2 Data Requirements. Regardless of whether deposition occurs on a land or water surface, much the same basic information is required for fallout characterization, contour construction, and model evaluation, specifically: (1) fallout buildup data, including time of arrival, rate of arrival, time of cessation, and particle-size variation with time; (2) fallout composition data, including the physical characteristics, chemical components, fission content, and radionuclide composition of representative particles and samples; (3) fallout radiation data, including photon emission rate and ionizing power as a function of time; and (4) total fallout data, including the number of fissions and amount of mass deposited per unit area, as well as the total gamma-ionization dose delivered to some late time.

1.3.3 Special Problems and Solutions. Models can be checked most readily by means of fallout-buildup data, because this depends only on the aerodynamic properties of the particles, their initial distribution in the cloud, and intervening meteorological conditions. The construction of land-equivalent radiation contours, on the other hand, requires characterization of the composition and radiations of the fallout in addition to information on the total amount deposited.

1.3.4 Radionuclide Composition and Radiation Characteristics. In the present case, for example, exploratory attempts to resolve beta-decay curves into major components failed, because at the latest times measured, the gross activity was generally still not decaying in accordance with the computed fission-product disintegration rate. It was known that, at certain times, induced activities in the actinides alone could upset the decay constant attributed to fission products, and that the salting agents present in some of the devices could be expected to influence the gross decay rate to a greater or lesser extent depending on the amounts, half lives, and decay schemes of the activated products. The extent to which the properties of the actual fission products resembled those of thermally fissioned U^{235} and fast fission of U^{238} was not known, nor were the effects of radionuclide fractionation. In order to establish the photon-emission characteristics of the source, a reliable method of calculating the gamma-ray properties of a defined quantity and distribution of nuclear-detonation products had to be developed. Without such information, measurements of gamma-ionization rate and sample activity, made at a variety of times, could not be compared, nor the results applied in biological-hazard studies.

Fission-product, induced-product, and fractionation corrections can be made on the basis of radiochemical analyses of samples for important nuclides. This leads to an average radionuclide composition from which the emission rate and energy distribution of gamma photons can be computed for various times. A photon-decay curve can then be prepared for any counter with known response characteristics and, by calculating ionization rates at the same times, a corresponding ionization-decay curve. These curves can in turn be compared with experimental curves to check the basic composition and used to reduce counter and survey-meter readings.

1.3.5 Sampling Bias. Because the presence of the collection system itself usually distorts the local air stream, corrections for sample bias are also required before the total fallout deposited at a point may be determined. To make such corrections, the sampling arrays at all stations must be geometrically identical, so that their collections may be compared when corrected for wind velocity, and an independent and absolute measure of the total fallout deposited at one or more of the stations must be obtained. The latter is often difficult, if not impossible, to do and for this reason it is desirable to express radiological effects, such as dose rate, in terms of a reference fission density. Insertion of the best estimate of the actual fission density then leads to the computed infinite-plane ionization rate for that case.

In principle, on the deck of a ship large enough to simulate an infinite plane, the same fallout-radiation measurements can be made as on a land mass. In actual fact, however, there are important differences: an additional deposition bias exists because of the distortion of the airflow around the ship; the collecting surfaces on the ship are less retentive than a land plane, and their geometric configuration is different; a partial washdown must be used if the ship is manned, and this requires headway into the surface wind in order to maintain position and avoid sample contamination in the unwashed area. For these reasons, the bias problem is even more severe aboard ship than on land.

The preceding considerations were applied in the development of the present experiment and will be reflected in the treatment of the data. All major sampling stations were constructed alike and included an instrument for measuring wind velocity. The buried-tray array surrounding the major station on Site How was intended to provide one calibration point, and it was hoped that another could be derived from the water-sampling measurements. In the analysis which follows, fractionation corrections will be made and radiological quantities expressed in terms of 10^4 fissions wherever possible. Relative-bias corrections will be included for each major station, and an attempt will also be made to assess absolute bias for these stations.

1.3.6 Overall Approach. It should be emphasized that, at the time this project was conceived, the need for controlled and correlated sets of fallout data for megaton bursts was critical. Because of the lack of experimental criteria, theoretical concepts could be neither proved nor disproved, and progress was blocked by disagreements over fundamental parameters. The distribution of particle sizes and radioactivity within the source cloud, the meteorological factors which determined the behavior of the particles falling through the atmosphere, the relationship of activity to particle size, and the decay and spectral characteristics of the fallout radiations: all were in doubt. Even the physical and chemical nature of the particulate from water-surface bursts was problematical, and all existing model theory was based on land-surface detonations. Corrections necessitated by collection bias and radionuclide fractionation were considered refinements.

The objectives stated in Section 1.1 were formulated primarily to provide such sets of data. However, the need to generalize the results so that they could be applied to other combinations of detonation conditions was also recognized, and it was felt that studies relating to basic radiological variables should receive particular emphasis. Only when it becomes possible to solve new situations by inserting the proper values of such detonation parameters as the yield of the device and the composition of environmental materials in generalized mathematical relationships will it become possible to truly predict fallout and combat its effects.

TABLE 2.3 STATION LOCATIONS IN THE ATOLL AREA

Station	Shot Cherokee North Latitude and East Longitude		Shot Zuni North Latitude and East Longitude		Shot Flathead North Latitude and East Longitude		Shot Navajo North Latitude and East Longitude		Shot Tewa North Latitude and East Longitude	
	deg	min	deg	min	deg	min	deg	min	deg	min
YFNB 13 (E)	11	35.3	11	40.0	11	40.0	11	39.1	11	37.5
	165	31.2	165	17.2	165	17.2	165	16.2	165	27.0
YFNB 29 (G,H)	11	37.5	11	37.5	11	37.5	11	36.2	11	37.4
	165	27.0	165	27.0	165	27.0	165	29.8	165	14.2
How Island (F) *	148,320 N		148,320 N		148,320 N		148,320 N		148,320 N	
	167,360 E		167,360 E		167,360 E		167,360 E		167,360 E	
How Island (K) *	148,450 N		148,450 N		148,450 N		148,450 N		148,450 N	
	167,210 E		167,210 E		167,210 E		167,210 E		167,210 E	
George Island (L) *	168,530 N		168,530 N		168,530 N		168,530 N		168,530 N	
	131,250 E		131,250 E		131,250 E		131,250 E		131,250 E	
William Island (M) *	109,030 N		109,030 N		109,030 N		—		—	
	079,540 E		079,540 E		079,540 E		—		—	
Charlie Island (M) *	—		—		—		172,150 N		172,150 N	
	—		—		—		081,150 E		081,150 E	
Raft-1 (P)	11	35.1	11	35.1	11	35.1	11	35.1	11	35.1
	165	27.6	165	27.6	165	27.6	165	27.6	165	27.6
Raft-2 (R)	11	34.6	11	34.6	11	34.6	11	34.6	11	34.6
	165	22.2	165	22.2	165	22.2	165	22.2	165	22.2
Raft-3 (S)	11	35.4	11	35.4	11	35.4	11	35.4	11	35.4
	165	17.2	165	17.2	165	17.2	165	17.2	165	17.2
Skiff-AA	12	06.1	12	06.1	12	06.1	12	05.4	12	05.4
	164	47.0	164	47.0	164	47.0	164	44.9	164	44.9
Skiff-BB	12	11.6	12	11.6	12	11.6	12	11.5	12	11.5
	165	10.0	165	10.0	165	10.0	165	07.5	165	07.5
Skiff-CC	12	11.3	12	11.3	12	10.7	12	11.8	12	11.8
	165	23.0	165	23.0	165	17.6	165	20.9	165	20.9
Skiff-DD	12	11.5	12	11.5	12	11.5	12	11.5	12	11.5
	165	40.0	165	40.0	165	40.0	165	40.0	165	40.0
Skiff-EE	12	11.3	12	11.3	12	11.3	12	11.3	12	11.3
	165	57.3	165	57.3	165	57.3	165	57.3	165	57.3
Skiff-FF	12	02.4	12	02.4	12	03.5	12	02.4	12	02.4
	166	15.5	166	15.5	166	14.2	166	15.5	166	15.5
Skiff-GG	11	57.8	11	57.8	11	57.8	—	—	12	01.1
	165	13.8	165	13.8	165	13.8	—	—	165	10.2
Skiff-HH	12	01.3	12	01.3	12	02.0	12	02.0	12	02.0
	165	22.9	165	22.9	165	21.6	165	21.6	165	21.6
Skiff-KK	12	02.0	12	02.0	12	02.0	12	02.0	12	02.0
	165	40.0	165	40.0	165	40.0	165	40.0	165	40.0
Skiff-LL	12	02.0	12	02.0	12	02.0	12	02.0	12	02.0
	165	58.0	165	58.0	165	58.0	165	58.0	165	58.0
Skiff-MM	11	52.8	11	52.8	11	52.8	11	52.7	11	52.7
	164	58.4	164	58.4	164	58.4	164	56.0	164	56.0
Skiff-PP	11	52.0	—	—	11	50.5	11	52.0	11	52.0
	165	22.8	—	—	165	23.9	165	22.8	165	22.8
Skiff-RR	11	51.0	11	51.0	11	53.3	11	52.3	11	52.3
	165	40.0	165	40.0	165	35.2	165	39.7	165	39.7
Skiff-SS	11	50.0	11	50.0	11	51.1	—	—	—	—
	165	58.0	165	58.0	165	58.0	—	—	—	—
Skiff-TT	11	50.8	11	50.8	11	50.8	11	50.8	11	50.8
	166	15.0	166	15.0	166	15.0	166	15.0	166	15.0
Skiff-UU	11	42.5	11	42.5	11	42.5	—	—	—	—
	165	47.5	165	47.5	165	47.5	—	—	—	—
Skiff-VV	11	21.7	11	21.7	—	—	—	—	—	—
	165	19.5	165	19.5	—	—	—	—	—	—
Skiff-WW	—	—	—	—	—	—	—	—	11	43.2
	—	—	—	—	—	—	—	—	165	11.5
Skiff-XX	—	—	—	—	—	—	—	—	11	41.2
	—	—	—	—	—	—	—	—	164	55.1
Skiff-YY	—	—	—	—	—	—	—	—	11	54.0
	—	—	—	—	—	—	—	—	164	36.4

* Holmes and Narver coordinates.

TABLE 2.4 SHIP LOCATIONS AT TIMES OF PEAK ACTIVITY

The symbols t_a and t_c represent the times of arrival and cessation of fallout, respectively; t_p is the time of peak observed ionization rate.

Station	Shot Cherokee			Shot Zuni			Shot Flathead			Shot Navajo			Shot Tewa		
	Time	North Latitude and East Longitude		Time	North Latitude and East Longitude		Time	North Latitude and East Longitude		Time	North Latitude and East Longitude		Time	North Latitude and East Longitude	
	TSD, hr	deg	min	TSD, hr	deg	min	TSD, hr	deg	min	TSD, hr	deg	min	TSD, hr	deg	min
YAG 40	6 (t_a) *	12	40.0	3.4 (t_a)	12	22.0	8.0 (t_a)	12	19.7	6.0 (t_a)	12	12.3	4.4 (t_a)	12	04.5
(A, B)		164	20.0		165	45.8		165	20.8		165	08.8		164	44.8
	9 (t_p) *	12	40.0	4.3	12	22.0	11.6	12	23.2	6.6	12	12.0	6.2	12	04.5
		164	35.0		165	37.0		165	31.2		165	11.0		164	46.9
				4.8	12	22.0	12.8	12	34.7	7.3	12	11.0	7.2 (t_p)	12	06.0
					165	30.3		165	34.0		165	10.0		164	49.2
				5.3	12	22.5	13.8	12	26.0	9.2	12	13.0	8.2	12	06.4
					165	24.5		165	37.1		165	04.3		164	53.0
				5.8	12	22.0	17.0 (t_p)	12	31.9	11.1	12	11.0	8.5 (t_c)	12	06.2
					165	19.0		165	43.5		165	04.8		164	52.8
				6.3	12	23.0	22 (t_c)	12	41.8	12.1	12	12.0			
					165	15.4		165	54.3		165	04.8			
				6.7 (t_p)	12	23.5				12.3 (t_p)	12	12.2			
					165	15.7					165	04.2			
				7.4 (t_c)	12	24.4				13.1	12	13.0			
					165	16.2					165	01.0			
										16 (t_c)	12	09.9			
											164	59.5			
YAG 39	10 (t_a) *	13	18.0	12 (t_a)	13	00.6	4.5 (t_a)	12	04.2	2.3 (t_a)	12	01.8	2.0 (t_a)	12	05.6
(C)		163	42.0		165	02.2		165	23.4		165	18.3		165	12.0
	12 (t_p) *	12	20.0	12.6	13	00.6	5.1	12	04.7	4.6	11	59.7	2.2	12	03.5
		163	40.0		165	03.0		165	18.0		165	20.0		165	12.0
				14.6	12	53.0	6.1	12	06.0	5.6	12	01.7	2.7	12	04.0
					165	02.8		165	25.0		165	19.5		165	13.1
				16.1	13	00.0	8.1	12	03.0	6.0 (t_p)	11	59.3	4.7	12	01.5
					165	07.1		165	26.0		165	20.7		165	18.0
				17.6	13	03.8	10.1	12	07.0	6.6	11	57.0	5.0 (t_p)	12	01.6
					165	00.0		165	27.0		165	22.0		165	18.2
				18.6	13	00.4	11.0 (t_p)	12	05.6	8.6	12	02.0	5.3 (t_c)	12	01.8
					165	00.6		165	27.0		165	20.0		165	18.3
				19.6	12	58.0	12.1	12	04.0	9.6	11	59.0			
					165	08.0		165	27.0		165	19.0			
				20.6	12	59.0	13 (t_c)	12	05.1	11.6	11	58.0			
					165	01.2		165	27.8		165	20.0			
				21.6	13	00.6				12.6	11	57.0			
					165	10.7					165	18.0			
				24.6	13	00.0				14.6	11	55.0			
					165	11.4					165	23.5			

TABLE 2.4 CONTINUED

The symbols t_a and t_c represent the times of arrival and cessation of fallout, respectively; t_p is the time of peak observed ionization rate.

Station	Shot Cherokee			Shot Zuni			Shot Flathead			Shot Navajo			Shot Tewa		
	Time	North Latitude and East Longitude		Time	North Latitude and East Longitude		Time	North Latitude and East Longitude		Time	North Latitude and East Longitude		Time	North Latitude and East Longitude	
	TSD, hr	deg	min	TSD, hr	deg	min	TSD, hr	deg	min	TSD, hr	deg	min	TSD, hr	deg	min
YAG 39				25 (t_p)	13	00.8				15 (t_c)	12	00.1			
(C)					165	10.6					165	20.1			
				26.6	13	03.0									
					165	08.0									
				29 (t_c)	13	02.4									
					165	10.7									
LST 611	20 (t_p) †	14	20.0	18 (t_p) †	13	41.5	6.6 (t_a)	12	06.9	3.0 (t_a)	11	38.2	7.0 (t_a)	12	27.8
(D)		163	40.0		164	22.0		164	40.0		164	39.5		164	40.5
							7.3	12	00.0	3.6	11	35.0	7.2	12	25.8
								164	40.0		164	40.0		164	38.9
							7.6	12	00.0	4.4	11	33.7	10.2	12	24.0
								164	42.0		164	41.8		164	48.3
							8.3	12	01.6	5.1	11	35.6	12.2	12	25.5
								164	43.5		164	41.5		164	49.0
							9.1 (t_p)	12	02.0	6.1 (t_p)	11	34.1	13.2	12	25.0
								164	47.0		164	42.4		164	50.5
							12.6	12	03.0	7.1	11	34.8	13.6 (t_p)	12	25.3
								165	01.0		164	41.5		164	50.4
							15.6	12	05.0	7.6	11	37.2	14 (t_c)	12	25.4
								165	13.0		164	41.0		164	50.3
							18.2	11	46.0	10.1	11	35.8			
								165	08.0		164	39.5			
							20 (t_c)	11	47.4	12.1	11	34.2			
								165	16.2		164	39.6			
										12.9	11	33.7			
											164	38.7			
										13 (t_c)	11	33.9			
											164	38.8			

* Questionable value; activity near background level.

† Predicted value; no fallout occurred.

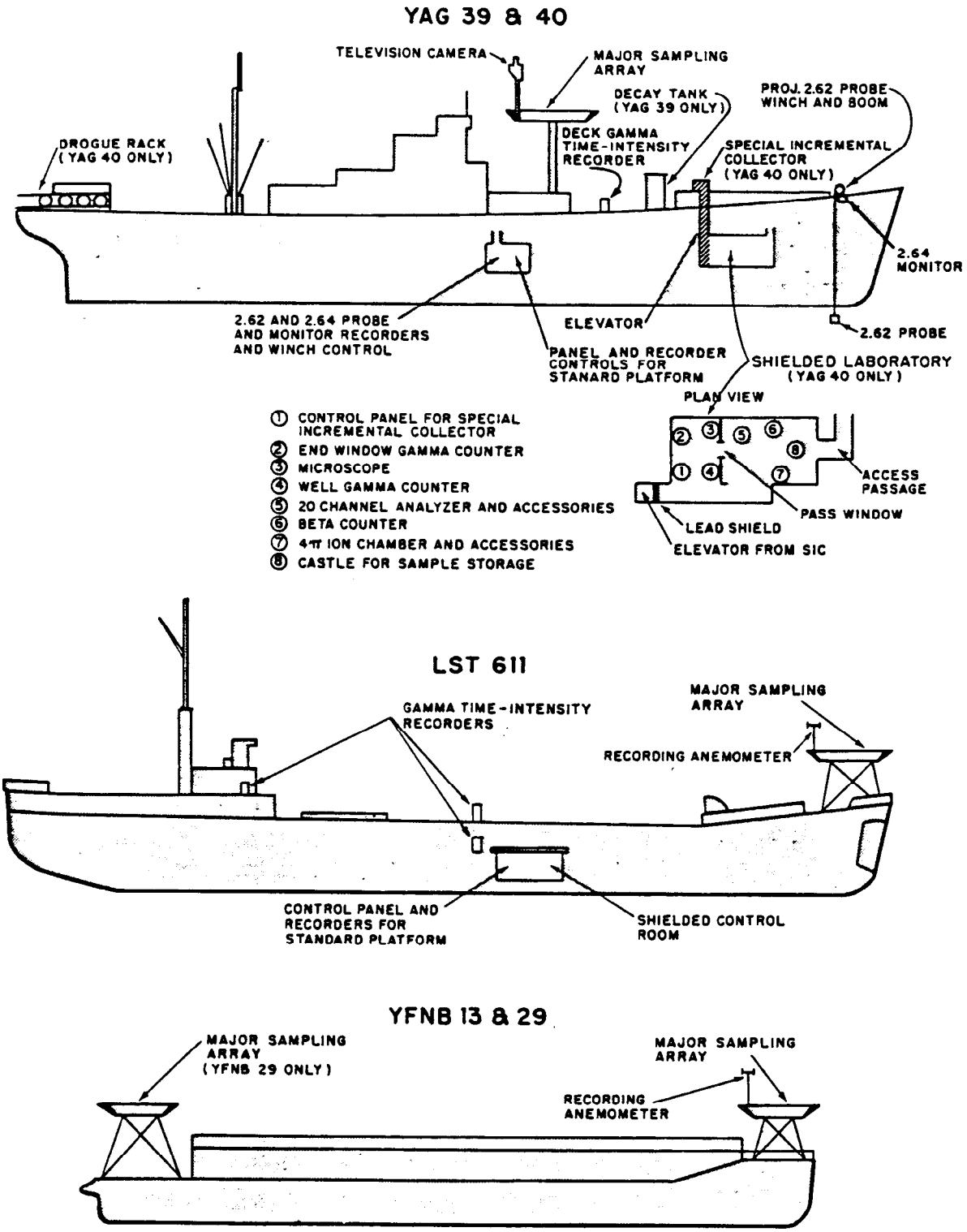

Figure 2.3 Ship and barge stations.

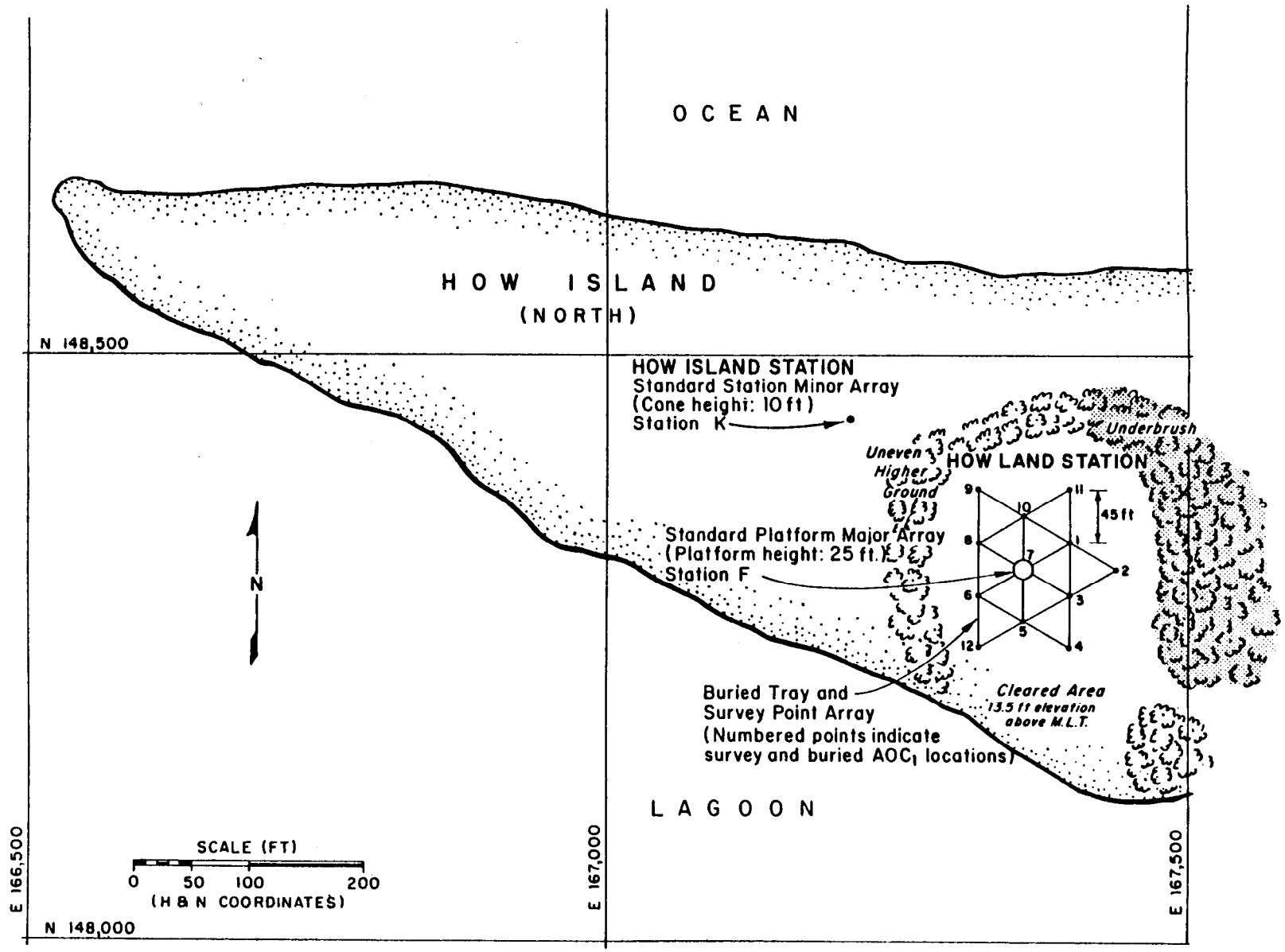

Figure 2.8 Location map and plan drawing of Site How.

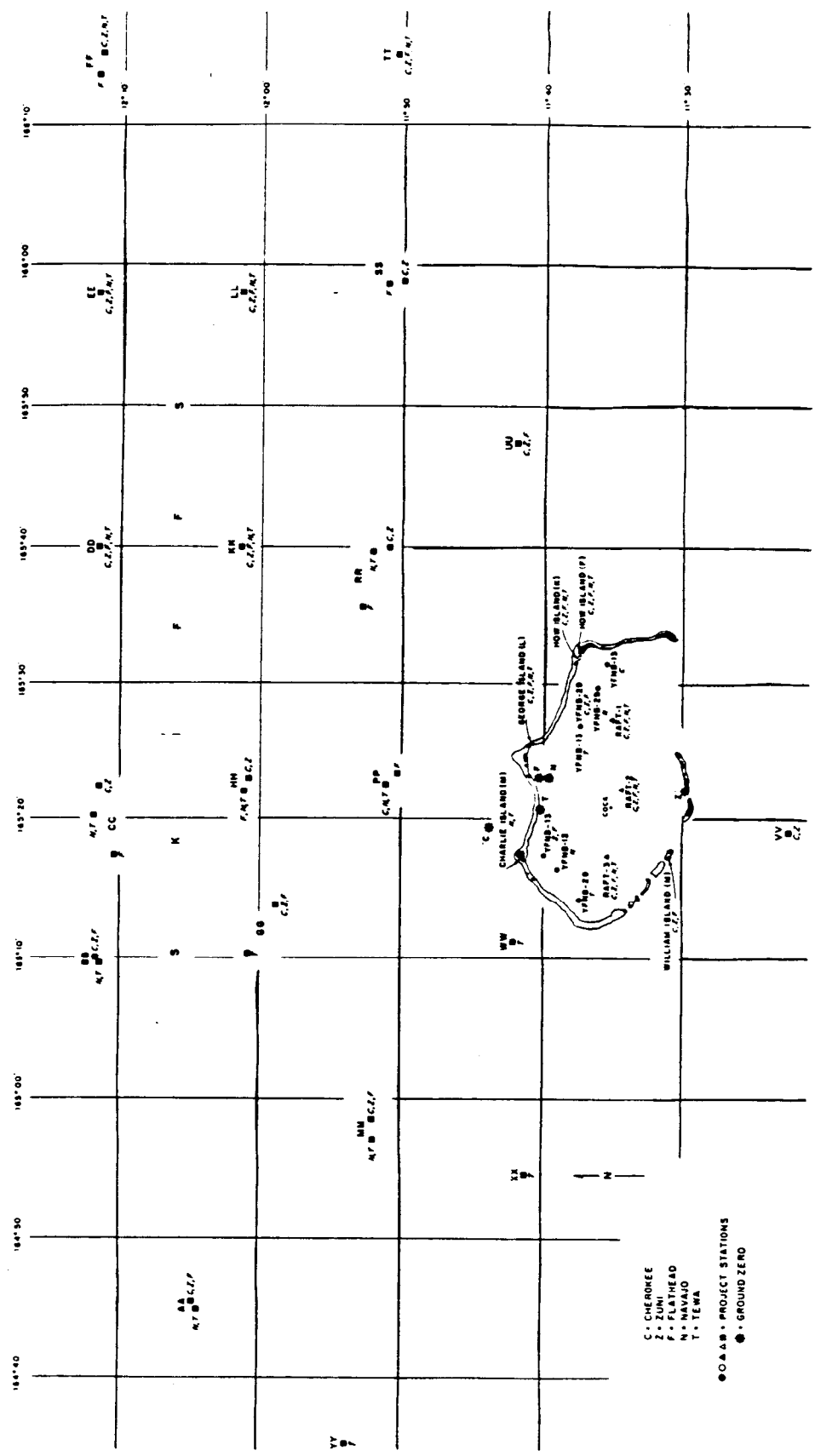

Figure 2.10 Station locations in the atoll area.

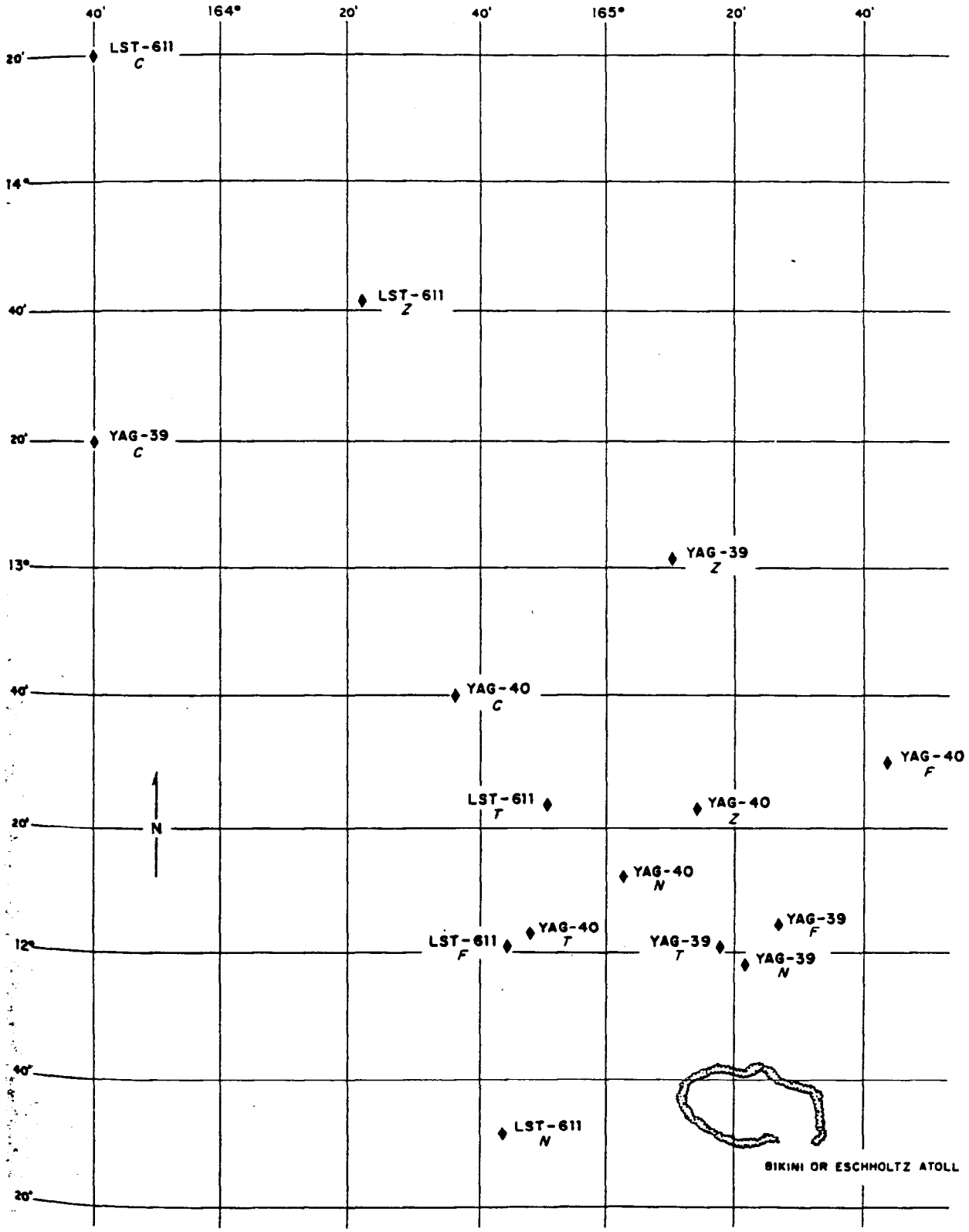

Figure 2.11 Ship locations at times of peak activity.

Chapter 3
RESULTS

3.1 DATA PRESENTATION

The data has been reduced and appears in comprehensive tables (Appendix B) that summarize certain kinds of information for all shots and stations. The text itself contains only derived results.

In general, the details of calculations, such as those involved in reducing gross gamma spectra to absolute photon intensities or in arriving at R-values, have not been included. Instead, original data and final results are given, together with explanations of how the latter were obtained and with references to reports containing detailed calculations.

Results for the water-surface Shots Flathead and Navajo, and the land-surface and near-land-surface Shots Zuni and Tewa, are presented in four categories: fallout-buildup characteristics (Section 3.2); physical, chemical, and radiochemical characteristics of the contaminated material (Section 3.3); its radionuclide composition and radiation characteristics (Section 3.4); and correlations of results (Section 4.3). Appendix B contains all reduced data for these shots separated into three types: that pertaining to the buildup phase (Section B.1); information on physical, chemical, and radiological properties (Section B.2); and data used for correlation studies (Section B.3).

Measurements and results for Shot Cherokee, an air burst during which very little fallout occurred, are summarized in Section 4.1.

Unreduced data are presented in Section B.4.

Each of the composite plots of TIR readings and IC tray activities presented in the section on buildup characteristics may be thought of as constituting a general description of the surface radiological event which occurred at that station. In this sense the information needed to complete the picture is provided by the remainder of the section on particle-size variation with time and mass-arrival rate, as well as by the following sections on the activity deposited per unit area, the particulate properties of the contaminated material, its chemical and radiochemical composition, and the nature of its beta- and gamma-ray emissions. Penetration rates and activity profiles in the ocean extend the description to subsurface conditions at the YAG locations. The radiological event that took place at any major station may be reconstructed in as much detail as desired by using Figures 3.1 through 3.4 as a guide and referring to the samples from that station for the results of interest. Each sample is identified by station, collector, and shot in all tables and figures of results, and the alphabetical and numerical designations assigned to all major array collectors are summarized in Figure A.1.

Throughout the treatment which follows, emphasis has been placed on the use of quantities such as fissions per gram and R^{99} values, whose variations show fundamental differences in fallout properties. In addition, radiation characteristics have been expressed in terms of unit fissions wherever possible. As a result, bias effects are separated, certain conclusions are made evident, and a number of correlations become possible. Some of the latter are presented in Sections 3.3, 3.4, and 4.3.

3.2 BUILDUP CHARACTERISTICS

3.2.1 Rate of Arrival. Reduced and corrected records of the ionization rates measured by one TIR and the sample activities determined from one IC at each major array station are plotted against time since detonation (TSD) in Figures 3.1 through 3.4 for Shots Flathead, Navajo,

Zuni, and Tewa. Numerical values are tabulated in Tables B.1 and B.2. Because the records of the TIR's and the deck (D-TIR) are plotted for the YAG's, the measurements made by the TIR's in the standard platform (P-TIR) have been included in Appendix B. The records of the IC's with shorter collection intervals have been omitted, because they show only the greater variability in the fine structure of the other curves and do not cover the entire fallout period.

TIR readings have been adjusted in accordance with the calibration factors applying to the four ionization chambers present in each instrument, and corrected to account for saturation loss over all ranges. (The adjustments were made in accordance with a private communication from H. Rinnert, NRDL, and based upon Co^{60} gamma rays incident on an unobstructed chamber, normal to its axis.) Recorder speeds have also been checked and the time applying to each reading verified. In those cases where saturation occurred in the highest range, readings have been estimated on the basis of the best information available and the curves dotted in on the figures.

It is pointed out that these curves give only approximate air-ionization rates. Because of the varying energy-response characteristics of each ionization chamber, and internal shielding effects resulting from the construction of the instrument, TIR response was nonuniform with respect both to photon energy and direction, as indicated in Figures A.2 through A.4. The overall estimated effect was to give readings as much as 20 percent lower than would have been recorded by an ideal instrument. (Measurements were made on the YAG 39 and YAG 40 during all four shots with a Cutie Pie or T1B hand survey meter held on top of an operating TIR. The TIR's indicated, on the average, 0.85 ± 25 percent of the survey meter readings, which themselves indicate only about 75 percent of the true dose rate 3 feet above a uniformly distributed plane source (Reference 17). Total doses calculated from TIR curves and measured by film-pack dosimeters (ESL) at the same locations are compared in Section 4.3.5.)

Detailed corrections are virtually impossible to perform, requiring source strength and spectral composition as functions of direction and time, combined with the energy-directional response characteristics of each chamber. It is also pointed out that these sources of error are inherent to some degree in every real detector and are commonly given no consideration whatsoever. Even with an ideal instrument, the measured dose rates could not be compared with theoretical land-equivalent dose rates because of irregularities in the distribution of the source material and shielding effects associated with surface conditions. However, a qualitative study of the performance characteristics of ship, barge, and island TIR's indicated that all performed in a manner similar for the average numbers of fissions deposited and identical radionuclide compositions.

The exposure interval associated with each IC tray has been carefully checked. In those cases where the time required to count all of the trays from a single instrument was unduly long, activities have been expressed at a common time of H+12 hours. Background and coincidence loss corrections have also been made.

The time interval during which each tray was exposed is of particular importance, not only because its midpoint fixes the mean time of collection, but also because all tray activities in counts per minute (counts/min) have been normalized by dividing by this interval, yielding counts per minute per minute of exposure (counts/min^2). Such a procedure was necessary, because collection intervals of several different lengths were used. The resulting quantity is an activity-arrival rate, and each figure shows how this quantity varied over the successive collection intervals at the reference time, or time when the trays were counted. If it can be established that mass is proportional to activity, these same curves can be used to study mass-arrival rate with time (Section 3.2.3, Shots Flathead and Navajo); if, on the other hand, the relationship of mass to activity is unknown, they may be used for comparison with curves of mass-arrival rate constructed by some other means (Section 3.2.3, Shots Zuni and Tewa).

Thus, while each point on a TIR curve expresses the approximate gamma ionization rate produced at that time by all sources of activity, the corresponding time point on the IC curve gives the decay-corrected relative rate at which activity was arriving. Both complementary kinds of information are needed for an accurate description of the radiological event that took place at a given station and are plotted together for this reason—not because they are comparable in any other way.

The activities of the IC trays have not been adjusted for sampling bias, although some undoubtedly exists, primarily because its quantitative effects are unknown. Relative rates may still be derived if it is assumed that all trays are biased alike, which appears reasonable for those cases in which wind speed and direction were nearly constant during the sampling period (Section 4.3.2). More extensive analysis would be required to eliminate uncertainties in the remaining cases.

It should also be mentioned that IC trays with alternating greased-disk and reagent-film collecting surfaces were intentionally used in all of the collectors for Shots Flathead and Navajo —with no detectable difference in efficiency for the resulting fallout drops—and of necessity for Shot Tewa. The late move of Shot Tewa to shallow water produced essentially solid particle fallout, for which the efficiency of the reagent film as a collector was markedly low. Thus, only the greased-disk results have been plotted for the YAG 40 in Figure 3.4, although it was necessary to plot both types for some of the other stations. Trays containing reagent-film disks, all of which were assigned numbers between 2994 and 3933, may be distinguished by reference to Table B.2. A few trays, designated by the prefix P, also contained polyethylene disks to facilitate sample recovery.

3.2.2 Times of Arrival, Peak Activity, and Cessation. The times at which fallout first arrived, reached its peak, and ceased at each major array station are summarized for all shots in Table 3.1. Peak ionization rates are also listed for convenient reference. Time of arrival detector (TOAD) results, covering all minor array stations and providing additional values for the major stations in the atoll area, are tabulated in Table 3.2.

The values given in Table 3.1 were derived from Figures 3.1 through 3.4, and the associated numerical values in Tables B.1 and B.2, by establishing certain criteria which could be applied throughout. These are stated in the table heading; while not the only ones possible, they were felt to be the most reasonable in view of the available data.

Arrival times (t_a) were determined by inspection of both TIR and IC records, the resulting values being commensurate with both. Because the arrival characteristics varied, arrival could not be defined in some simple way, such as "1 mr/hr above background." The final values, therefore, were chosen as sensible-arrival times, treating each case individually. It should be mentioned that, within the resolving power of the instruments used, no time difference existed between the onset of material collections on the IC trays and the toe of the TIR buildup curve. The IC's on the ships were manually operated and generally were not triggered until the arrival of fallout was indicated by the TIR or a survey meter, thus precluding any arrival determination by IC; those at the unmanned stations, however, triggered automatically at shot time, or shortly thereafter, and could be used. The SIC on the YAG 40 also provided usable data, ordinarily yielding an earlier arrival time than IC B-7 on the same ship. In order to conserve trays, however, the number exposed before fallout arrival was kept small, resulting in a larger time uncertainty within the exposure interval of the first active tray.

Once defined, times of peak activity (t_p) could be taken directly from the TIR curves. Because peaks were sometimes broad and flat, however, it was felt to be desirable to show also the time interval during which the ionization rate was within 10 percent of the peak value. Examination of these data indicated that $t_p \sim 2t_a$; this point is discussed and additional data are presented in Reference 18.

Cessation time (t_c) is even more difficult to define than arrival time. In almost every case, for example, fallout was still being deposited at a very low rate on the YAG 40 when the ship departed station. Nevertheless, an extrapolated cessation time which was too late would give an erroneous impression, because 90 or 95 percent of the fallout was down hours earlier. For this reason, IC-tray activities measured at a common time were cumulated and the time at which 95 percent of the fallout had been deposited read off. A typical curve rises abruptly, rounds over, and approaches the total amount of fallout asymptotically. Extrapolated cessation times were estimated primarily from the direct IC plots (Figures 3.1 through 3.4), supplemented by the cumulative plots, and the TIR records replotted on log-log paper. It must be emphasized

that the cessation times reported are closely related to the sensitivity of the measuring systems used and the fallout levels observed.

All values for time of arrival given in Table 3.2 were determined from TOAD measurements. They were obtained by subtracting the time interval measured by the instrument clock, which started when fallout arrived, from the total period elapsed between detonation and the time when the instrument was read.

Because the TOAD's were developed for use by the project and could not be proof-tested in advance, certain operational problems were encountered in their use; these are reflected by Footnotes §, ¶ and † in Table 3.2. Only Footnote † indicates that no information was obtained by the units; however, Footnotes § and ¶ are used to qualify questionable values. Because the TOAD's from the barge and island major stations were used elsewhere after Shot Flathead, Footnote * primarily expresses the operational difficulties involved in servicing the skiffs and keeping them in place.

The fact that a station operated properly and yet detected no fallout is indicated in both tables by Footnote ‡. In the case of the major stations, this means that the TIR record showed no measurable increase and all of the IC trays counted at the normal background rate. For the minor stations, however, it means that the rate of arrival never exceeded 20 mr/hr per half hour, because the radiation trigger contained in the TOAD was set for this value.

3.2.3 Mass-Arrival Rate. A measure of the rate at which mass was deposited at each of the major stations during Shots Zuni and Tewa is plotted in Figure 3.5 from data contained in Table B.4; additional data are contained in Table B.6. Corresponding mass-arrival rates for Shots Flathead and Navajo may be obtained, where available, by multiplying each of the IC-tray activities (count/min^2) in Figures 3.1 and 3.2 by the factor, micrograms per square feet per hour per counts per minute per minute, [μg/(ft^2-hr-count/min^2)]. For the YAG 40, YAG 39, and LST 611, the factor is 0.0524 for Shot Flathead and 0.701 for Shot Navajo. For the YFNB 29, the factor is 0.343 for Shot Flathead. For the YFNB 13 and How-F, the factor is 3.69 for Shot Navajo.

The former values of mass-arrival rate, micrograms per square foot per hour [μg/(ft^2/hr)], were calculated from the particle-size distribution studies in Reference 19, discussed in more detail in Section 3.2.4. The number of solid particles in each size increment deposited per square foot per hour was converted to mass by assuming the particles to be spheres with a density of 2.36 gm/cm^3. Despite the fact that a few slurry particles might have been present (Section 3.3.1), these values were then summed, over all size increments, to obtain the total mass-arrival rate for each tray, or as a function of time since detonation (TSD). These results may not be typical for the geographic locations from which the samples were taken, because of collector bias (Section 4.3.2).

Because this result will be affected by any discrepancy between the number of particles of a certain size, which would have passed through an equal area in free space had the tray not been present, and the number ultimately collected by the tray and counted, both sampling bias (Section 4.3.2) and counting error (Section 3.2.4) are reflected in the curves of Figure 3.5. For this reason they, like the curves of Section 3.2.1, are intended to provide only relative-rate information and should not be integrated to obtain total-mass values, even over the limited periods when it would be possible to do so. The total amount of mass (mg/ft^2) deposited at each major station, determined from chemical analysis of OCC collections, is given in Table 3.16.

The constants to be used for the water-surface shots follow from the slurry-particle sodium chloride analyses in Reference 31 and were derived on the basis of experimentally determined values relating well-counter gamma activity to sodium chloride weight in the deposited fallout. These values and the methods by which they were obtained are presented in Section 3.3.2. The factors were calculated from the ratio of counts per minute per minute (count/min^2) for the IC-tray area to counts per minute per gram [(counts/min)/gm] of NaCl from Table 3.12. The grams of NaCl were converted to grams of fallout, with water included, in the ratio of 1/2.2; and the gamma well counts from the table were expressed as end-window gamma counts by use of the ratio 1/62. An average value of specific activity for each shot was used for the ship stations,

while a value more nearly applicable for material deposited from 1 to 3 hours after detonation was used for the barge and island stations.

It is to be noted that the insoluble solids of the slurry particles (Section 3.3.2) were not included in the conversion of grams of NaCl to grams of fallout. Even though highly active, they constituted less than 2 to 4 percent of the total mass and were neglected in view of measurement errors up to ±5 percent for sodium chloride, ±15 percent for specific activity, and ±25 percent for water content.

3.2.4 Particle-Size Variation. The way in which the distribution of solid-particle sizes varied over the fallout buildup period at each of the major stations during Shots Zuni and Tewa is shown in Figures 3.6 through 3.9. The data from which the plots were derived are tabulated in Table B.3, and similar data for a number of intermediate collection intervals are listed in Table B.5. All of the slurry particles collected over a single time interval at a particular location during Shots Flathead and Navajo tended to fall in one narrow size range; representative values are included in Table 3.12.

The information contained in Tables B.3 through B.6 and plotted in the figures represents the results of studies described in detail in Reference 19. All IC trays were inserted in a fixed setup employing an 8-by-10-inch-view camera and photographed with a magnification of 2., soon after being returned to NRDL. Backlighting and low-contrast film were used to achieve maximum particle visibility. A transparent grid of 16 equal rectangular areas was then superimposed on the negative and each area, enlarged five times, printed on 8-by-10-inch paper at a combined linear magnification of 10.

Since time-consuming manual methods had to be used in sizing and counting the photographed particles, three things were done to keep the total number as small as possible, consistent with good statistical practice and the degree of definition required. (1) The total number of trays available from each collector was reduced by selecting a representative number spaced at more or less equal intervals over the fallout-buildup period. Reference was made to the TIR and IC curves (Figures 3.1 to 3.4) during the selection process, and additional trays were included in time intervals where sharp changes were indicated. (2) Instead of counting the particles in all areas of heavily loaded trays, a diagonal line was drawn from the most dense to the least dense edge and only those areas selected which were intersected by the line. (3) No particles smaller than 50 microns in diameter were counted, this being arbitrarily established as the size defining the lower limit of significant local fallout. (The lower limit was determined from a fallout model, using particle size as a basic input parameter (Section 4.3.1). Particles down to ~20 microns in diameter will be present, although the majority of particles between 20 and 50 microns will be deposited at greater distances than those considered.)

Actual sizing and counting of the particles on the selected ten times enlargements was accomplished by the use of a series of gages consisting of four sets of black circular spots of the same magnification, graduated in equal-diameter increments of 5, 10, 30, and 100 microns. These were printed on a sheet of clear plastic so that the largest spot which could be completely inscribed in a given particle area could be determined by superimposition. Thus, all of the particle sizes listed refer to the diameter of the maximum circle which could be inscribed in the projected area of the particle. A preliminary test established that more-consistent results could be achieved using this parameter than the projected diameter, or diameter of the circle equal to the projected area of the particle.

A number of problems arose in connection with the counting procedure: touching particles were difficult to distinguish from single aggregates; particles which were small, thin, translucent, or out of focus were difficult to see against the background; particles falling on area borderlines could not be accurately sized and often had to be eliminated; some elongated particles, for which the inscribed-circle method was of questionable validity, were observed; a strong tendency existed to overlook particles smaller than about 60 microns, because of the graininess of the print and natural human error. Most of these problems were alleviated, however, by having each print processed in advance by a specially trained editor. All particles to be counted were first marked by the editor, then sized by the counter.

Once the basic data, consisting of the number of particles in each arbitrary size interval between 50 and 2,600 microns, were obtained for the selected trays, they were normalized to a 1-micron interval and smoothed, to compensate in part for sample sparsity, by successive applications of a standard smoothing function on a digital computer. These, with appropriate unit conversions, are the results listed in Tables B.3 and B.5: the numbers of particles, within a 1-micron interval centered at the indicated sizes, collected per hour for each square foot of surface.

Figures 3.6 through 3.9 show how the concentration of each particle size varied over the buildup period by providing, in effect, successive frequency distributions on time-line sections. The curves representing the 92.5- and 195-micron particles have been emphasized to bring out overall trends and make the figures easier to use. Measures of central tendency have been avoided, because the largest particles which make the most-significant contribution to the activity are not significantly represented in the calculation of the mean particle size, while the small particles which make the greatest contribution in the calculation of the mean particle size are most subject to errors from counting and background dust deposits. It should also be remembered that sampling bias is present and probably assumes its greatest importance for the small particles.

Plots of pure background collections for the ship and barge stations resemble the plot of the YAG 39 data for Shot Zuni, but without the marked peaks in the small particles or the intrusions of the large particles from below, both of which are characteristic of fallout arrival. This is not necessarily true for the How land station, however, where such features may result from disturbances of the surface dust; the series of peaks at about 4 hours during Shot Zuni, for example, appears to be the result of too close an approach by a survey helicopter.

3.2.5 Ocean Penetration. Figure 3.10 shows the general penetration behavior of fallout activity in the ocean for Shot Navajo, a water-surface shot, and Shot Tewa, resembling a land-surface shot. These simplified curves show a number of successive activity profiles measured during and after the fallout period with the oceanographic probe (SIO-P) aboard the YAG 39 and demonstrate the changing and variable nature of the basic phenomena. The best estimates of the rate at which the main body of activity penetrated at the YAG 39 and YAG 40 locations during Shots Flathead, Navajo, and Tewa are summarized in Table 3.3, and the depths at which this penetration was observed to cease are listed in Table 3.4. The data from which the results were obtained are presented in graphical form in Figure B.1; reduced-activity profiles similar to those shown in Figure 3.10 were used in the preparation of the plots. Estimates of the maximum penetration rates observed for Shots Zuni, Navajo, and Tewa appear in Table 3.5.

The values tabulated in Reference 20 represent the result of a systematic study of measured profiles for features indicative of penetration rate. Various shape characteristics, such as the depth of the first increase in activity level above normal background and the depth of the juncture of the gross body of activity with the thin body of activity below, were considered; but none was found to be applicable in every case.

The concept of equivalent depth was devised so that: (1) all the profile data (i.e., all the curves giving activity concentration as a function of depth) could be used, and (2) the results of the Project 2.63 water-sampling effort could be related to other Program 2 studies, in which the determination of activity per unit volume of water near the surface (surface concentration) was a prime measurement. The equivalent depth is defined as the factor which must be applied to the surface concentration to give the total activity per unit water surface area as represented by the measured profile. Because the equivalent depth may be determined by dividing the planimetered area of any profile by the appropriate surface concentration, it is relatively independent of profile shape and activity level and, in addition, can utilize any measure of surface concentration which can be adjusted to the time when the profile was taken and expressed in the same units of activity measurement. Obviously, if the appropriate equivalent depth can be determined, it may be applied to any measurement of the surface concentration to produce an estimate of the activity per unit area when no other data are available.

The penetration rates in Table 3.3 were obtained by plotting all equivalent-depth points avail-

able for each ship and shot (Figure B.1), dividing the data into appropriate intervals on the basis of the plots, and calculating the slopes of the least-squares lines for these intervals. The maximum depths of penetration listed in Table 3.4 were derived from the same plots by establishing that the slopes did not differ significantly from zero outside of the selected intervals. Erratic behavior or failure of the probes on both ships during Shot Zuni and on the YAG 40 during Shot Flathead prevented the taking of data which could be used for equivalent-depth determinations. It did prove possible in the former case, however, to trace the motion of the deepest tip of the activity profile from the YAG 39 measurements; and this is reported, with corresponding values from the other events, as a maximum penetration rate in Table 3.5.

It is important to emphasize that the values given in Tables 3.3 and 3.4, while indicating remarkably uniform penetration behavior for the different kinds of events, refer only to the gross body of the fallout activity as it gradually settles to the thermocline. When the deposited material consists largely of solid particles, as for Shots Zuni and Tewa, it appears that some fast penetration may occur. The rates listed for these shots in Table 3.5 were derived from a fast-traveling component which may have disappeared below the thermocline, leaving the activity profile open at the bottom (Figure 3.10). On the other hand, no such penetration was observed for Shot Flathead and was questionable in the case of Shot Navajo. This subject is discussed further in Section 4.3.2, and estimates of the amount of activity disappearing below the thermocline are presented.

It is also important to note that the linear penetration rates given in Table 3.3 apply only from about the time of peak onward and after the fallout has penetrated to a depth of from 10 to 20 meters. Irregular effects at shallower depths, like the scatter of data points in the vicinity of the thermocline, no doubt reflect the influence both of differences in fallout composition and uncontrollable oceanographic variables. The ships did move during sampling and may have encountered nonuniform conditions resulting from such localized disturbances as thermal gradients, turbulent regions, and surface currents.

In addition to penetration behavior, decay and solubility effects are present in the changing activity profiles of Figure 3.10. The results of the measurements made by the decay probe (SIO-D) suspended in the tank filled with ocean water aboard the YAG 39 are summarized in Table 3.6. Corresponding values from Reference 15 are included for comparison; although similar instrumentation was used, these values were derived from measurements made over slightly different time intervals in contaminated water taken from the ocean some time after fallout had ceased.

Two experiments were performed to study the solubility of the activity associated with solid fallout particles and give some indication of the way in which activity measurements made with energy-dependent instruments might be affected. Several attempts were also made to make direct measurements of the gamma-energy spectra of water samples, but only in one case (Sample YAG 39-T-IC-D, Table B.20) was there enough activity present in the aliquot.

The results of the experiments are summarized in Figures 3.11 and 3.12. Two samples of particles from Shot Tewa, giving 4-π ionization chamber readings of 208×10^{-9} and 674×10^{-8} ma respectively, were removed from a single OCC tray (YAG 39-C-34 TE) and subjected to measurements designed to indicate the solubility rates of various radionuclides in relation to the overall solubility rate of the activity in ocean water.

The first sample (Method I) was placed on top of a glass-wool plug in a short glass tube. A piece of rubber tubing connected the top of this tube to the bottom of a 10-ml microburet filled with sea water. The sea water was passed over the particles at a constant rate, and equivolume fractions were collected at specified time intervals. In 23 seconds, 3 ml passed over the particles, corresponding to a settling rate of 34 cm/min—approximately the rate at which a particle of average diameter in the sample (115 microns) would have settled. The activity of each fraction was measured with the well counter soon after collection and, when these measurements were combined with the total sample activity, the cumulative percent of the activity dissolved was computed (Figure 3.11). Gamma-energy spectra were also measured on fractions corresponding roughly to the beginning (10 seconds), middle (160 seconds) and end (360 seconds) of the run (Figure 3.12). The time of the run was D+5 days.

On D+4 the second sample (Method II) was placed in a vessel containing 75 ml of sea water. After stirring for a certain time interval, the solution was centrifuged and a 50-λ aliquot removed from the supernate. This procedure was repeated several times over a 48-hour period, with the activity of each fraction being measured shortly after separation and used to compute the cumulative percent of the total activity in solution (Figure 3.11). The gamma spectrum of the solution stirred for 48 hours was also measured for comparison with the spectra obtained by Method I (Figure 3.12).

As indicated in Figure 3.11, more than 1 percent of the total activity went into solution in less than 10 seconds, followed by at least an additional 19 percent before equilibrium was achieved. This was accompanied by large spectral changes, indicating marked radionuclide fractionation (Figure 3.12); nearly all of the I^{131}, for example, appears to have been dissolved in 360 seconds.

The dip-counter activities of all water samples taken by Projects 2.63 and 2.62a are tabulated in Table B.32. Ocean background corrections have not been attempted but may be estimated for each shot at the YAG 39 and YAG 40 locations from the activities of the background samples collected just prior to the arrival of fallout. All other corrections have been made, however, including those required by the dilution of the designated 1,100-ml depth samples to the standard 2,000-ml counting volume. Normalized dip-counter decay curves for each event (Figure B.14), and the records of the surface-monitoring devices (NYO-M, Figures B.8 through B.13) are also included in Section B.4.

3.3 PHYSICAL, CHEMICAL, AND RADIOCHEMICAL CHARACTERISTICS

3.3.1 Solid Particles. All of the active fallout collected during Shot Zuni, and nearly all collected during Shot Tewa, consisted of solid particles which closely resembled those from Shot M during Operation Ivy and Shot 1 during Operation Castle (References 21 and 22). Alternate trays containing greased disks for solid-particle collection and reagent films for slurry-particle collection were used in the IC's during Shot Tewa. Microscopic examination of the latter revealed an insignificant number of slurry particles; these results are summarized in Table B.10. No slurry particles were observed in the Zuni fallout, although a small number may have been deposited.

As illustrated in Figure 3.13, the particles varied from unchanged irregular grains of coral sand to completely altered spheroidal particles or flaky agglomerates, and in a number of cases included dense black spheres (Reference 19). Each of these types is covered in the discussion of physical, chemical, radiochemical, and radiation characteristics which follows. Basic data for about 100 particles from each shot, selected at random from among those removed from the SIC trays in the YAG 40 laboratory, are included in Table B.34.

Physical and Chemical Characteristics. A number of irregular and spheroidal particles collected on the YFNB 29 during Shots Zuni and Tewa were thin-sectioned and studied under a petrographic microscope (Reference 23); some from Shot Zuni were also subjected to X-ray diffraction analysis (Table 3.7). Typical thin sections of both types of particles are presented in Figures 3.14, 3.15 and 3.16 for Shot Zuni and Figures 3.17 and 3.18 for Shot Tewa. Although the particles shown in the figures were taken from samples of close-in fallout, those collected 40 miles or more from the shot point by the SIC on the YAG 40 were observed to be similar, except for being smaller in size.

Both methods of analysis showed the great majority of irregular particles to consist of fine-grained calcium hydroxide, $Ca(OH)_2$, with a thin surface layer of calcium carbonate, $CaCO_3$ (Figure 3.17). A few, however, had surface layers of calcium hydroxide with central cores of unchanged coral ($CaCO_3$), and an even smaller number were composed entirely of unchanged coral (Figure 3.14). It is likely that the chemically changed particles were formed by decarbonation of the original calcium carbonate to calcium oxide followed by hydration to calcium hydroxide and subsequent reaction with CO_2 in the atmosphere to form a thin coat of calcium carbonate. Particles of this kind were angular in appearance and unusually white in color (Figure 3.13, A and G).

Many of the irregular particles from Shot Zuni were observed to carry small highly active

spherical particles 1 to 25 microns in diameter on their surfaces (Figures 3.13G and 3.15). Shot Tewa particles were almost entirely free from spherical particles of this kind, although a few with diameters less than 1 micron were discovered when some of the irregular particles were powdered and examined with an electron microscope. A few larger isolated spherical particles were also found in the Zuni fallout (Figures 3.13, B and H). Such particles varied in color from orange-red for the smallest sizes to opaque black for the largest sizes.

While these particles were too small to be subjected to petrographic or X-ray diffraction analysis, it was possible to analyze a number of larger particles collected during Shot Inca which appeared to be otherwise identical (Figure 3.19). The Inca particles were composed primarily of Fe_3O_4 and calcium iron oxide ($2\ CaO.Fe_2O_3$) but contained smaller amounts of Fe_2O_3 and CaO. Some were pure iron oxide but the majority contained calcium oxide in free form or as calcium iron oxide (Reference 24).

Most of the spheroidal particles consisted of coarse-grained calcium hydroxide with a thin surface layer of calcium carbonate (Figure 3.16). Nearly all contained at least a few grains of calcium oxide, however, and some were found to be composed largely of this material (Figure 3.18)—5 to 75 percent by volume. Although melted, particles of this kind probably underwent much the same chemical changes as the irregular particles, the principal difference being that they were incompletely hydrated. They varied in appearance from irregular to almost perfect spheres and in color from white to pale yellow (Figure 3.13, C, H, and K). Many had central cavities, as shown in Figure 3.16 and were in some cases open on one side.

Because of their delicacy, the agglomerated particles could not be thin-sectioned and had to be crushed for petrographic and X-ray diffraction analysis. They were found to be composed primarily of calcium hydroxide and some calcium carbonate. It has been observed that similar particles are formed by the expansion of calcium oxide pellets placed in distilled water, and that the other kinds of fallout particles sometimes change into such aggregates if exposed to air for several weeks. The particles were flaky in appearance, with typical agglomerated structures, and a transparent white in color (Figure 3.13, D, I, and J); as verified by examination of IC trays in the YAG 40 laboratory immediately after collection, they were deposited in the forms shown.

The densities of 71 yellow spheroidal particles, 44 white spheroidal particles, and 7 irregular particles from Shot Zuni were determined (Reference 25) using a density gradient tube and a bromoform-bromobenzene mixture with a range from 2.0 to 2.8 gm/cm^3. These results, showing a clustering of densities at 2.3 and 2.7 gm/cm^3, are summarized in Table 3.8. The yellow spheres are shown to be slightly more dense than the white, and chemical spot tests made for iron gave relatively high intensities for the former with respect to the latter. No density determinations were made for agglomerated particles, but one black spherical particle (Table 3.7) was weighed and calculated to have a density of 3.4 gm/cm^3.

The subject of size distribution has been covered separately in Section 3.2.4, and all information on particle sizes is included in that section.

Radiochemical Characteristics. Approximately 30 irregular, spheroidal and agglomerated particles from Shot Zuni were subjected to individual radiochemical analysis (Reference 26), and the activities of about 30 more were assayed in such a way that certain of their radiochemical properties could be inferred. A number of particles of the same type were also combined in several cases so that larger amounts of activity would be available. These data are tabulated in Tables B.7 and B.8.

Radiochemical measurements of Sr^{89}, Mo^{99}, Ba^{140}-La^{140} and Np^{239} were made. (All classified information such as the product/fission ratio for Np^{239}, which could not be included in Reference 26, and the limited amount of data obtained for Shots Tewa and Flathead were received in the form of a private communication from the authors of Reference 26.) For the most part, conventional methods of analysis (References 27 and 28) were used, although the amounts of Np^{239} and Mo^{99} (actually Tc^{99m}) were determined in part from photopeak areas measured on the single-channel gamma analyzer (Section 2.2 and Reference 29). The total number of fissions in each sample was calculated from the number of atoms of Mo^{99} present, and radiochemical results were expressed as R-values using Mo^{99} as a reference. (R-values, being defined as the ratio

of the observed amount of a given nuclide to the amount expected from thermal neutron fission of U^{235}, relative to some reference nuclide, combine the effects of fractionation and variations in fission yield and contain a number of experimental uncertainties. Values between 0.5 and 1.5 cannot be considered significantly different from 1.0.) Selected particles were also weighed so that the number of fissions per gram could be computed.

Radioactivity measurements were made in the gamma well counter (WC) and the 4-π gamma ionization chamber (GIC), both of which are described in Section 2.2. Because the efficiency of the former decreased with increasing photon energy, while the efficiency of the latter increased, samples were often assayed in both instruments and the ratio of the two measurements (counts per minute per 10^4 fissions to milliamperes per 10^4 fissions) used as an indication of differences in radionuclide composition.

It will be observed that the particles in Table B.7 have been classified according to color and shape. For purposes of comparing radiochemical properties, spheroidal and agglomerated particles have been grouped together and designated as "altered particles," while irregular particles have been designed "unaltered particles." The latter should not be interpreted literally, of course; it will be evident from the foregoing section that the majority of irregular particles have undergone some degree of chemical change. Particles were classified as altered if they exhibited the obvious physical changes of spheroidal or agglomerated particles under the optical microscope.

Radiochemical results for all altered and unaltered particles from Shot Zuni are summarized in Table 3.9, and activity ratios of the particles from this shot and Shot Tewa are compared in Table 3.10. The differences in radiochemical composition suggested in the tables are emphasized in Figure 3.20, which shows how the energy-dependent ratios (counts per minute per 10^4 fissions, milliamperes per 10^4 fissions and counts per minute per milliamperes) varied with time, and in Figure 3.21, wherein the data used for computing the R-values and product/fission (p/f) ratios (number of atoms of induced product formed per fission) in Tables B.7 and B.8 are presented graphically by plotting the numbers of atoms of each nuclide in a sample versus the number of atoms of Mo^{99}. Data obtained from calibration runs with neutron-irradiated U^{235} are plotted in the former for comparison; and the standard cloud sample data for Np^{239}, as well as those derived from the estimated device fission yields for Ba^{140} and Sr^{89}, are included in the latter.

It is interesting to note that these results not only establish that marked differences exist between the two types of particles, but also show the altered particles to be depleted in both Ba^{140}-La^{140} and Sr^{89}, while the unaltered particles are enriched in Ba^{140}-La^{140} and perhaps slightly depleted in Sr^{89}. The altered particles are also seen to be about a factor of 100 higher than the unaltered in terms of fissions per gram. When these R-values are compared with those obtained from gross fallout samples (Tables 3.17 and 3.21), it is further found that the values for altered particles resemble those for samples from the lagoon area, while the values for the unaltered particles resemble those from cloud samples.

Activity Relationships. All of the particles whose gamma activities and physical properties were measured in the YAG 40 laboratory (Table B.34), as well as several hundred additional particles from the incremental collectors on the other ships and barges, were studied systematically (Reference 30) in an attempt to determine whether the activities of the particles were functionally related to their size. These data are listed in Table B.9 and the results are plotted in Figures 3.22 and 3.23. Possible relationships between particle activity, weight, and density were also considered (Reference 25), using a separate group of approximately 135 particles collected on the YFNB 29 during Shots Zuni and Tewa and the YAG 39 during Shot Tewa only; Figures 3.24 and 3.25 show the results.

As implied by the differences in radiochemical composition discussed in the preceding section, marked differences exist in the gamma-radiation characteristics of the different types of particles. Compared with the variations in decay rate and energy spectrum observed for different particles collected at about the same time on the YAG 40 (Figures B.2, B.3 and B.4), altered particles show large changes relative to unaltered particles. Figures 3.26 and 3.27 from Reference 26 illustrate this point. The former, arbitrarily normalized at 1,000 hours, shows how

well-counter decay rates for the two types of particles deviate on both sides of the interval from 200 to 1,200 hours, and how the same curves fail to coincide, as they should for equivalent radionuclide compositions, when plotted in terms of 10^4 fissions. The latter shows the regions in which the primary radionuclide deficiencies exist.

The previous considerations suggest that particles should be grouped according to type for the study of activity-size relationships.

Figures 3.22 and 3.23 show the results of a study made in this way (Table B.9). A large number of the particles for which size and activity data were obtained in the YAG 40 laboratory during Shots Zuni and Tewa were first grouped according to size (16 groups, about 32 microns wide, from 11 to 528 microns), then subdivided according to type (irregular or angular, spheroidal or spherical, and agglomerated) within each size group. The distribution of activities in each size group and subgroup was considered and it was found that, while no regular distribution was apparent for the size group, the subgroup tended toward normal distribution. Median activities were utilized for both, but maximum and minimum values for the overall size group were included in Table B.9 to show the relative spread. It will be observed that activity range and median activity both increase with size.

Similar results for groups of particles removed from IC trays exposed aboard the YAG 39, LST 611, YFNB 13, and YFNB 29 during Shot Tewa are also included in Table B.9. These have not been plotted or used in the derivation of the final relationships, because the particles were removed from the trays and well-counted between 300 and 600 hours after the shot, and many were so near background that their activities were questionable. (This should not be interpreted to mean that the fallout contained a significant number of inactive particles. Nearly 100 percent of the particles observed in the YAG 40 laboratory during Shots Zuni and Tewa were active.)

In the figures, the median activity of each size group from the two sets of YAG 40 data has been plotted against the mean diameter of the group for the particles as a whole and several of the particle type subgroups. Regression lines have been constructed, using a modified least-squares method with median activities weighted by group frequencies, and 95-percent-confidence bands are shown in every case. Agglomerated particles from Shot Zuni and spheroidal particles from Shot Tewa have not been treated because of the sparsity of the data.

It should also be noted that different measures of diameter have been utilized in the two cases. The particles from both shots were sized under a low-power microscope using eyepiece micrometer disks; a series of sizing circles was used during Shot Zuni, leading to the diameter of the equivalent projected area D_a, while a linear scale was used for Shot Tewa, giving simply the maximum particle diameter D_m. The first method was selected because it could be applied under the working conditions in the YAG 40 laboratory and easily related to the method described in Section 3.2.4 (Figure B.5); the second method was adopted so that more particles could be processed and an upper limit established for size in the development of activity-size relationships.

The equations for the regression lines are given in the figures and summarized as follows: all particles, Shot Zuni, $A \propto D_a^{2.4}$, Shot Tewa, $A \propto D_m^{1.8}$; irregular particles, Shot Zuni, $A \propto D_a^{2.2}$, Shot Tewa, $A \propto D_m^{1.7}$; spheroidal particles, Shot Zuni, $A \propto D_a^{3.7}$; and agglomerated particles, Shot Tewa, $A \propto D_m^{2.1}$.

(Analogous relationships for Tewa particles from the YFNB 29 were derived on the basis of much more limited data in Reference 25, using maximum diameter as the measure of size. These are listed below; error not attributable to the linear regression was estimated at about 200 percent for the first two cases and 400 percent for the last: all particles, $A \propto D_m^{2.01}$; irregular particles, $A \propto D_m^{1.92}$; and spheroidal particles, $A \propto D_m^{3.37}$.)

It may be observed that the activity of the irregular particles varies approximately as the square of the diameter. This is in good agreement with the findings in Reference 23; the radioautographs in Figures 3.14 and 3.17 show the activity to be concentrated largely on the surfaces of the irregular particles. The activity of the spheroidal particles, however, appears to vary as the third or fourth power of the diameter, which could mean either that it is a true function of particle volume or that it diffused into the molten particle in a region of higher activity concentration in the cloud. The thin-section radioautographs suggest the latter to be true, showing the activity to be distributed throughout the volume in some cases (Figure 3.16) but confined to

the surface in others (Figure 3.18). It may also be seen that the overall variation of activity with size is controlled by the irregular particles, which appear to predominate numerically in the fallout (Table B.9), rather than by the spheroidal particles. Table 3.11 illustrates how the activity in each size group was divided among the three particle types.

No correlation of particle activity with density was possible (Figure 3.25) but a rough relationship with weight was derived for a group of Tewa particles from the YFNB 29 on the basis of Figure 3.24: $A \propto W^{0.7}$, where W refers to the weight in micrograms and nonregression error is estimated at ~140 percent (Reference 25). (An additional study was performed at NRDL, using 57 particles from the same source and a more stable microbalance. The resulting relation was: $A \propto W^{0.57}$.) This result is consistent with the diameter functions, because $D^2 \propto W^{2/3}$. The relative activities of the white and yellow spheroidal particles referred to earlier were also compared and the latter were found to be slightly more active than the former.

3.3.2 Slurry Particles. All of the fallout collected during Shots Flathead and Navajo consisted of slurry particles whose inert components were water, sea salts, and a small amount of insoluble solids. (Although IC and SIC trays containing greased disks were interspersed among those containing reagent films for shots, no isolated solid particles that were active were observed.) Large crystals displaying the characteristic cubic shape of sodium chloride were occasionally observed in suspension. The physical and chemical, radiochemical, and radiation characteristics of these particles are discussed below. Table B.35 contains representative sets of data, including data on particles collected on the YAG 40 and at several other stations during each shot.

Physical and Chemical Characteristics. Slurry particles have been studied extensively and are discussed in detail in Reference 31. The results of preliminary studies of the insoluble solids contained in such particles are given in Reference 32. Figure 3.28 is a photomicrograph of a typical deposited slurry droplet, after reaction with the chloride-sensitive reagent film surface. The chloride-reaction area appears as a white disk, while the trace or impression of the impinging drop is egg shaped and encloses the insoluble solids. The concentric rings are thought to be a Liesegang phenomenon. An electronmicrograph of a portion of the solids is shown in Figure 3.29, illustrating the typical dense agglomeration of small spheres and irregular particles.

The physical properties of the droplets were established in part by microscopic examination in the YAG 40 laboratory soon after their arrival, and in part by subsequent measurements and calculations. For example, the dimensions of the droplets that appeared on the greased trays provided a rapid approximation of drop diameter, but the sphere diameters reported in Table 3.12 were calculated from the amount of chloride (reported as NaCl equivalent) and H_2O measured later from the reagent films. It will be noted that particle size decreased very slowly with time; and that for any given time period, size distribution need not be considered, because standard deviations are small. Average densities for the slurry particles, calculated from their dimensions and the masses of NaCl and H_2O present, are also given in Table 3.12.

On the basis of the data in Table 3.12, and a calibration method for solids volume that involved the collection on reagent film of simulated slurry droplets containing aluminum oxide suspensions of appropriate diameter at known concentrations, it was estimated that the particles were about 80 percent NaCl, 18 percent H_2O, and 2 percent insoluble solids by volume. The latter were generally amber in color and appeared under high magnification (Figure 3.29) to be agglomerates composed of irregular and spherical solids ranging in size from about 15 microns to less than 0.1 micron in diameter. The greatest number of these solids were spherical and less than 1 micron in diameter, although a few were observed in the size range from 15 to 60 microns.

Chemical properties were determined by chloride reagent film, X-ray diffraction, and electron diffraction techniques. (The gross chemistry of slurry drops is of course implicit in the analyses of the OCC collections from Shots Flathead and Navajo (Table B.18); no attempt has been made to determine the extent of correlation.) The first featured the use of a gelatin film containing colloidal red silver dichromate, with which the soluble halides deposited on the film

react when dissolved in saturated, hot water vapor. The area of the reaction disk produced, easily measured with a microscope, is proportional to the amount of NaCl present (Reference 33). The values of NaCl mass listed in Table 3.12 were obtained by this method; the values of H_2O mass were obtained by constructing a calibration curve relating the volume of water in the particle at the time of impact to the area of its initial impression, usually well defined by the insoluble solids trace (Figure 3.28). Because the water content of slurry fallout varies with atmospheric conditions at the time of deposition, mass is expressed in terms of the amount of NaCl present; the weight of water may be estimated by multiplying the NaCl mass by 1.2, the average observed factor.

Conventional X-ray diffraction methods were used for qualitative analysis of the insoluble solids, stripped from the reagent film by means of an acrylic spray coating, and they were found to consist of calcium iron oxide ($2\ CaO \cdot Fe_2O_3$), oxides of calcium and iron, and various other compounds (Table 3.13). Some of these were also observed by electron diffraction.

Radiochemical Characteristics. Thirteen of the most-active slurry particles removed from the SIC trays in the YAG 40 laboratory during Shot Flathead were combined (Reference 26), and analyzed radiochemically in much the same way as the solid particles described earlier in Section 3.3.1. The sample was assayed in the gamma well counter (WC) and the 4-π gamma ionization chamber (GIC), then analyzed for Mo^{99}, Ba^{140}-La^{140}, Sr^{89}, and Np^{239}; total fissions, activity ratios, R-values and the product/fission ratio were computed as before. The results are presented in Table 3.14.

It may be seen that the product/fission ratio and $R^{99}(89)$ value are comparable with the values obtained for gross fallout samples (Tables 3.17, 3.18, and 3.21), and that the overall radionuclide composition resembles that of the unaltered solid particles. Slight depletion of both Ba^{140}-La^{140} and Sr^{89} is indicated.

Activity Relationships. Since the mass of slurry-particle fallout was expressed in terms of NaCl mass, it was decided to attempt to express activity relationships in the same terms. This was accomplished in two steps. First, the H+12-hours well-counter activities measured on the IC trays from the majority of the stations listed in Table 3.12 were summed to arrive at the total amounts of activity deposited per unit area (counts per minute per square foot). These values were then divided by the average specific activity calculated for each station (counts per minute per microgram NaCl) to obtain the total amount of NaCl mass deposited per unit area (micrograms NaCl per square foot). Results for Shot Flathead are plotted in Figure 3.30, and numerical values for both shots are tabulated in Table B.11; the Navajo results were not plotted because of insufficient data. (Figure 3.30 and Table B.11 have been corrected for recently discovered errors in the tray activity summations reported in Reference 31.)

While this curve may be used to estimate the amount of activity associated with a given amount of slurry-fallout mass in outlying areas, it must be remembered that the curve is based on average specific activity. It should also be noted that the unusually high values of NaCl mass obtained for the YFNB 29 during Shot Flathead have not been plotted. A correspondingly high value for the YFNB 13 during Shot Navajo appears in the table. These were felt to reflect differences in composition which are not yet well understood.

A preliminary effort was also made to determine the way in which the activity of slurry particles was divided between the soluble and insoluble phases. As illustrated in Figure 3.31, radioautographs of chloride reaction areas on reagent films from all of the Flathead collections and a few of the Navajo shipboard collections indicated that the majority of the activity was associated with the insoluble solids. This result was apparently confirmed when it was found that 84 percent of the total activity was removable by physical stripping of the insoluble solids; however, more careful later studies (private communication from N. H. Farlow, NRDL) designed to establish the amount of activity in solids that could not be stripped from the film, and the amount of dissolved activity in gelatin removed with the strip coating, decreased this value to 65 percent. It must be noted that the stripping process was applied to a Flathead sample from the YAG 40 only, and that solubility experiments on OCC collections from other locations at Shot Navajo (Reference 32) indicated the partition of soluble-insoluble activity may vary with collector location or time of arrival. The latter experiments, performed in duplicate, yielded

average insoluble percentages of 93 and 14 for the YAG 39 (two aliquots) and the YFNB 13 respectively.

While such properties of barge shot fallout as the slurry nature of the droplets, diameters, densities, and individual activities have been adequately measured, it is evident that more extensive experimentation is required to provide the details of composition of the solids, their contribution to the weight of the droplets, and the distribution of activity within the contents of the droplets.

3.3.3 Activity and Fraction of Device. An estimate of the total amount of activity deposited at every major and minor station during each shot is listed in Table 3.15. Values are expressed both as fissions per square foot and fraction of device per square foot for convenience. In the case of the major stations the weighted mean and standard deviation of measurements made on the four OCC's and two AOC_1's on the standard platform are given, while the values tabulated for the minor stations represent single measurements of AOC_2 collections. Basic data for both cases are included in Tables B.12 and B.14. (Tray activities were found to pass through a maximum and minimum separated by about 180 degrees when plotted against angular displacement from a reference direction; ten values at 20-degree intervals between the maximum and minimum were used to compute the mean and standard deviation (Section 4.3.2).)

The number of fissions in one OCC tray from each major station and one standard cloud sample was determined by radiochemical analysis for Mo^{99} after every shot (Reference 34). Because these same trays and samples had previously been counted in the doghouse counter (Section 2.2), the ratio of doghouse counts per minute at 100 hours could then be calculated for each shot and location, as shown in Table B.13, and used to determine the number of fissions in the remaining OCC trays (fissions per 2.60 ft^2, Table B.12). Final fissions per square foot values were converted to fraction of device per square foot by means of the fission yields contained in Table 2.1 and use of the conversion factor 1.45×10^{26} fissions/Mt(fission). (Slight discrepancies may be found to exist in fraction of device values based on Mo^{99}, because only interim yields were available at the time of calculation.)

Aliquots from some of the same OCC trays analyzed radiochemically for Mo^{99} were also measured on the dip counter. Since the number of fissions in the aliquots could be calculated and the fallout from Shots Flathead and Navajo was relatively unfractionated, the total number of fissions in each AOC_2 from these shots could be computed directly from their dip-counter activities using a constant ratio of fissions per dip counts per minute at 100 hours. Table B.14I gives the results.

Shot Zuni, and to a lesser extent Shot Tewa, fallout was severely fractionated, however, and it was necessary first to convert dip-counter activities to doghouse-counter activities, so that the more-extensive relationships between the latter and the fissions in the sample could be utilized. With the aliquot measurements referred to above, an average value of the ratio of doghouse activity per dip-counter activity was computed (Table B.15), and this used to convert all dip counts per minute at 100 hours to doghouse counts per minute at 100 hours (Table B.14II). The most appropriate value of fissions per doghouse counts per minute at 100 hours was then selected for each minor station, on the basis of its location and the time of fallout arrival, and the total number of fissions calculated for the collector area, 0.244 ft^2. Final fission per square foot values were arrived at by normalizing to 1 ft^2, and fraction of device per square foot was computed from the total number of device fissions as before.

Many of the results presented in this report are expressed in terms of 10^4 fissions. For example, all gamma- and beta-decay curves in Section 3.4 (Figures 3.34 to 3.38) are plotted in units of counts per second per 10^4 fissions, and the final ionization rates as a function of time for each shot (Figure 3.39) are given in terms of roentgens per hour per 10^4 fissions per square foot. Thus, the estimates in Table 3.15 are all that is required to calculate the radiation intensities which would have been observed at each station under ideal conditions any time after the cessation of fallout. It should be noted, however, that the effects of sampling bias have not been entirely eliminated from the tabulated values and, consequently, will be reflected in any quantity determined by means of them. Even though the use of weighted-mean collector values for the

major stations constitutes an adjustment for relative platform bias, the question remains as to what percent of the total number of fissions per unit area, which would have been deposited in the absence of the collector, were actually collected by it. This question is considered in detail in Section 4.3.2.

3.3.4 Chemical Composition and Surface Density. The total mass of the fallout collected per unit area at each of the major stations is summarized for all four shots in Table 3.16. Results are further divided into the amounts of coral and sea water making up the totals, on the assumption that all other components in the device complex contributed negligible mass. These values were obtained by conventional quantitative chemical analysis of one or more of the OCC tray collections from each station for calcium, sodium, chlorine, potassium, and magnesium (References 35 through 38); in addition analyses were made for iron, copper and uranium (private communication from C. M. Callahan and J. R. Lai, NRDL). The basic chemical results are presented in Tables B.16 and B.18. (Analyses were also attempted for aluminum and lead; possibly because of background screening, however, they were quite erratic and have not been included.)

The chemical analysis was somewhat complicated by the presence in the collections of a relatively large amount of debris from the fiberglass honeycomb (or hexcell) inserts, which had to be cut to collector depth and continued to spall even after several removals of the excess material. It was necessary, therefore, to subtract the weight of the fiberglass present in the samples in order to arrive at their gross weights (Table B.18I). The weight of the fiberglass was determined in each case by dissolving the sample in hydrochloric acid to release the carbonate, filtering the resultant solution, and weighing the insoluble residue. In addition, the soluble portion of the resin binder was analyzed for the elements listed above and subtracted out as hexcell contribution to arrive at the gross amounts shown (References 39 and 40). Aliquots of the solution were then used for the subsequent analyses.

It was also necessary to subtract the amount of mass accumulated as normal background. These values were obtained by weighing and analyzing samples from a number of OCC trays which were known to have collected no fallout, although exposed during the fallout period. Many of the trays from Shot Cherokee, as well as a number of inactive trays from other shots, were used; and separate mean weights with standard deviations were computed for each of the elements under ocean and land collection conditions (Tables B.16 and B.18).

After the net amount of each element due to fallout was determined, the amounts of original coral and sea water given in Table 3.16 could be readily computed with the aid of the source compositions shown in Table B.16. In most cases, coral was determined by calcium; however, where the sea water/coral ratio was high, as for the barge shots, the sea water contribution to the observed calcium was accounted for by successive approximation. Departure from zero of the residual weights of the coral and sea water components shown in Table B.18 reflect combined errors in analyses and compositions. It should be noted that all ± values given in these data represent only the standard deviation of the background collections, as propagated through the successive subtractions. In the case of Shot Zuni, two OCC trays from each platform were analyzed several months apart, with considerable variation resulting. It is not known whether collection bias, aging, or inherent analytical variability is chiefly responsible for these discrepancies.

The principal components of the device and its immediate surroundings, exclusive of the naturally occurring coral and sea water, are listed in Table B.17. The quantities of iron, copper and uranium in the net fallout are shown in Table B.18I to have come almost entirely from this source. Certain aliquots from the OCC trays used for radiochemical analysis were also analyzed independently for these three elements (Table B.18II). These data, when combined with the tabulated device complex information, allow computation of fraction of device; the calculations have been carried out in Section 4.3.4 for uranium and iron and compared with those based on Mo^{99}.

3.4 RADIONUCLIDE COMPOSITION AND RADIATION CHARACTERISTICS

3.4.1 Approach. If the identity, decay scheme, and disintegration rate of every nuclide in

a sample are known, then all emitted particle or photon properties of the mixture can be computed. If, in addition, calibrated radiation detectors are available, then the effects of the sample emissions in those instruments may also be computed and compared with experiment. Finally, air-ionization or dose rates may be derived for this mixture under specified geometrical conditions and concentrations.

In the calculations to follow, quantity of sample is expressed in time-invariant fissions, i.e., the number of device fissions responsible for the gross activity observed; diagnostically, the quantity is based on radiochemically assayed Mo^{99} and a fission yield of 6.1 percent. This nuclide, therefore, becomes the fission indicator for any device and any fallout or cloud sample. The computation for slow-neutron fission of U^{235}, as given in Reference 41, is taken as the reference fission model; hence, any $R^{99}(x)$ values in the samples differing from unity, aside from experimental uncertainty, represent the combined effects of fission kind and fractionation, and necessitate modification of the reference model if it is to be used as a basis for computing radiation properties of other fission-product compositions. (An R-value may be defined as the ratio of the amount of nuclide x observed to the amount expected for a given number of reference fissions. The notation $R^{99}(x)$ means the R-value of mass number x referred to mass number 99.)

Two laboratory instruments are considered: the doghouse counter employing a 1-inch-diameter-by-1-inch-thick NaI(Tl) crystal detector, and the continuous-flow proportional beta counter (Section 2.2). The first was selected because the decay rates of many intact OCC collections and all cloud samples were measured in this instrument; the second, because of the desirability of checking calculated decay rates independent of gamma-ray decay schemes. Although decay data were obtained on the 4-π gamma ionization chamber, response curves (Reference 42) were not included in the calculations. However, the calculations made in this section are generally consistent with the data presented in Reference 42. The data obtained are listed in Table B.26.

3.4.2 Activities and Decay Schemes. The activities or disintegration rates of fission products for 10^4 fissions were taken from Reference 41; the disintegration rates are used where a radioactive disintegration is any spontaneous change in a nuclide. Other kinds of activities are qualified, e.g., beta activity. (See Section 3.4.4.) Those of induced products of interest were computed for 10^4 fissions and a product/fission ratio of 1, that is, for 10^4 initial atoms (Reference 43).

Prepublication results of a study of the most-important remaining nuclear constants—the decay schemes of these nuclides—are contained in References 42 and 44. The proposed schemes, which provide gamma and X-ray photon energies and frequencies per disintegration, include all fission products known up to as early as ~45 minutes, as well as most of the induced products required. All of the following calculations are, therefore, limited to the starting time mentioned and are arbitrarily terminated at 301 days.

3.4.3 Instrument Response and Air-Ionization Factors. A theoretical response curve for the doghouse counter, based on a few calibrating nuclides, led to the expected counts/disintegration of each fission and induced product as a function of time, for a point-source geometry and 10^4 fissions or initial atoms (Reference 43). The condensed decay schemes of the remaining induced nuclides were also included. To save time, the photons emitted from each nuclide were sorted into standardized energy increments, 21 of equal logarithmic width comprising the scale from 20 kev to 3.25 Mev. The response was actually computed for the average energy of each increment, which in general led to errors no greater than ~10 percent.

Counting rates expected in the beta counter were obtained from application of the physical-geometry factor to the theoretical total-beta and positron activity of the sample. With a response curve essentially flat to beta E_{max} over a reasonably wide range of energies, it was not necessary to derive the response to each nuclide and sum for the total. Because the samples were essentially weightless point sources, supported and covered by 0.80 mg/cm^2 of pliofilm, scattering and absorption corrections were not made to the observed count rates; nor were gamma-ray contributions subtracted out. Because many of the detailed corrections are self-

canceling, it is assumed the results are correct to within ~20 percent. The geometries (or counts/beta) for Shelves 1 through 5 are given in Section A.2.

Air-ionization rates 3 feet above an infinite uniformly contaminated plane, hereafter referred to as standard conditions (SC), are based on the curve shown in Figure B.6, which was originally obtained in another form in Reference 7. The particular form shown here, differing mainly in choice of parameters and units, has been published in Reference 45. Points computed in Reference 46 and values extracted from Reference 47 are also shown for comparison. The latter values are low, because air scattering is neglected.

The ionization rate (SC) produced by each fission-product nuclide as a function of time for 10^4 reference fissions/ft^2 (Reference 17), was computed on a line-by-line basis; the induced products appear in Table B.19 for 10^4 fissions/ft^2 and a product/fission ratio of 1, with lines grouped as described for the doghouse-counter-response calculations.

The foregoing sections provide all of the background information necessary to obtain the objectives listed in the first paragraph of Section 3.4.1, with the exception of the actual radionuclide composition of the samples. The following sections deal with the available data and methods used to approximate the complete composition.

3.4.4 Observed Radionuclide Composition. Radiochemical R-values of fission products are given in Table 3.17 and observed actinide product/fission ratios appear in Table 3.18, the two tables summarizing most of the radiochemistry done by the Nuclear and Physical Chemistry, and Analytical and Standards Branches, NRDL (Reference 34).

The radiochemical results in Reference 34 are expressed as device fractions, using fission yields estimated for the particular device types. These have been converted to R-values by use of the equation:

$$R_{\theta}^{99}(x) = \frac{FOD_E(x)}{FOD(99)} \cdot \frac{FY_E(x)}{FY_{\theta}(x)}$$

Where $R_{\theta}^{99}(x)$ is the R-value of nuclide x relative to Mo^{99}; $FOD_E(x)$ and $FY_E(x)$ are respectively the device fraction and estimated yield of nuclide x reported in Reference 34, $FY_{\theta}(x)$ is the thermal yield of nuclide x, and FOD(99) is the device fraction by Mo^{99}. The thermal yields used in making this correction were taken from ORNL 1793 and are as follows: Zr^{95}, 6.4 percent; Te^{132}, 4.4 percent; Sr^{89}, 4.8 percent; Sr^{90}, 5.9 percent; Cs^{137}, 5.9 percent; and Ce^{144}, 6.1 percent. The yield of Mo^{99} was taken as 6.1 percent in all cases. The R-values for all cloud-sample nuclides were obtained in that form directly from the authors of Reference 34.

Published radiochemical procedures were followed (References 48 through 54), except for modifications of the strontium procedure, and consisted of two $Fe(OH)_3$ and $BaCrO_4$ scavenges and one extra $Sr(NO_3)_2$ precipitation with the final mounting as $SrCO_3$. Table 3.19 lists principally product/fission ratios of induced activities other than actinides for cloud samples; sources are referenced in the table footnotes.

Supplementary information on product/fission ratios in fallout and cloud samples was obtained from gamma-ray spectrometry (Tables B.20 and B.21) and appears in Table 3.20.

3.4.5 Fission-Product-Fractionation Corrections. Inspection of Tables 3.17 through 3.20, as well as the various doghouse-counter and ion-chamber decay curves, led to the conclusion that the radionuclide compositions of Shots Flathead and Navajo could be treated as essentially unfractionated. It also appeared that Shots Zuni and Tewa, whose radionuclide compositions seemed to vary continuously from lagoon to cloud, and probably within the cloud, might be covered by two compositions: one for the close-in lagoon area, and one for the more-distant ship and cloud samples. The various compositions are presented as developed, starting with the simplest. The general method and supporting data are given, followed by the results.

Shots Flathead and Navajo. Where fission products are not fractionated, that is, where the observed $R^{99}(x)$ values are reasonably close to 1 (possible large R-values among low-yield valley and right-wing mass numbers are ignored), gross fission-product properties may

be readily extracted from the sources cited. Induced product contributions may be added in after diminishing the tabular values (product/fission = 1) by the proper ratio. After the resultant computed doghouse-counter decay rate is compared with experiment, the ionization rate (SC) may be computed for the same composition. Beta activities may also be computed for this composition—making allowance for those disintegrations that produce no beta particles. The Navajo composition was computed in this manner, as were the rest of the compositions, once fractionation corrections had been made.

Shot Zuni. A number of empirical corrections were made to the computations for unfractionated fission products in an effort to explain the decay characteristics of the residual radiations from this shot. The lagoon-area composition was developed first, averaging available lagoon area R-values. As shown in Figure 3.32, R-values of nuclides which, in part at least, are decay products of antimony are plotted against the half life of the antimony precursor, using the fission-product decay chains tabulated in Reference 56. (Some justification for the assumptions are made that, after ~45 minutes, the R-values of all members of a given chain are identical, and related to the half life of the antimony precursor, then Figure 3.32 may be used to estimate R-values of other chains containing antimony precursors with different half lives. The R-value so obtained for each chain is then used as a correction factor on the activity (Reference 41) of each nuclide in that chain, or more directly, on the computed doghouse activity or ionization (SC) contribution (Table 3.21). The partial decay products of two other fractionating precursors, xenon and krypton, are also shown in Figure 3.32, and are similarly employed. These deficiencies led to corrections in some 22 chains, embracing 54 nuclides that contributed to the activities under consideration at some time during the period of interest. The R-value of I^{131} was taken as 0.03; a locally measured but otherwise unreported I^{133}/I^{131} ratio of 5.4 yields an I^{133} R-value of 0.16.

Although the particulate cloud composition might have been developed similarly, using a different set of curves based on cloud R-values, it was noticed that a fair relation existed between cloud and lagoon nuclide R-values as shown in Figure 3.33. Here $R^{99}(x)$ cloud/$R^{99}(x)$ lagoon is plotted versus $R^{99}(x)$ lagoon average. The previously determined lagoon chain R-values were then simply multiplied by the indicated ratio to obtain the corresponding cloud R-values. The dotted lines indicate the trends for two other locations, YAG 39 and YAG 40, although these were not pursued because of time limitations. It is assumed that the cloud and lagoon compositions represent extremes, with all others intermediate. No beta activities were computed for this shot.

Shot Tewa. Two simplifying approximations were made. First, the cloud and outer station average R-values were judged sufficiently close to 1 to permit use of unfractionated fission products. Second, because the lagoon-area fission-product composition for Shot Tewa appeared to be the same as for its Zuni counterpart except in mass 140, the Zuni and Tewa lagoon fission products were therefore judged to be identical, except that the Ba^{140}-La^{140} contribution was increased by a factor of 3 for the latter.

The induced products were added in, using product/fission ratios appropriate to the location wherever possible; however, the sparsity of ratio data for fallout samples dictated the use of cloud values for most of the minor induced activities.

3.4.6 Results and Discussion. Table B.22 is a compilation of the computed doghouse counting rates for the compositions described; these data and some observed decay rates are shown in Figures 3.34 through 3.37. All experimental doghouse-counter data is listed in Table B.23. Table B.24 similarly summarizes the Flathead and Navajo computed beta-counting rates; they are compared with experiment in Figure 3.38, and the experimental data are given in Table B.25. Results of the gamma-ionization or dose rate (SC) calculations for a surface concentration of 10^4 fissions/ft^2 are presented in Table 3.22 and plotted in Figure 3.39. It should be emphasized that these computed results are intended to be absolute for a specified composition

and number of fissions as determined by Mo^{99} content, and no arbitrary normalization has been employed to match theory and experiment. Thus, the curves in Figure 3.39, for instance, represent the best available estimates of the SC dose rate produced by 10^4 fissions/ft^2 of the various mixtures. The Mo^{99} content of each of the samples represented is identical, namely the number corresponding to 10^4 fissions at a yield of 6.1 percent. The curves are displaced vertically from one another solely because of the fractionation of the other fission products with respect to Mo^{99}, and the contributions of various kinds and amounts of induced products.

It may be seen that the computed and observed doghouse-counter decay rates are in fairly good agreement over the time period for which data could be obtained. The beta-decay curves for Shots Flathead and Navajo, initiated on the YAG 40, suggest that the computed gamma and ionization curves, for those events at least, are reasonably correct as early as 10 to 15 hours after detonation.

The ionization results may not be checked directly against experiment; it was primarily for this reason that the other effects of the proposed compositions were computed for laboratory instruments. If reasonable agreement can be obtained for different types of laboratory detectors, then the inference is that discrepancies between computed and measured ionization rates in the field are due to factors other than source composition and ground-surface fission concentration.

The cleared area surrounding Station F at How Island (Figure 2.8) offers the closest approximation to the standard conditions for which the calculations were made, and Shot Zuni was the only event from which sufficient fallout was obtained at this station to warrant making a comparison. With the calculated dose rates based on the average buried-tray value of $2.08 \pm 0.22 \times 10^{14}$ fissions/ft^2 (Table B.27) and the measured rates from Table B.28, (plotted in Figure B.7), the observed/calculated ratio varies from 0.45 at 11.2 hours to 0.66 from 100 to 200 hours, falling to an average of 0.56 between 370 and 1,000 hours. Although detailed reconciliation of theory and experiment is beyond the scope of this report, some of the factors operating to lower the ratio from an ideal value of unity were: (1) the cleared area was actually somewhat less than infinite in extent, averaging ~120 feet in radius, with the bulldozed sand and brush ringing the area in a horseshoe-shaped embankment some 7 feet high; (2) the plane was not mathematically smooth; and (3) the survey instruments used indicate less than the true ionization rate, i.e., the integrated response factor, including an operator, is lower than that obtained for Co^{60} in the calibrating direction.

It is estimated that, for average energies from 0.15 Mev to 1.2 Mev, a cleared radius of 120 feet provides from ~0.80 to ~0.70 of an infinite field (Reference 46). The Cutie Pie survey meter response, similar to the T1B between 100 kev and 1 Mev, averages about 0.85 (Reference 17). These two factors alone, then, could depress the observed/calculated ratio to ~0.64.

TABLE 3.1 TIMES OF ARRIVAL, PEAK ACTIVITY, AND CESSATION AT MAJOR STATIONS

Time of arrival (t_a) indicates the earliest reliable arrival time of fallout as determined from the incremental collector and gamma time-intensity recorder results. Time of peak activity (t_p) indicates the time of peak ionization rate (in parentheses) and the times during which the ionization rate was within 10 percent of the peak rate. I_p refers to the peak ionization rate. Time of cessation (t_c) indicates, first, the time by which 95 percent of the fallout had been deposited and, next, the extrapolated time of cessation.

Shot	Station	t_a	t_p			I_p	t_c
		TSD, hr	TSD, hr			r/hr	TSD, hr
Flathead	YAG 40 (A, B)	8.0	12	(17.0)	20	0.259	22 to 23
	YAG 39 (C)	4.5	10	(11.0)	13	0.141	13 to 15
	LST 611 (D)	6.6	9.0	(9.1)	9.2	0.098	20 to 25
	YFNB 13 (E)	0.35	1.1	(1.3)	1.5 *	21.8 *	2.0 to †
	YFNB 29 (G, H)	0.62	1.2	(1.52)	1.9	0.98	1.5 to 9.0
	How Island (F)	‡		‡		‡	‡
Navajo	YAG 40 (A, B)	6.0	11	(12.3)	13	0.129	16 to 20
	YAG 39 (C)	2.3	5.9	(6.0)	6.2	1.49	15 to 16
	LST 611 (D)	3.0	5.6	(6.1)	6.7	0.043	13 to 18
	YFNB 13 (E)	0.20	0.58	(0.63)	0.73	8.5	1.9 to 9.0 §
	YFNB 29 (G, H)	0.68	1.2	(1.33)	1.9	0.116	3.2 to 14 §
	How Island (F)	0.75		¶		¶	4.5 to 7.0 §
Zuni	YAG 40 (A, B)	3.4	6.2	(6.7)	7.7	7.6	7.4 to 13
	YAG 39 (C)	12	20	(25)	33	0.038	29 to 33
	LST 611 (D)	‡		‡		‡	‡
	YFNB 13 (E)	0.33	0.97	(1.25)	1.6 *	6 *	1.9 to 9.3
	YFNB 29 (G, H)	0.32	0.70	(0.82)	1.2	9.6	2.4 to 3.3
	How Island (F)	0.38	0.98	(1.05)	1.4	2.9	1.9 to 2.6
Tewa	YAG 40 (A, B)	4.4	6.2	(7.2)	7.6	7.43	8.5 to 16
	YAG 39 (C)	2.0	4.4	(5.0)	5.7	20.2	5.3 to 16
	LST 611 (D)	7.0	13	(13.6)	15	0.256	14 to 18
	YFNB 13 (E)	0.25	1.8	(1.9)	3.0	2.5	7.0 to 16
	YFNB 29 (G, H)	0.23	1.4	(1.7)	2.8 *	40 *	4.3 to 16
	How Island (F)	1.6	2.5	(2.9)	3.4	2.5	3.3 to 9.0

* Estimated value; gamma time-intensity recorder saturated.
† No determination possible; incremental collector failed.
‡ No fallout occurred.
§ Minimum value.
¶ Instrument failed.

IN THE ATOLL AREA

Time of arrival (t_a) indicates the arrival time of fallout as determined from the time of arrival detector results.

Station	Shot Flathead t_a	Shot Navajo t_a	Shot Zuni t_a	Shot Tewa t_a
	TSD, hr	TSD, hr	TSD, hr	TSD, hr
YFNB 13 (E)	*	*	†	*
YFNB 29 (G)	0.77	*	0.40	*
YFNB 29 (H)	0.68	*	0.40	*
How Island (F)	‡	*	0.35	*
How Island (K)	‡	*	0.40 §	*
George Island (L)	0.02 †	†	0.33	†
Charlie Island (M)	—	†	—	†
William Island (M)	‡	—	0.22	—
Raft-1 (P)	‡	‡	0.33	†
Raft-2 (R)	†	0.73	†	†
Raft-3 (S)	0.5	0.05 †	0.23	0.48
Skiff-AA	9.1 ¶	9.4	*	5.0
Skiff-BB	†	†	3.8 §	†
Skiff-CC	4.7	‡	*	4.2
Skiff-DD	‡	‡	*	‡
Skiff-EE	‡	‡	3.0 §	‡
Skiff-FF	‡	‡	†	‡
Skiff-GG	*	*	2.0 §	2.9 §
Skiff-HH	†	†	†	2.2
Skiff-KK	‡	†	*	‡
Skiff-LL	‡	‡	†	‡
Skiff-MM	*	4.3	2.9	2.0
Skiff-PP	†	1.4	*	†
Skiff-RR	4.1	†	1.7	†
Skiff-SS	10.6	—	†	—
Skiff-TT	‡	‡	†	‡
Skiff-UU	‡	—	†	—
Skiff-VV	—	—	*	—
Skiff-WW	—	—	—	†
Skiff-XX	—	—	—	1.2 §
Skiff-YY	—	—	—	†

* Skiff or instrument lost, or no instrument present.
† Instrument malfunctioned or may have malfunctioned.
‡ Activity level insufficient to trigger instrument; no fallout or only light fallout occurred.
§ Estimated value; clock reading corrected by ± an integral number of days.
¶ Instrument may have triggered at peak; low arrival rate.

TABLE 3.3 PENETRATION RATES DERIVED FROM EQUIVALENT-DEPTH DETERMINATIONS

Shot	Station	Number of Points	Time Studied From	Time Studied To	Rate	± Limits 95 pct Confidence
			TSD, hr		m/hr	m/hr
Flathead	YAG 39	10	8.3	12.8	3.0	2.5
Navajo	YAG 39	10	7.4	18.6	2.6	0.2
Navajo	YAG 40	4	10.0	13.0	4.0	2.1
Tewa	YAG 39	26	5.1	14.8	3.0	0.7
Tewa	YAG 40	5	5.2	8.1	4.0	2.9

TABLE 3.4 DEPTHS AT WHICH PENETRATION CEASED FROM EQUIVALENT-DEPTH DETERMINATIONS

Shot	Station	Number of Points	Time Studied From	Time Studied To	Depth	± Limits 95 pct Confidence	Estimated Thermocline Depth *
			TSD, hr		meters	meters	meters
Navajo	YAG 39	13	30.9	40.1	62	15	40 to 60
Tewa	YAG 39	17	15.3	20.5	49	10	40 to 60
			31.8	34.8			

* See Reference 15.

TABLE 3.5 MAXIMUM PENETRATION RATES OBSERVED

Shot	Station	Number of Points	Time Studied From	Time Studied To	Rate	± Limits 95 pct Confidence
			TSD, hr		m/hr	m/hr
Zuni	YAG 39	3	15.2	16.8	~30	—
		9	17.8	29.8	2.4	0.9
Navajo	YAG 39	5	3.1	5.2	23.0	9.8
Tewa	YAG 39	2	3.8	4.1	~300	—

TABLE 3.6 EXPONENT VALUES FOR PROBE DECAY MEASUREMENTS

The tabulated numbers are values of n in the expression: $A = A_0 (t/t_0)^n$, where A indicates the activity at a reference time, t, and A_0 the activity at the time of observation, t_0.

Shot	Exponent Values	
	Project 2.63	Project 2.62a
Zuni	0.90	1.13
Flathead	0.90	1.05
Navajo	1.39	1.39
Tewa	*	1.34

* Instrument malfunctioned.

TABLE 3.7 X-RAY DIFFRACTION ANALYSES AND SPECIFIC ACTIVITIES OF INDIVIDUAL PARTICLES, SHOT ZUNI

Serial Number	Type	Size	Activity at H + 240 hrs	Net Weight	Specific Activity	Compounds Present			Particle Description
						$CaCO_3$	CaO	$Ca(OH)_2$	
		mm	well counts/min	mg	(counts/min)/mg				
165	Sphere	2	17,500,000	6.9	2,540,000	X	X	X	Creamy-white; surface protuberances.
166	Sphere	2	36,500,000	17.3	2,110,000	X	XX*	XX	White, off-white; green-yellow; patchy.
167	Irregular	†	2,410,000	40.1	60,200	X			Rubbery; fibrous; shapeless.
168	Sphere	2	36,200,000	8.7	4,160,000	X	X	X	Pale yellow; white patches.
169	Irregular	2 × 2.5	101,140	11.9	8,500	XX			Resembles actual coral; easily fractured.
170	Irregular	2 × 6	955,340	†	†	X		X	Columnar structure.
171	Agglomerate	†	6,300,000	†	†		X	X	Broken; extremely friable.
172	Agglomerate	†	16,700,000	†	†	X	X	X	Broken; white and pale yellow-green; friable.
173	Irregular	2.5 × 5.0	2,200,000	11.4	193,000	XX		XX	Cavities and tunnels throughout.
174	Sphere	2.1	24,500,000	7.1	3,450,000	X	X	X	Off-white; slightly ellipsoidal.
175	Sphere	†	9,100,000	2.5	3,640,000		X	X	Clear cubic and yellowish irregular crystals.
176	Irregular	2 × 5	443,620	48.8	9,070	XX			Gray mass with embedded shells.
177	Agglomerate	†	2,600,000	†	†		X	X	Broken; white and pale green; very friable.
178	Irregular	8 × 8	1,900,000	388.0	4,900	X		X	Manmade, concretelike material.
179	Sphere	1.5	6,600,000	5.1	1,300,000	X	XX	XX	Yellowish mosaic surface.
180	Irregular	6 × 10	1,860,000	457.3	4,070	X		X	Same as Particle 178.
181	Irregular	2.5 × 4	27,300,000	25.8	1,060,000	X	XX	XX	Yellowish; finer-grained CaO.
182	Black sphere	1.7	70,600	9.0	7,840				$Fe_3O_4 + Fe_2O_3 \cdot H_2O$

* Examination was also made of interior of particle; XX indicates a compound detected both on exterior surface and interior.
† No data available.

TABLE 3.8 DISTRIBUTION OF PARTICLE DENSITIES, SHOT ZUNI

Total number of particles = 122. Total number of irregular particles = 7. Total number of yellow spheres = 71. Total number of white spheres = 44. Mean density of all spheres = 2.46 gm/cm^3. Mean density of yellow spheres = 2.53 gm/cm^3. Mean density of white spheres = 2.33 gm/cm^3.

Density	Percentage of Total Particles	Percentage of Yellow Spheres	Percentage of White Spheres
gm/cm^3			
2.0	2.5	1.4	4.7
2.1	6.7	2.8	11.6
2.2	7.5	2.8	16.3
2.3	22.5	14.0	35.0
2.4	9.2	9.9	9.1
2.5	10.7	8.5	13.9
2.6	15.0	22.6	4.7
2.7	19.2	29.6	4.7
2.8	5.8	8.5	2.3

TABLE 3.9 RADIOCHEMICAL PROPERTIES OF ALTERED AND UNALTERED PARTICLES, SHOT ZUNI

Quantity	Time	Altered Particles		Unaltered Particles	
		Number of Samples	Value	Number of Samples	Value
	TSD, hr				
fissions/gm ($\times 10^{14}$)	—	6	3.8 ± 3.1	9	0.090 ± 0.12
fissions/gm ($\times 10^{14}$) *	—	14	4.2 ± 2.7	24	0.033 ± 0.035
(counts/min)/10^4 fissions	71	4	0.34 ± 0.06	4	0.53 ± 0.19
(counts/min)/10^4 fissions	105	3	0.35 ± 0.08	7	1.1 ± 0.4
(counts/min)/10^4 fissions	239	1	0.054	1	0.12
(counts/min)/10^4 fissions	532	2	0.013	1	0.024
ma/10^4 fissions ($\times 10^{-17}$)	71	4	30 ± 5	4	59 ± 24
ma/10^4 fissions ($\times 10^{-17}$)	105	3	24 ± 7	7	109 ± 31
ma/10^4 fissions ($\times 10^{-17}$)	239	1	3.4	1	20
ma/10^4 fissions ($\times 10^{-17}$)	481	2	1.7	1	5.1
(counts/min)/ma ($\times 10^{14}$)	71	5	11 ± 1	4	9.3 ± 2.0
(counts/min)/ma ($\times 10^{14}$)	105	4	14 ± 3	13	8.6 ± 1.5
(counts/min)/ma ($\times 10^{14}$)	239	10	16 ± 2	6	8.2 ± 1.3

* Calculated from activity ratios on the basis of particles analyzed for total fissions.

TABLE 3.10 ACTIVITY RATIOS FOR PARTICLES FROM SHOTS ZUNI AND TEWA

Activity Ratio	Shot Zuni				Shot Tewa	
	Altered Particles		Unaltered Particles		All Particles	
	Value	Time	Value	Time	Value	Time
		TSD, hr		TSD, hr		TSD, hr
(counts/min)/ma ($\times 10^{14}$)	14. ± 3.	105	8.6 ± 1.5	105	11. ± 6.	96
	16. ± 2.	239	8.2 ± 1.3	239		
(counts/min)/10^4 fissions	0.35 ± 0.08	105	1.1 ± 0.4	105	0.38 ± 0.12	97
	0.054	239	0.12	239	0.18 ± 0.02	172
ma/10^4 fissions ($\times 10^{-17}$)	24. ± 7.	105	109. ± 31.	105	37. ± 15.	97
	3.4	239	20.	239		

TABLE 3.11 DISTRIBUTION OF ACTIVITY OF YAG 40 TEWA PARTICLES WITH SIZE AND TYPE

Size Group	Percent of Composite Total Activity	Percent of Size Group Activity		
		Irregular	Spheroidal	Agglomerated
microns				
16 to 33	<0.1	23.4	76.6	0.0
34 to 66	2.2	88.1	5.0	6.9
67 to 99	6.0	46.4	37.5	16.0
100 to 132	11.6	68.6	6.7	24.6
133 to 165	18.2	43.4	5.7	50.9
166 to 198	18.9	49.3	1.9	48.8
199 to 231	8.1	58.0	0.0	41.9
232 to 264	9.9	14.7	0.0	85.3
265 to 297	7.0	14.6	0.1	85.3
298 to 330	11.5	18.5	0.0	81.4
331 to 363	0.7	—	—	100.0
364 to 396	1.7	0.0	2.2	97.7
397 to 429	—	—	—	—
430 to 462	0.6	23.8	76.2	0.0
463 to 495	—	—	—	—
496 to 528	3.4	100.0	0.0	0.0

TABLE 3.12 PHYSICAL, CHEMICAL, AND RADIOLOGICAL PROPERTIES OF SLURRY PARTICLES

All indicated errors are standard deviations of the mean.

Time of Arrival Interval	Station	Number of Particles Measured	Average NaCl Mass	Average H_2O Mass	Average Density ± Standard Deviation	Average Diameter* ± Standard Deviation	Average Specific Activity ± Standard Deviation
TSD, hr			μg	μg	gm/cm^3	microns	$\times 10^{10}$ (counts/min)/gm†
Shot Flathead:							
1 to 3	YFNB 29	4 to 10	0.06	0.08	1.28 ± 0.1	57 ± 6	43 ± 8‡
7 to 9	YAG 39 and LST 611	50 to 52	0.42	0.62	1.29 ± 0.01	112 ± 2	282 ± 20
11 to 12	YAG 40	10	0.94	1.20	1.35 ± 0.05	129 ± 16	285 ± 160
15 to 18	YAG 40	3 to 4	0.50	0.69	1.34 ± 0.08	121 ± 6	265 ± 90
Totals		67 to 76			1.30 ± 0.01		282 ± 30§
Shot Navajo:							
1 to 3	YFNB 13	5 to 20	7.77	7.94	1.38 ± 0.04	272 ± 14	4 ± 0.6‡
3 to 5	YAG 39	9 to 14	7.62	4.49	1.50 ± 0.01	229 ± 24	16 ± 3
5 to 6	LST 611	14	1.61	1.83	1.41 ± 0.04	166 ± 6	14 ± 2
7 to 9	YAG 40	4 to 10	1.25	1.08	1.45 ± 0.04	142 ± 22	9 ± 3
9 to 10	YAG 40	5 to 23	0.44	0.60	1.31 ± 0.02	110 ± 5	11 ± 2
10 to 11	YAG 40	11 to 15	0.66	0.50	1.43 ± 0.03	111 ± 4	16 ± 4
11 to 12	YAG 40	33	0.30	0.44	1.32 ± 0.01	94 ± 4	26¶
12 to 13	YAG 40	28	0.31	0.31	1.37 ± 0.01	96 ± 2	21¶
13 to 14	YAG 40	6	0.17	0.27	1.28 ± 0.02	86 ± 7	29¶
14 to 15	YAG 40	5	0.10	0.18	1.30 ± 0.03	75 ± 2	23¶
15 to 18	YAG 40	13 to 14	0.06	0.32	1.15 ± 0.02	84 ± 4	56 ± 7
Totals		133 to 182			1.35 ± 0.01		21 ± 3§

* Diameter of spherical slurry droplet at time of arrival.

† Photon count in well counter at H + 12.

‡ Not included in calculation of total.

§ Based on summation of individual-particle specific activities.

¶ Calculated value based on total tray count, number of particles per tray, and average NaCl mass per particle; not included in calculation of total.

TABLE 3.13 COMPOUNDS IDENTIFIED IN SLURRY-PARTICLE INSOLUBLE SOLIDS

All compounds were identified by X-ray diffraction except Fe_2O_3 and $NaCa(SiO_4)$, which were identified by electron diffraction; $2CaO \cdot Fe_2O_3$ was also observed in one sample by electron diffraction. The presence of Cu in the Navajo sample was established by X-ray diffraction. I indicates definite identification and PI possible identification.

Compound	Shot Flathead	Shot Navajo
$2CaO \cdot Fe_2O_3$	I	
$CaCO_3$	I	I
Fe_2O_3	I	
Fe_3O_4	I	I
$CaSO_4 \cdot 2H_2O$	I	
NaCl	I	I
$NaCa(SiO_4)$		PI
SiO_2		PI
$MgO \cdot Fe_2O_3$		PI

TABLE 3.14 RADIOCHEMICAL PROPERTIES OF SLURRY PARTICLES, YAG 40, SHOT FLATHEAD

Analysis of the combined particles led to the following data: Description, essentially NaCl; WC, 0.872×10^6 counts/min; time of WC, 156 TSD, hrs; GIC, 88×10^{-11} ma; time of GIC, 196 TSD, hrs; fissions, 6.83×10^{10}; Ba^{140} Sr^{89}; Np^{239} product/fission ratio, 0.41; activity ratios at 196 TSD, hrs, 9.9×10^{14} (counts/min)/ma, 0.13 (counts/min)/10^4 fissions, and 13.0×10^{-17} ma/10^4 fissions.

Field Number	WC	Time of WC
	$\times 10^6$ counts/min	TSD, hrs
2680-1	0.0668	189
2682-2	0.116	190
2334-1	0.0730	190
2677-1	0.0449	193
2333-1	0.131	190
2682-1	0.0607	189
2331-1	0.249	189
2333-2	0.064	191
2334-4	0.146	190
2333-3	0.0487	190
2332-1	0.0295	190
2681-3	0.235	190
2681-1	0.141	190

TABLE 3.16 SURFACE DENSITY OF FALLOUT COMPONENTS IN TERMS OF ORIGINAL COMPOSITION

Shot	Collector	Weight, mg/ft²		
		Coral	Sea Water	Total
Flathead	YAG 40-B-19 FL	14.0 ± 1.0	195.2 ± 16.2	209.2 ± 16.2
	LST 611-D-51 FL	0.0 ± 1.0	89.2 ± 16.2	89.2 ± 16.2
	YFNB 13-E-56 FL	1.6 ± 1.0	6,155.0 ± 31.3	6,156.7 ± 31.3
	How F-67 FL	0.0 ± 2.57	32.6 ± 17.7	32.6 ± 17.9
	YFNB 29-H-81 FL	5.4 ± 1.0	564.2 ± 31.3	569.5 ± 31.3
Navajo	YAG 40-B-19 NA	4.3 ± 1.0	646.8 ± 31.3	651.1 ± 31.3
	YAG 39-C-36 NA	3.2 ± 1.0	1,416.4 ± 31.3	1,418.6 ± 31.3
	LST 611-D-51 NA	13.0 ± 1.0	1,299.5 ± 31.3	1,312.5 ± 31.3
	YFNB 13-E-54 NA	51.6 ± 1.0	5,129.8 ± 31.3	5,181.5 ± 31.3
	How F-67 NA	12.0 ± 2.6	561.3 ± 35.4	573.3 ± 35.4
	YFNB 29-H-81 NA	24.0 ± 1.0	0.0 ± 31.3	24.0 ± 31.3
Zuni	YAG 40-B-17 ZU	1,810.1 ± 1.0	116.8 ± 16.2	1,927.0 ± 16.2
	YAG 40-B-19 ZU	522.6 ± 1.0	166.1 ± 31.3	688.7 ± 31.3
	YAG 39-C-23 ZU	17.8 ± 1.0	88.6 ± 16.2	106.4 ± 16.2
	YAG 39-C-36 ZU	19.2 ± 1.0	55.0 ± 31.3	74.2 ± 31.3
	YFNB 13-E-56 ZU	1,574.8 ± 1.0	1,121.6 ± 16.2	2,696.4 ± 16.2
	YFNB 13-E-58 ZU	797.9 ± 1.0	583.9 ± 16.2	1,381.8 ± 16.2
	How F-63 ZU	989.5 ± 2.6	86.7 ± 0.3	1,076.2 ± 2.6
	How F-67 ZU	592.3 ± 2.6	221.8 ± 17.7	814.2 ± 17.9
	YFNB 29-H-79 ZU	2,912.9 ± 1.0	561.0 ± 16.2	3,473.8 ± 16.2
	YFNB 29-H-81 ZU	2,788.4 ± 1.0	1,274.2 ± 16.2	4,062.6 ± 16.2
Tewa	YAG 40-B-19 TE	661.7 ± 1.0	273.6 ± 16.2	935.3 ± 16.2
	YAG 39-C-36 TE	1,726.8 ± 1.0	517.5 ± 16.2	2,244.4 ± 16.2
	LST 611-D-51 TE	62.9 ± 1.0	0.0 ± 31.3	62.9 ± 31.3
	YFNB 13-E-56 TE	54.1 ± 1.0	199.0 ± 16.2	253.2 ± 16.2
	How F-67 TE	15.0 ± 2.4	13.6 ± 0.2	28.6 ± 2.4
	YFNB 29-H-81 TE	4,533.1 ± 1.0	0.0 ± 31.3	4,533.1 ± 31.3

Page 66 Deleted.
Pages 68 thru 75 Deleted

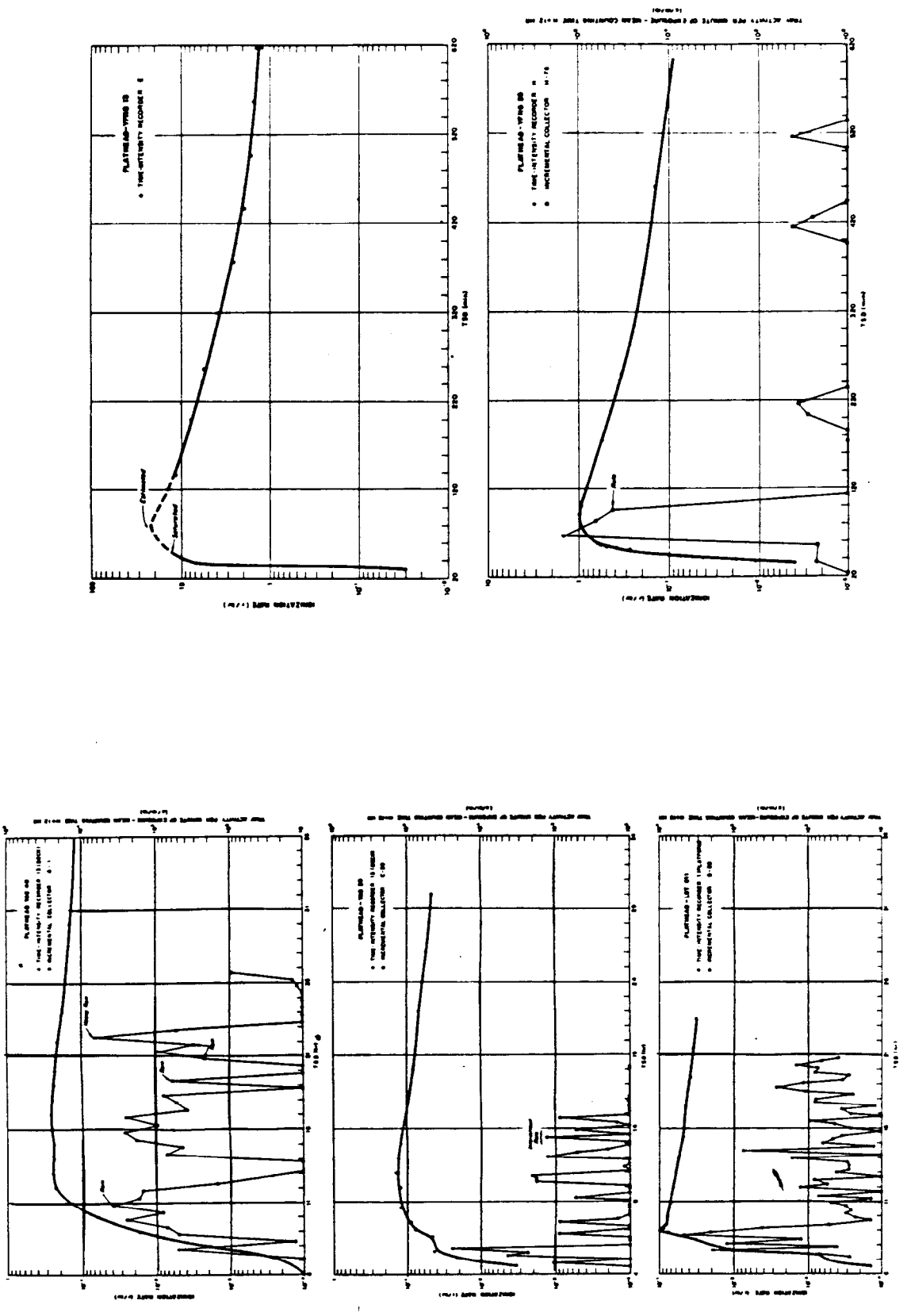

Figure 3.1 Rates of arrival at major stations, Shot Flathead.

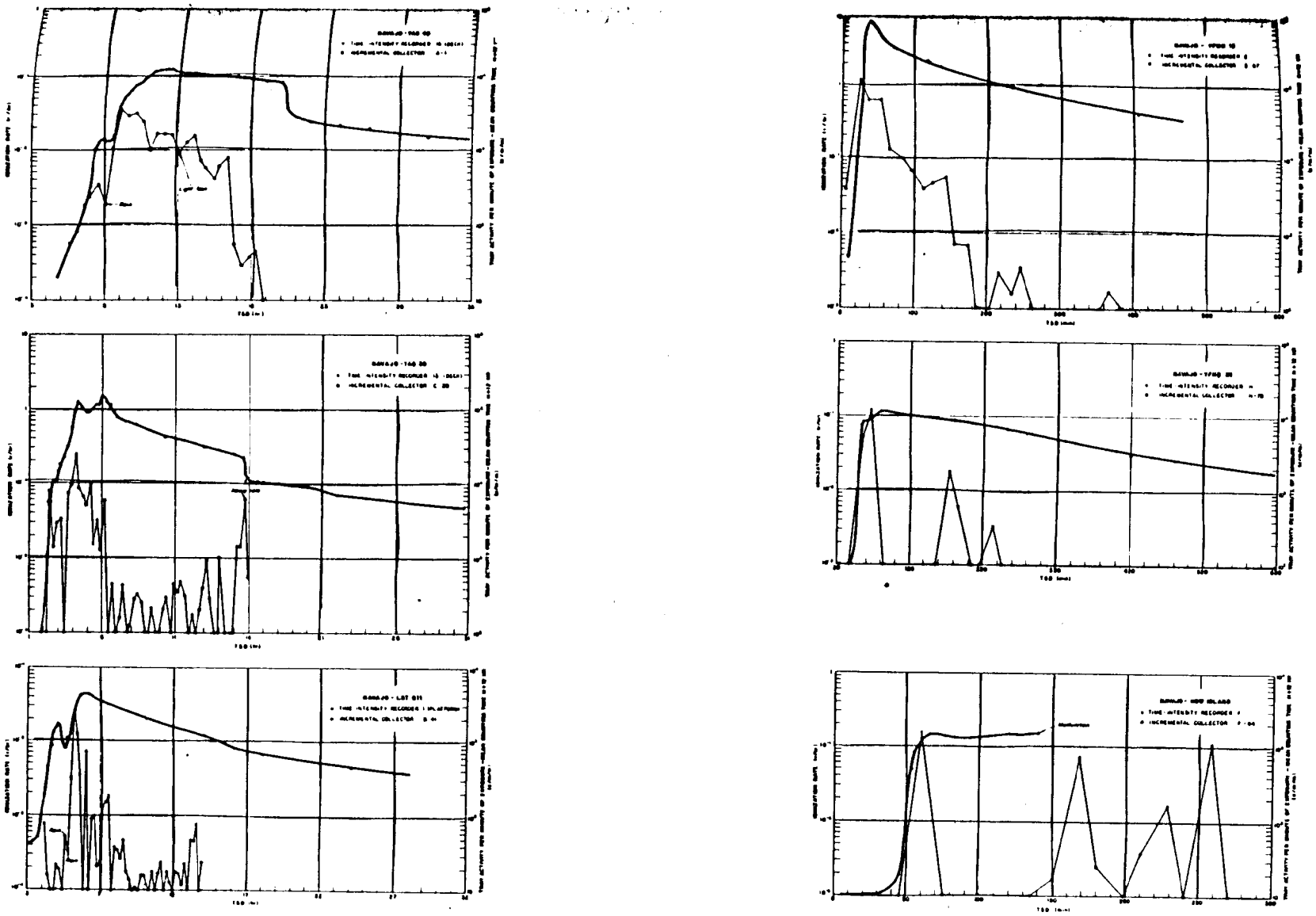

Figure 3.2 Rates of arrival at major stations, Shot Navajo.

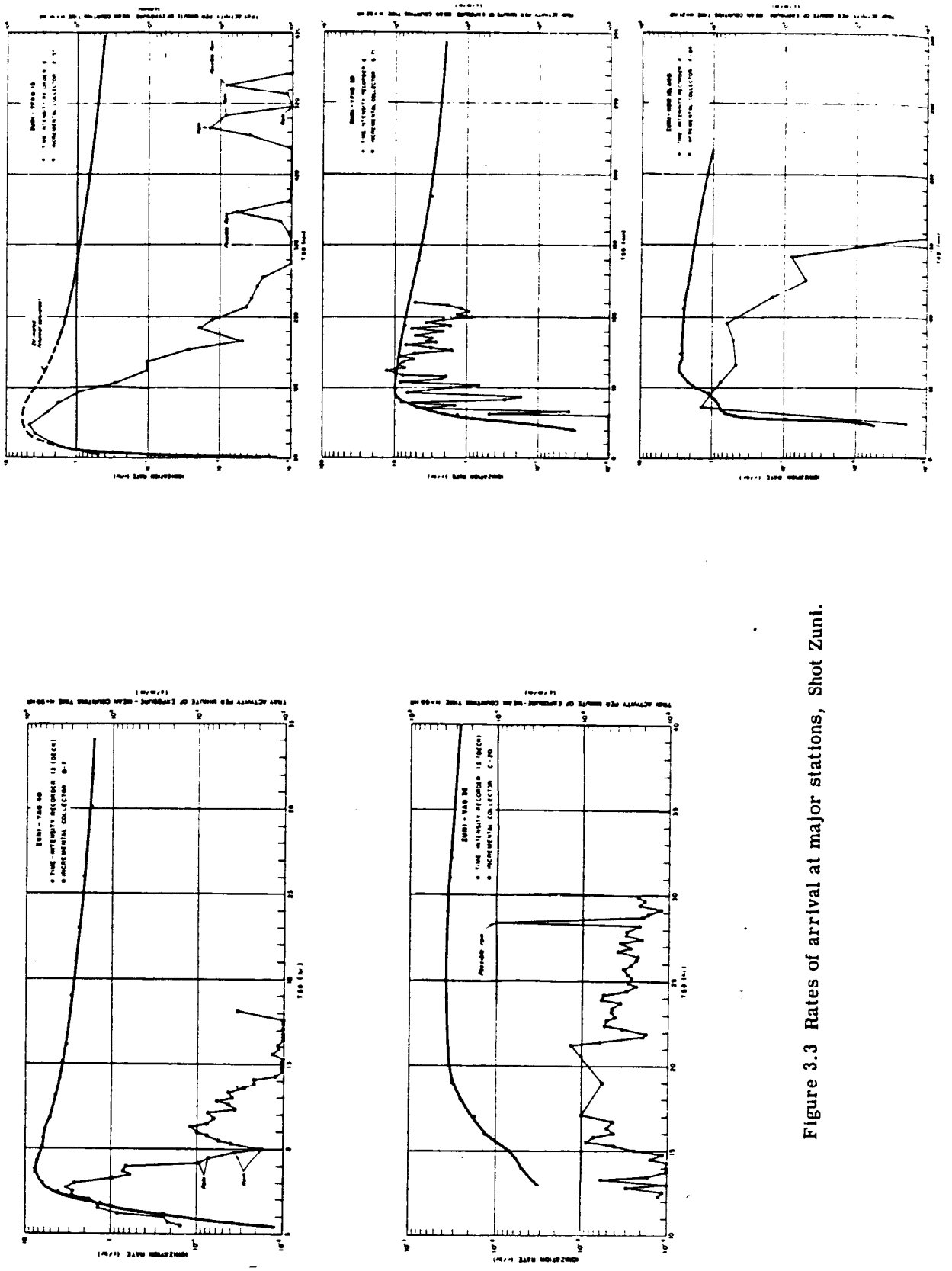

Figure 3.3 Rates of arrival at major stations, Shot Zuni.

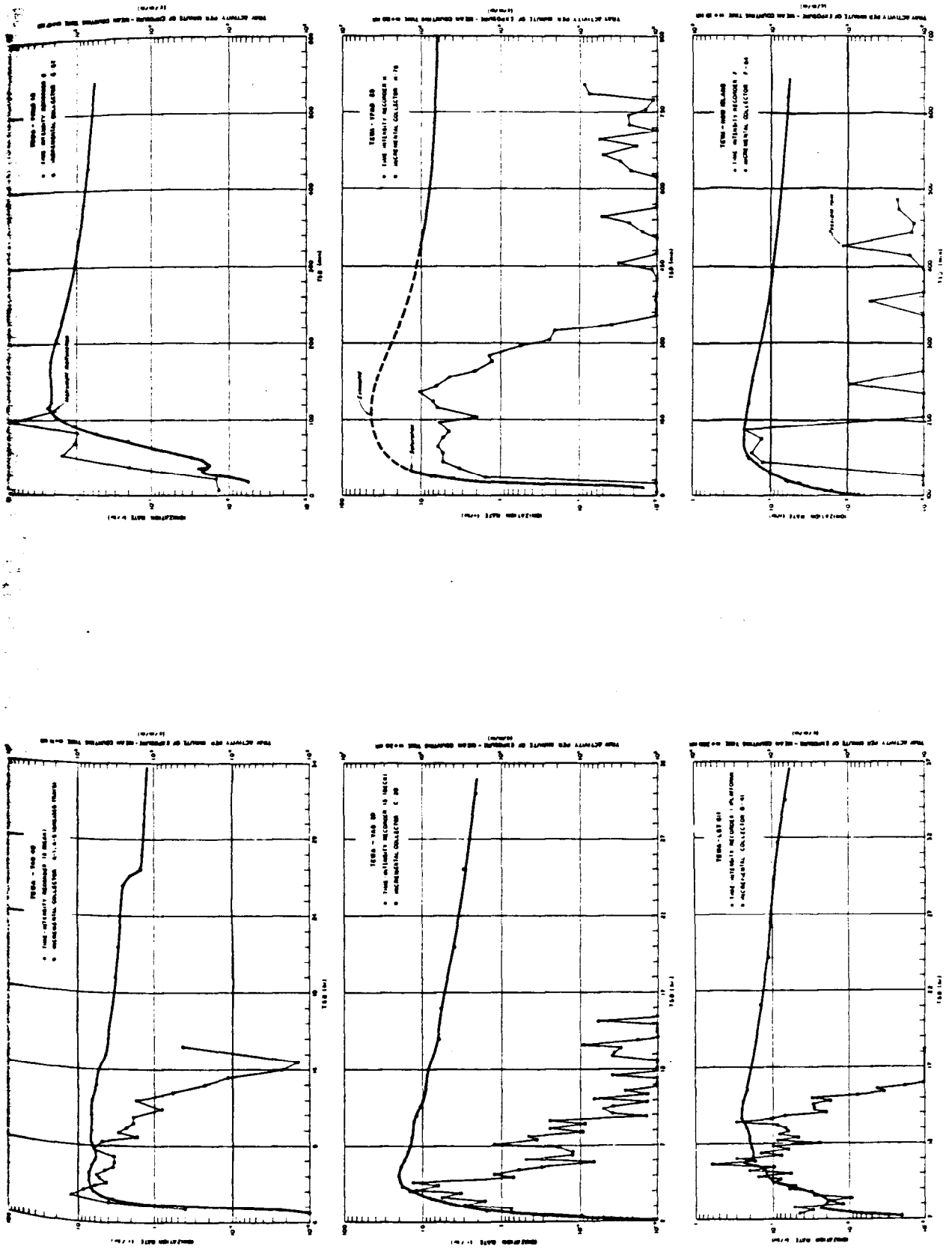

Figure 3.4 Rates of arrival at major stations, Shot Tewa.

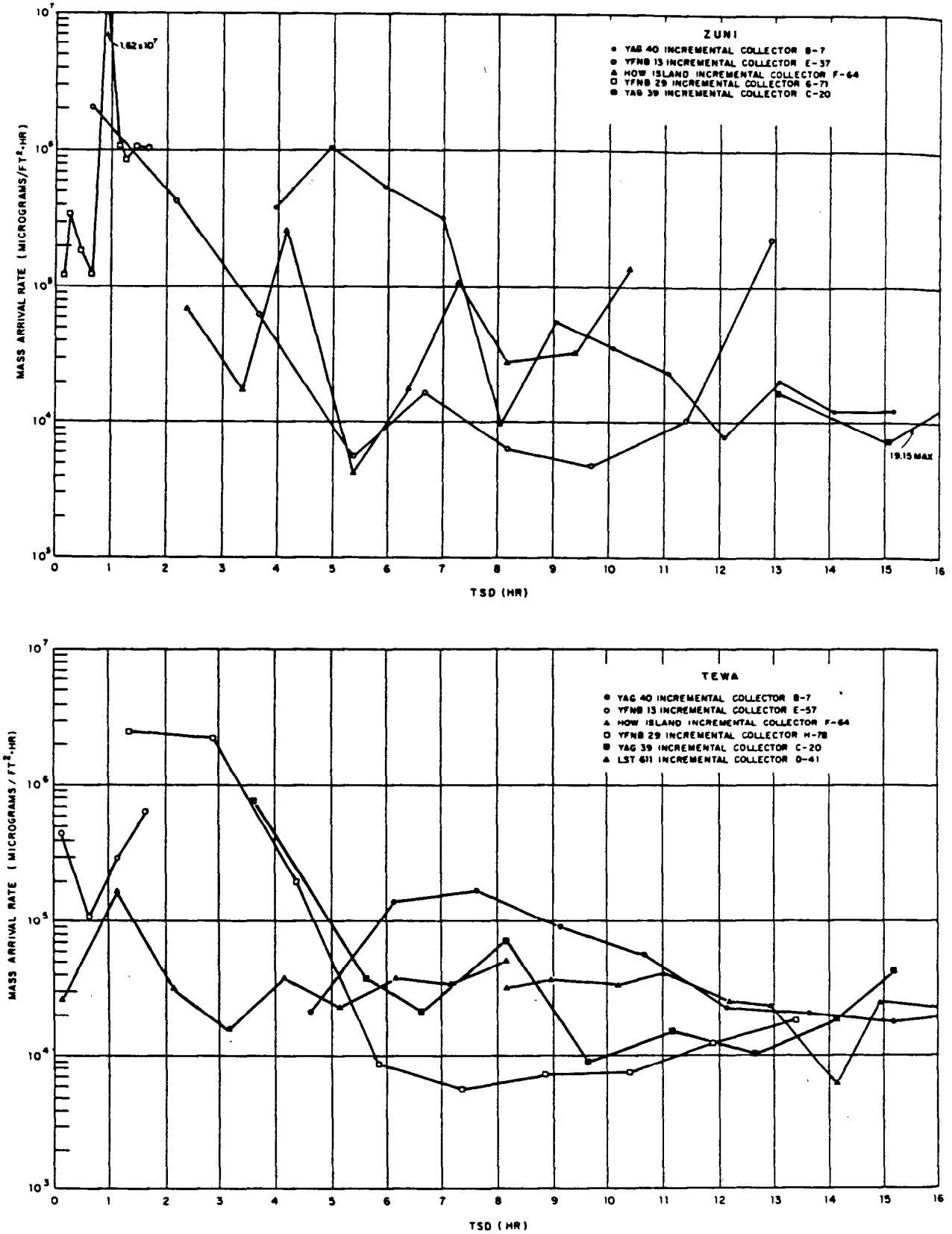

Figure 3.5 Calculated mass-arrival rate, Shots Zuni and Tewa.

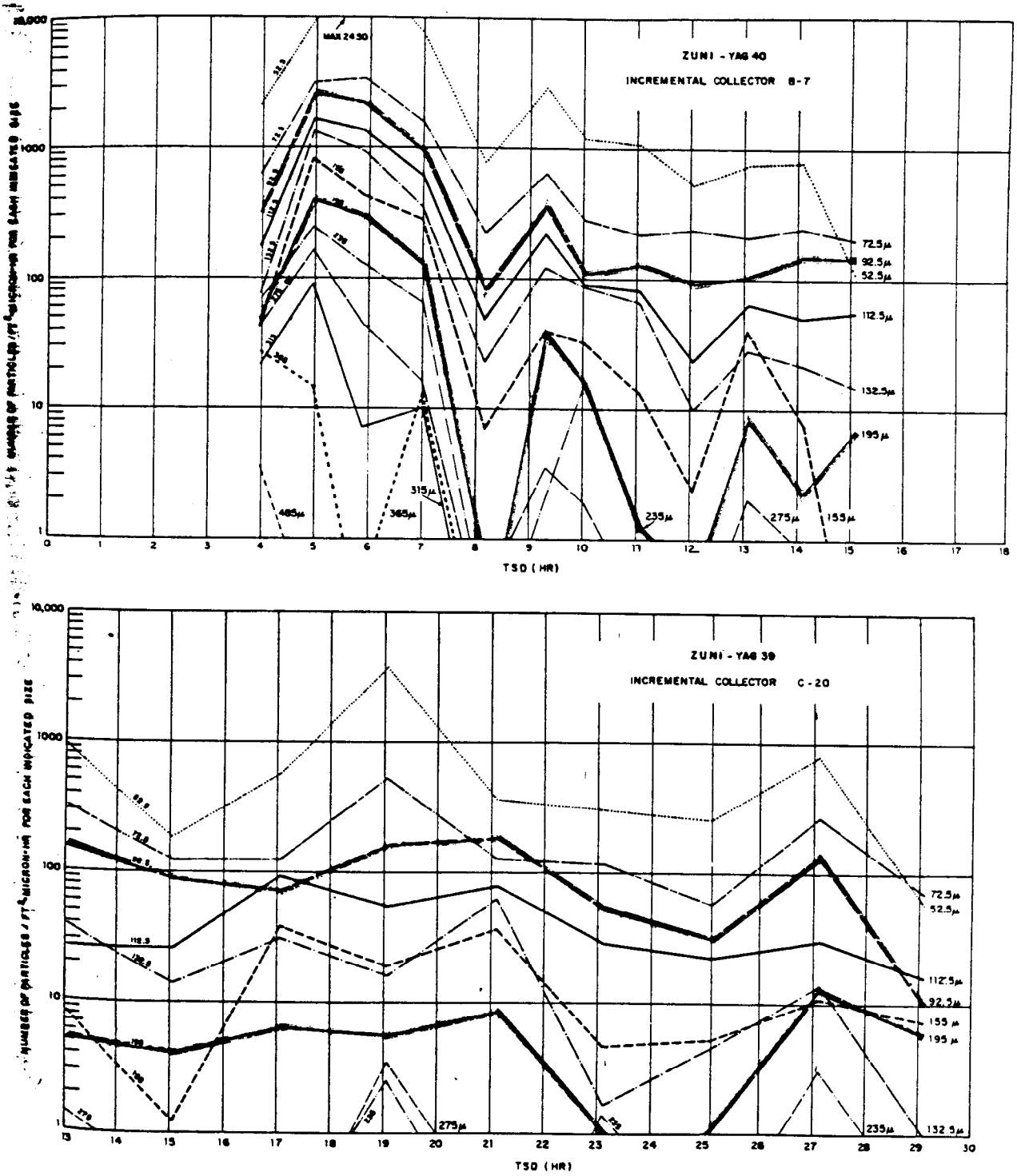

Figure 3.6 Particle-size variation at ship stations, Shot Zuni.

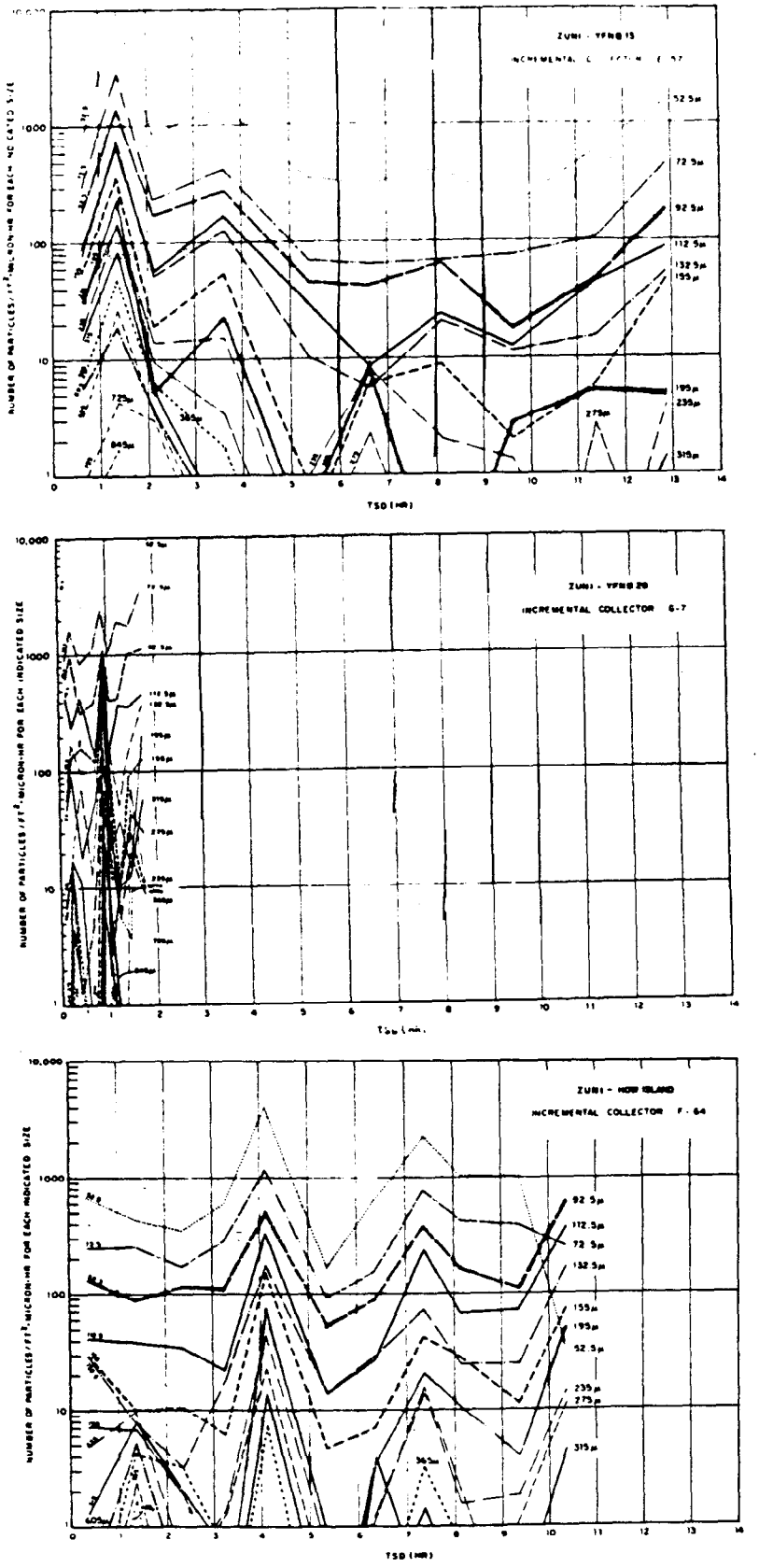

Figure 3.7 Particle-size variation at barge and island stations, Shot Zuni.

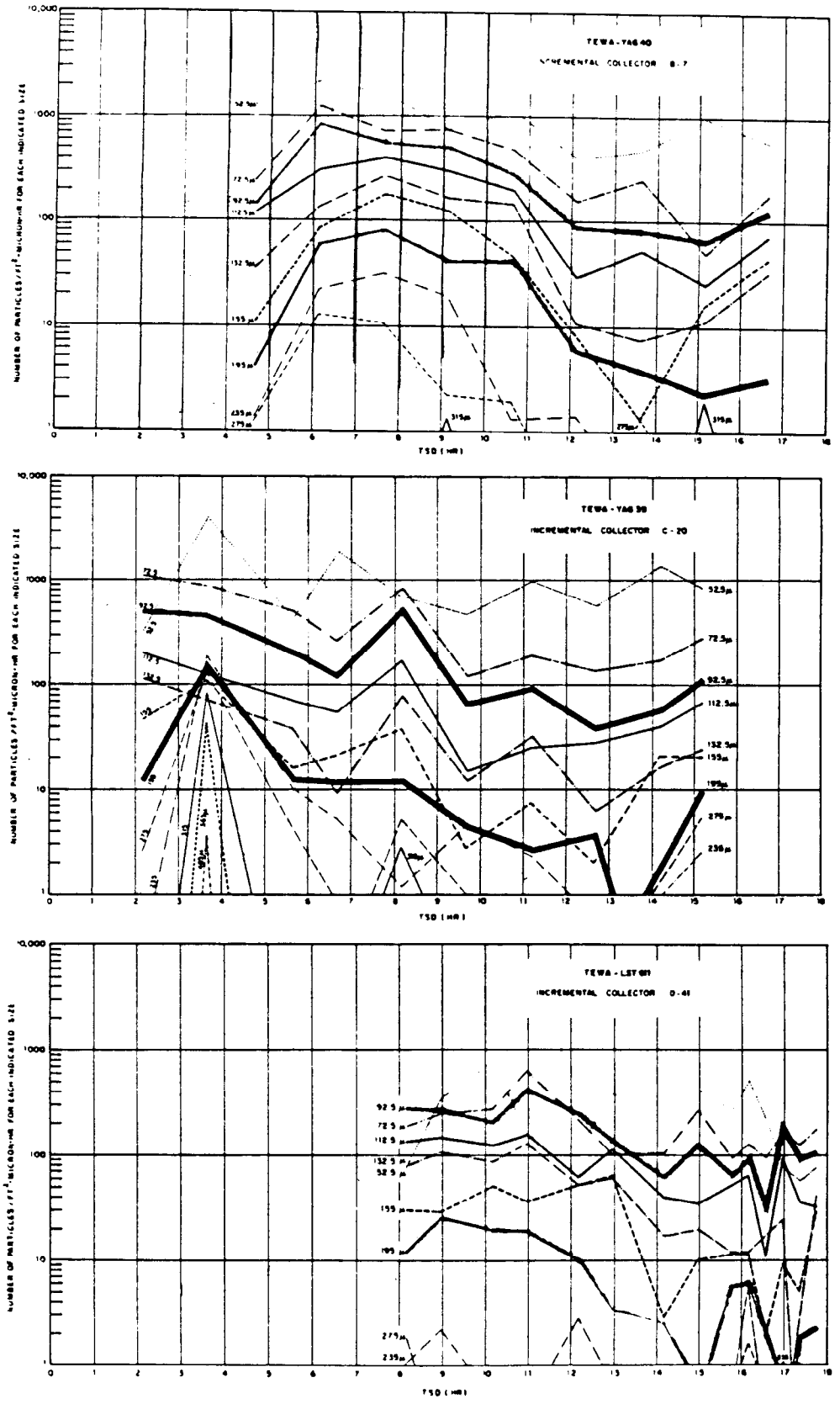

Figure 3.8 Particle-size variation at ship stations, Shot Tewa.

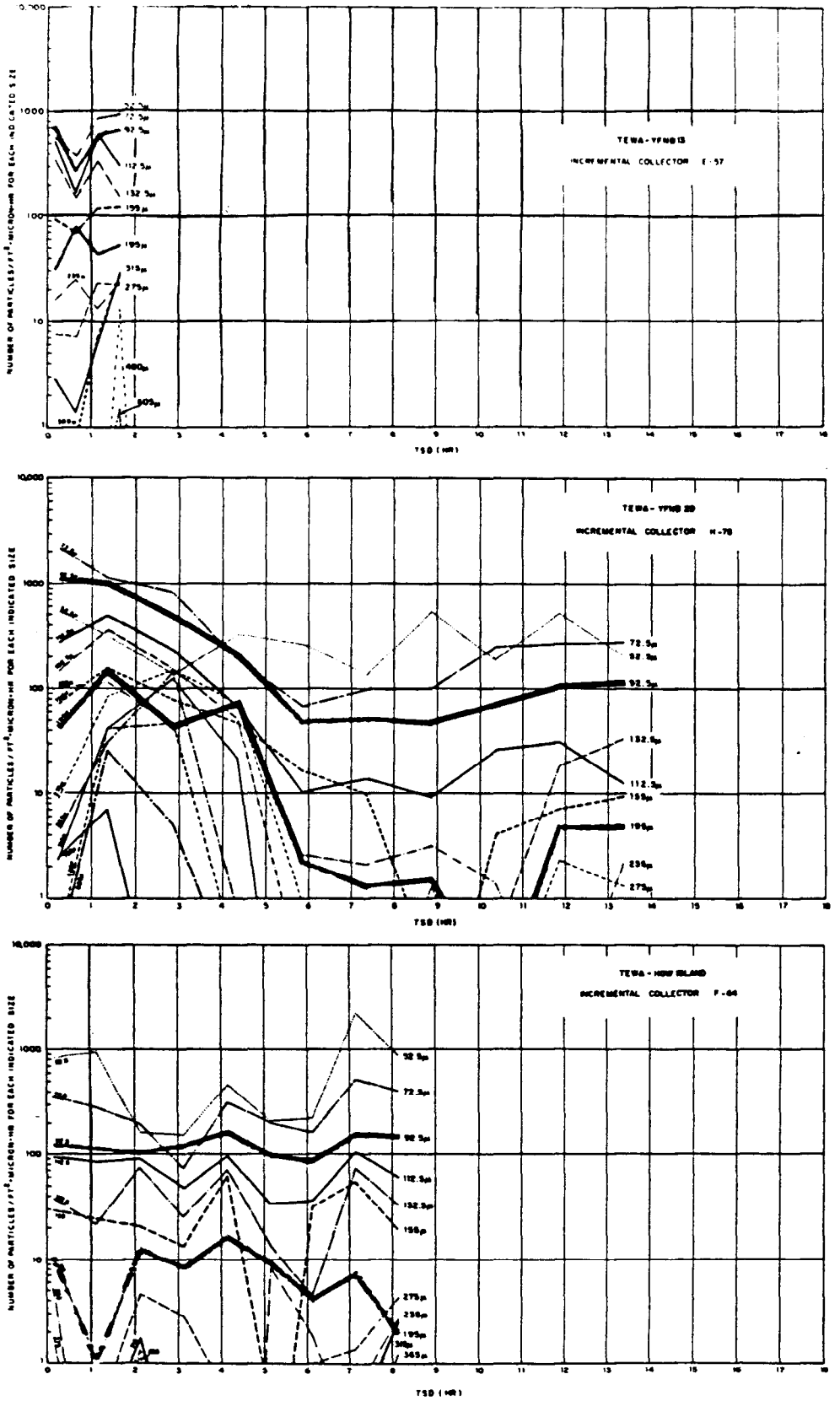

Figure 3.9 Particle-size variation at barge and island stations, Shot Tewa.

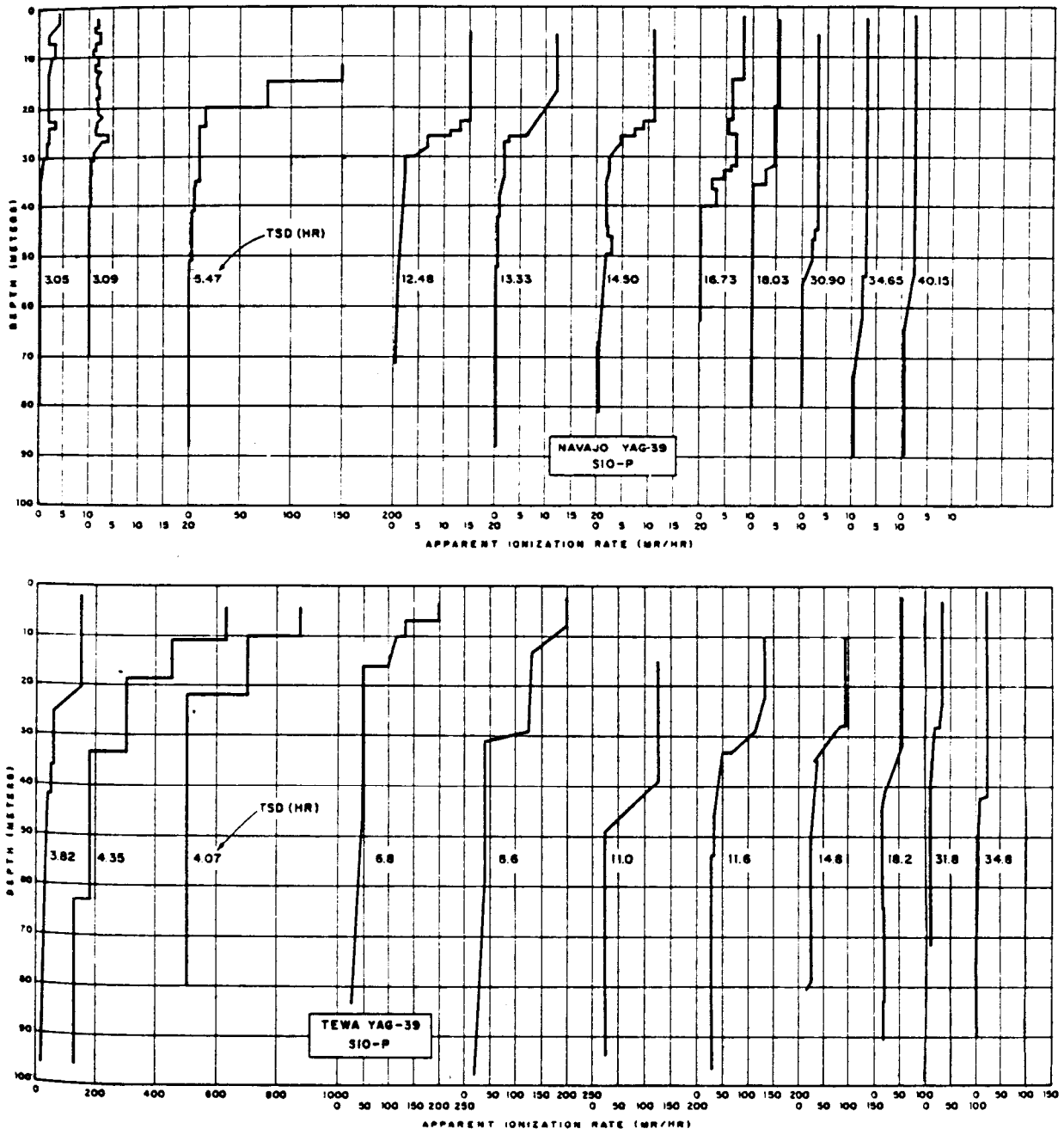

Figure 3.10 Ocean activity profiles, Shots Navajo and Tewa.

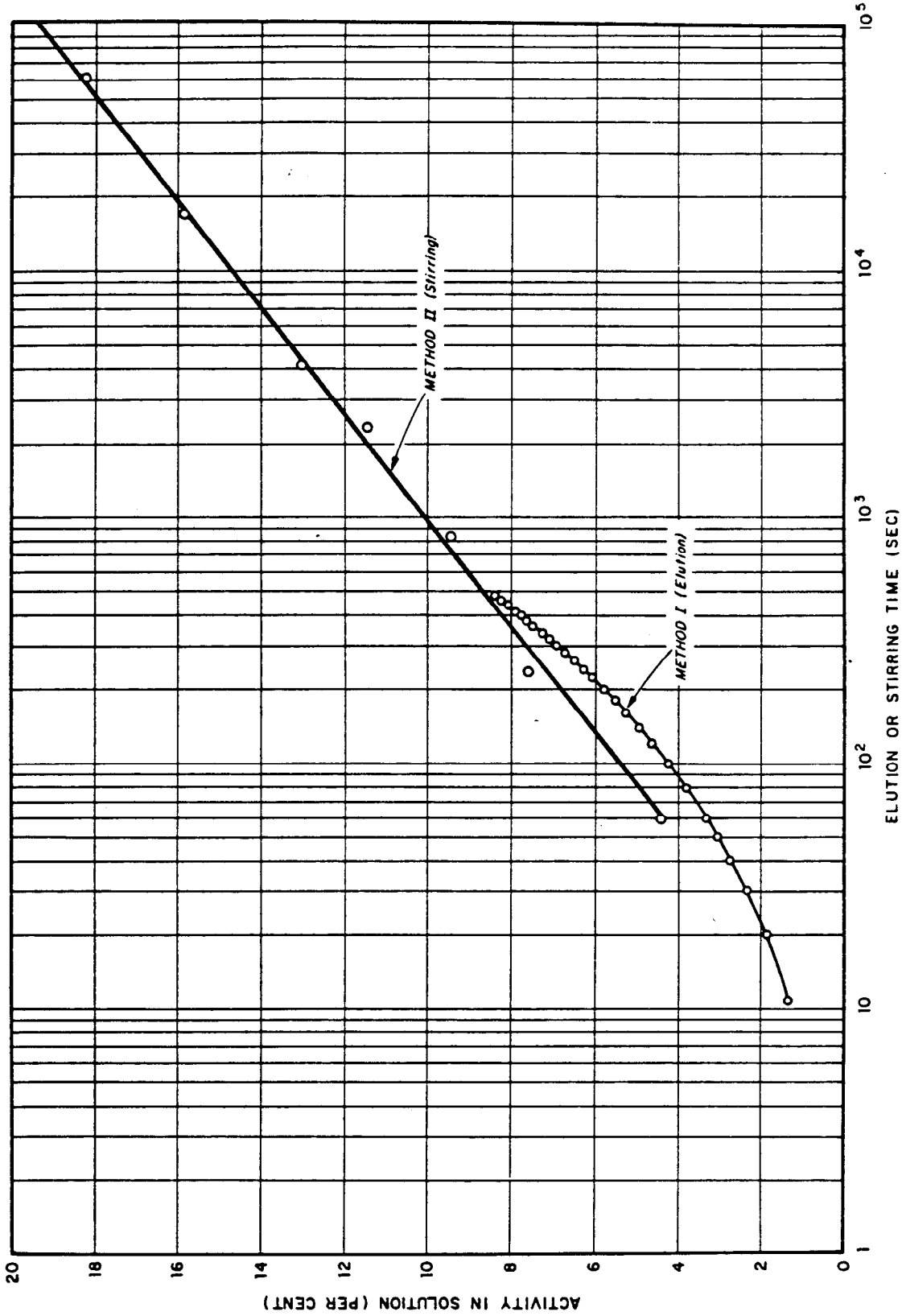

Figure 3.11 Solubility of solid fallout particles.

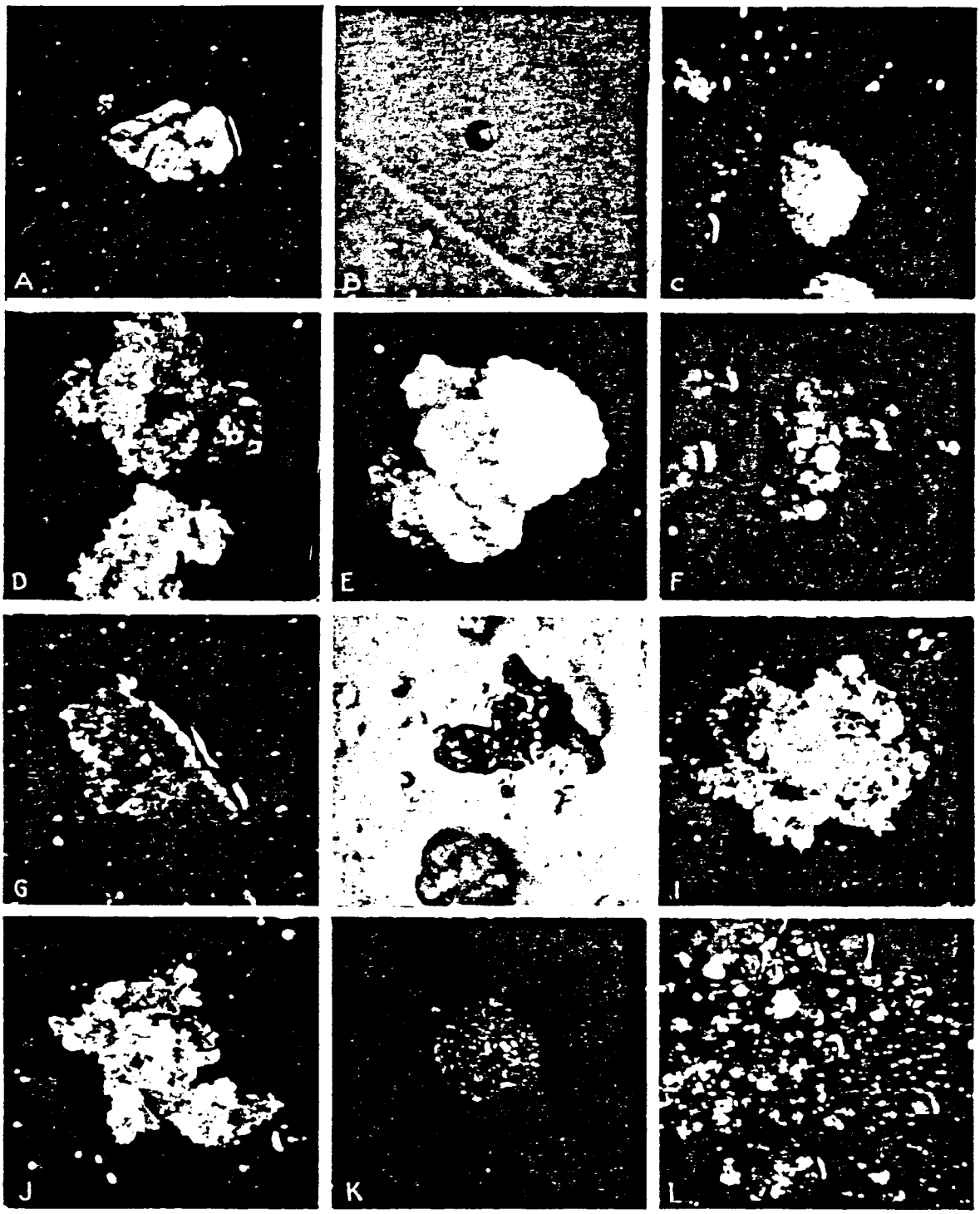

Figure 3.13 Typical solid fallout particles.

PAGE 87 Deleted

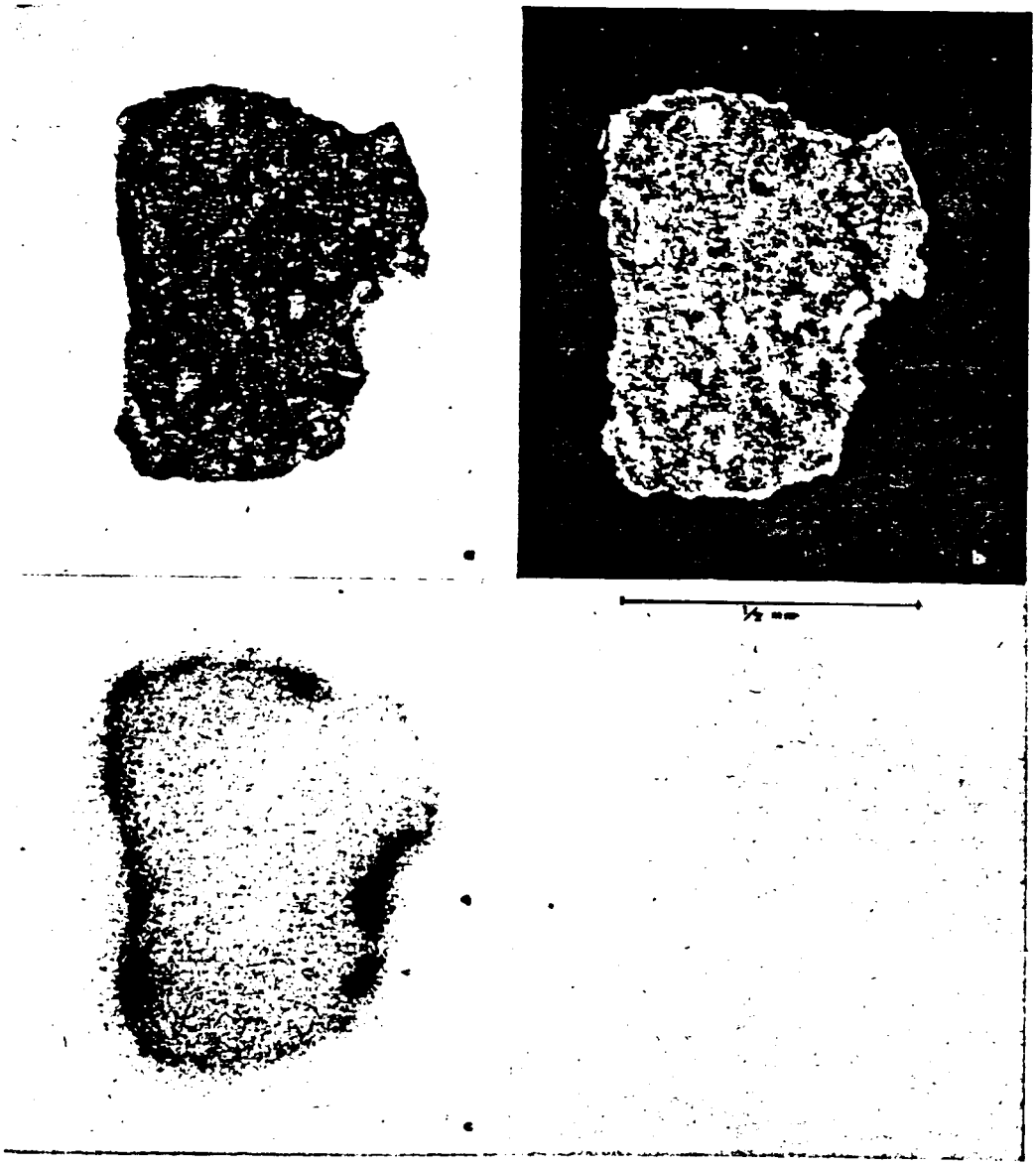

Figure 3.14 Angular fallout particle, Shot Zuni.
a. Ordinary light. b. Crossed nicols. c. Radioautograph.

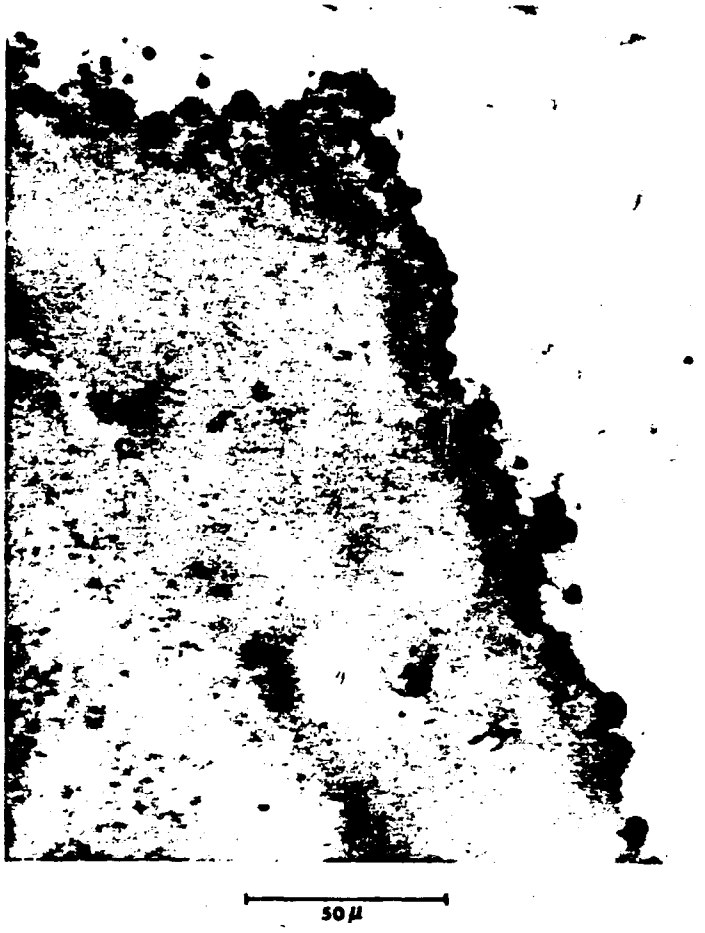

Figure 3.15 High magnification of part of an angular fallout particle, Shot Zuni.

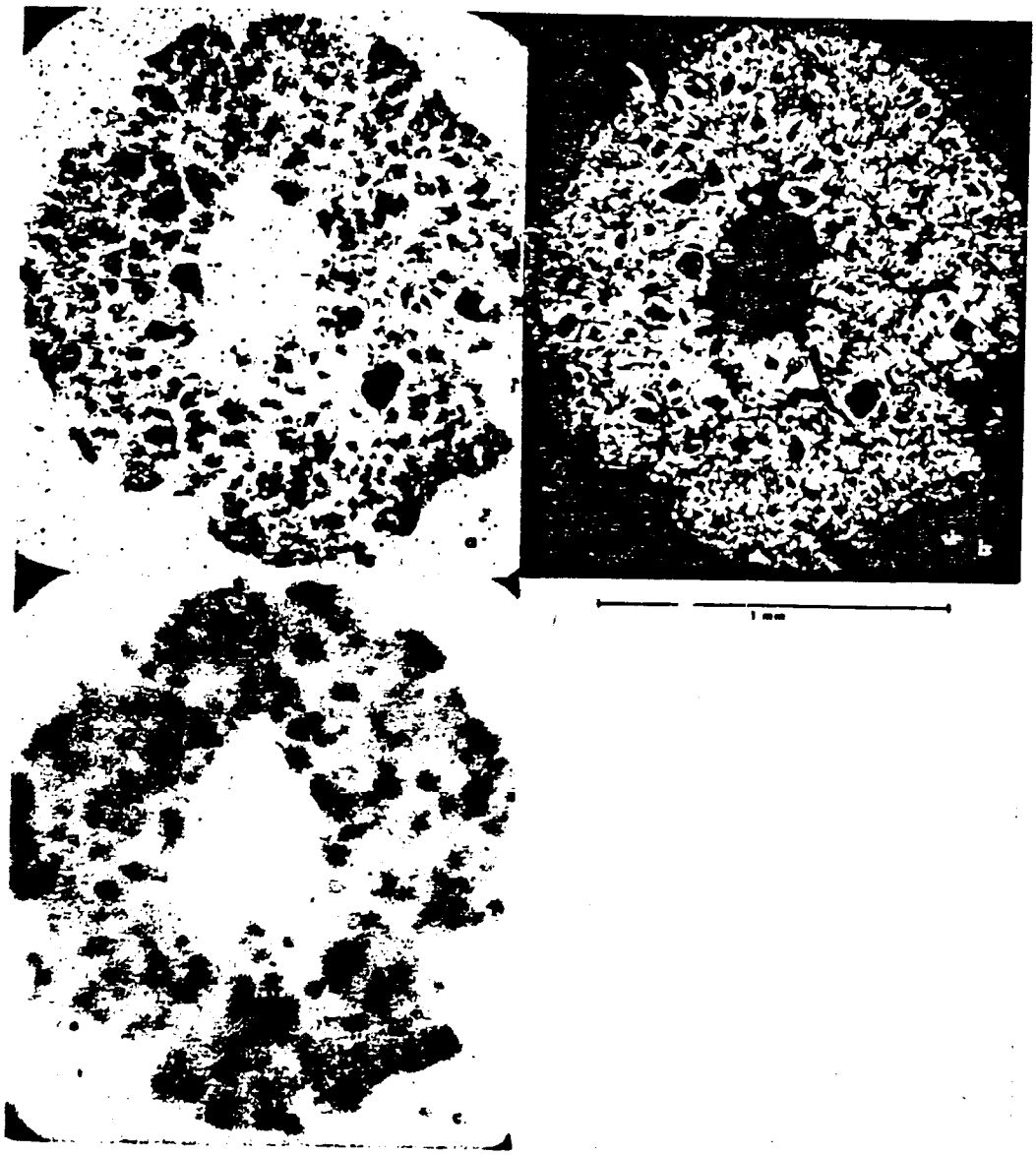

Figure 3.16 Spheroidal fallout particle, Shot Zuni.
a. Ordinary light. b. Crossed nicols. c. Radioautograph.

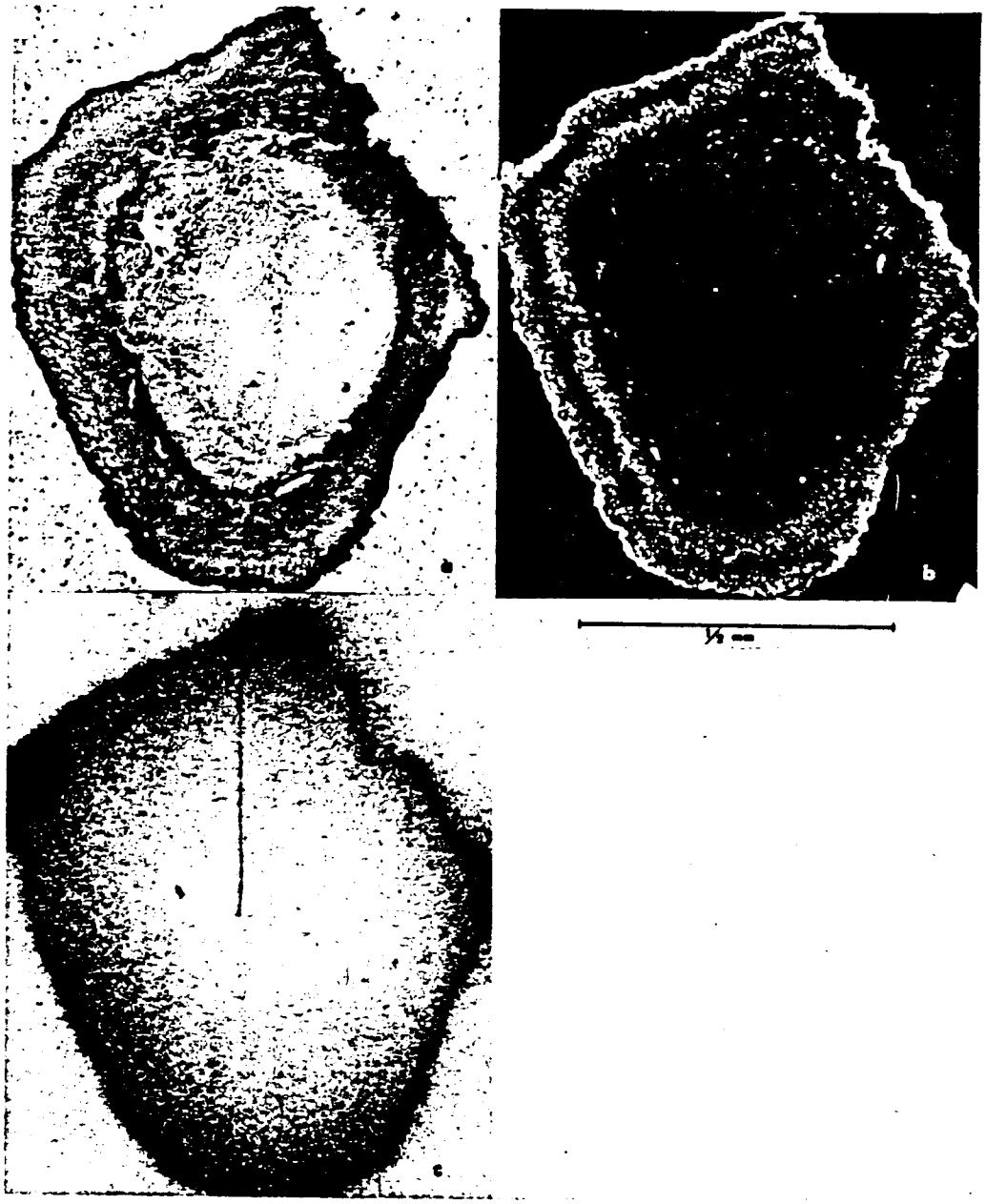

Figure 3.17 Angular fallout particle, Shot Tewa.
a. Ordinary light. b. Crossed nicols. c. Radioautograph.

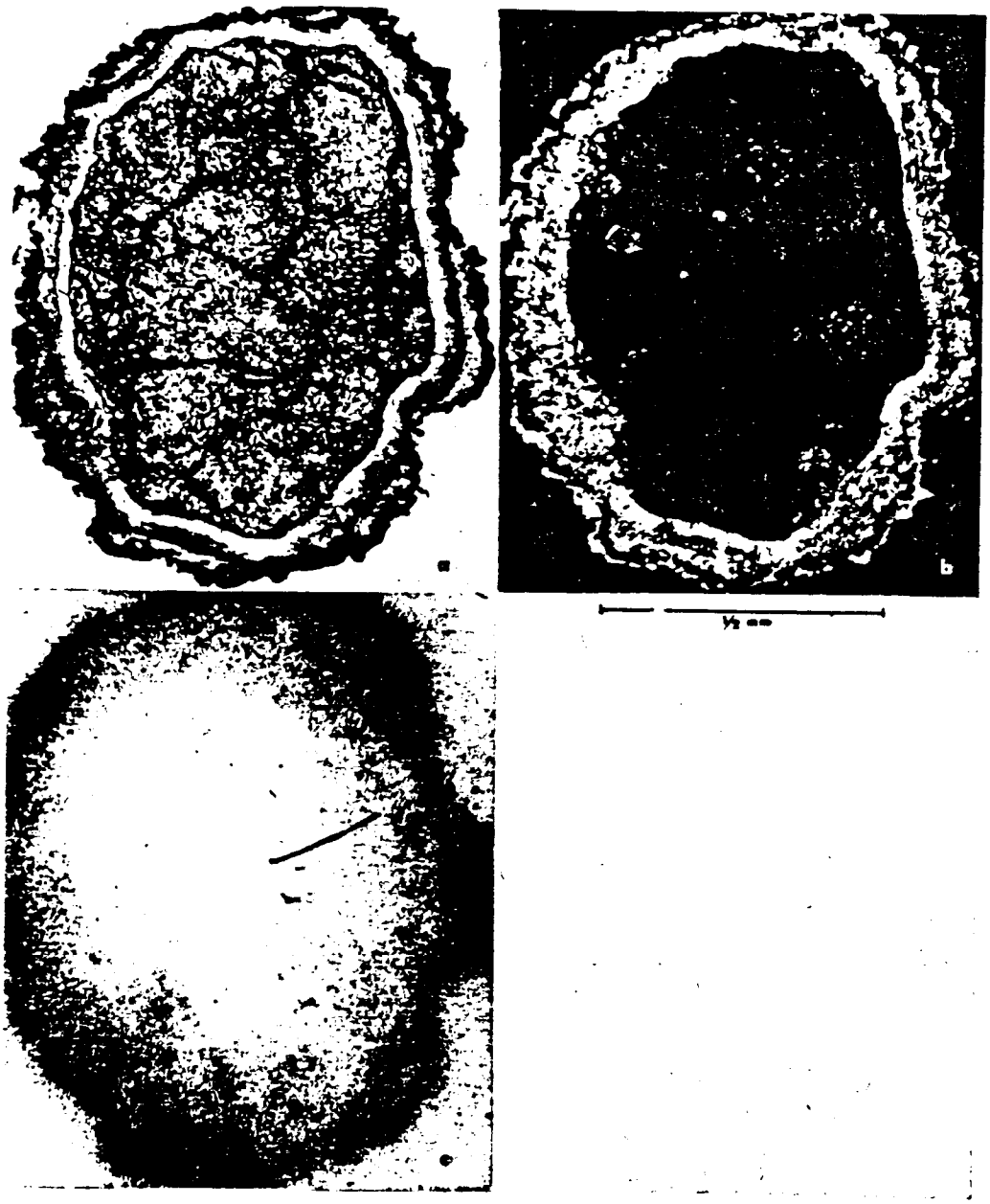

Figure 3.18 Spheroidal fallout particle, Shot Tewa.
a. Ordinary light. b. Crossed nicols. c. Radioautograph.

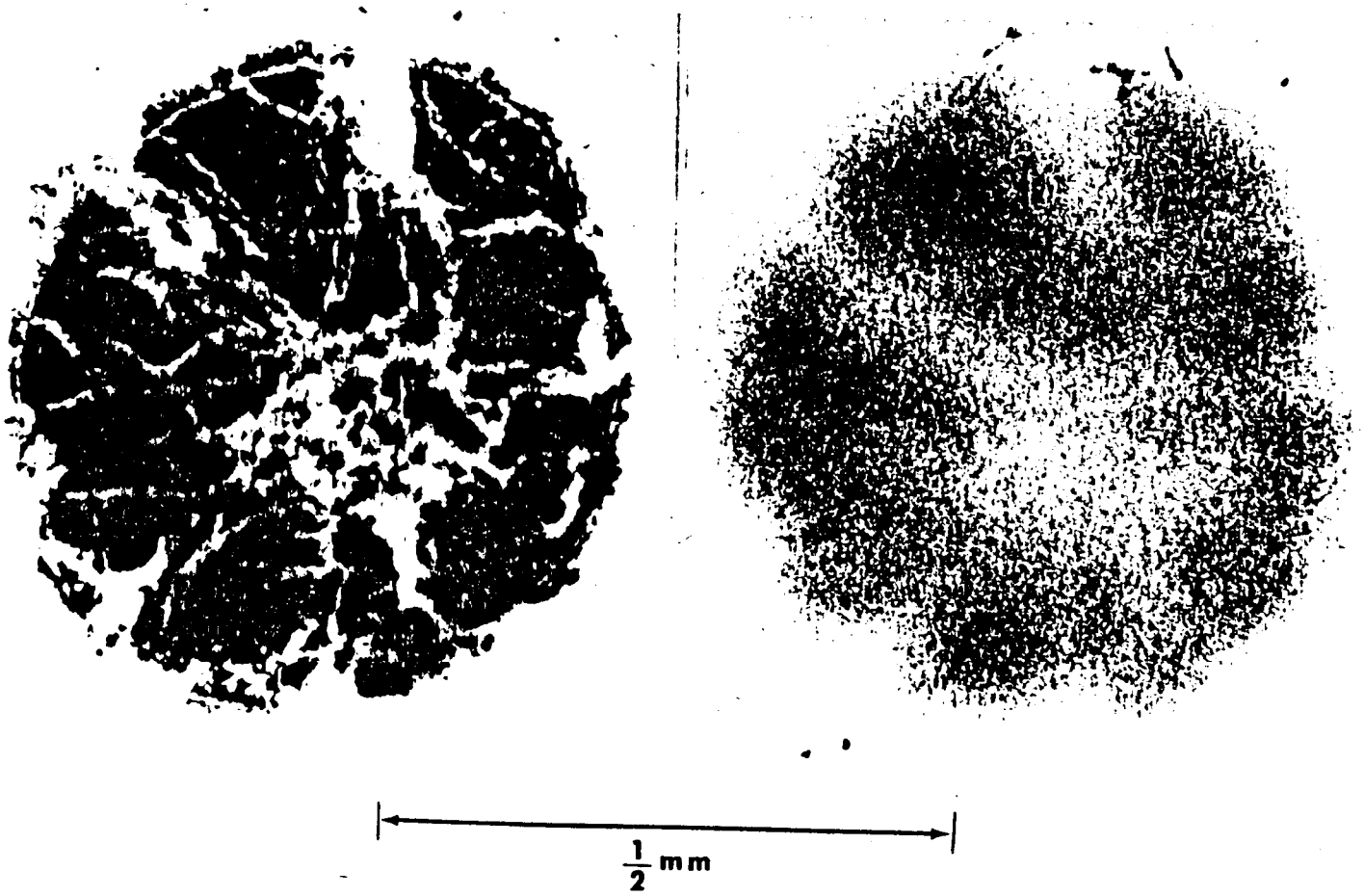

Figure 3.19 Thin section and radioautograph of spherical fallout particle, Shot Inca.

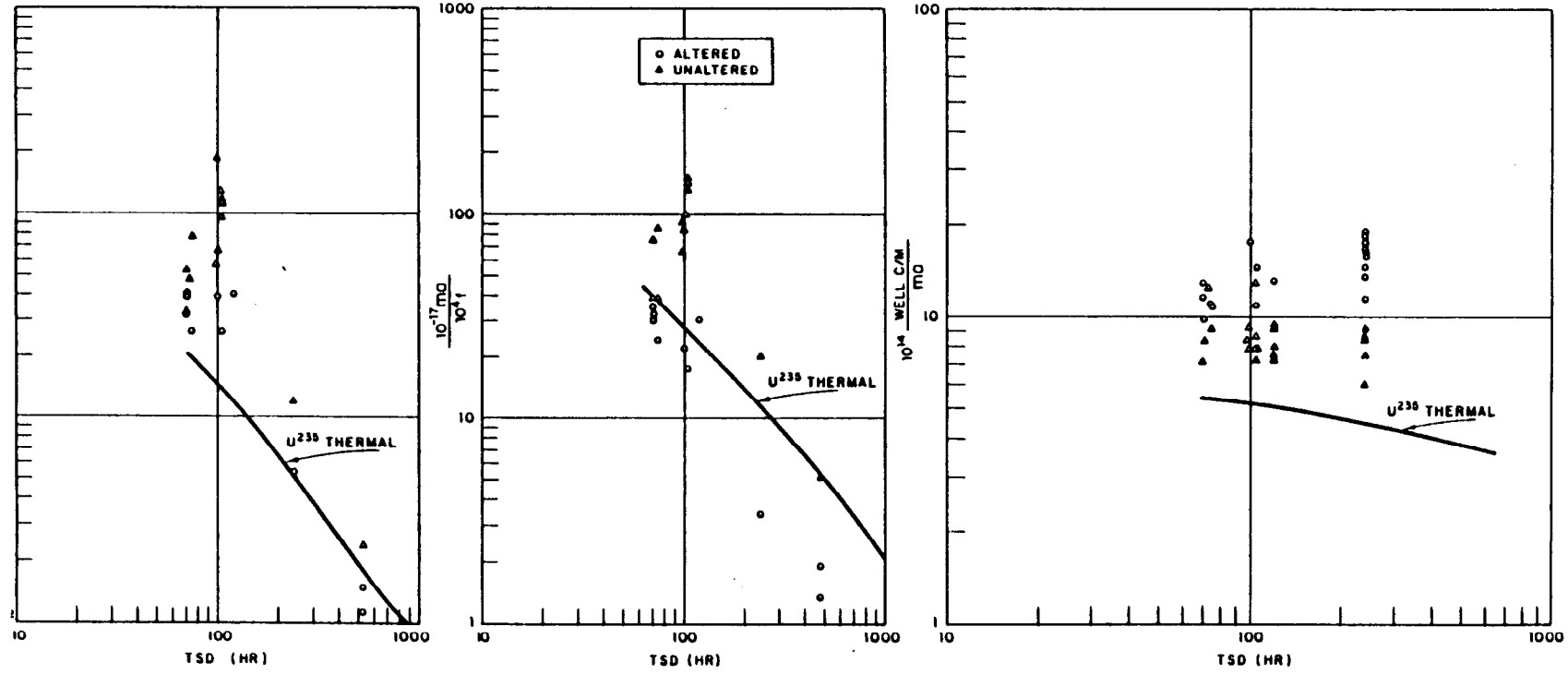

Figure 3.20 Energy-dependent activity ratios for altered and unaltered particles, Shot Zuni.

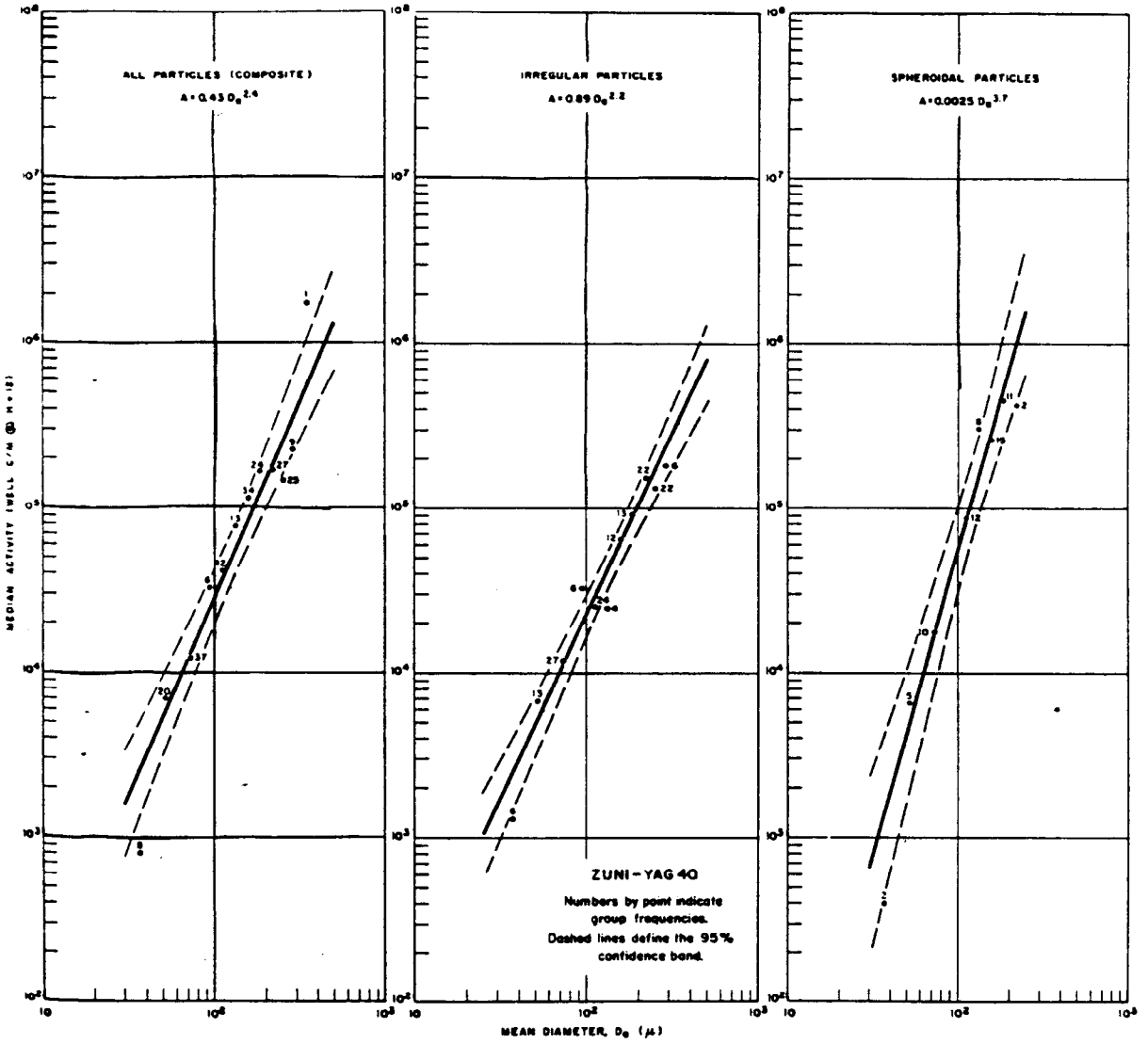

Figure 3.22 Particle group median activity versus mean size, Shot Zuni.

PAGE 96 DELETED

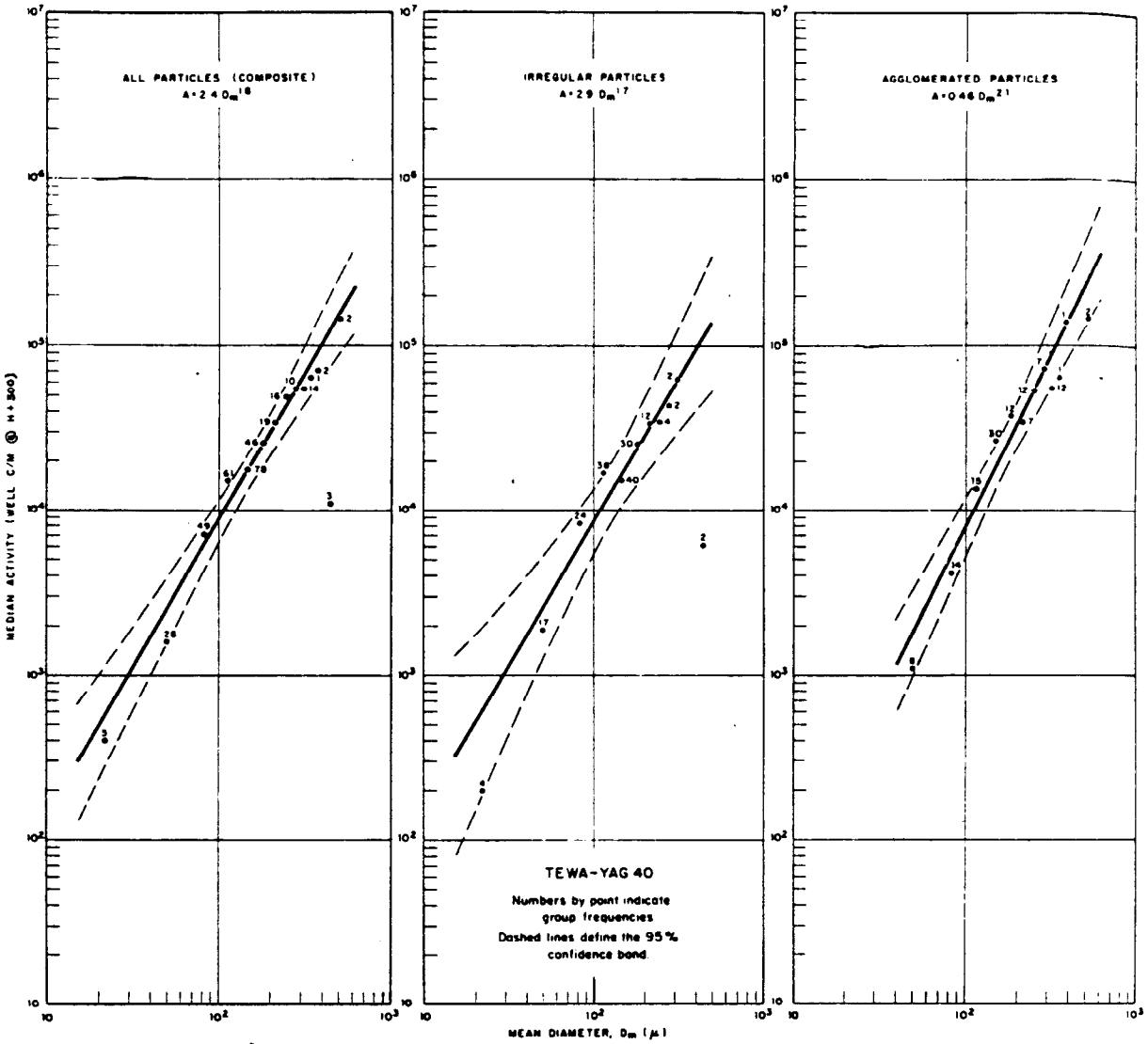

Figure 3.23 Particle group median activity versus mean size, Shot Tewa.

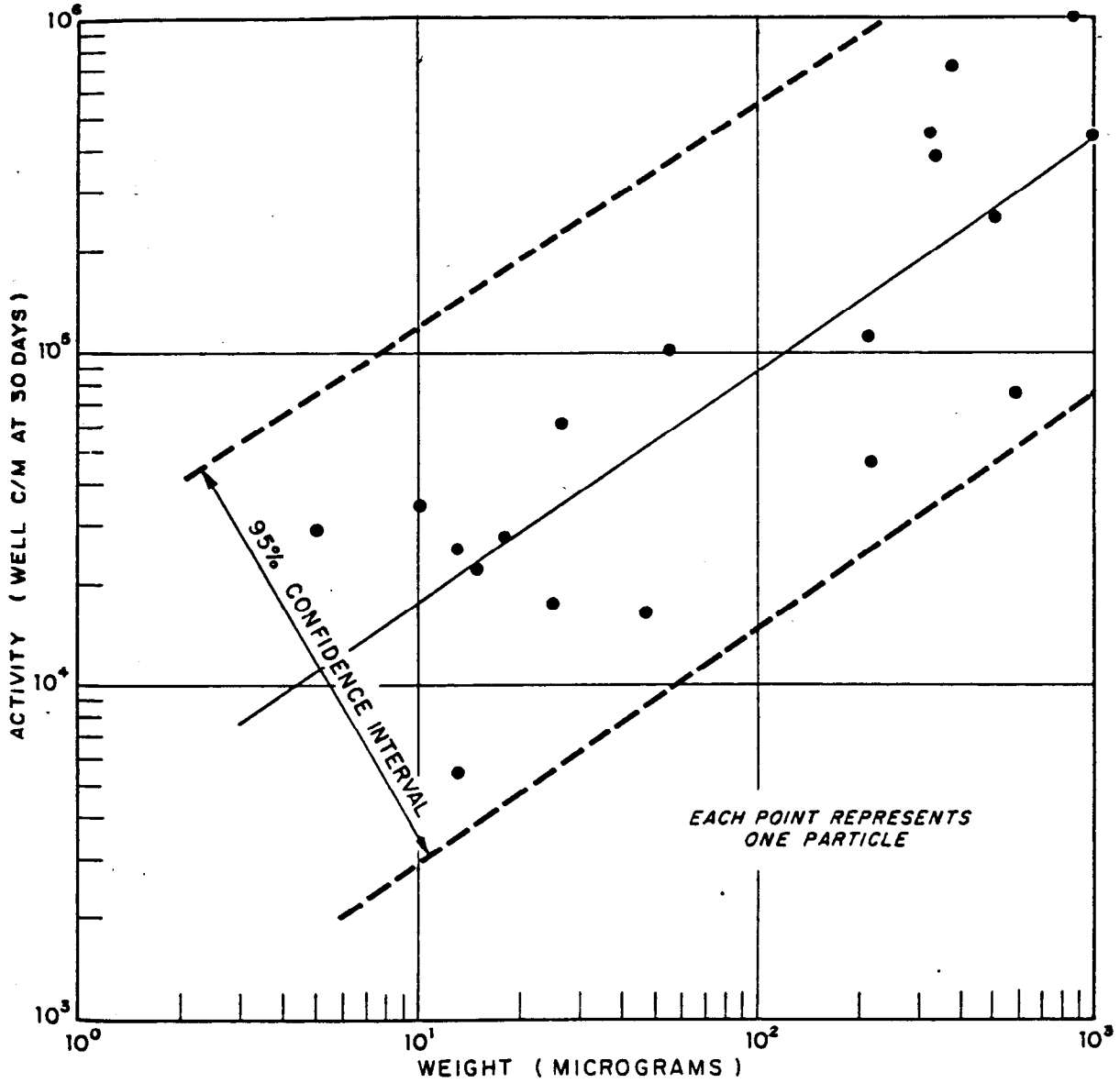

Figure 3.24 Relation of particle weight to activity, Shot Tewa.

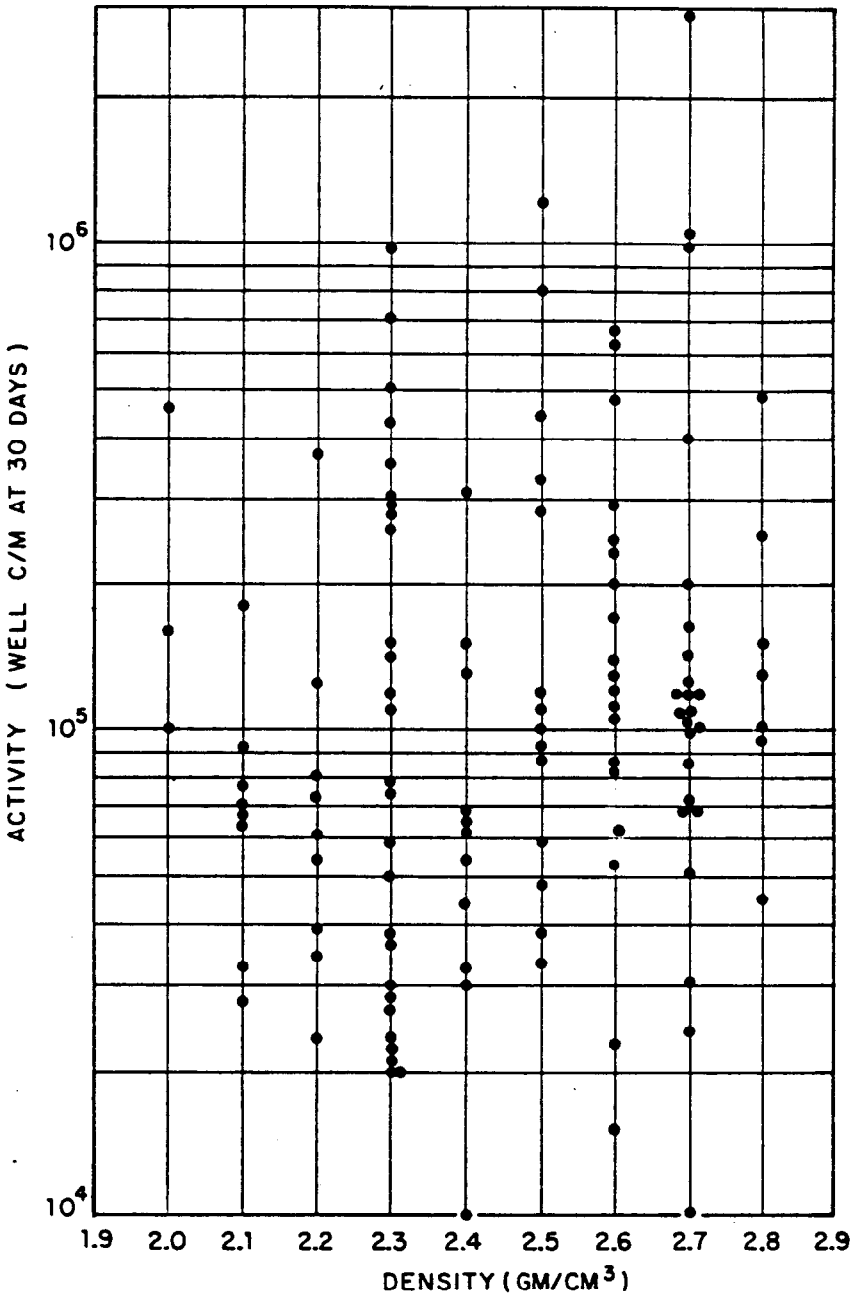

Figure 3.25 Relation of particle density to activity, Shot Zuni.

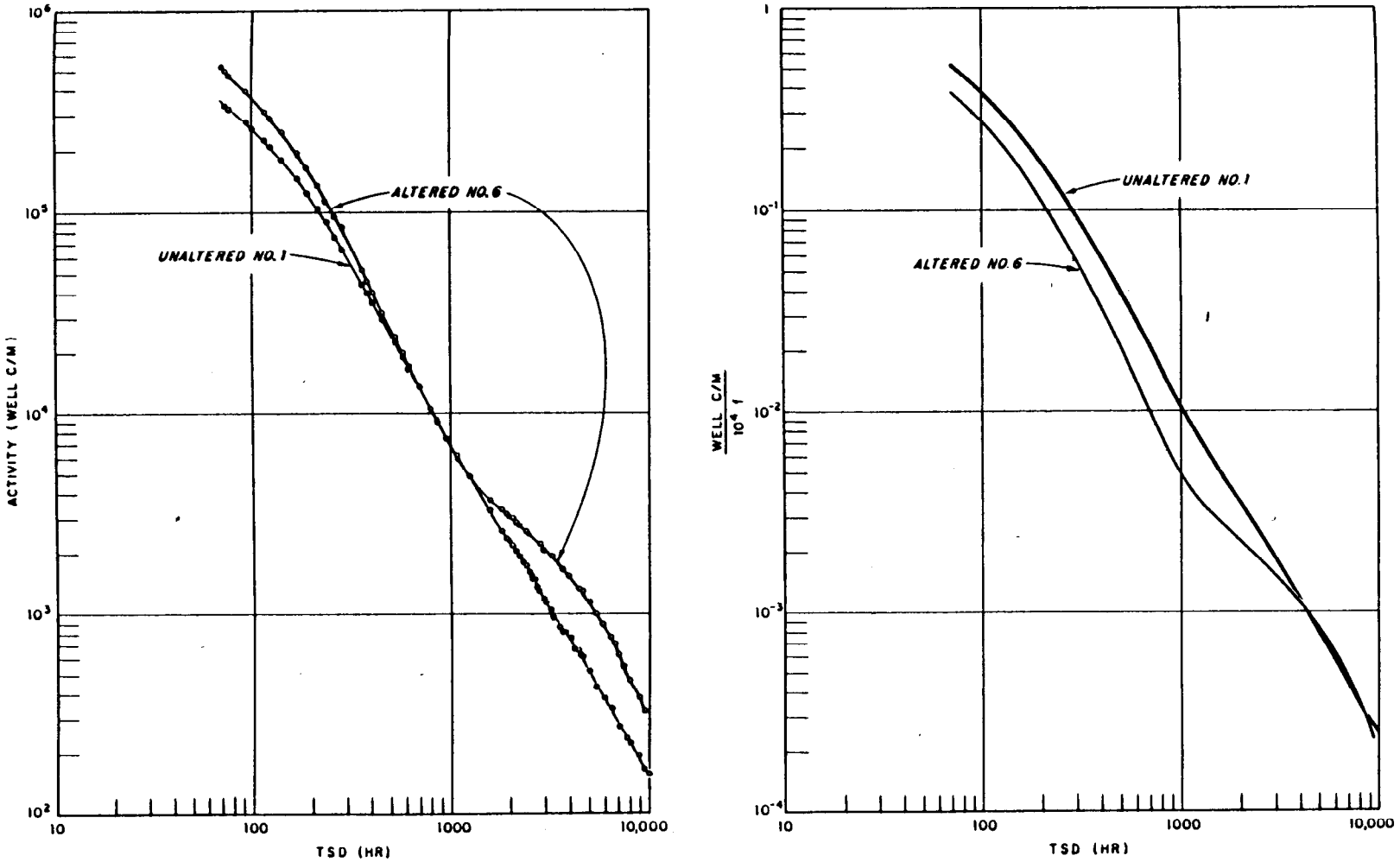

Figure 3.26 Gamma decay of altered and unaltered particles, Shot Zuni.

page 102 deleted

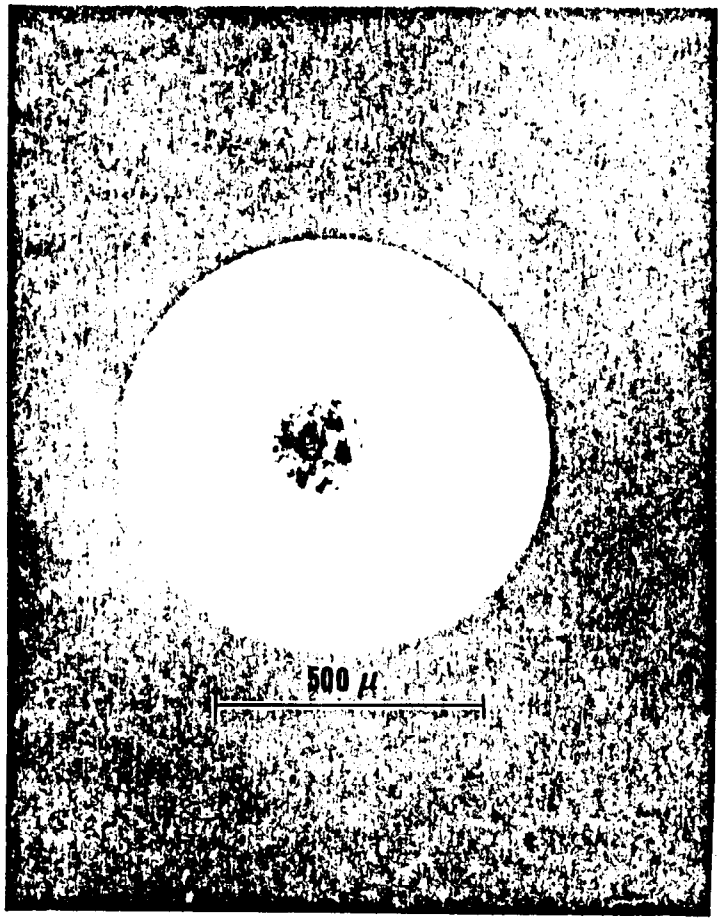

Figure 3.28 Photomicrograph of slurry-particle reaction area and insoluble solids.

Figure 3.29 Electronmicrograph of slurry-particle insoluble solids.

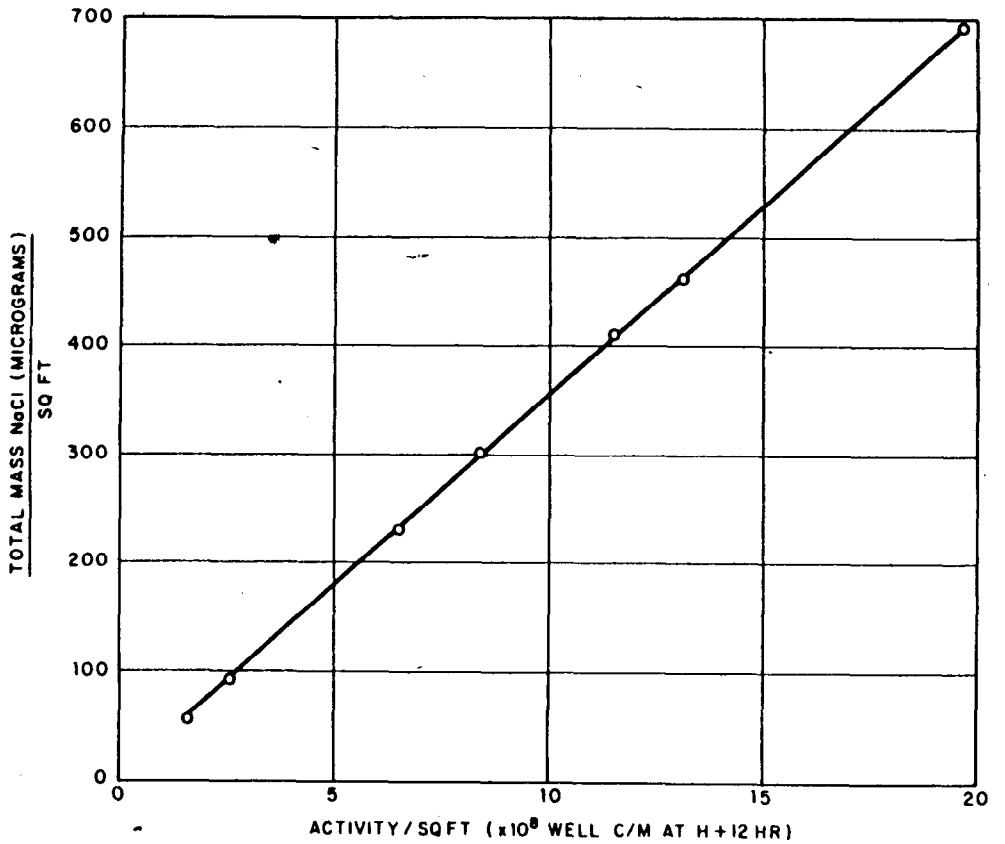

Figure 3.30 NaCl mass versus activity per square foot, Shot Flathead.

Figure 3.31 Radioautograph of slurry-particle trace and reaction area.

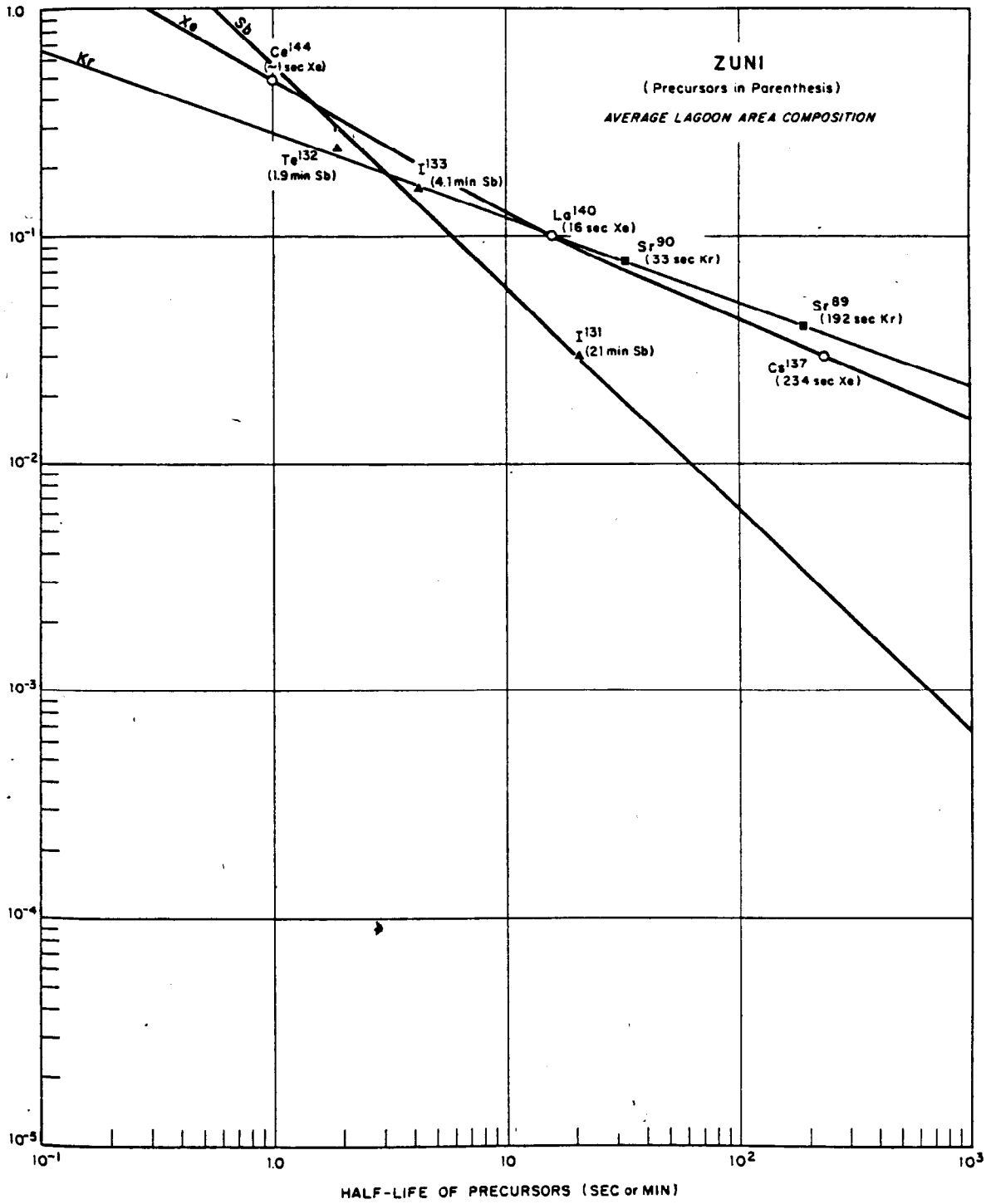

Figure 3.32 Radionuclide fractionation of xenon, krypton, and antimony products, Shot Zuni.

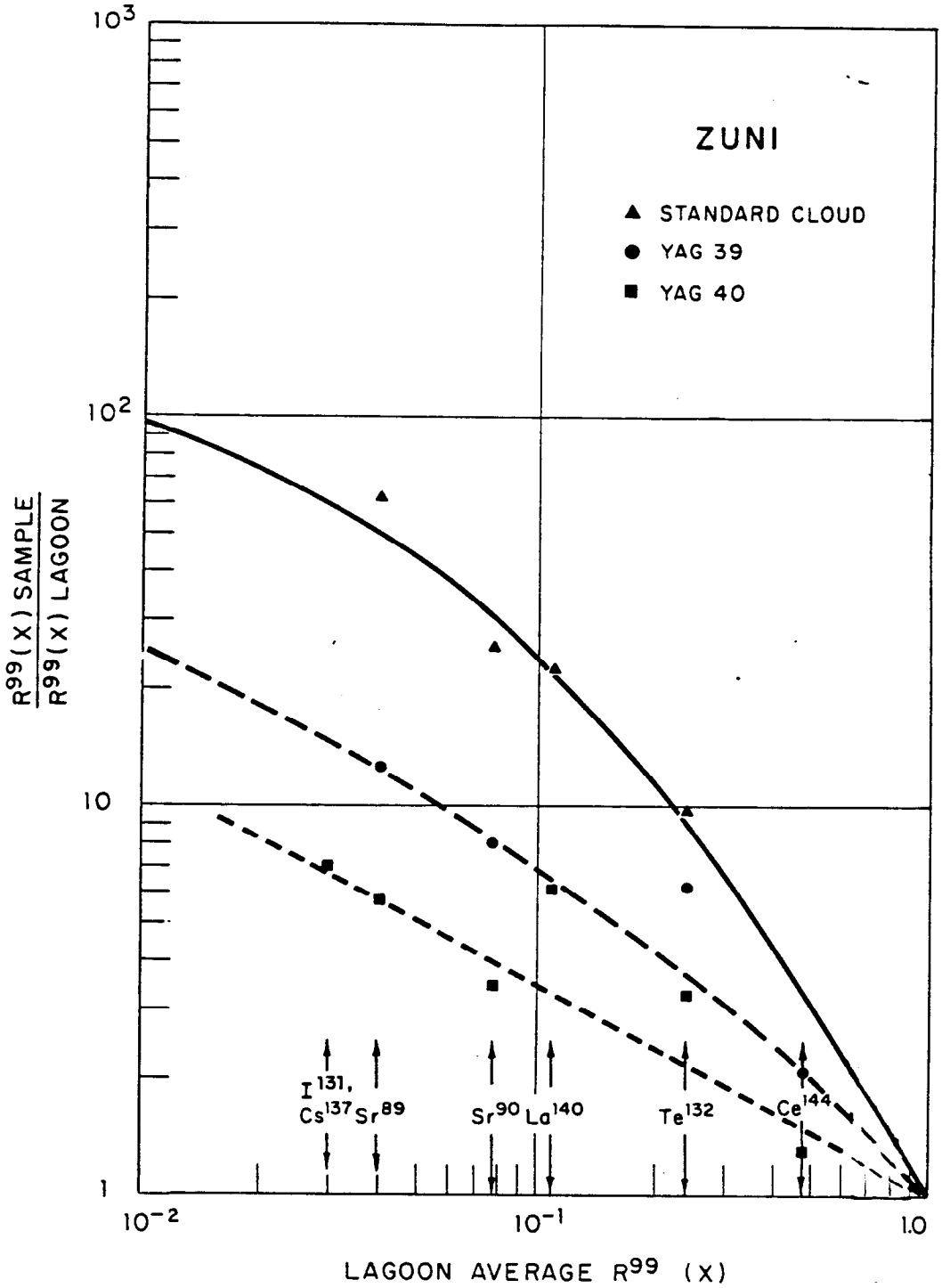

Figure 3.33 R-value relationships for several compositions, Shot Zuni.

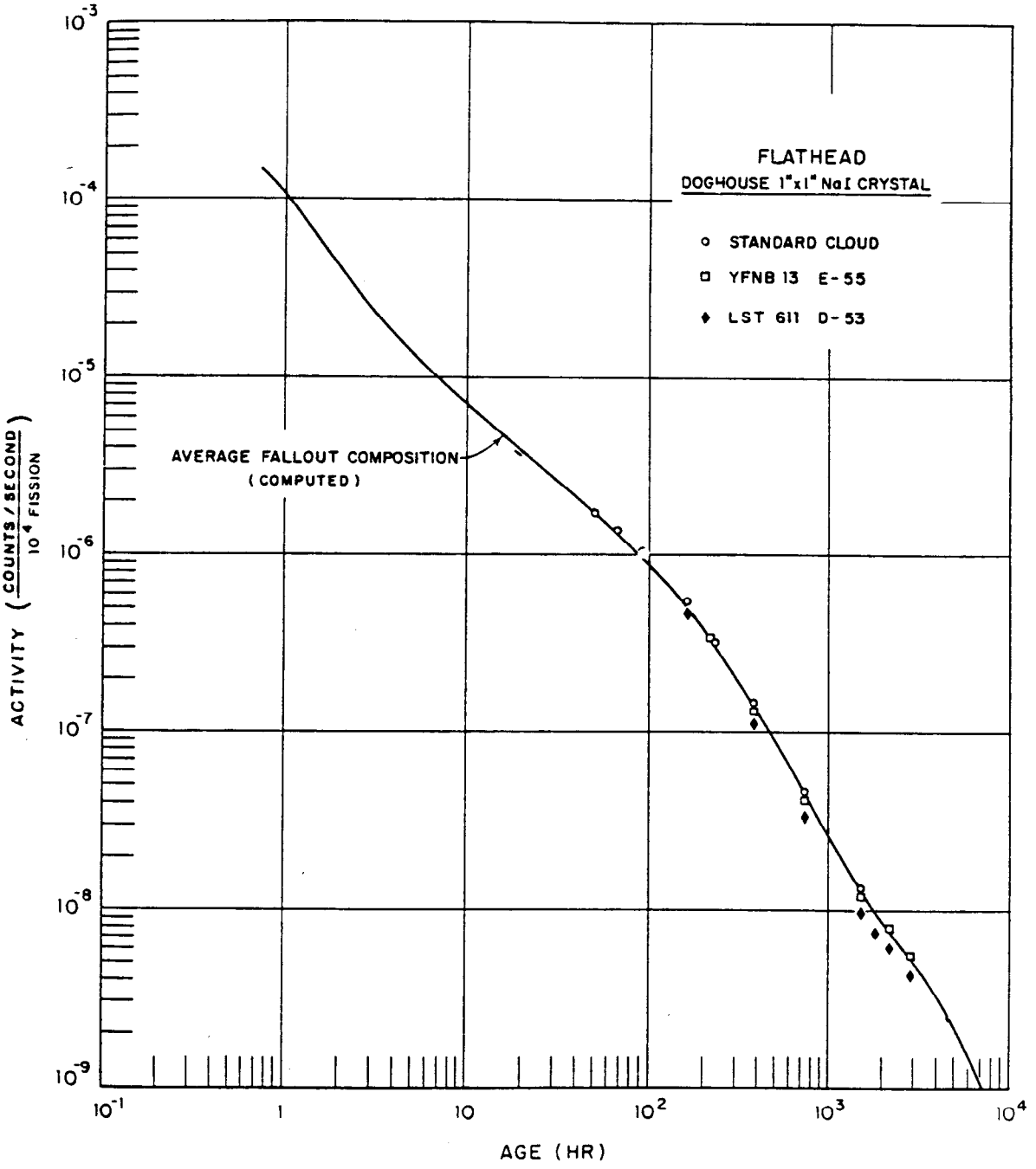

Figure 3.34 Photon-decay rate by doghouse counter, Shot Flathead.

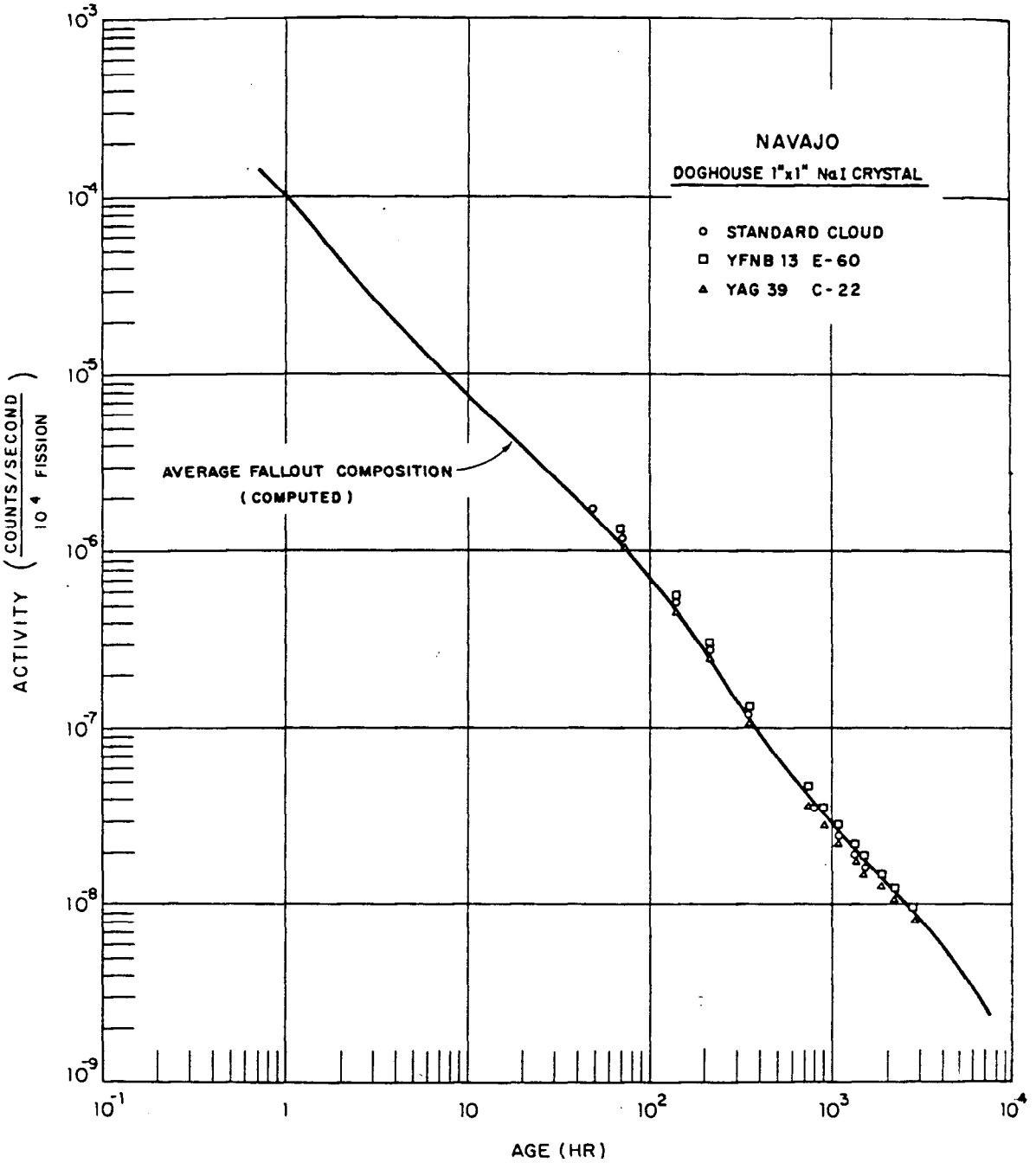

Figure 3.35 Photon-decay rate by doghouse counter, Shot Navajo.

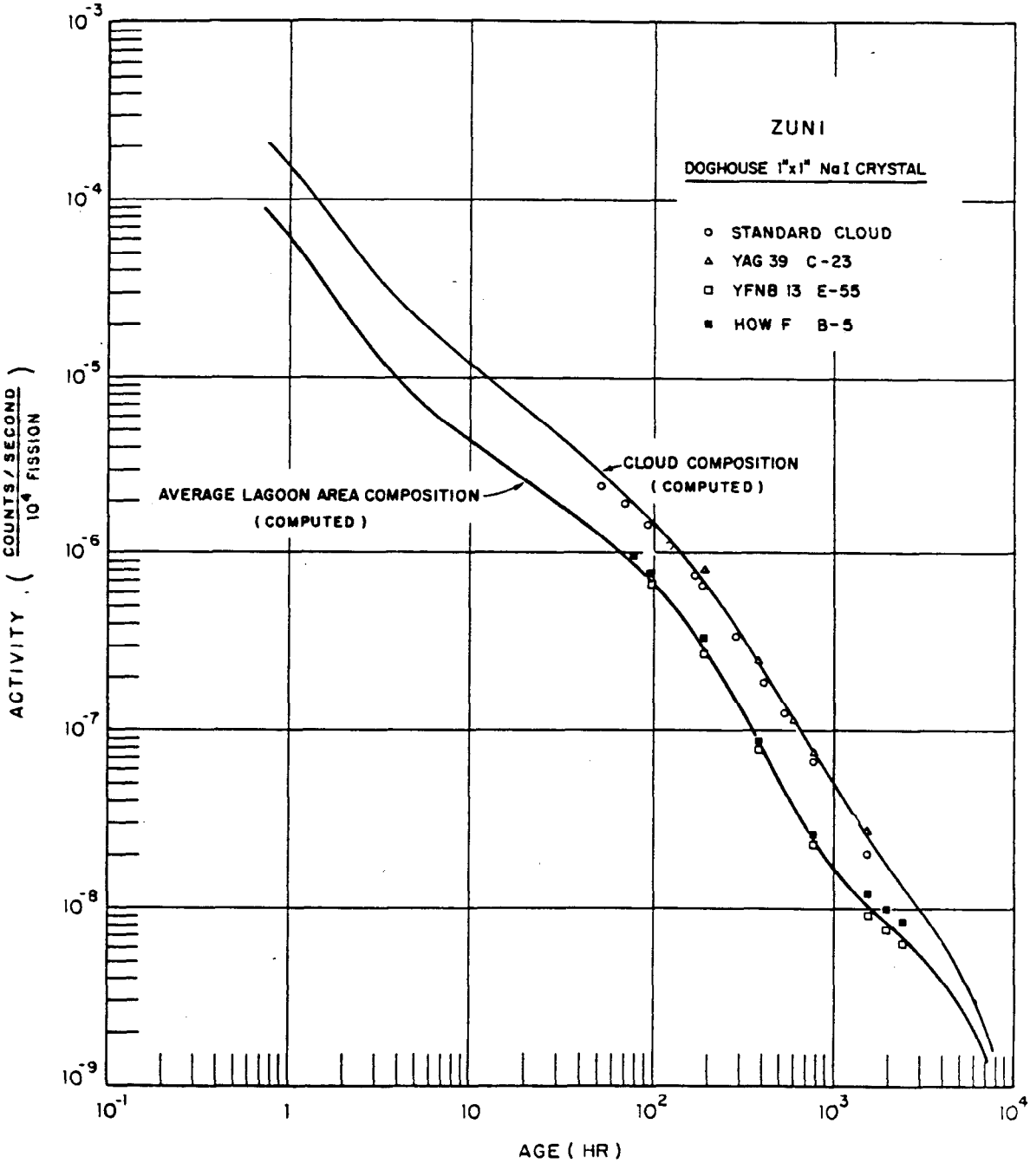

Figure 3.36 Photon-decay rate by doghouse counter, Shot Zuni.

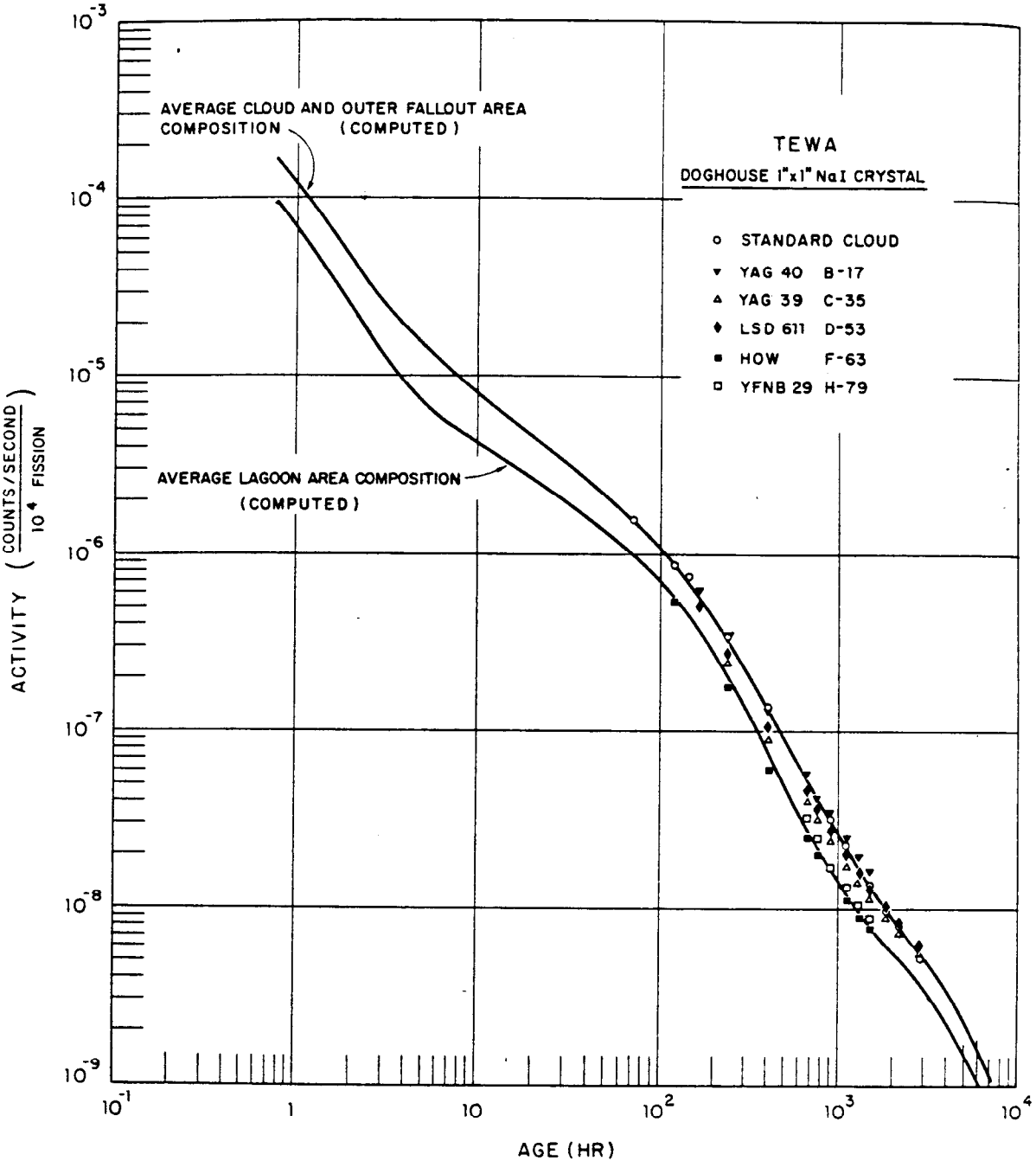

Figure 3.37 Photon-decay rate by doghouse counter, Shot Tewa.

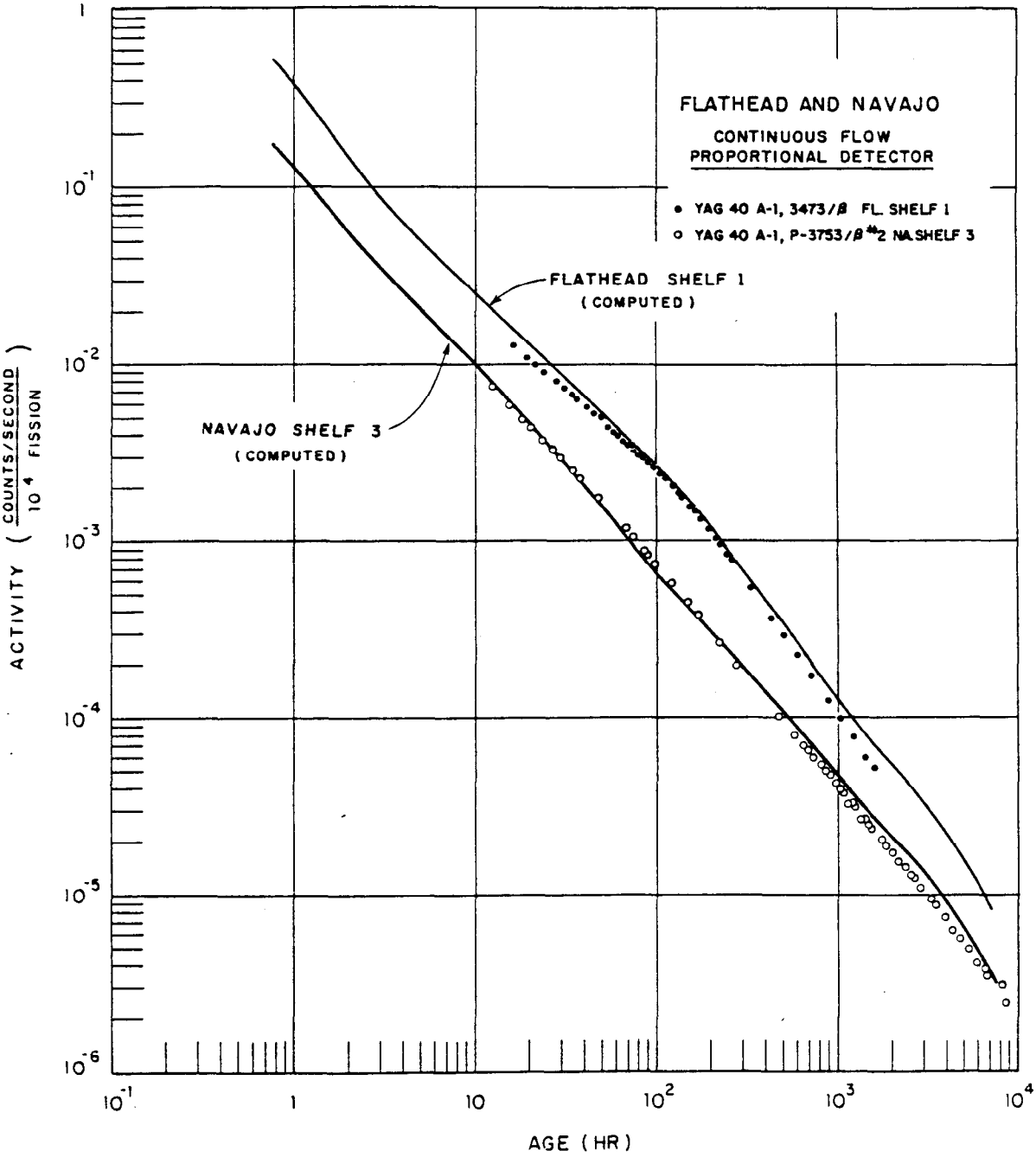

Figure 3.38 Beta-decay rates, Shots Flathead and Navajo.

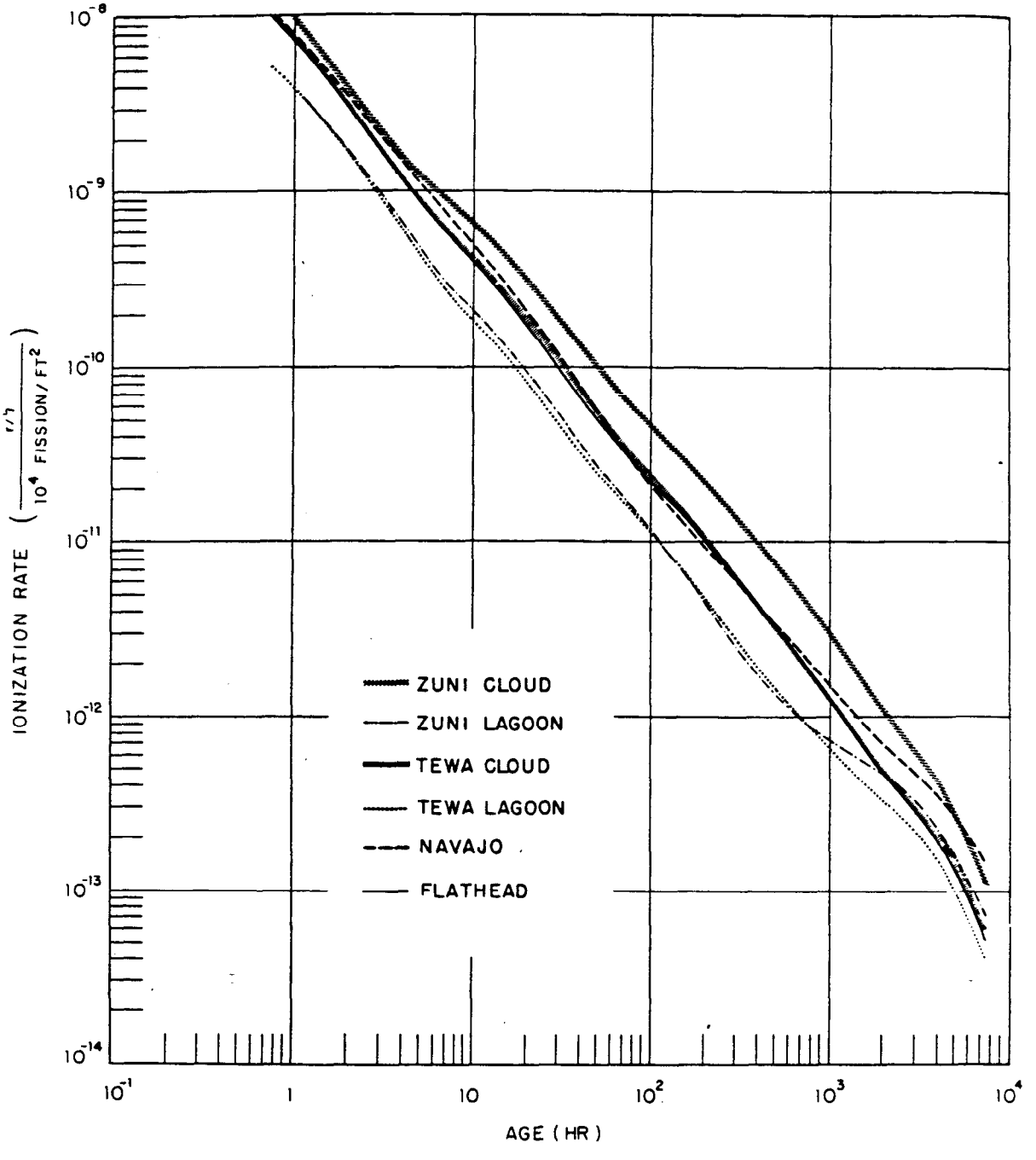

Figure 3.39 Computed ionization-decay rates, Shots Flathead, Navajo, Zuni, and Tewa.

Chapter 4
DISCUSSION

4.1 SHOT CHEROKEE

Because the residual radiation level from Shot Cherokee was too low to be of any military significance, the results were omitted from Chapter 3. However, this should not be interpreted to mean that no fallout occurred; the evidence is clear that very light fallout was deposited over a large portion of the predicted area.

Partly to obtain background data and provide a full-scale test of instrumentation and procedures, and partly to verify that the fallout was as light as anticipated, all stations were activated for the shot, and all exposed sampling trays were processed according to plan (Section 2.4). Small amounts of fallout were observed on the YAG 40 and YAG 39; the collectors removed from Skiffs AA, BB, CC, DD, GG, HH, MM, and VV were slightly active; and low levels of activity were also measured in two water samples collected by the SIO vessel DE 365. Results from all other stations were negative.

The approximate position of each station during the collection interval is shown in Figure 4.1; more exact locations for the skiffs and project ships are included in Tables 2.3 and 2.4. The boundaries of the fallout pattern predicted by the methods described in Section 4.3.1 are also given in the figure, and it may be seen that nearly all of the stations falling within the pattern received some fallout. (Skiff PP and the LST 611 probably do not constitute exceptions, because the former was overturned by the initial shock wave and the incremental collectors on the latter were never triggered.)

On the YAG 40, an increase in normal background radiation was detected with a survey meter at about H+6 hours, very close to the predicted time of fallout arrival. Although the ionization rate never became high enough for significant TIR measurements, open-window survey meter readings were continued until the level began to decrease. The results, plotted in Figure 4.2, show a broad peak of about 0.25 mr/hr centered roughly on H+9 hours. In addition, a few active particles were collected in two SIC and two IC trays during the same period; these results, expressed in counts per minute per minute as before (Section 3.2.1), are given in Figure 4.3. The spread along the time axis reflects the fact that the SIC trays were exposed for longer intervals than usual.

Radioautographs of the tray reagent films showed that all of the activity on each one was accounted for by a single particle, which appeared in every case to be a typical slurry droplet of the type described in Section 3.3.2. Successive gamma-energy spectra and the photon-decay rate of the most active tray (No. 729, ~6,200 counts/min at H+10 hours) were measured and are presented in Figures 4.4 and 4.5. The prominent peaks appearing at ~100 and 220 kev in the former appear to be due to Np^{239}.

A slight rise in background radiation was also detected with a hand survey meter on the YAG 39. The open-window level increased from about 0.02 mr/hr at H+10 hours to 0.15 mr/hr at H+12 hours, before beginning to decline. Only one IC tray was found to be active (No. 56 ~9,200 counts/min at H+10 hours), and this was the control tray exposed on top of the collector for 20 hours from 1300 on D-day to 0900 on D+1. Although about 25 small spots appeared on the reagent film, they were arranged in a way that suggested the breakup of one larger slurry particle on impact; as on the YAG 40 trays, only NaCl crystals were visible under low-power optics in the active regions.

Plots of the gamma-energy spectrum and decay for this sample are included in Figures 4.4 and 4.5; the similarities of form in both cases suggest a minimum of radionuclide fractionation.

By means of the Flathead conversion factor [$\sim 1.0 \times 10^6$ fissions/(dip counts/min at 100 hours)], the dip-counter results for the AOC's from the skiffs have been converted to fissions per square foot in Table 4.1, so that they may be compared with the values for the other shots (Table 3.15). The dip-counter activities of all water samples, including those for the DE 365, are summarized in Table B.32.

4.2 DATA RELIABILITY

The range and diversity of the measurements required for a project of this size virtually precludes the possibility of making general statements of accuracy which are applicable in all cases. Nevertheless, an attempt has been made in Table 4.2 to provide a qualitative evaluation of the accuracy of the various types of project measurements. Quantitative statements of accuracy, and sometimes precision, are given and referenced where available. No attempt has been made, however, to summarize the errors listed in the tables of results in the text; and certain small errors, such as those in station locations in the lagoon area and instrument exposure and recovery times, have been neglected.

Although the remaining estimates are based primarily on experience and judgment, comments have been included in most cases containing the principal factors contributing to the uncertainty. The following classification system is employed, giving both a quality rating and, where applicable, a probable accuracy range:

Class	Quality	Accuracy Range
A	Excellent	± 0 to 10 percent
B	Good	± 10 to 25 percent
C	Fair	± 25 to 50 percent
D	Poor	± ≥ 50 percent
N	No information available	

4.3 CORRELATIONS

4.3.1 Fallout Predictions. As a part of operations in the Program 2 Control Center (Section 2.4), successive predictions were made of the location of the boundaries and hot line of the fallout pattern for each shot. (The hot line is defined in Reference 67 as that linear path through the fallout area along which the highest levels of activity occur relative to the levels in adjacent areas. The measured hot line in the figures was estimated from the observed contours, and the boundary established at the lowest isodose-rate line which was well delineated.) The final predictions are shown superimposed on the interim fallout patterns from Reference 13 in Figures 4.6 through 4.9. Allowance has been made for time variation of the winds during Shots Flathead and Navajo, and for time and space variation during Shots Zuni and Tewa. Predicted and observed times of fallout arrival at most of the major stations, as well as the maximum particle sizes predicted and observed at times of arrival, peak, and cessation, are also compared in Table 4.3. The marked differences in particle collections from close and distant stations are illustrated in Figure 4.10. In the majority of cases, agreement is close enough to justify the assumptions used in making the predictions; in the remaining cases, the differences are suggestive of the way in which these assumptions should be altered.

The fallout-forecasting method is described in detail in Reference 67. This method begins with a vertical-line source above the shot point, and assumes that all particle sizes exist at all altitudes; the arrival points of particles of several different sizes (75, 100, 200, and 350 microns in diameter in this case), originating at the centers of successive 5,000-foot altitude increments are then plotted on the surface. The measured winds are used to arrive at single vectors representative of the winds in each layer, and these vectors are applied to the particle for the period of time required for it to fall through the layer. The required times are calculated from

equations for particle terminal velocity, of the form described by Dallavalle. Such equations consider the variables of particle density, air density, particle diameter, air viscosity, and constants incorporating the effects of gravity and particle shape. (Modified versions of the original Dallavalle equations are presented in Reference 67; data on the Marshall Islands atmosphere required to evaluate air density and air viscosity are also given in this reference.) The last two steps are simplified, however, by the use of a plotting template, so designed that vectors laid off in the wind direction, to the wind speed, automatically include terminal velocity adjustments (Reference 68).

Size lines result from connecting the surface-arrival points for particles of the same size from increasing increments of altitude; height lines are generated by connecting the arrival points of particles of different sizes from the same altitudes. These two types of lines form a network from which the arrival times of particles of various sizes and the perimeter of the fallout pattern may be estimated, once the arrival points representing the line source have been expanded to include the entire cloud diameter. This last step requires the use of a specific cloud model. The model that was used in arriving at the results of Figures 4.6 through 4.9 and Table 4.3 is shown in Figure 4.11. Particles larger than 1,000 microns in diameter were restricted to the stem radius, or inner 10 percent of the cloud radius, while those from 500 to 1,000 microns in diameter were limited to the inner 50 percent of the cloud radius; all particle sizes were assumed to be concentrated primarily in the lower third of the cloud and upper third of the stem.

The dimensions shown in the figures were derived from empirical curves available in the field, relating cloud height and diameter to device yield (Reference 67). Actual photographic measurements of the clouds from Reference 69 were used wherever possible, however, for subsequent calculations leading to results tabulated in Table 4.3.

The location of the hot line follows directly from the assumed cloud model, being determined by the height lines from the lower third of the cloud, successively corrected for time and, sometimes, space variation of the winds. Time variation was applied in the field in all cases, but space variation later and only in cases of gross disagreement. The procedure generally followed was to apply the variation of the winds in the case of the 75- and 100-micron particles and use shot-time winds for the heavier particles. Wind data obtained from balloon runs at 3-hour intervals by the Task Force were used both to establish the initial shot-time winds and make the corrections for time and space variation. The calculations for Shot Zuni are summarized for illustrative purposes in Table B.29.

It is of particular interest to note that it was necessary to consider both time and space variation of the winds for Shots Zuni and Tewa in order to bring the forecast patterns into general agreement with the measured patterns. Vertical air motions were considered for Shot Zuni but found to have little effect on the overall result. It is also of interest to observe that the agreement achieved was nearly as good for Shots Flathead and Navajo with no allowance for space variation as for Shots Zuni and Tewa with this factor included, in spite of the fact that the fallout from the former consisted of slurry rather than solid particles below the freezing level (Sections 3.3.1 and 3.3.2). Whether this difference can be attributed to the gross differences in the nature of the fallout is not known.

4.3.2 Sampling Bias. When a solid object such as a collecting tray is placed in a uniform air stream, the streamlines in its immediate vicinity become distorted, and small particles falling into the region will be accelerated and displaced. As a result, a nonrepresentative or biased sample may be collected. Although the tray will collect a few particles that otherwise would not have been deposited, the geometry is such that a larger number that would have fallen through the area occupied by the tray will actually fall elsewhere. In an extreme case of small, light particles and high wind velocity, practically all of the particles could be deposited elsewhere, because the number deposited elsewhere generally increases with increasing wind velocity and decreasing particle size and density.

This effect has long been recognized in rainfall sampling, and some experimental collectors have been equipped with a thin horizontal windshield designed to minimize streamline distortion

(Reference 72). The sampling of solid fallout particles presents even more severe problems, however, because the particles may also blow out of the tray after being collected, producing an additional deficit in the sample.

In addition, samples collected in identical collectors located relatively close together in a fixed array have been found to vary with the position of the collector in the array and its height above the ground (References 10 and 72). It follows from such studies that both duplication and replication of sampling are necessary to obtain significant results.

Consideration was given to each of these problems in the design of the sampling stations. An attempt was made to minimize and standardize streamline distortion by placing horizontal windshields around all major array platforms and keeping their geometries constant. (The flow characteristics of the standard platform were studied both by small-scale wind-tunnel tests and measurements made on the mounted platform prior to the operation (Reference 73). It was found that a recirculatory flow, resulting in updrafts on the upwind side and downdrafts on the downwind side, developed inside the platform with increasing wind velocity, leading to approximately the same streamline distortion in every case.) Similar windshields were used for the SIC on the YAG 40 and the decay probe tank on the YAG 39, and funnels were selected for the minor array collectors partly for the same reason.

Honeycomb inserts, which created dead-air cells to prevent loss of material, were used in all OCC and AOC collectors. This choice represented a compromise between the conflicting demands for high collection efficiency, ease of sample removal, and freedom from adulterants in subsequent chemical and radiochemical analyses.

Retentive grease surfaces, used in the IC trays designed for solid-particle sampling, facilitated single-particle removal.

All total collectors were duplicated in a standard arrangement for the major arrays; and these arrays, like the minor arrays, were distributed throughout the fallout area and utilized for all shots to provide adequate replication.

At the most, such precautions make it possible to relate collections made by the same kind of sampling arrays; they do not insure absolute, unbiased collections. In effect, this means that, while all measurements made by major arrays may constitute one self-consistent set, and those made by minor arrays another, it is not certain what portion of the total deposited fallout these sets represent. As explained earlier (Section 3.1), this is one reason why radiological properties have been expressed on a unit basis wherever possible. Efforts to interpret platform collections include a discussion and treatment of the relative bias observed within the platforms, as well as comparisons of the resulting platform values with buried-tray and minor array collections on How Island, water sampling and YAG 39 tank collections, and a series of postoperation rainfall measurements made at NRDL.

Relative Platform Bias. The amount of fallout collected by the OCC and AOC_1 collectors in the upwind part of the standard platform was lower than that collected in the downwind portion. It was demonstrated in Reference 74 that these amounts usually varied symmetrically around the platform with respect to wind direction, and that the direction established by the line connecting the interpolated maximum and minimum collections (observed bias direction) coincided with the wind direction. A relative wind varying with time during fallout was treated by vectorial summation, with the magnitude of each directional vector proportional to the amount of fallout occurring in that time. (Variations in the relative wind were caused principally by ship maneuvers, or by oscillation of the anchored barges under the influence of wind and current; directions varying within ± 15 degrees were considered constant.) The resulting collection pattern with respect to the weighted wind resultant (computed bias direction) was similar to that for a single wind, although the ratio of the maximum to the minimum collection (bias ratio) was usually nearer unity, and the bias direction correspondingly less certain.

The variability in relative-wind direction and fallout rate, which could under certain conditions produce a uniform collection around the platform, may be expressed as a bias fraction (defined in Reference 74 as the magnitude of the resultant vector mentioned above divided by the arithmetic sum of the individual vector magnitudes). In effect, this fraction represents a measure of the degree of single-wind deposition purity, because the bias fraction in such a case

would be 1; on the other hand, the resultant vector would vanish for a wind that rotated uniformly around the platform an integral number of times during uniform fallout, and the fraction would be 0.

Where necessary, the mean value of the four OCC and two AOC_1 collectors was chosen as representative for a platform; but when a curve of fallout amount versus angular displacement from the bias direction could be constructed using these collections, the mean value of the curve was obtained from 10 equispaced values between 0 and 180 degrees. The latter applied to all platforms except the LST 611 and the YFNB's, probably indicating disturbances of the air stream incident on the platform by the geometry of the carrier vessel. These platforms, however, were mounted quite low; while the YAG platforms were high enough and so placed as to virtually guarantee undisturbed incidence for all winds forward of the beam.

Pertinent results are summarized in Table 4.4. Fallout amounts per collector are given as doghouse-counter activities at 100 hours, convertible to fissions by the factors given in Table B.13; the mean values so converted appear in Table 3.15. Wind velocities are listed in Table B.37; as in the summary table, the directions given are true for How Island and relative to the bow of the vessel for all other major stations.

No attempt was made to account quantitatively for the values of the bias ratio observed, even for a single-wind system; undoubtedly, the relative amount deposited in the various parts of the platform depends on some function of the wind velocity and particle terminal velocity. As indicated earlier, the airflow pattern induced by the platform itself appeared to be reproducible for a given wind speed, and symmetrical about a vertical plane parallel with the wind direction. Accordingly, for a given set of conditions, collections made on the platform by different instruments with similar intrinsic efficiencies will vary only with location relative to the wind direction. Further experimentation is required to determine how the collections are related to a true ground value for different combinations of particle characteristics and wind speeds.

A limited study of standard-platform bias based on incremental collector measurements was also made, using the data discussed in Section 3.2.4 (Reference 19). These results are presented in Figures 4.12, 4.13, and 4.14. The first compares particle-size frequency distributions of collections made at the same time by different collectors located at the same station; studies for the YAG 39 and YAG 40 during Shots Zuni and Tewa are included. The second compares the total relative mass collected as a function of time, and the variation of relative mass with particle size, for different collectors located at the same station; as above, YAG 39 and YAG 40 collections during Shots Zuni and Tewa were used. The last presents curves of the same type given in Section 3.2.4 for the two IC's located on the upwind side of the YAG 39 platform; these may be compared with the curves in Figure 3.8 which were derived from the IC on the downwind side.

The results show that, except at late times, the overall features of collections made by different instruments at a given station correspond reasonably well, but that appreciable differences in magnitude may exist for a particular time or particle size. In the case of collections made on a single platform (YAG 39), the differences are in general agreement with the bias curves discussed above; and these differences appear to be less than those between collections made near the deck and in the standard platform (A-1 and B-7, YAG 40). It is to be noted that incremental-collector comparisons constitute a particularly severe test of bias differences because of the small size (~ 0.0558 ft^2) of the collecting tray.

How Island Collections. One of the primary purposes of the Site How station was to determine the overall collection efficiency of the total collectors mounted in the standard platform. An area was cleared on the northern end of the island, Platform F with its supporting tower was moved from the YFNB 13 to the center of this area, and 12 AOC_1 trays were filled with local soil and buried in a geometrical array around the tower with their collecting surfaces flush with the ground (Figure 2.8). After every shot, the buried trays were returned to NRDL and counted in the same manner as the OCC trays from the platform.

It is assumed that the collections of these buried trays represent a near-ideal experimental approach to determining the amount of fallout actually deposited on the ground. (Some differences, believed minor, were present in OCC and AOC_1-B doghouse-counter geometries. Very

little differential effect is to be expected from a lamina of activity on top of the 2 inches of sand versus activity distributed on the honeycomb insert and bottom of the tray. The more serious possibility of the active particles sifting down through the inert sand appears not to have occurred, because the survey-meter ratios of AOC_1-B's to OCC's taken at Site Nan, Site Elmer, and NRDL did not change significantly with time.)

In Table 4.5, weighted-mean platform values, obtained as described above, are converted to fissions per square foot and compared to the average buried-tray deposit taken from Table B.27. It may be seen that, within the uncertainty of the measurements, the weighted-mean platform values are in good agreement with the ground results. It must be recalled, however, that single winds prevailed at How Island for all shots, and that the observed bias ratios were low (< 2).

The AOC_2 collections at Station K (Table 3.15) are also included in Table 4.5 for comparison. They appear to be consistently slightly lower than the other determinations, with the exception of the much lower value for Shot Navajo. The latter may be due to recovery loss and counting error resulting from the light fallout experienced at the station during this shot. Because only one collector was present in each minor sampling array, bias studies of the kind conducted for the major arrays were not possible. As mentioned earlier, however, an attempt was made to minimize bias in the design of the collector and, insofar as possible, to keep geometries alike. Although it was necessary to reinforce their mounting against blast and thermal damage on the rafts and islands (Figure 2.7), identical collectors were used for all minor arrays.

Shipboard Collections and Sea Water Sampling. The platform collections of the YAG 39 and YAG 40 may be compared with the water-sampling results reported in Reference 20, decay-tank data from the YAG 39, and in some cases with the water-sampling results from the SIO vessel Horizon (Reference 15). Strictly speaking, however, shipboard collections should not be compared with post-fallout ocean surveys, because, in general, the fallout to which the ship is exposed while attempting to maintain geographic position is not that experienced by the element of ocean in which the ship happens to be at cessation.

The analysis of an OCC collection for total fission content is straightforward, although the amount collected may be biased; the ocean surface, on the other hand, presents an ideal collector but difficult analytical problems. For example, background activities from previous shots must be known with time, position, and depth; radionuclide fractionation, with depth, resulting from leaching in sea water should be known; and the decay rates for all kinds of samples and instruments used are required. Fallout material which is fractionated differently from point-to-point in the fallout field before entry into the ocean presents an added complication.

Table 4.6 summarizes the results of the several sampling and analytical methods used. The ocean values from Reference 20 were calculated as the product of the equivalent depth of penetration (Section 3.2.5) at the ship and the surface concentration of activity (Method I). The latter was determined in every case by averaging the dip-count values of appropriate surface samples listed in Table B.32 and converting to equivalent fissions per cubic foot. When penetration depths could not be taken from the plots of equivalent depth given in Figure B.1, however, they had to be estimated by some other means. Thus, the values for both ships during Shot Zuni were assumed to be the same as that for the YAG 39 during Shot Tewa; the value for the YAG 39 during Shot Flathead was estimated by extrapolating the equivalent depth curve, while that for the YAG 40 was taken from the same curve; and the values for the YAG 40 during Shots Navajo and Tewa were estimated from what profile data was available.

The conversion factor for each shot (fissions/(dip counts/min at 200 hours) for a standard counting volume of 2 liters) was obtained in Method I from the response of the dip counter to a known quantity of fissions. Although direct dip counts of OCC aliquots of known fission content became available at a later date (Table B.15), it was necessary at the time to derive these values from aliquots of OCC and water samples measured in a common detector, usually the well counter. The values for the decay tank listed under Method I in Table 4.6 were also obtained from dip counts of tank samples, similarly converted to fissions per cubic foot. Dip-counter response was decay-corrected to 200 hours by means of the normalized curves shown in Figure B.14.

Another estimate of activity in the ocean was made (private communication from R. Caputi, NRDL), using the approach of planimetering the total areas of a number of probe profiles meas-

ured at late times in the region of YAG 39 operations during Shots Navajo and Tewa (Method II). (The probe profiles were provided, with background contamination subtracted out and converted from microamperes to apparent milliroentgens per hour by F. Jennings, Project 2.62a, SIO. Measurements were made from the SIO vessel Horizon.) The integrated areas were converted to fissions per square foot by applying a factor expressing probe response in fissions per cubic foot. This factor was derived from the ratio at 200 hours of surface probe readings and surface sample dip counts from the same station, after the latter had been expressed in terms of fissions using the direct dip counter-OCC fission content data mentioned above. These results are also listed in Table 4.6.

The set of values for the YAG 39 decay tank labeled Method III in the same table is based on direct radiochemical analyses of tank (and ocean surface) samples for Mo^{99} (Table B.30). The results of Methods I and II were obtained before these data became available and, accordingly, were accomplished without knowledge of the actual abundance distribution of molybdenum with depth in sea water.

Table 4.7 is a summary of the dip-to-fission conversion factors indicated by the results in Table B.30; those used in Methods I and II are included for comparison. It is noteworthy that, for the YAG 39, the ocean surface is always enriched in molybdenum, a result which is in agreement with the particle dissolution measurements described earlier (Figures 3.11 and 3.12); in this experiment Mo^{99}, Np^{239}, and probably I^{131} were shown to begin leaching out preferentially within 10 seconds. The tank value for Shot Zuni, where the aliquot was withdrawn before acidifying or stirring, shows an enrichment factor of ~3.5 relative to the OCC; acidification and stirring at Shot Tewa eliminated the effect. The slurry fallout from Shots Flathead and Navajo, however, shows only a slight tendency to behave in this way.

Finally, Table 4.6 also lists the representative platform values obtained earlier, as well as the maximum values read from the platform-collection curves for the cases where deposition occurred under essentially single-wind conditions (Table 4.4). These values are included as a result of postoperation rainfall measurements made at NRDL (Table B.31). (Although the data have not received complete statistical analysis, the ratio of the maximum collection of rainfall by an OCC on the LST 611 platform to the average collection of a ground array of OCC trays is indicated to be 0.969 ± 0.327 for a variety of wind velocities (Reference 75).)

It may be seen by examination of Table 4.6 that the most serious discrepancies between ocean and shipboard collections arise in two cases: the YAG 39 during Shot Zuni, where the ocean/OCC (maximum) ratio of ~2 may be attributed entirely to the fission/dip conversions employed —assuming the OCC value is the correct average to use for a depth profile; and the YAG 39 during Shot Navajo, where the ocean/OCC ratio is ~10, but the tank radiochemical value and the Horizon profile value almost agree within their respective limits. While the OCC value appears low in this multiwind situation, the difference between the YAG 39 and Horizon profiles may be the background correction made by SIO.

In the final analysis, the best and most complete data were obtained at the YAG 39 and Horizon stations during Shot Tewa. Here, preshot ocean surface backgrounds were negligibly small; equipment performed satisfactorily for the most part; the two vessels ran probe profiles in sight of each other; and the Horizon obtained depth samples at about the same time. The YAG 39 did not move excessively during fallout, and the water mass of interest was marked and followed by drogue buoys. In addition to the values reported in Table 4.6, the value 1.82×10^{15} fissions/ft^2 was obtained for the depth-sample profile, using the dip-to-fission factor indicated in Table 4.7. (Because of the variations in the fission conversion factor with the fractionation exhibited from sample to sample, a comparison was made of the integral value of the dip counts (dip counts/min)/2 liters) feet from the depth-sample profile with the OCC YAG 39-C-21 catch expressed in similar units. The ratio ocean integral/OCC-C-21 = 1.08 was obtained.)

It may be seen that all values for this shot and area agree remarkably well, in spite of the fact that Method I measurements extend effectively down to the thermocline, some of the Method II profiles to 500 meters, and the depth sample cast to 168 meters. If the maximum OCC catch is taken as the total fallout, then it must be concluded that essentially no activity was lost to depths greater than those indicated. Although the breakup of friable particles and dissolution

of surface-particle activity might provide an explanation, contrary evidence exists in the rapid initial settling rates observed in some profiles, the solid nature of many particles from which only ~20 percent of the activity is leachable in 48 hours, and the behavior of Zuni fallout in the YAG 39 decay tank. Relative concentrations of 34, 56, and 100 were observed for samples taken from the latter under tranquil, stirred, and stirred-plus-acidified conditions. (Based on this information and the early Shot Tewa profiles of Figure 3.10, the amount lost is estimated at about 50 percent at the YAG 39 locations in Reference 20.) If on the other hand it is assumed that a certain amount of activity was lost to greater depths, then the curious coincidence that this was nearly equal to the deficit of the maximum OCC collection must be accepted.

It is unlikely that any appreciable amount of activity was lost below the stirred layer following Shots Flathead and Navajo. No active solids other than the solids of the slurry particles, which existed almost completely in sizes too small to have settled below the observed depth in the time available, were collected during these shots (Section 3.3.2).

In view of these considerations and the relative reliability of the data (Section 4.2), it is recommended that the maximum platform collections (Table B.12) be utilized as the best estimate of the total amount of activity deposited per unit area. An error of about ±50 percent should be associated with each value, however, to allow for the uncertainties discussed above. Although strictly speaking, this procedure is applicable only in those cases where single-wind deposition prevailed, it appears from Table 4.6 that comparable accuracy may be achieved for cases of multiwind deposition by retaining the same percent error and doubling the mean platform value.

4.3.3 Gross Product Decay. The results presented in Section 3.4.6 allow computation of several other radiological properties of fission products, among them the gross decay exponent. Some discussion is warranted because of the common practice of applying a $t^{-1.2}$ decay function to any kind of shot, at any time, for any instrument.

This exponent, popularized by Reference 58, is apparently based on a theoretical approximation to the beta-decay rate of fission products made in 1947 (Reference 59), and some experimental gamma energy-emission rates cited in the same reference. Although these early theoretical results are remarkably good when restricted to the fission-product properties and times for which they were intended, they have been superseded (References 41, 60, 61, and 62); and, except for simple planning and estimating, the more-exact results of the latter works should be used.

If fractionation occurs among the fission products, they can no longer be considered a standard entity with a fixed set of time-dependent properties; a fractionated mixture has its own set of properties which may vary over a wide range from that for normal fission products.

Another source of variation is induced activities which, contrary to Section 9.19 of Reference 47, can significantly alter both the basic fission-product-decay curve shape and gross property magnitudes per fission. The induced products contributed 63 percent of the total dose rate in the Bikini Lagoon area 110 hours after Shot Zuni; and 65 percent of the dose rate from Shot Navajo products at an age of 301 days was due to induced products, mainly Mn^{54} and Ta^{182}. Although many examples could be found where induced activities are of little concern, the a priori assumption that they are of negligible importance is unsound.

Because the gross disintegration rate per fission of fission products may vary from shot to shot for the reason mentioned above, it is apparent that gamma-ray properties will also vary, and the measurement of any of these with an instrument whose response varies with photon energy further complicates matters.

Although inspection of any of the decay curves presented may show an approximate $t^{-1.2}$ average decay rate when the time period is judiciously chosen, it is evident that the slope is continuously changing, and more important, that the absolute values of the functions, e.g., photons per second per fission or roentgens per hour per fissions per square foot, vary considerably with sample composition.

As an example of the errors which may be introduced by indiscriminate use of the $t^{-1.2}$

tion or by assuming that all effects decay alike, consider the lagoon-area ionization curve for Shot Tewa (Figure 3.39) which indicates that the 1-hour dose rate may be obtained by multiplying the 24-hour value by 61.3. A $t^{-1.2}$ correction yields instead a factor of 45.4 (−26 percent error), and if the doghouse-decay curve is assumed proportional to the ionization-decay curve, a factor of 28.3 (−54 percent) results. To correct any effect to another time it is important, therefore, to use a theoretical or observed decay rate for that particular effect.

4.3.4 Fraction of Device by Chemistry and Radiochemistry. The size of any sample may be expressed as some fraction of device. In principle, any device component whose initial weight is known may serve as a fraction indicator; and in the absence of fractionation and analytical errors, all indicators would yield the same fraction for a given sample. In practice, however, only one or two of the largest inert components will yield enough material in the usual fallout sample to allow reliable measurements. These measurements also require accurate knowledge of the amount and variability of background material present, and fractionation must not be introduced in the recovery of the sample from its collector.

The net amounts of several elements collected have been given in Section 3.4.4, with an assessment of backgrounds and components of coral and sea water. The residuals of other elements are considered to be due to the device, and may therefore be converted to fraction of device (using Table B.17) and compared directly with results obtained from Mo^{99}. This has been done for iron and uranium, with the results shown in Table 4.8. Fractions by copper proved inexplicably high (factors of 100 to 1,000 or more), as did a few unreported analyses for lead; these results have been omitted. The iron and uranium values for the largest samples are seen to compare fairly well with Mo^{99}, while the smaller samples tend to yield erratic and unreliable results.

4.3.5 Total Dose by Dosimeter and Time-Intensity Recorder. Standard film-pack dosimeters, prepared and distributed in the field by the U. S. Army Signal Engineering Laboratories, Project 2.1, were placed at each major and minor sampling array for all shots. Following sample recovery, the film packs were returned to this project for processing and interpretation as described in Reference 76; the results appear in Table 4.9.

The geometries to which the dosimeters were exposed were always complicated and, in a few instances, varied between shots. In the case of the ship arrays, they were located on top of the TIR dome in the standard platform. On How-F and YFNB 29, Shot Zuni, they were taped to an OCC support ~2 feet above the deck of the platform before the recovery procedure became established. All other major array film packs were taped to the RA mast or ladder stanchion ~2.5 feet above the rim of the platform to facilitate their recovery under high-dose-rate conditions. Minor array dosimeters were located on the exterior surface of the shielding cone ~4.5 feet above the base in the case of the rafts and islands, and ~5 feet above the deck on the masts of all skiffs except Skiffs BB and DD where they were located ~10 feet above the deck on the mast for Shot Zuni; subsequently the masts were shortened for operational reasons.

Where possible, the dose recorded by the film pack is compared with the integrated TIR readings (Table B.1) for the period between the time of fallout arrival at the station and the time when the film pack was recovered; the results are shown in Table 4.9. It has already been indicated (Section 3.4.6) that the TIR records only a portion of the total dose in a given radiation field because of its construction features and response characteristics. This is borne out by Table 4.10, which summarizes the percentages of the film dose represented in each case by the TIR dose.

It is interesting to observe that for the ships, where the geometry was essentially constant, this percentage remains much the same for all shots except Navajo, where it is consistently low. The same appears to be generally true for the barge platforms, although the results are much more difficult to evaluate. A possible explanation may lie in the energy-response curves of the TIR and film dosimeter, because Navajo fallout at early times contained Mn^{56} and Na^{24} —both of which emit hard gamma rays—while these were of little importance or absent in the other shots.

4.3.6 Radiochemistry-Spectrometry Comparison. Calibrated spectrometer measurements on samples of known fission content allow expected counting rates to be computed for the samples in any gamma counter for which the response is simply related to the gross photon frequency and energy. Accordingly, the counting rate of the doghouse counter was computed for the standard-cloud samples by application of the calibration curve (Reference 43) to the spectral lines and frequencies reported in Reference 57 and reproduced in Table B.20. These results are compared with observations in Table 4.11, as well as with those obtained previously using radiochemical-input information with the same calibration curve. Cloud samples were chosen, because the same physical sample was counted both in the spectrometer and doghouse counter, thereby avoiding uncertainties in composition or fission content introduced by aliquoting or other handling processes.

Several of the spectrometers used by the project were uncalibrated, that is, the relation between the absolute number of source photons emitted per unit time at energy E and the resulting pulse-height spectrum was unknown. A comparison method of analysis was applied in these cases, requiring the area of a semi-isolated reference photopeak, whose nuclide source was known, toward the high-energy end of the spectrum. From this the number of photons per seconds per fissions per area can be computed. The area of the photopeak ascribed to the induced product, when roughly corrected by assuming efficiency to be inversely proportional to energy, yields photons per seconds per fissions. The latter quantity leads serially, via the decay scheme, to disintegration rate per fission at the time of measurement, then to atoms at zero time per fission, which is the desired product/fission ratio. The γ line at 0.76 Mev provides a satisfactory reference from ~30 days to 2 years, but the gross spectra are usually not simple enough to permit use of this procedure until an age of ~½ year has been reached.

A few tracings of the recorded spectra appear in Figure 4.15, showing the peaks ascribed to the nuclides of Table 3.20. Wherever possible, spectra at different ages were examined to insure proper half-life behavior, as in the Mn^{56} illustration. The Zuni cloud-sample spectrum at 226 days also showed the 1.7-Mev line of Sb^{124}, though not reproduced in the figure. This line was barely detectable in the How Island spectrum, shown for comparison, and the 0.60-Mev line of Sb^{124} could not be detected at all.

Average energies, photon-decay rates and other gamma-ray properties have been computed from the reduced spectral data in Table B.20 and appear in Table B.21.

4.3.7 Air Sampling. As mentioned earlier, a prototype instrument known as the high volume filter (HVF) was proof-tested during the operation on the ship-array platforms. This instrument, whose intended function was incremental aerosol sampling, is described in Section 2.2. All units were oriented fore and aft in the bow region of the platform between the two IC's shown in Figure A.1. The sampling heads opened vertically upward, with the plane of the filter horizontal, and the airflow rate was 10 ft^3/min over a filter area of 0.0670 ft^2, producing a face velocity of 1.7 mph.

The instruments were manually operated according to a fixed routine from the secondary control room of the ship; the first filter was opened when fallout was detected and left open until the TIR reading on the deck reached ~1 r/hr; the second through the seventh filters were exposed for ½-hour intervals, and the last filter was kept open until it was evident that the fallout rate had reached a very low level. This plan was intended to provide a sequence of relative air concentration measurements during the fallout period, although when 1 r/hr was not reached only one filter was exposed. Theoretically, removal of the dimethylterephalate filter material by sublimation will allow recovery of an unaltered, concentrated sample; in practice however, the sublimation process is so slow that it was not attempted for this operation.

After the sampling heads had been returned to NRDL, the filter material containing the activity was removed as completely as possible and measured in the 4-π ionization chamber; these data are summarized in Table B.36. It may be seen that the indicated arrival characteristics generally correspond with those shown in Figures 3.1 to 3.4.

A comparative study was also made for some shots of the total number of fissions per square foot collected by HVF's, IC's, and OCC's located on the same platform. Ionization-chamber

activities were converted to fissions by means of aliquots from OCC YAG 39-C-21, Shots Flathead and Navajo, and YAG 40-B-6, Shot Zuni, which had been analyzed for Mo^{99}. It may be seen in Table 4.12 that, with one exception, the HVF collected about the same or less activity than the other two instruments. In view of the horizontal aspect of the filter and the low airflow rate used, there is little question that the majority of the activity the HVF collected was due to fallout. The results obtained should not, therefore, be interpreted as an independent aerosol hazard.

TABLE 4.1 ACTIVITY PER UNIT AREA FOR SKIFF STATIONS, SHOT CHEROKEE

No fallout was collected on the skiffs omitted from the table.

Station	Dip counts/min at H + hr		Approximate fissions/ft^2
AA	3,094	196.6	2.5×10^{10}
BB	3,094	196.6	2.5×10^{10}
CC	4,459	150.3	2.8×10^{10}
DD	9,885	214.2	8.7×10^{10}
GG	5,720	196.2	4.6×10^{10}
HH	858	196.1	6.9×10^{9}
MM	8,783	214.0	7.7×10^{10}
VV	452	432.0	8.0×10^{9}

TABLE 4.2 EVALUATION OF MEASUREMENT AND DATA RELIABILITY

I. Field Measurements and Deposition Properties

Class	Measurement	Instrument	Comments
A	Station location, ships	—	±500 to 1,000 yards.
A	Station location, skiffs	—	±1,000 yards.
A-C	Time of arrival	TIR	Arbitrary selection of significant increase above background.
A-C	Time of arrival	IC	Uncertainty in first tray significantly above background; arrival uncertain within time interval tray exposed.
A-D	Time of arrival	TOAD	Uncertain for initially low rates of field increase; malfunctions on skiffs; clock-reading difficulties.
A	Time of peak ionization rate	TIR	—
A-C	Time of peak fallout arrival rate	IC	Uncertain for protracted fallout duration and sharp deposition rate peaks.
D	Time of cessation	TIR	Depends on knowledge of decay rate of residual material.
B-D	Time of cessation	IC	Rate plot for protracted fallout and fallout with sharp deposition-rate peaks may continue to end of exposure period; cumulative activity slope approaches 1.
C	Ionization rate, in situ	TIR	Poor directional-energy response (Appendix A.2); variations in calibration; poor inter-chamber agreement.
C	Apparent ionization rate, in ocean	SIO-P	Calibration variable, mechanical difficulties.
C	Apparent ionization rate, in tank	SIO-D	Calibration variable, electrical difficulties.
N	Ionization rate, above sea surface	NYO-M	High self-contamination observed.
B	Ionization rate, in situ	T1B, Cutie Pie	Calibration for point source in calibration direction; readings ~20 percent low above extended source.
C	Total dose	TIR	See above: Ionization rate, TIR.
N	Total dose	ESL film pack	Assumed ±20 percent.
D	Weight of fallout/area	OCC	Bias uncertainty (Section 4.3.2); variability of background collections; see below: Elemental composition, fallout.
D	Fraction of device/area (Fe, U)	OCC	Bias uncertainty(Section 4.3.2); uncertainty of indicator abundance in device surroundings; see below: Elemental composition, fallout.
D	Original coral-sea-water constituents	OCC	Variations in atoll, reef, and lagoon bottom composition; see below: Elemental composition, fallout.
C	Fissions and fraction of device/area (Mo^{99})	OCC	Bias uncertainty (Section 4.3.2); device fission yield uncertainty.
D	Fissions/area	SIO-P, dip	Uncertainties in dip to fission conversion factor, ocean backgrounds, fractionation of radionuclides, motion of water; see above: Apparent ionization rate, in ocean.

TABLE 4.2 CONTINUED

II. Laboratory Activity Measurements.

Class	Measurement	Sample	Comments
A	Gamma activity, doghouse	OCC, AOC_1, AOC_1-B	Precision better than ±5 percent, except for end portion of decay curves.
A-C	Gamma activity, dip	AOC_2 aliquots, tank, sea water	Aliquoting uncertainty with occasional presence of solids in high specific-activity sample.
A	Gamma activity, end-window	IC trays	Precision better than ±5 percent.
A	Gamma activity, well	Individual particles, aliquots of most samples	Precision for single particles ±3 percent (Reference 26).
B	Gamma activity, 4-π ion chamber	Aliquots of most samples	Some skill required in operation; precision ±5 to 20 percent at twice background (Reference 26).
A	Mo^{99} assay, radiochemical	OCC, cloud	Accuracy ±10 percent (Reference 34).
B	Radiochemical R-values, product/fission ratios	OCC, cloud	Accuracy of nuclide determination ±20 to 25 percent (Reference 34).
D	Spectrometry R-values, product/fission ratios	OCC, cloud, IC	Factor of 2 or 3; misidentification possible.
A	Relative decay rates, all instruments	All required	With few exceptions, necessary decay corrections made from observed decay rates of appropriate samples in counters desired.

III. Laboratory Physical and Chemical Measurements

Class	Measurement	Sample	Comments
A	Chloride content, slurry drops	IC reagent film	Accuracy ±5 percent (Reference 31).
B	Water volume, slurry drops	IC reagent film	Accuracy ±25 percent (Reference 31).
D	Identification, compounds and elements of slurry solids	IC reagent films, OCC	Possible misidentification; small samples, small number of samples.
A	Solid particle weights	IC trays, OCC, unscheduled	Accuracy and precision ±5 μg, leading to ±1 percent or better on most particles (Reference 26).
A	Solid particle densities	IC trays, OCC, unscheduled	Precision better than ±5 percent.
C	Elemental composition, fallout	OCC	Large deviations in composition from duplicate trays; recovery loss, and possible fractionation, ~40 mg; honeycomb interference.
D	Identification, compounds and elements of slurry solids	IC reagent film, OCC	Possible misidentification; small samples; small number of samples.
B-C	Particle size-frequency distributions, concentrations and relative weights versus time	IC trays	Difficulties in recognition of discrete particles, treatment of flaky or aggregated particles; uncertain application of defined diameter to terminal-velocity equations; tray backgrounds and photographic resolution in smaller size ranges.

IV. Radiation Characteristics Data

Class	Item	Comments
A-C	Gamma-ray decay schemes	Amount of decay scheme data available dependent on particular nuclide.
A-B	Fission-product-disintegration rates	About ±20 percent for time period considered (Reference 41).
N	Computed $\frac{\text{r/hr at 3 ft above infinite plane}}{\text{photon/time/area}}$ versus photon energy	Error assumed small compared to errors in fallout concentration, radionuclide composition, and decay scheme data.
B	Absolute calibration, beta counter	Personal communication from J. Mackin, NRDL.
B	Absolute calibration, doghouse counter	Uncertainty in disintegration rate of calibrating nuclides; dependence on gamma-ray decay schemes.

TABLE 4.3 COMPARISON OF PREDICTED AND OBSERVED TIMES OF ARRIVAL AND MAXIMUM PARTICLE-SIZE VARIATION WITH TIME

Shot *	Station	Time of Arrival		Maximum Particle Size (microns) at					
				Time of Arrival		Time of Peak Activity †		Time of Cessation †	
		Predicted	Observed †	Predicted	Observed ‡	Predicted	Observed ‡	Predicted	Observed ‡
		TSD, hr							
Flathead	YFNB 13	§	0.35	—	—	—	—	—	—
	How I	§	§	—	—	—	—	—	—
	YAG 39	3	4.5	200	—	¶	—	¶	—
	YAG 40	9	8.0	125	—	70	120	<70	—
	LST 611	6	6.6	120	112	¶	—	¶	—
Navajo	YFNB 13	<0.5	0.20	>1,000	—	>1,000	—	—	—
	How I	1.5	0.75	500	—	500	—	¶	—
	YAG 39	2	2.3	500	—	180	—	~100	—
	YAG 40	4	6.0	200	—	130	96	~75	84
	LST 611	3	3.0	300	—	180	166	—	—
Zuni	YFNB 13	<1	0.33	500	1,400	500	695	500	545
	How I	<1.5	0.38	>500	—	>500	365	>500	—
	YAG 40	~6	3.4	§	325	150	300	125	245
	YAG 39	9	12	100	—	¶	—	¶	—
	LST 611	§	§	—	—	—	—	—	—
Tewa	YFNB 13	<0.5	0.25	2,000	285	350	—	¶	—
	YFNB 29	<1	0.23	800	1,100	500	1,000	¶	—
	How I	1	1.6	1,000	205	250	285	¶	—
	YAG 39	2	2.0	500	—	180	395	¶	—
	YAG 40	3.5	4.4	200	—	100	285	90	255
	LST 611	7	7.0	150	285	80	205	—	—

* The following cloud dimensions were used in the calculations:

	Shot Flathead	Shot Navajo	Shot Zuni	Shot Tewa
Top, × 1,000 ft	65	85	80	90
Base, × 1,000 ft	35	50	50	50
Diameter, naut mi	6	40	40	60

† Table 3.1.

‡ Section 3.2.4 and Tables B.3 and B.5.

§ No fallout, or no fallout at reference time.

¶ Fallout completed by reference time.

TABLE 4.4 RELATIVE BIAS OF STANDARD-PLATFORM COLLECTIONS

Platform	Shot	Collection Curve		Bias Ratio	Bias Fraction	Bias Direction		Weighted Mean Platform Value
		Maximum	Minimum			Observed	Computed	
		doghouse counts/min at 100 hrs				deg	deg	doghouse counts/min at 100 hrs
How F	Zuni	2.91×10^6	1.59×10^6	1.8	1.0	75	77	$2.24 \pm 0.51 \times 10^6$
	Flathead	*	*	*	*	*	*	*
	Navajo	1.98×10^4	1.45×10^4	1.4	1.0	75	79	$1.72 \pm 0.20 \times 10^4$
	Tewa	3.31×10^5	2.02×10^5	1.6	1.0	69	92	$2.65 \pm 0.50 \times 10^5$
YAG 40-B	Zuni	7.48×10^6	3.76×10^6	2.0	0.68	152	126	$5.61 \pm 1.45 \times 10^6$
	Flathead	4.57×10^5	0.229×10^5	20.	0.98	0	342	$2.25 \pm 1.85 \times 10^5$
	Navajo	9.04×10^4	5.14×10^4	1.8	0.16	356	37	$7.07 \pm 1.47 \times 10^4$
	Tewa	15.8×10^6	1.30×10^6	12.	0.85	358	350	$8.39 \pm 5.72 \times 10^6$
YAG 39-C	Zuni	13.8×10^4	1.45×10^4	9.5	0.97	345	353	$7.54 \pm 4.68 \times 10^4$
	Flathead	11.5×10^4	2.12×10^4	5.4	0.41	327	12	$6.79 \pm 3.61 \times 10^4$
	Navajo	2.33×10^5	1.12×10^5	2.1	0.44	352	343	$1.71 \pm 0.46 \times 10^5$
	Tewa	2.82×10^7	0.282×10^7	10.	0.97	358	357	$1.50 \pm 1.03 \times 10^7$
LST 611-D	Zuni	*	*	*	*	*	*	*
	Flathead	†	†	†	†	†	†	$7.42 \pm 6.12 \times 10^4$ ‡
	Navajo	§	§	§	§	§	§	$1.47 \pm 0.47 \times 10^4$ ‡
	Tewa	18.8×10^5	8.34×10^5	2.3	¶	332	¶	$1.35 \pm 0.57 \times 10^6$
YFNB 13-E	Zuni	5.12×10^6	2.54×10^6	2.0	¶	15	¶	$3.84 \pm 1.02 \times 10^6$
	Flathead	7.36×10^6	4.42×10^6	1.7	¶	13	¶	$5.86 \pm 1.08 \times 10^6$
	Navajo	8.43×10^5	6.39×10^5	1.3	¶	354	¶	$7.41 \pm 0.79 \times 10^5$
	Tewa	6.90×10^6	1.92×10^6	3.6	¶	349	¶	$4.28 \pm 1.99 \times 10^6$
YFNB 29-G	Zuni	5.81×10^6	3.49×10^6	1.7	¶	342	¶	$4.65 \pm 0.90 \times 10^6$
	Flathead	3.12×10^5	2.01×10^5	1.6	¶	350	¶	$2.56 \pm 0.40 \times 10^5$
	Navajo	1.21×10^4	0.85×10^4	1.4	¶	17	¶	$1.03 \pm 0.13 \times 10^4$
	Tewa	3.90×10^7	1.56×10^7	2.5	¶	10	¶	$2.73 \pm 0.93 \times 10^7$
YFNB 29-H	Zuni	9.10×10^6	4.98×10^6	1.8	¶	346	¶	$6.97 \pm 1.60 \times 10^6$
	Flathead	§	§	§	¶	§	¶	$2.91 \pm 0.84 \times 10^5$ ‡
	Navajo	§	§	§	¶	§	¶	$1.45 \pm 0.24 \times 10^4$ ‡
	Tewa	6.73×10^7	3.32×10^7	2.0	¶	0	¶	$4.99 \pm 1.40 \times 10^7$

* Very light or no fallout occurred. † Instrument malfunction; analysis not attempted. ‡ Average of six total collectors in platform. § Collection curve could not be constructed. ¶ Vectorial analysis not attempted.

TABLE 4.5 COMPARISON OF HOW ISLAND COLLECTIONS

Shot	Standard Platform	Buried Trays	AOC_2	Platform/Buried Trays
	weighted mean fissions/ft^2	weighted mean fissions/ft^2	fissions/ft^2	
Zuni	$2.07 \pm 0.47 \times 10^{14}$	$2.08 \pm 0.22 \times 10^{14}$	1.87×10^{14}	0.995 ± 0.249
Flathead	$6.14 \pm 2.72 \times 10^{10}$ *	†	2.16×10^{10}	—
Navajo	$1.49 \pm 0.17 \times 10^{12}$	$1.24 \pm 0.51 \times 10^{12}$	2.67×10^{11}	1.202 ± 0.512
Tewa	$2.61 \pm 0.49 \times 10^{13}$	$2.30 \pm 0.35 \times 10^{13}$	1.53×10^{13}	1.135 ± 0.274

* Mean of six total collectors.

† No activity resolvable from Zuni background.

TABLE 4.6 SURFACE DENSITY OF ACTIVITY DEPOSITED ON THE OCEAN

Shot	Station	Ocean, Probe Analysis		Decay Tank, YAG 39		OCC, Ship Platform	
		Method I	Method II	Method I	Method III	Weighted Mean	Maximum Extrapolation *
		fissions/ft^2		fissions/ft^2		fissions/ft^2	
Zuni	YAG 39	9×10^{12} †	—	8.3×10^{12}	—	$2.74 \pm 1.70 \times 10^{12}$	5.02×10^{12}
	YAG 40	1×10^{14} ‡	—	—	—	$3.67 \pm 0.95 \times 10^{14}$	—
Flathead	YAG 39	1.1×10^{13}	—	7.0×10^{12}	$6.96 \pm 2.89 \times 10^{12}$	$4.36 \pm 2.32 \times 10^{12}$	—
	YAG 40	3×10^{13}	—	—	—	$1.55 \pm 1.27 \times 10^{13}$	3.15×10^{13}
Navajo	YAG 39	1.6×10^{14}	—	5.2×10^{13}	$3.40 \pm 0.72 \times 10^{13}$	$1.54 \pm 0.41 \times 10^{13}$	—
	Horizon	—	$5.98 \pm 1.02 \times 10^{13}$ §	—	—	—	—
	YAG 40	4.4×10^{13}	—	—	—	$6.05 \pm 1.26 \times 10^{12}$	—
Tewa	YAG 39	2.2×10^{15} †	—	3.6×10^{15}	$2.75 \pm 0.88 \times 10^{15}$	$1.11 \pm 0.76 \times 10^{15}$	2.08×10^{15}
	Horizon	—	$3.00 \pm 0.77 \times 10^{15}$ ¶	—	—	—	—
	YAG 40	1.1×10^{15} †	—	—	—	$4.70 \pm 3.20 \times 10^{14}$	8.85×10^{14}

* For cases of essentially single-wind deposition.

† Not corrected for material possibly lost by settling below stirred layer.

‡ Considerable motion of ship during fallout period.

§ Average of profiles taken at Horizon stations 4, 4A, 5, 7, and 8 from 18.6 to 34.3 hours (Table B.33).

¶ Average of profiles taken at Horizon stations 2-5, 5A, 6, and 12 from 21.3 to 81.2 hours (Table B.33).

TABLE 4.7 DIP-COUNTER CONVERSION FACTORS

Unless otherwise noted, all factors given are based on a direct dip count and radiochemical analysis for Mo^{99}. Sample designators and bottle numbers are given in parentheses.

Station	Source	Shot Zuni	Shot Flathead	Shot Navajo	Shot Tewa
		$\times 10^6$	$\times 10^6$	$\times 10^6$	$\times 10^6$
A. Fissions/(dip counts/min at 100 hrs)					
YAG 39	OCC	0.530 (C-21) *	0.945 (C-21)	1.285 (C-21)	1.02 (C-21)
	Decay tank	1.853 (T-1B, 8,035) †	0.774 (T-1B, 8,549)	0.960 (T-3B, 8,585)	0.645 (T-1B, 8,350)
	Ocean surface	4.537 (S-1B, 8,030)	1.137 (S-1B, 8,544)	1.430 (S-3B, 8,581)	1.525 (S-1B, 8,326)
YAG 40	OCC	1.02 (B-6)	1.006 (B-4) *	1.248 (B-4) *	0.817 (B-4) *
	Ocean surface	0.906 (S-1B, 8,254)	—	—	1.709 (S-2B, 8,289)
McGinty	Ocean surface	—	—	0.726 (MS-5A, 8,052)	—
	Ocean surface	—	—	1.09 (MS-5B, 8,053)	—
B. Fissions/(dip counts/min at 200 hrs) ‡					
YAG 39	OCC	1.37	2.16	3.36	2.45
	Decay tank	4.80	1.77	2.51	1.55
	Ocean surface	11.75	2.61	3.73	3.66
	Method I	2.33	2.46	4.03	2.46
	Method II			3.23 ± 0.39	2.90 ± 0.51

* No OCC aliquot counted in dip counter; computed from Table B.13 and doghouse/dip average ratio in Table B.15.

† Tank unacidified and unstirred when sample taken.

‡ Values in A corrected to 200 hours by average photon-decay factors 2.59, 2.29, 2.61, and 2.40 for Shots Zuni, Flathead, Navajo, and Tewa, respectively. These decay-curve shapes are practically identical to those shown in Figure B.14 over this time period.

TABLE 4.9 GAMMA DOSAGE BY ESL FILM DOSIMETER AND INTEGRATED TIR MEASUREMENTS

Station	Shot Zuni			Shot Flathead			Shot Navajo			Shot Tewa		
	Film Dose	TIR Dose	Exposure Time	Film Dose	TIR Dose	Exposure Time	Film Dose	TIR Dose	Exposure Time	Film Dose	TIR Dose	Exposure Time
	r	r	to H+hr	r	r	to H+hr	r	r	to H+hr	r	r	to H+hr
YAG 40-B	30	19.8	28.2	2.5	1.7	33.6	1.77	0.8	32.8	41.6	31.0	32.6
YAG 39-C	0.2	0.2	34.6	0.05	0.5	26.1	10	4.6	50.3	68	67.0	51.3
LST 611-D	<0.05	0.0	62.0	1.7	1.3	51.6	0.81	0.3	26.6	3.62	3.4	31.7
YFNB 13-E	44	17.8 *	26.7	400	74.6 *	26.7	68.5	13.7	58.3	20.3	8.7	7.8
YFNB 29-G	20	23.6	6.9	7.5	3.7	5.7	1.64	0.2	6.5	310	158.0 *	51.1
YFNB 29-H	43	41.7	27.7	12	3.9	25.9	1.65	0.7	5.5	320	284.0 *	75.6
How F	19	6.7	11.1	0.22	0.0	6.3	1.82	†	6.7	4.5	0.8	8.3
How K	51	—	30.2	3.1	—	6.3	3.37	—	10.7	6.7	—	8.4
George L	260	—	32.7	230	—	31.7	150	—	32.5	†	—	†
Charlie M	—	—	—	—	—	—	107	—	32.7	†	—	†
William M	110	—	31.6	5.2	—	30.9	—	—	—	—	—	—
Raft 1	25	—	30.8	1.5	—	29.4	1.32	—	27.3	3.35	—	31.7
Raft 2	40	—	29.8	24	—	28.6	4.62	—	28.1	45.5	—	32.3
Raft 3	34	—	28.6	19	—	27.8	16.1	—	28.8	204	—	33
Skiff AA	17	—	52.1	25	—	24.2	13.2	—	59.9	45.5	—	63.25
Skiff BB	33	—	56.9	59	—	28.3	†	—	†	141	—	37.9
Skiff CC	20	—	72.9	9.4	—	30.6	5.2	—	53.2	42.5	—	36.6
Skiff DD	17	—	74.6	†	—	†	2.56	—	50.3	1.28	—	33.4
Skiff EE	2.3	—	171.9	0.6	—	48.4	1.45	—	48.8	9.87	—	31.7
Skiff FF	‡	—	‡	1.1	—	55.1	0.56	—	29.3	0.3	—	26.5
Skiff GG	10	—	59.3	‡	—	‡	—	—	—	295	—	60.1
Skiff HH	16	—	60.8	20	—	32.7	29.5	—	52.3	61	—	39.8
Skiff KK	6.8	—	75.7	2.0	—	51.4	6.3	—	33.0	0.62	—	34.7
Skiff LL	†	—	†	1.0	—	53.4	2.05	—	31.0	1.40	—	29.8
Skiff MM	1.8	—	50.1	‡	—	‡	†	—	†	410	—	61.5
Skiff PP	—	—	—	16	—	34.8	77	—	35.4	60	—	58.3
Skiff RR	2.4	—	77.1	2.0	—	60.8	11.7	—	33.8	0.6	—	41.9
Skiff SS	1.1	—	155.3	3.6	—	58.0	—	—	—	—	—	—
Skiff TT	1.2	—	168.7	1.2	—	56.4	1.09	—	27.8	0.3	—	28.0
Skiff UU	†	—	†	0.45	—	59.3	—	—	—	—	—	—
Skiff VV	†	—	†	—	—	—	—	—	—	—	—	—
Skiff WW	—	—	—	—	—	—	—	—	—	154	—	56.7
Skiff XX	—	—	—	—	—	—	—	—	—	2.05	—	54.6
Skiff YY	—	—	—	—	—	—	—	—	—	1.41	—	52.6

* Estimated value, TIR saturated. † Instrument malfunctioned or lost. ‡ Not instrumented.

Page 130 Deleted

TABLE 4.10 PERCENT OF FILM DOSIMETER READING RECORDED BY TIR

Station	Shot Zuni	Shot Flathead	Shot Navajo	Shot Tewa
	pct	pct	pct	pct
YAG 40-B	66	68	45	75
YAG 39-C	100	~100	46	97
LST 611-D	*	76	37	94
YFNB 13-E	41 †	19 †	20	43
YFNB 29-G	~100 ‡	49	12	51 †
YFNB 29-H	97	32	42	89 †
How F	35 ‡	*	§	18

* No fallout occurred.
† TIR saturated.
‡ Dosimeter location varied from other shots.
§ Instrument malfunctioned.

TABLE 4.11 COMPARISON OF THEORETICAL DOGHOUSE ACTIVITY OF STANDARD-CLOUD SAMPLES BY GAMMA SPECTROMETRY AND RADIOCHEMISTRY

Time of Spectral Run	Observed Dog-house Activity	Computed Activity and Errors			
		Spectrometer	Error	Radiochemical	Error
H+hr	counts/min	counts/min	pct	counts/min	pct
Shot Zuni Standard Cloud, 9.84×10^{12} fissions					
53	142,500	95,300	−33.1	163,541	+14.8
117	70,000	47,450	−32.2	74,981	+7.11
242	26,700	20,640	−22.7	29,107	+9.01
454	9,500	7,516	−20.9	10,745	+13.1
790	3,700	3,790	+2.43	4,546	+22.9
1,295	1,550	1,973	+27.3	1,984	+28.0
Shot Flathead Standard Cloud, 2.79×10^{13} fissions					
96.5	171,000	142,090	−16.9	154,008	−9.93
195	72,000	51,490	−28.5	66,960	−7.00
262	45,000	29,850	−33.7	43,022	−4.39
334	30,500	22,760	−25.4	29,128	−4.49
435	19,300	14,920	−22.7	19,084	−1.11
718	8,200	6,778	−17.3	7,985	−2.62
1,031	4,400	3,341	−22.5	4,152	−5.63
1,558	2,130	2,243	+5.31	2,076	−2.53
Shot Navajo Standard Cloud, 3.46×10^{12} fissions					
51.5	34,000	27,470	−19.2	31,350	−7.79
69	25,500	20,724	−18.7	22,630	−11.3
141	11,000	9,432	−14.2	9,757	−11.3
191	7,000	7,411	+5.87	6,290	−10.1
315	3,050	2,834	−7.08	2,927	−4.03
645	980	958	−2.24	1,038	+5.92
Shot Tewa Standard Cloud, 4.71×10^{13} fissions					
71.5	442,000	244,930	−44.6	429,600	−2.81
93.5	337,000	194,170	−42.4	325,000	−3.56
117	262,000	157,890	−39.7	255,800	−2.37
165	169,000	134,910	−20.2	161,000	−4.73
240	97,000	74,780	−22.9	91,000	−6.19
334	54,000	38,770	−28.2	52,280	−3.19
429	34,500	25,200	−27.0	33,200	−3.77
579	20,200	14,770	−26.9	19,640	−2.77
766	12,400	10,860	−12.4	12,150	−2.02
1,269	5,200	5,660	+8.85	4,974	−4.35
1,511	3,850	4,550	+18.2	3,759	−2.36

TABLE 4.12 COMPARISON OF ACTIVITIES PER UNIT AREA COLLECTED BY THE HIGH VOLUME FILTER AND OTHER SAMPLING INSTRUMENTS

Shot	Designation and Exposure Period, H+hr					Fissions/ft^2 (Mo^{99})		
	HVF		IC		OCC and AOC_1	HVF (area = 0.06696 ft^2)	IC (area = 0.05584 ft^2)	OCC and AOC_1 (area = 2.60 ft^2)
Zuni	YAG 40-B-9	3.4 to 4.8				10.14×10^{13}		
	YAG 40-B-10	5.3				23.48		
	YAG 40-B-11	5.8				23.73		
	YAG 40-B-12	6.3				21.79		
	YAG 40-B-13	6.8				6.42		
	YAG 40-B-14	7.3				6.93		
	YAG 40-B-15	7.8				0.39		
	YAG 40-B-8	16.4				3.97		
	HVF to	16.4	YAG 40-B-7	to 15.6	To 16.3 and 28.2 *	9.68×10^{14}	6.06×10^{14}	$3.71 \pm 0.88 \times 10^{14}$
Flathead	YAG 40-B-8	to 26.4	YAG 40-B-7	to 19.9	To 26.4	2.03×10^{12}	3.87×10^{12}	$16.3 \pm 13.4 \times 10^{12}$
	YAG 39-C-25	to 26.1	YAG 39-C-20	to 18.2	To 23.8	1.57×10^{12} †	4.85×10^{12}	$4.37 \pm 2.37 \times 10^{12}$
Navajo	YAG 40-B-8	to 19.1	YAG 40-B-7	to 15.5	To 8.7 and 19.7 *	3.72×10^{12}	3.70×10^{12}	$6.08 \pm 1.26 \times 10^{12}$
	YAG 39-C-25	to cessation	YAG 39-C-20	to 16.1	To 15.9 and 24.1 *	5.50×10^{12}	11.9×10^{12}	$14.6 \pm 3.5 \times 10^{12}$

* Short-exposure trays as active as long.

† DMT spilled on recovery.

TABLE 4.13 NORMALIZED IONIZATION RATE (SC), CONTAMINATION INDEX, AND YIELD RATIO

A number in parentheses indicates the number of zeros between the decimal point and first significant figure.

Shot	Age	r/hr / fissions/ft^2
Hypothetical, 100 pct fission, unfractionated fission products, no induced activities	1.12 hrs	(12)6254
	1.45 days	(14)6734
	9.82 days	(15)6748
	30.9 days	(15)1816
	97.3 days	(16)3713
	301 days	(17)5097
Zuni, lagoon-area composition	1.12 hrs	(12)3356
	1.45 days	(14)4134
	9.82 days	(15)3197
	30.9 days	(16)9165
	97.3 days	(16)4097
	301 days	(17)7607
Zuni, cloud composition	1.12 hrs	(12)7093
	1.45 days	(13)1407
	9.82 days	(14)1766
	30.9 days	(15)4430
	97.3 days	(16)8755
	301 days	(16)1121
Flathead, average composition	1.12 hrs	(12)5591
	1.45 days	(14)6994
	9.82 days	(15)7924
	30.9 days	(15)1893
	97.3 days	(16)3832
	301 days	(17)5230
Navajo, average composition	1.12 hrs	(12)6864
	1.45 days	(14)9481
	9.82 days	(15)7816
	30.9 days	(15)2160
	97.3 days	(16)5933
	301 days	(16)1477
Tewa, lagoon-area composition	1.12 hrs	(12)3321
	1.45 days	(14)3564
	9.82 days	(15)3456
	30.9 days	(16)9158
	97.3 days	(16)2843
	301 days	(17)4208
Tewa, cloud and outer fallout composition	1.12 hrs	(12)6446
	1.45 days	(14)8913
	9.82 days	(15)8670
	30.9 days	(15)1971
	97.3 days	(16)4019
	301 days	(17)6009

* Ratio of (r/hr)/(Mt(total)/ft^2) at t for device to (r/hr)/(Mt(total)/ft^2) at t for hypothetical device.

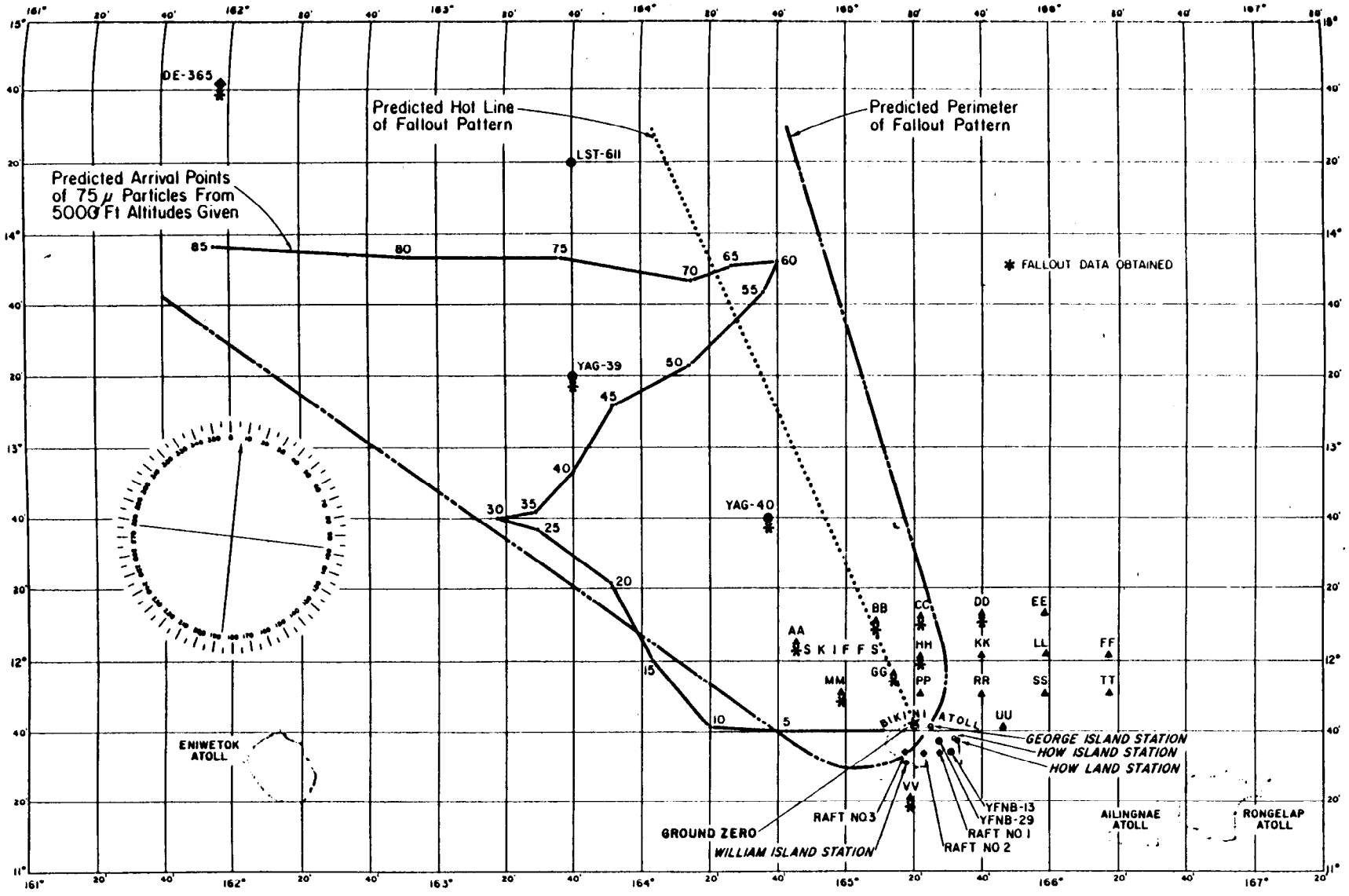

Figure 4.1 · Approximate station locations and predicted fallout pattern, Shot Cherokee.

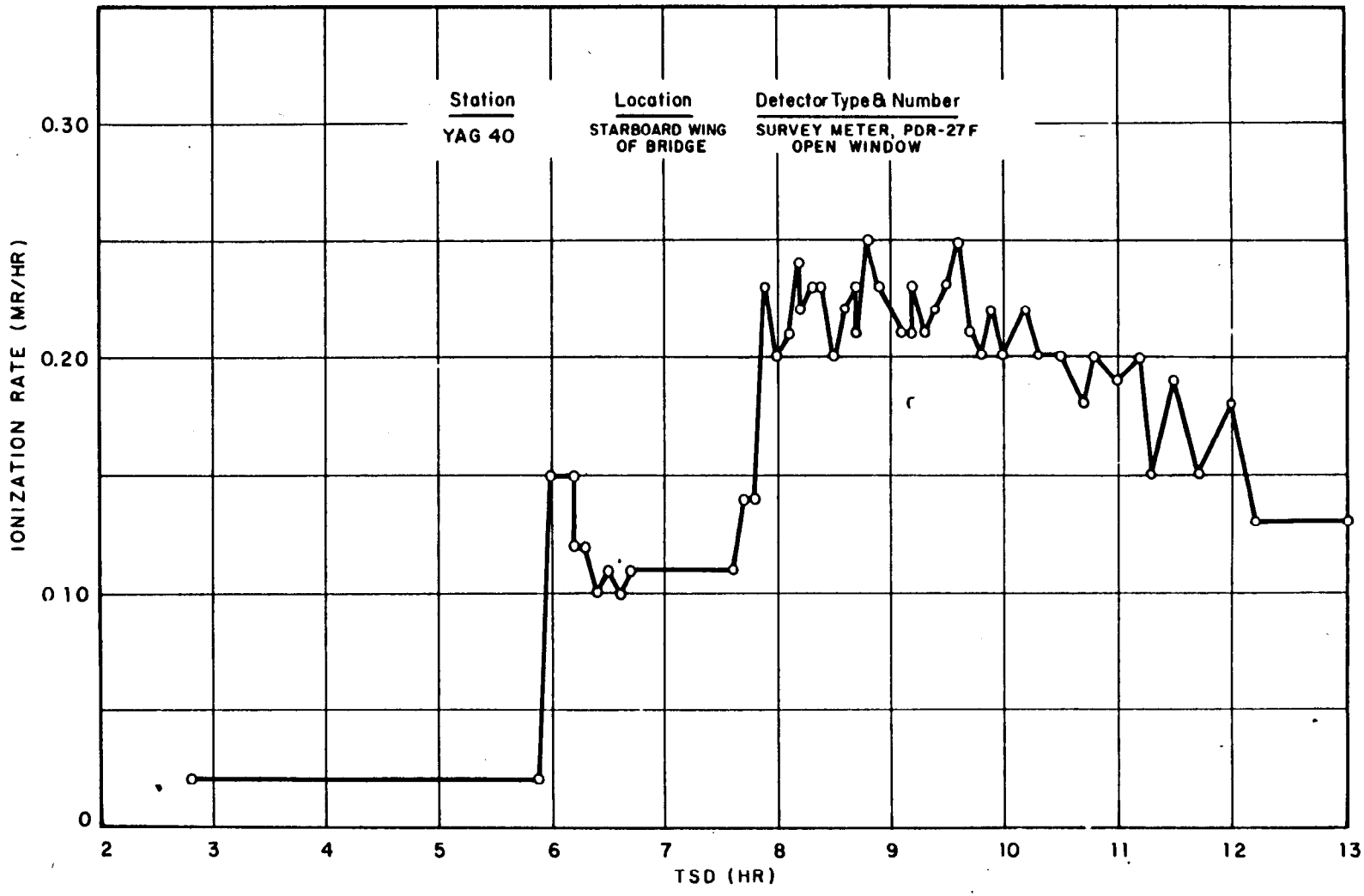

Figure 4.2 Survey-meter measurement of rate of arrival on YAG 40, *Shot Cherokee*.

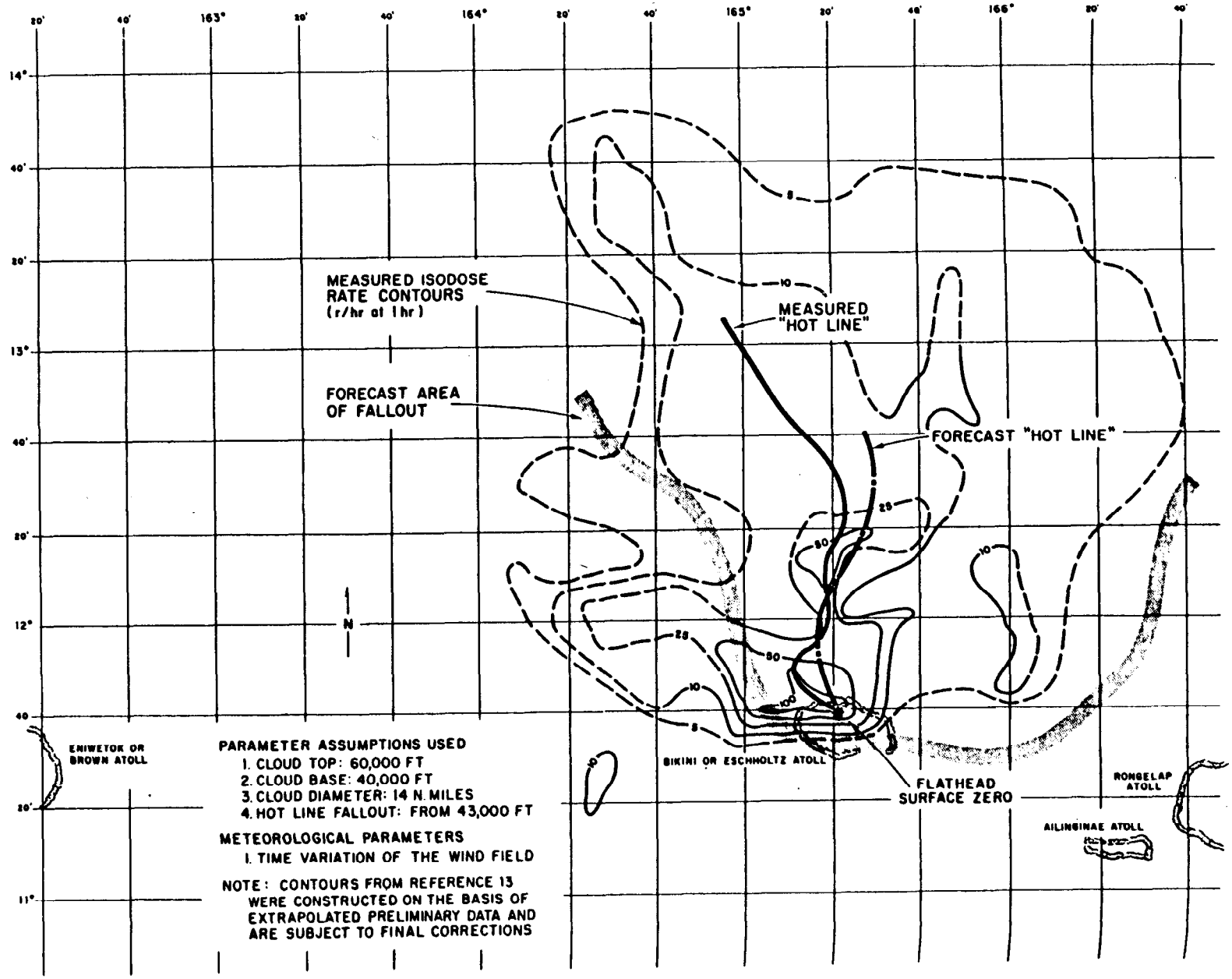

Figure 4.6 Predicted and observed fallout pattern, *Shot Flathead.*

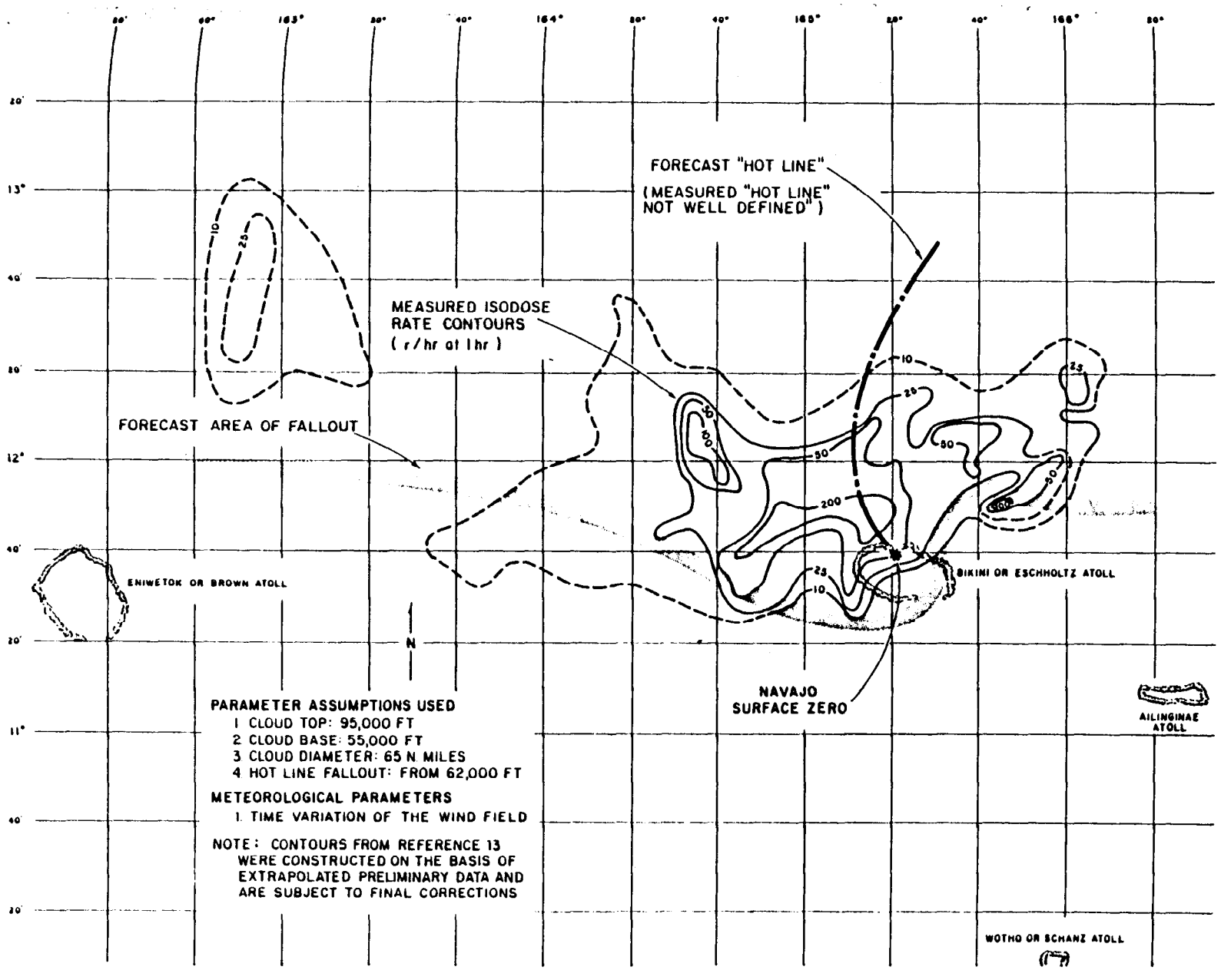

Figure 4.7 Predicted and observed fallout pattern, Shot Navajo.

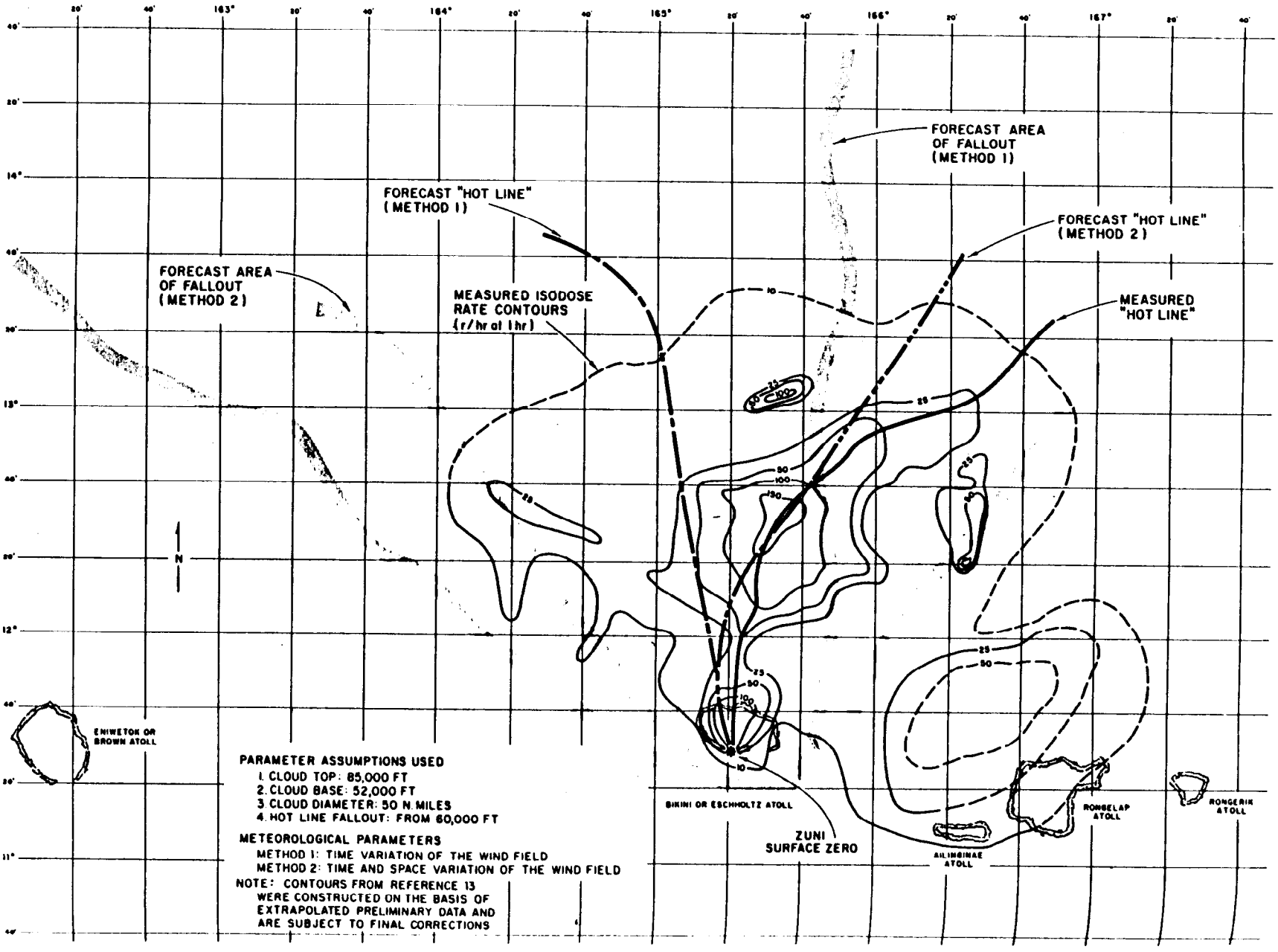

Figure 4.8 Predicted and observed fallout pattern, Shot Zuni.

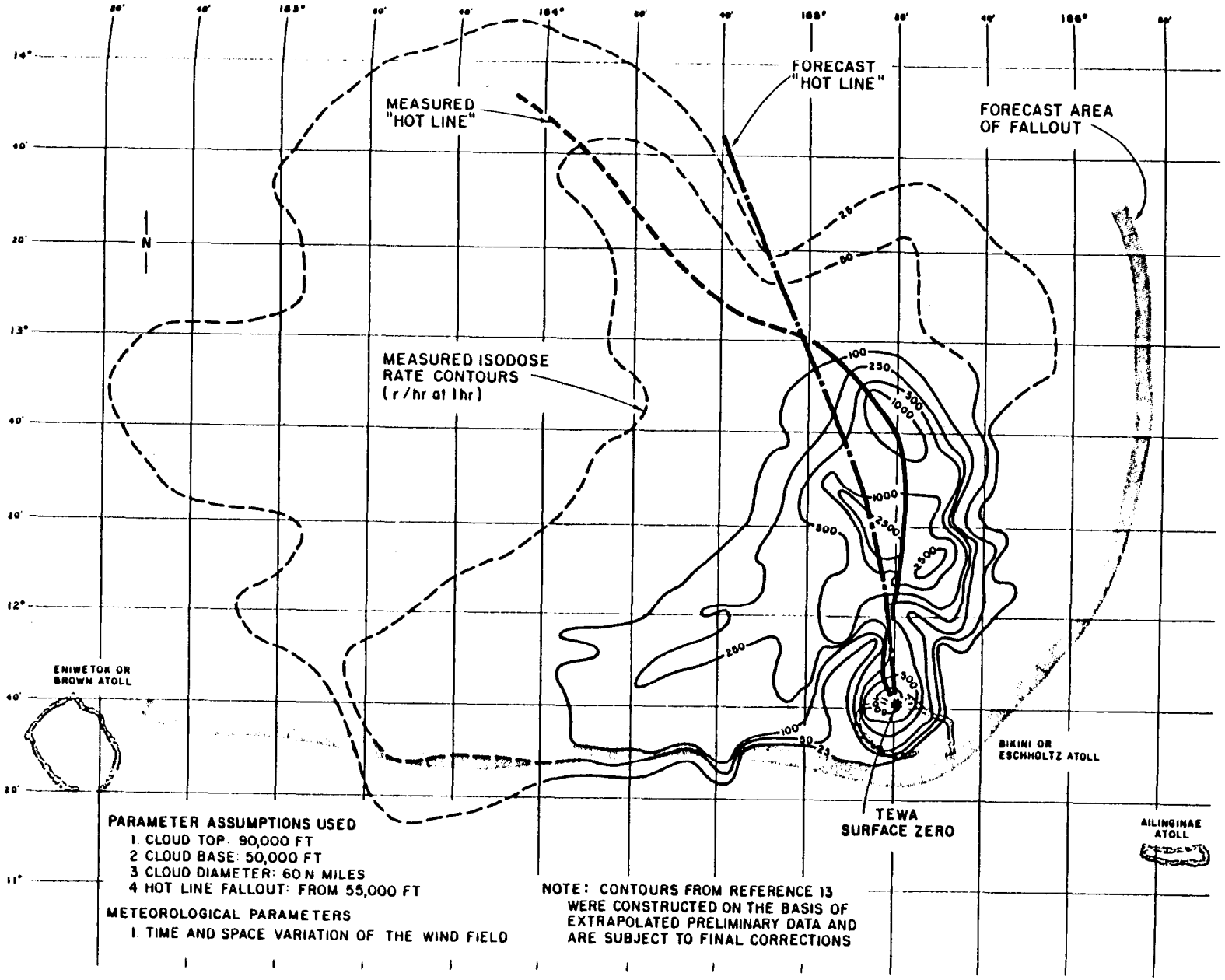

Figure 4.9 Predicted and observed fallout pattern, Shot Tewa.

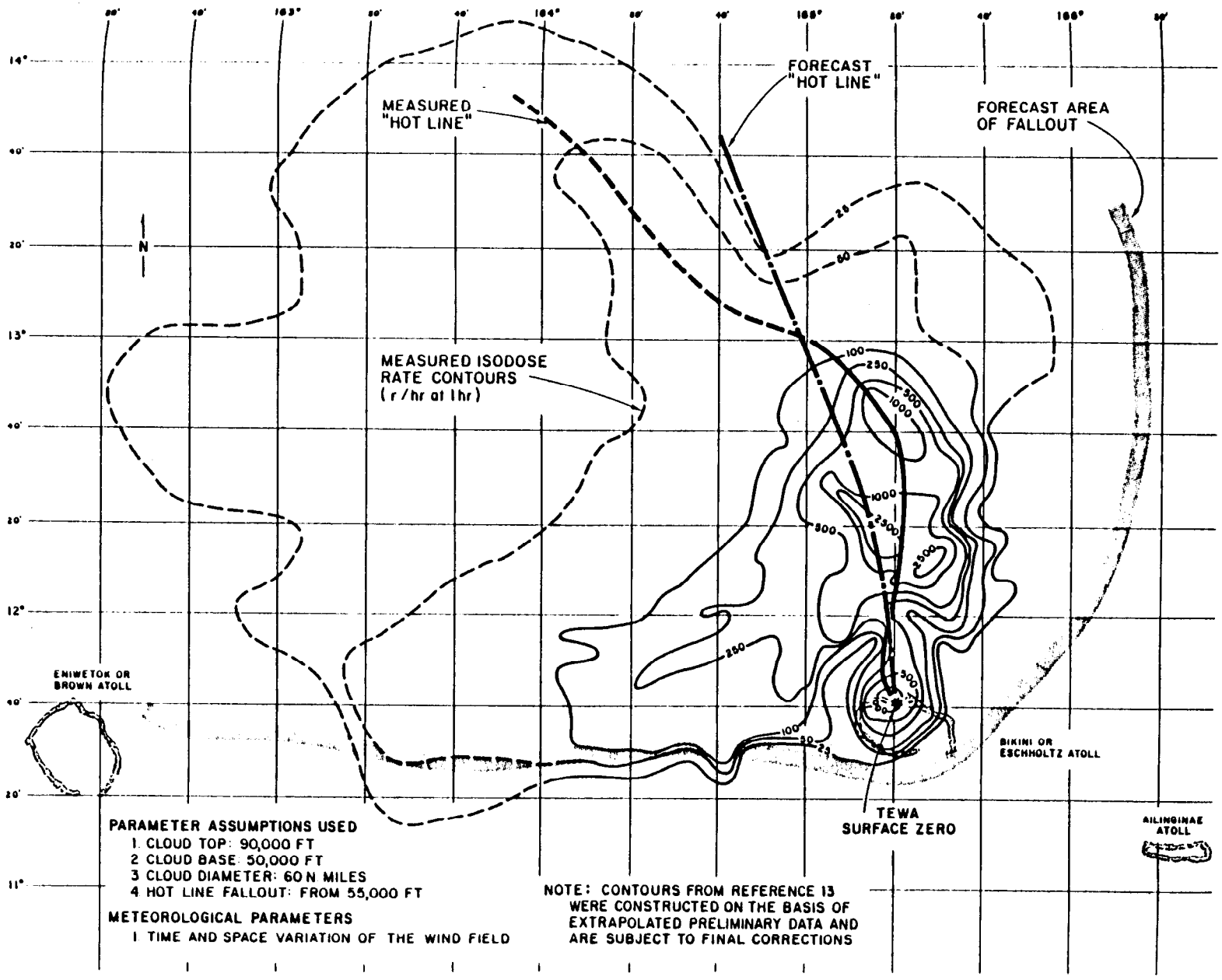

Figure 4.9 Predicted and observed fallout pattern, Shot Tewa.

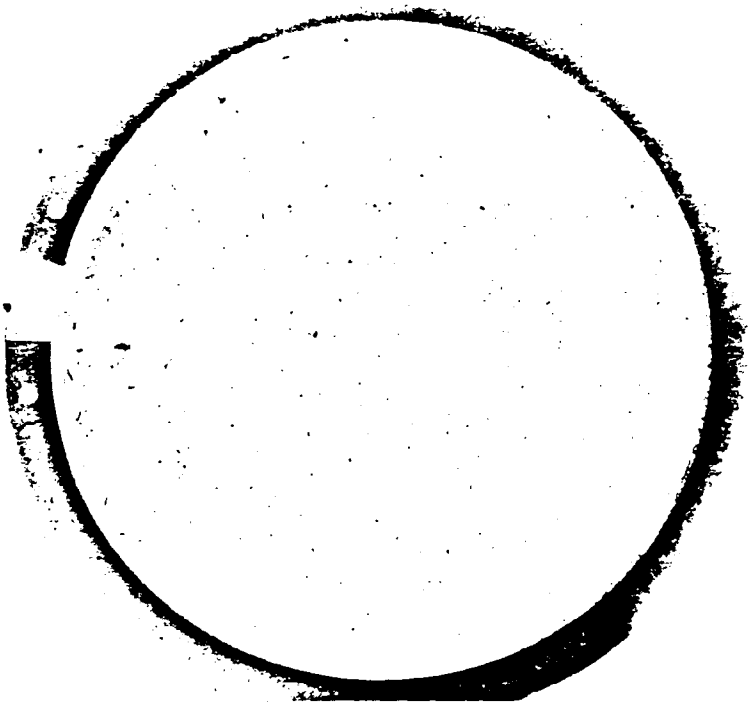

A HEAVY
COLLECTION
FAR OUT
15 MINUTE EXPOSURE

TRAY NO. 411

YAG 40, B-7
ZUNI

A HEAVY
COLLECTION
CLOSE IN
15 MINUTE EXPOSURE

TRAY NO. 1204

YFNB 13, E-57
ZUNI

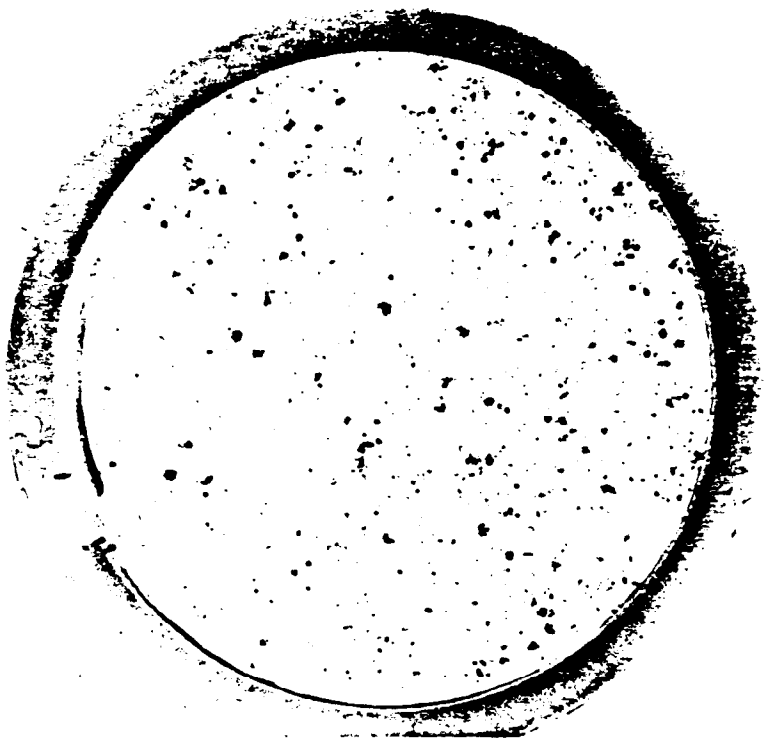

Figure 4.10 Close and distant particle collections, Shot Zuni.

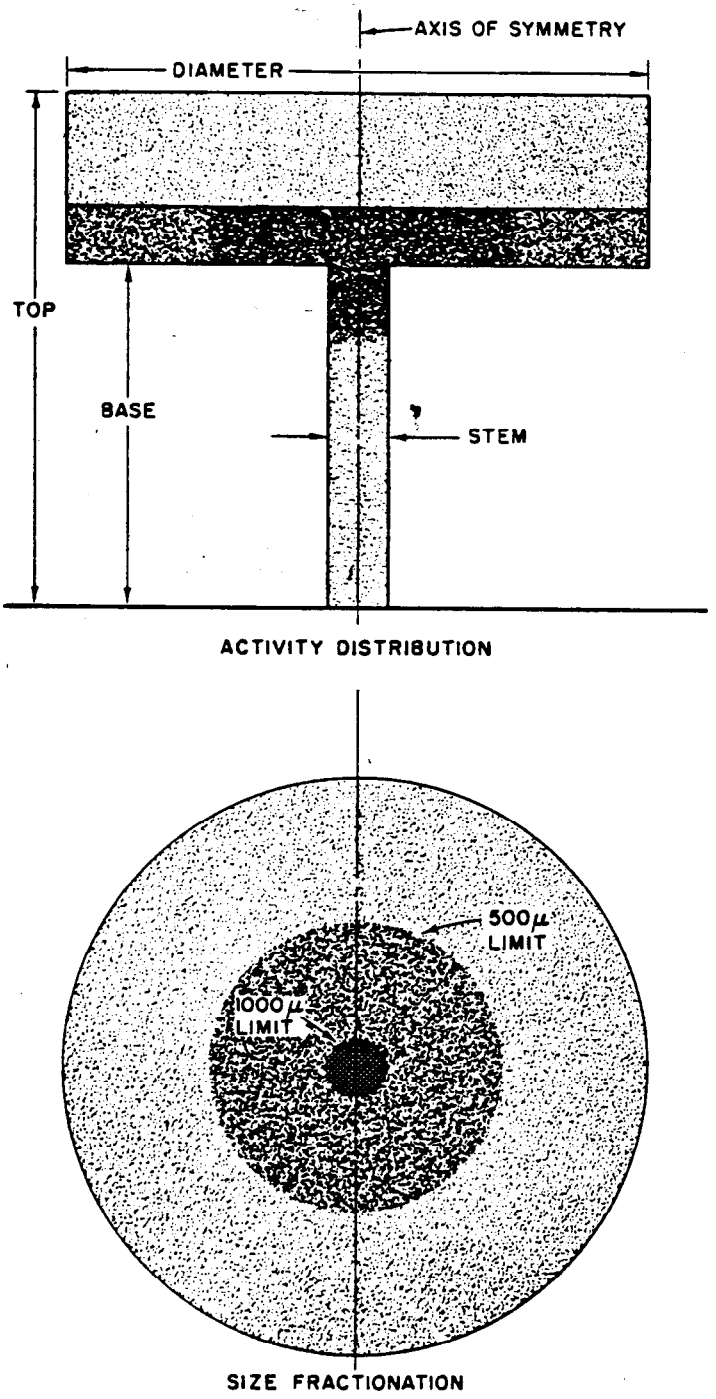

Figure 4.11 Cloud model for fallout prediction.

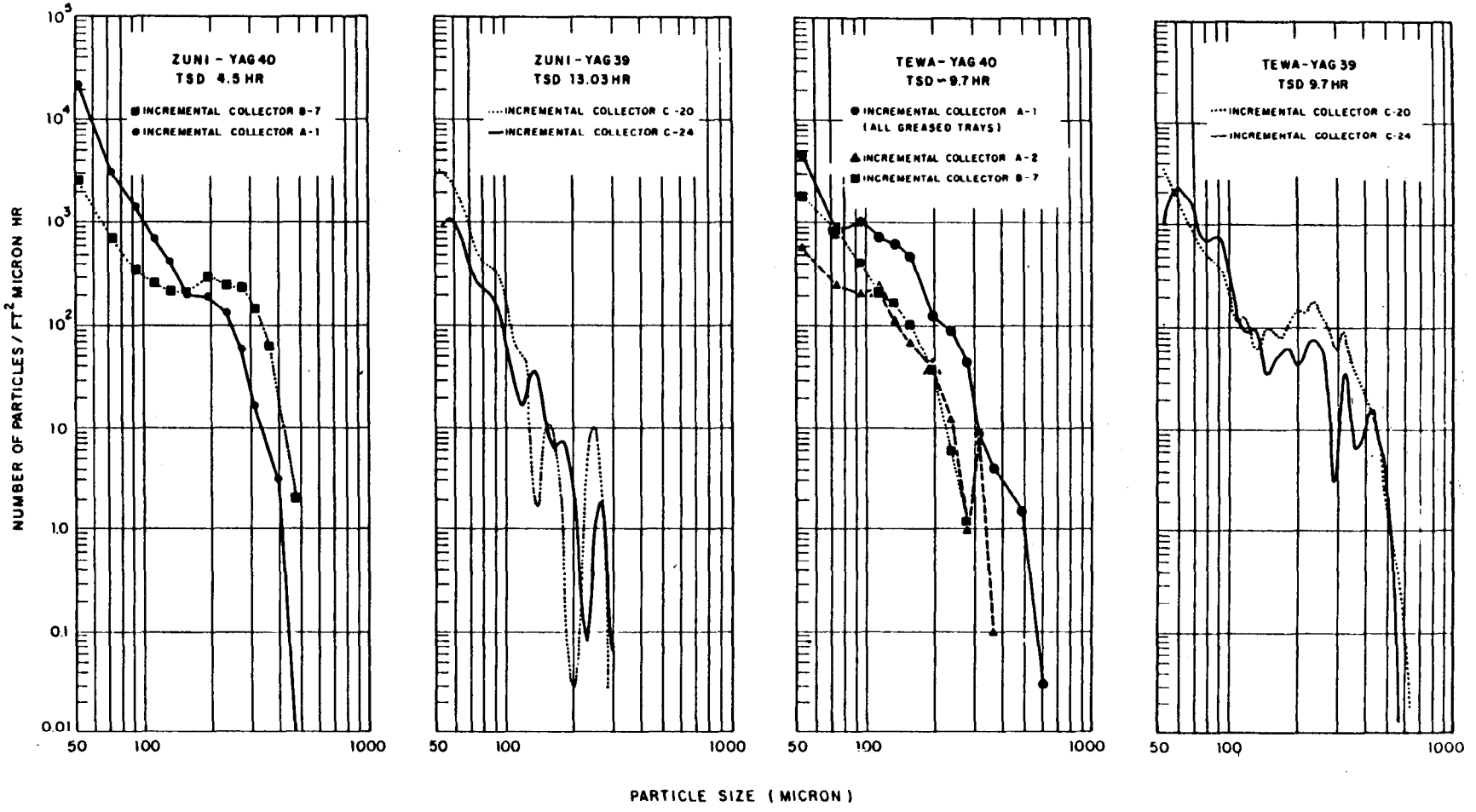

Figure 4.12 Comparison of incremental-collector, particle-size frequency distributions, Shots Zuni and Tewa.

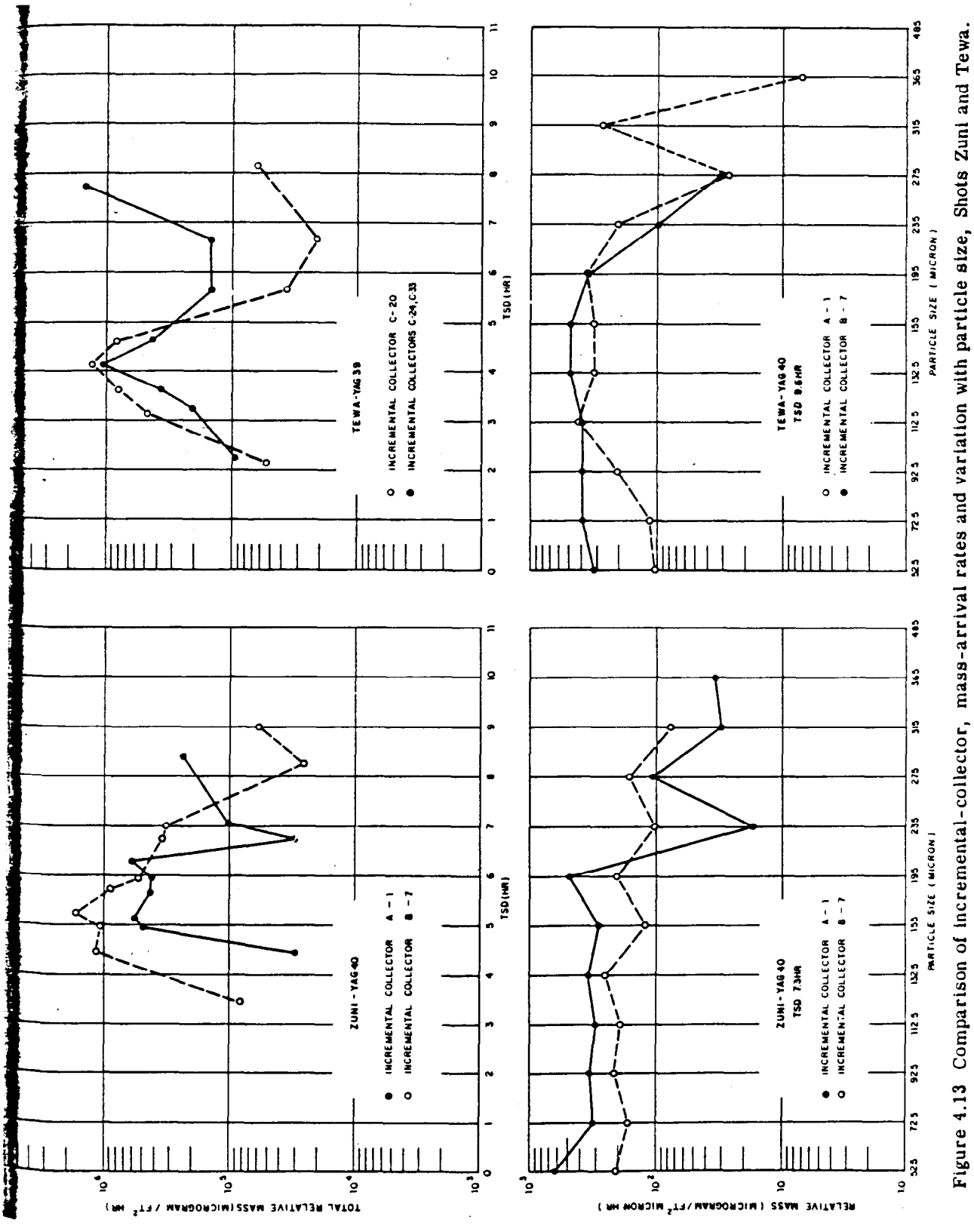

Figure 4.13 Comparison of incremental-collector, mass-arrival rates and variation with particle size, Shots Zuni and Tewa.

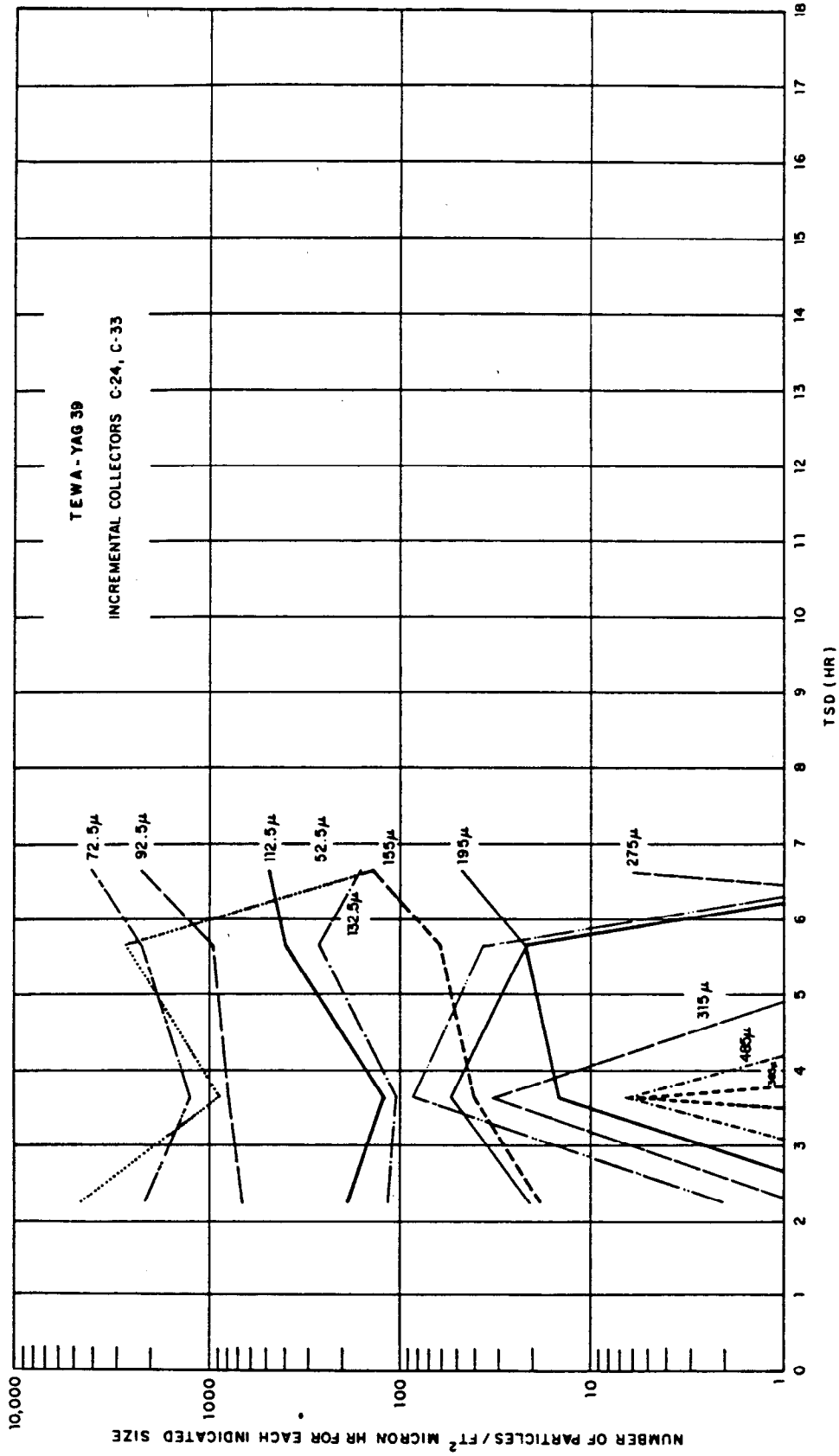

Figure 4.14 Comparative particle-size variation with time, YAG 39, Shot Tewa.

Chapter 5
CONCLUSIONS and RECOMMENDATIONS

5.1 CONCLUSIONS

5.1.1 Operational. The following features of project operations are concluded to have been satisfactory:

1. Emphasis on complete documentation of the fallout at a few points, rather than limited documentation at a large number of points. Because of this, integrated sets of data were obtained, better control of all measurements was achieved, and a number of important correlations became possible for the first time. It is a related conclusion that the care taken to locate project stations, and the close coordination maintained with the aerial and oceanographic survey projects, were necessary.

2. Concentration on specific measurements required by fallout theory, instead of on general observations and data collection. The results obtained by emphasizing time-dependent data promise to be of particular value in fallout research, as do the early-time measurements of particle properties made in the YAG 40 laboratory.

3. Devotion of laboratory work on the YAG 40 and Site Elmer to relative activity and associated measurements. In several cases, data were obtained that would otherwise have been lost or obscured by radioactive decay. Counting statistics were improved, and the confidence in all measurements and observations was increased by the elimination of intermediate handling. Conversely, chemical and radiochemical measurements, which require a disproportionate amount of effort in the field, could be made under more favorable conditions, although at the sacrifice of information on short-lived induced activities.

4. Utilization of standardized instrument arrays and procedures. Without this, measurements made at different locations could not have been easily related, and various correlations could not have been achieved. Instrument maintenance, sample recovery, and laboratory processing were considerably simplified. Because the use of the How Island station as a datum plane for all standardized instrumentation was an integral part of the overall concept, it should be noted that the station functioned as intended and obtained information of fundamental importance for data reduction and correlation.

5. Preservation of station mobility. It if had not been possible to move both major and minor sampling arrays to conform with changes in shot location and wind conditions, much valuable data would have been lost. Some of the most useful samples came from the barges that were relocated between shots. Coordination of ship sampling operations from the Program 2 Control Center on the basis of late meteorological information and early incoming data also proved practical; sampling locations were often improved and important supplementary measurements added.

6. Determination of station locations by Loran. Despite the fact that it was difficult for the ships to hold position during sampling, adequate information on their locations as a function of time was obtained. Ideally, of course, it would be preferable for ships to remain stationary during sampling, using Loran only to check their locations. The deep-anchoring method used for the skiffs gave good results and appears to be appropriate for future use.

7. Establishment of organizational flexibility. The use of small teams with unified areas of responsibility and the capability of independent action during the instrument-arming and sample-recovery periods was a primary factor in withstanding operational pressures. The stabilizing influence provided by the sample-processing centers on Bikini and Eniwetok contributed significantly to the effectiveness of the system.

There were also certain features of project operations which were unsatisfactory:

Page 149 Deleted.

1. The large size of the project. If more-limited objectives had been adopted, and the measurements to accomplish these objectives allotted to several smaller projects, the amount of field administrative work and the length of time key personnel were required to spend in the field could probably have been reduced. In future tests, the total number of shot participations should be kept to the minimum compatible with specific data requirements.

2. The difficulty of maintaining adequate communications between the test site and NRDL. Despite arrangements to expedite dispatches, frequent informal letters, and messages transmitted by sample couriers, several cases occurred where important information was delayed in transit.

3. The use of instruments developed by other projects. Malfunctions were frequent in such cases but were probably due partly to lack of complete familiarity with the design of the instrument. This is the principal reason why the water-sampling results are incomplete and of uncertain reliability.

4. The operational characteristics of certain project instruments. The time-of-arrival detectors (TOAD) were developed for the operation and had not been proof-tested in the field. They tended to give good results when located on stable stations, such as barges or islands, and poor results when located on stations like the skiffs. It seems probable that minor design modifications would suffice to make this a dependable instrument. The honeycomb inserts used in the open-close total collector (OCC) exhibited a tendency to spall and should be modified for future use. The sizes of the collecting areas of the always-open collector, Type 2 (AOC_2), and incremental collector (IC) should be increased if possible. Complete redesign of the gamma time-intensity recorder (TIR) to improve its response characteristics, reduce its size, and make it a self-contained unit was obviously required for future work and was initiated during the field phase.

5. The commitments of the project to supply early evaluations of field data. Because of the nature of fallout studies, inferences drawn from unreduced data may be misleading. Despite the urgency associated with studies of this kind, interim project reports should be confined to presenting the results of specific field measurements.

5.1.2 Technical. The general conclusions given below are grouped by subject and presented for the most part in the same order that the subjects are discussed in the preceding chapters. In a sense, the values tabulated and plotted in the text constitute the detailed conclusions, because they represent the numerical results derived from the reduced data of the appendixes. For this reason, numerical values will be extracted from the text only if some generality is evident or to illustrate an observed range. Although the conclusions presented are not necessarily those of the authors whose works have been referenced in the text, interpretations are usually compatible.

Buildup Characteristics.

1. The time from fallout arrival to peak radiation rate was approximately equal to the time of arrival for all stations and shots. Activity-arrival rate was roughly proportional to mass-arrival rate for the solid-particle shots, Zuni and Tewa. A similar result was obtained for outlying stations during Shot Flathead, although this proportionality did not hold for Shot Navajo nor for the close-in collections from Shot Flathead.

2. The shape of the activity-arrival-rate curve was not markedly different for solid- and slurry-particle shots. In both types of events, the time from the onset of fallout to the time when the radiation rate peaked was usually much shorter than the time required for the remainder of the fallout to be deposited. There was some tendency for slurry fallout to be more protracted and less concentrated in a single major arrival wave; however, statistical fluctuations due to low concentrations of particles and small collector areas were responsible for most of the rapid changes observed after the time of peak. Where fallout concentrations were sufficiently high, good time correlation was ordinarily obtained between peak rate of arrival and peak radiation rate.

3. Particle-size distributions varied continuously with time at each station during the solid-particle shots, activity arrival waves being characterized by sharp increases in the concentra-

tions of the larger particles. Because of background dust and unavoidable debris on the trays, correlation of the concentrations of smaller particles with radiological measurements was more difficult. The concentrations of the smallest sizes remained almost constant with time. Particle diameters gradually decreased with time at each station during the slurry-particle shots, though remaining remarkably constant at ~100 to 200 microns on the ships during the entire fallout period.

4. In the vicinity of the ships, the gross body of fallout activity for the slurry-particle shots penetrated to the thermocline from a depth of 10 to 20 meters at the rate of 3 to 4 m/hr. A considerable fraction of the activity for the solid-particle shots penetrated to the thermocline at about the same rate. This activity remained more or less uniformly distributed above the thermocline up to at least 2 days after the shot, and is presumed to have been in solution or associated with fine particles present either at deposition or produced by the breakup of solid aggregates in sea water. An unknown amount of activity, perhaps as much as 50 percent of the total, penetrated at a higher rate and may have disappeared below the thermocline during the solid-particle shots. It is unlikely that any significant amount of activity was lost in this way during the slurry-particle shots.

5. Fractionation of Mo^{99}, Np^{239}, and I^{131} occurred in the surface water layer following solid-particle deposition; a continuous variation in composition with depth is indicated. Only slight tendencies in this direction were noted for slurry fallout.

Physical, Chemical, and Radiological Characteristics.

1. The fallout from Shots Zuni and Tewa consisted almost entirely of solid particles similar to those observed after the land-surface shots during Operations Ivy and Castle, consisting of irregular, spheroidal, and agglomerated types varying in color from white to yellow and ranging in size from < 20 microns to several millimeters in diameter. Most of the irregular particles consisted primarily of calcium hydroxide with a thin surface layer of calcium carbonate, although a few unchanged coral particles were present; while the spheroidal particles consisted of calcium oxide and hydroxide, often with the same surface layer of calcium carbonate. The agglomerates were composed of calcium hydroxide with an outer layer of calcium carbonate. The particles almost certainly were formed by decarbonation of the original coral to calcium oxide in the fireball, followed by complete hydration in the case of the irregular particles, and incomplete hydration in the case of the other particles; the surface layer, which may not have been formed by deposition time, resulted from reaction with CO_2 in the atmosphere. The densities of the particles were grouped around 2.3 and 2.7 gm/cm^3.

2. Radioactive black spherical particles, usually less than 1 micron in diameter, were observed in the fallout from Shot Zuni, but not in the fallout from Shot Tewa. Nearly all such particles were attached to the surfaces of irregular particles. They consisted partially of calcium iron oxide and could have been formed by direct condensation in the fireball.

3. The radionuclide composition of the irregular particles varied from that of the spheroidal and agglomerated particles. The irregular particles tended to typify the cloud-sample and distant-fallout radiochemistry, while the spheroidal and agglomerated particles were more characteristic of the gross fallout near ground zero. The irregular particles tended to be enriched in Ba^{140}-La^{140} and slightly depleted in Sr^{89}; the spheroidal and agglomerated particles were depleted in these nuclides but were much higher in specific activity. It should be recognized that this classification by types may be an oversimplification, and that a large sample of individual particles of all types might show a continuous variation of the properties described. The inference is strong, nevertheless, that the fractionation observed from point to point in the fallout field at Shot Zuni was due to the relative abundance and activity contribution of some such particle types at each location.

4. The activities of the irregular particles varied roughly as their surface area or diameter squared, while those of the spheroidal particles varied as some power higher than the third. Indications are that the latter were formed in a region of higher activity concentration in the cloud, with the activity diffusing into the interior while they were still in a molten state. Activity was not related to particle density but varied with the weight of irregular particles in a manner consistent with a surface-area function.

5. The fallout from Shots Flathead and Navajo collected at the ship stations was made up entirely of slurry particles consisting of about 80 percent sodium chloride, 18 percent water, and 2 percent insoluble solids composed primarily of oxides of calcium and iron. The individual insoluble solid particles were generally spherical and less than 1 micron in diameter, appearing to be the result of direct condensation in the fireball.

6. The radionuclide composition of individual slurry drops could not be assessed because of insufficient activity, but the results of combining a number of droplets were similar to those obtained from gross fallout collections. In general, much less fractionation of radionuclides was evident in the slurry-particle shots than in the solid-particle shots. The amount of chloride in a slurry drop appeared to be proportional to the drop activity for the ship stations at Shot Flathead; however, variability was experienced for Shot Navajo, and the relation failed for both shots at close-in locations. Conflicting data was obtained on the contribution of the insoluble solids to the total drop activity. While the slurry nature of the fallout and certain properties such as drop diameters, densities, and concentrations have been adequately described, further experimentation is required to establish the composition of the insoluble solids, and the partition of activity among the components of the drop.

Radionuclide Composition and Radiation Characteristics.

1. The activities of products resulting from slow-neutron fission of U^{235} are sufficiently similar to those resulting from device fission to be quantitatively useful. It should also be noted that the absolute calibration of gamma counters is feasible, permitting calculation of the count-per-disintegration ratio of any nuclide whose photon-decay scheme is known. For establishing the quantity of a given nuclide in a complex mixture, radiochemistry is the method of choice; at the present time, gamma-ray spectrometry appears less reliable, even for nuclides readily identifiable. In addition, gross spectra obtained with a calibrated spectrometer led to computed counting rates for a laboratory gamma counter which were generally low.

2. Fractionation of radionuclides occurred in the fallout of all surface shots considered. By several criteria, such as R-values and capture ratios, Shot Navajo was the least fractionated, with fractionation increasing in Shots Flathead, Tewa, and Zuni. For Shot Zuni, the fractionation was so severe that the ionization per fission of the standard cloud sample was ~5 to 6 times greater than for close-in fallout samples. Important nuclides usually deficient in the fallout were members of the decay chains of antimony, xenon, and krypton, indicating that the latter products, because of their volatilities or rare-gas state, do not combine well with condensing or unaltered carrier particles. Although empirical methods have been employed to correct for fractionation in a given sample, and to relate the fractionation observed from sample to sample at Shot Zuni, the process is not well understood. As yet, no method is known for predicting the extent of fractionation to be expected for arbitrary yield and detonation conditions.

3. Tables of values are given for computing the infinite-field ionization rate for any point in the fallout field where the composition and fission density are known. The same tables permit easy calculation of the contribution of any induced nuclide to the total ionization rate. Based on How Island experience, rates so obtained are approximately twice as high as a survey meter would indicate. It is evident that unless fractionation effects, terrain factors, and instrument-response characteristics are quantitatively determined, accurate estimates of the fraction of the device in the local fallout cannot be obtained by summing observed dose-rate contours.

Correlations.

1. The maximum fission densities observed during the various shots were, in fissions per square foot, approximately 4×10^{15} for Shot Tewa, 8×10^{14} for Shot Zuni, 6×10^{14} for Shot Flathead, 9×10^{13} for Shot Navajo, and 9×10^{10} for Shot Cherokee. The fallout which was deposited during Shot Cherokee arrived as slurry particles similar to those produced by Shots Flathead and Navajo and appeared to be relatively unfractionated with regard to radionuclide composition; the total amount deposited was small, however, and of no military significance.

2. Reasonable agreement between the predicted and observed perimeters and central axes of the preliminary fallout patterns for Shots Zuni and Tewa was achieved by assuming the radioactive material to be concentrated largely in the lower third of the cloud and upper third of the stem, restricting particles larger than 1,000 and 500 microns in diameter to the inner 10 per-

cent and 50 percent of the cloud radius, respectively, and applying methods based on accepted meteorological procedures. Modified particle fall-rate equations were used and corrections were made for time and spatial variation of the winds. With the same assumptions, rough agreement was also achieved for Shots Flathead and Navajo by neglecting spatial variation of the winds, in spite of the gross differences in the character of the fallout. The reason for this agreement is not well understood. Predicted fallout arrival times were often shorter by 10 to 25 percent than the measured times, and the maximum particle sizes predicted at the times of arrival, peak, and cessation were usually smaller by 10 to 50 percent than the measured sizes.

3. The weighted mean values of the activity collected per unit area on the standard platform constitute a set of relative measurements, varying as a function of wind velocity and particle terminal velocity. The exact form of this function is not known; it appears, however, that the airflow characteristics of the platform were sufficiently uniform over the range of wind velocities encountered to make particle terminal velocity the controlling factor. The activity-per-unit-area measurements made on the samples from the skiffs may constitute a second set of relative values, and those made on samples from the raft and island minor arrays, a third set, closely related to the second.

4. The maximum platform collections should be utilized as the best estimate of the total amount of activity deposited per unit area. An error of about ±50 percent should be associated with each value, however, to allow for measurement error, collection bias, and other uncertainties. Although this procedure is strictly applicable only in those cases where single-wind deposition prevailed, comparable accuracy may be achieved by doubling the mean platform value and retaining the same percent error.

5. Decay of unfractionated fission products according to $t^{-1.2}$ is adequate for planning and estimating purposes. Whenever fractionation exists or significant induced activities are present, however, an actual decay curve measured in a counter with known response characteristics, or computed for the specific radionuclide composition involved, should be used. Errors of 50 percent or more can easily result from misapplication of the $t^{-1.2}$ rule in computations involving radiological effects.

6. It is possible to determine fraction of device by iron or residual uranium with an accuracy comparable to a Mo^{99} determination, but the requirements for a large sample, low background, and detailed device information are severe. In general, fractions calculated from these elements tended to be high. Analysis of copper, aluminum, and lead produced very high results which were not reported. It is probable that backgrounds from all sources were principally responsible, because the amounts of these elements expected from the Redwing devices were quite small.

7. The time-intensity recorders consistently measured less gamma ionization dose than film dosimeters located on the same platforms. In those cases where the geometry remained nearly constant and comparisons could be made, this deficiency totaled ~30 to 60 percent, in qualitative agreement with the response characteristics of the instrument estimated by other methods.

8. Because nearly equal amounts of fallout per unit area were collected over approximately the same time interval by the incremental collector, high volume filter, and open-close collectors on the ship platforms, it appears that air filtration through a medium exposed to direct fallout at face velocities up to 1.7 mph offers no substantial advantage over passive fallout sampling. It is apparent that under such conditions the collections are not proportional to the volume of air filtered, and should not be interpreted as implying the existence of an independent aerosol hazard.

9. The contamination index, which provides a measure of the relative fallout ionization rate for unit device yield per unit area, is approximately proportional to the ratio of fission yield to total yield of the device.

5.2 RECOMMENDATIONS

It is believed that the preceding results emphasize the desirability of making the following additional measurements and analyses.

1. Time of fallout arrival, rate of arrival, time of peak, and time of cessation should be

measured at a number of widely separated points for as many different sets of detonation conditions as possible. Because these quantities represent the end result of a complex series of interactions between device, particle, and meteorological parameters, additional relationships between them would not only provide interim operational guides, but would also be useful as general boundary conditions to be satisfied by model theory.

2. The particle-size distributions with time reported herein should be further assessed to remove the effects of background dust collections and applied to a more detailed study of particle size-activity relationships. For future use, an instrument capable of rapidly sizing and counting fallout particles in the diameter-size range from about 20 to 3,000 microns should be developed. Several promising instruments are available at the present time, and it is probable that one of these could be adapted for the purpose. While appropriate collection and handling techniques would have to be developed as an integral part of the effort, it is likely that improved accuracy, better statistics, and large savings in manpower could be achieved.

3. Controlled measurements should be made of the amount of solid-particle activity which penetrates to depths greater than the thermocline at rates higher than ~ 3 to 4 m/hr. Supporting measurements sufficient to define the particle size and activity distribution on arrival would be necessary at each point of determination. Related to this, measurements should be made of radionuclide fractionation with depth for both solid and slurry particles; in general, the solubility rates and overall dispersion behavior of fallout material in ocean water should be studied further. Underwater gamma detectors with improved performance characteristics and underwater particle collectors should be developed as required. Underwater data are needed to make more-accurate estimates from measured contours of the total amount of activity deposited in the immediate vicinity of the Eniwetok Proving Ground.

4. A formation theory for slurry particles should be formulated. Separation procedures should be devised to determine the way in which the total activity and certain important radionuclides are partitioned according to physical-chemical state. Microanalytical methods of chemical analysis applicable both to the soluble and insoluble phases of such particles are also needed. The evidence is that the solids present represent one form of the fundamental radiological contaminant produced by nuclear detonations and are for this reason deserving of the closest study. The radiochemical composition of the various types of solid particles from fallout and cloud samples should also receive further analysis, because differences related to the history of the particles and the radiation fields produced by them appear to exist.

5. A fallout model appropriate for shots producing only slurry particles should be developed. At best, the fact that it proved possible to locate the fallout pattern for shots of this kind, using a solid-particle model, is a fortuitous circumstance and should not obscure the fact that the precipitation and deposition mechanisms are unknown. Considering the likelihood in modern warfare of detonations occurring over appreciable depths of ocean water near operational areas, such a model is no less important than a model for the land-surface case. It would also be desirable to expand the solid-particle model applied during this operation to include the capability of predicting radiation contours on the basis of conventional scaling principles or the particle size-activity relationships given earlier.

6. Theoretical and experimental studies of radionuclide fractionation with particle type and spatial coordinates should be continued. This is a matter of the first importance, for if the systematic variations in composition suggested herein can be established, they will not only make possible more accurate calculation of the radiation fields to be expected, but may also lead to a better understanding of the basic processes of fallout-particle formation and contamination.

7. A series of experiments should be conducted to determine the true ionization rates and those indicated by available survey meters for a number of well-known individual radionuclides deposited on various kinds of terrain. Although the absolute calibration of all gamma counters and a good deal of logistic and analytical effort would be required, the resulting data would be invaluable for comparison with theoretical results. Also in this connection, the proposed decay schemes of all fission products and induced activities should be periodically revised and brought up to date.

8. Some concept of fraction of device which is meaningful in terms of relative gamma-radiation hazard should be formulated. The total ionization from all products of a given device could, for example, be computed for a 4-π ionization chamber. Decay-corrected measurement in the chamber of any fallout sample, whether fractionated or not, would then give a quantity representing a fraction of the total gamma-ray hazard. The definition of contamination index should also be expanded to include the concept of contamination potential at any point in the fallout area. In addition to the effects of the fission-to-total-yield ratio of the device on the resultant radiation field, the final value should include the effects of the particle characteristics and chemical composition of the material as they affect chemical availability and decontamination. Ideally, the value should be derivable entirely from the parameters of the device and its environment, so that it could be incorporated in model theory and used as part of conventional prediction procedures.

9. Additional bias studies of collecting instruments and instrument arrays should be performed. If possible, a total collector, an incremental collector, and a standard collector array should be developed whose bias characteristics as a function of wind velocity and particle terminal velocity are completely known. This problem, which can be a source of serious error in fallout measurements, has never been satisfactorily solved. To do so will require full-scale tests of operational instruments using controlled airflow and particles of known shape, density, and size distribution. Collectors should be designed to present the largest collecting areas possible, compatible with other requirements, in order to improve the reliability of subsequent analyses.

10. More-detailed measurements of oceanographic and micro-meteorological variables should accompany any future attempt to make oceanographic or aerial surveys of fallout regions, if contour construction is to be attempted. It appears, in fact, that because of the difficulty of interpreting the results of such surveys, their use should be restricted to locating the fallout area and defining its extent and general features.

11. Based on the results presented in this report, and the final reports of other projects, a corrected set of fraction-of-device contours should be prepared for the Redwing shots. These contours may represent the best estimate of local fallout from megaton detonations available to date; however, more-accurate estimates could be made in the future by collecting and analyzing enough total-fallout samples of known bias to permit the construction of iso-amount contours for various important radionuclides.

REFERENCES

1. C. E. Adams, F. R. Holden, and N. R. Wallace; "Fall-Out Phenomenology"; Annex 6.4, Operation Greenhouse, WT-4, August 1951; U. S. Naval Radiological Defense Laboratory, San Francisco 24, California; Confidential.

2. I. G. Poppoff and others; "Fall-Out Particle Studies"; Project 2.5a-2, Operation Jangle, WT-395 (in WT-371), April 1952; U. S. Naval Radiological Defense Laboratory, San Francisco 24, California; Secret Restricted Data.

3. R. K. Laurino and I. G. Poppoff; "Contamination Patterns at Operation Jangle"; USNRDL-399, 30 April 1953; U. S. Naval Radiological Defense Laboratory, San Francisco 24, California; Unclassified.

4. W. B. Heidt, Jr. and others; "Nature, Intensity, and Distribution of Fall-Out from Mike Shot"; Project 5.4a, Operation Ivy, WT-615, April 1953; U. S. Naval Radiological Defense Laboratory, San Francisco 24, California; Unclassified.

5. R. L. Stetson and others; "Distribution and Intensity of Fallout"; Project 2.5a, Operation Castle, WT-915, January 1956; U. S. Naval Radiological Defense Laboratory, San Francisco 24, California; Secret Restricted Data.

6. Headquarters, Joint Task Force Seven, letter; Subject: "Radiological Surveys of Several Marshall Island Atolls," 18 March 1954.

7. T. R. Folsom and L. B. Werner; "Distribution of Radioactive Fallout by Survey and Analyses of Sea Water"; Project 2.7, Operation Castle, WT-935, April 1959; Scripps Institution of Oceanography, La Jolla, California, and U. S. Naval Radiological Defense Laboratory, San Francisco 24, California; Secret Restricted Data.

8. H. D. LeVine and R. T. Graveson; "Radioactive Debris from Operation Castle Aerial Survey of Open Sea Following Yankee-Nectar"; NYO-4618.

9. M. B. Hawkins; "Determination of Radiological Hazard to Personnel"; Project 2.4, Operation Wigwam, WT-1012, May 1957; U. S. Naval Radiological Defense Laboratory, San Francisco 24, California; Official Use Only.

10. R. L. Stetson and others; "Distribution and Intensity of Fallout from the Underground Shot"; Project 2.5.2, Operation Teapot, WT-1154, March 1958; U. S. Naval Radiological Defense Laboratory, San Francisco 24, California; Unclassified.

11. D. C. Borg and others; "Radioactive Fall-Out Hazards from Surface Bursts of Very High Yield Nuclear Weapons"; AFSWP-507, May 1954; Headquarters, Armed Forces Special Weapons Project, Washington 13, D. C.; Secret Restricted Data.

12. "Fall-Out Symposium"; AFSWP-895, January 1955; Armed Forces Special Weapons Project, Washington 25, D. C.; Secret Restricted Data.

13. V. A. J. VanLint and others; "Fallout Studies During Operation Redwing"; Program 2, Operation Redwing, ITR-1354, October 1956; Field Command, Armed Forces Special Weapons Project, Sandia Base, Albuquerque, New Mexico; Secret Restricted Data.

14. R. T. Graveson; "Fallout Location and Delineation by Aerial Surveys"; Project 2.64, Operation Redwing, ITR-1318, February 1957; U. S. AEC Health and Safety Laboratory, New York, New York; Secret Restricted Data.

15. F. D. Jennings and others; "Fallout Studies by Oceanographic Methods"; Project 2.62a, Operation Redwing, ITR-1316, November 1956; University of California, Scripps Institution of Oceanography, La Jolla, California; Secret Restricted Data.

16. M. Morgenthau and others; "Land Fallout Studies"; Project 2.65, Operation Redwing, ITR-1319, December 1956; Radiological Division, Chemical Warfare Laboratories, Army Chemical Center, Maryland; Secret Restricted Data.

17. C. F. Miller and P. Loeb; "The Ionization Rate and Photon Pulse Rate Decay of Fission Products from Slow Neutron Fission of U^{235}"; USNRDL-TR-247, August 1958; U. S. Naval Radiological Defense Laboratory, San Francisco 24, California; Unclassified.

18. P. D. LaRiviere; "The Relationship of Time of Peak Activity from Fallout to Time of Arrival"; USNRDL-TR-137, February 1957; U. S. Naval Radiological Defense Laboratory, San Francisco 24, California; Unclassified.

19. J. W. Hendricks; "Fallout Particle Size Measurements from Operation Redwing"; USNRDL-TR-264, July 1958; U. S. Naval Radiological Defense Laboratory, San Francisco 24, California; Confidential.

20. S. Baum; "Behavior of Fallout Activity in the Ocean"; NRDL Technical Report (in publication); U. S. Naval Radiological Defense Laboratory, San Francisco 24, California; Secret.

21. C. E. Adams; "The Nature of Individual Radioactive Particles. II. Fallout Particles from M-Shot, Operation Ivy"; USNRDL-408, 1 July 1953; U. S. Naval Radiological Defense Laboratory, San Francisco 24, California; Confidential.

22. C. E. Adams; "The Nature of Individual Radioactive Particles. IV. Fallout Particles from the First Shot, Operation Castle"; USNRDL-TR-26, 17 January 1955; U. S. Naval Radiological Defense Laboratory, San Francisco 24, California; Confidential.

23. C. E. Adams; "The Nature of Individual Radioactive Particles. V. Fallout Particles from Shots Zuni and Tewa, Operation Redwing"; USNRDL-TR-133, 1 February 1957; U. S. Naval Radiological Defense Laboratory, San Francisco 24, California; Confidential.

24. C. E. Adams and J. D. O'Connor; "The Nature of Individual Radioactive Particles. VI. Fallout Particles from a Tower Shot, Operation Redwing"; USNRDL-TR-208, December 1957; U. S. Naval Radiological Defense Laboratory, San Francisco 24, California; Unclassified.

25. W. Williamson, Jr.; "Investigation and Correlation of Some Physical Parameters of Fallout Material"; USNRDL-TR-152, 28 March 1957; U. S. Naval Radiological Defense Laboratory, San Francisco 24, California; Unclassified.

26. J. Mackin and others; "Radiochemical Analysis of Individual Radioactive Fallout Particles from a Land Surface Detonation"; USNRDL-TR-386, September 1958; U. S. Naval Radiological Defense Laboratory, San Francisco 24, California; Unclassified.

27. C. D. Coryell and N. Sugarman; "Radiochemical Studies: The Fission Products"; Book 3; McGraw-Hill, 1951.

28. "Radiochemical Procedures in Use at the University of California Radiation Laboratory, Livermore"; UCRL-4377, 10 August 1954; University of California Radiation Laboratory, Livermore, California.

29. L. D. McIsaac; "Determination of Np^{239}, "Total Fissions," Mo^{99}, and Ce^{141} in Fission Product Mixtures by Gamma-Ray Scintillation Spectrometry"; USNRDL-TR-72, 5 January 1956; U. S. Naval Radiological Defense Laboratory, San Francisco 24, California; Unclassified.

30. H. K. Chan; "Activity-Size Relationship of Fallout Particles from Two Shots, Operation Redwing"; USNRDL-TR-314, February 1959; U. S. Naval Radiological Defense Laboratory, San Francisco 24, California; Unclassified.

31. N. H. Farlow and W. R. Scheil; "Physical, Chemical, and Radiological Properties of Slurry Particulate Fallout Collected During Operation Redwing"; USNRDL-TR-170, 5 May 1957; U. S. Naval Radiological Defense Laboratory, San Francisco 24, California; Unclassified.

32. W. R. Schell; "Physical Identification of Micron-Sized, Insoluble Fallout Particles Collected During Operation Redwing"; USNRDL-TR-364, 24 September 1959; U. S. Naval Radiological Defense Laboratory, San Francisco 24, California; Unclassified.

33. N. H. Farlow; "Quantitative Analysis of Chloride Ion in 10^{-6} to 10^{-12} Gram Particles"; Analytical Chemistry; 29: 883, 1957.

34. L. R. Bunney and N. E. Ballou; "Bomb-Fraction Measurement Techniques"; USNRDL-TR-176, September 1957; U. S. Naval Radiological Defense Laboratory, San Francisco 24, California; Secret Restricted Data.

35. M. Honma; "Flame Photometric Determination of Na, K, Ca, Mg, and Sr in Seawater"; USNRDL-TR-62, September 1955; U. S. Naval Radiological Defense Laboratory, San Francisco 24, California; Unclassified.

36. M. Honma; "Flame Photometric Determination of Na, K, Ca, Mg, and Sr in Coral"; Unpublished data; U. S. Naval Radiological Defense Laboratory, San Francisco 24, California.

37. F. D. Snell and C. T. Snell; "Colorimetric Methods of Analysis"; Vol. II Third Edition; D. Van Nostrand Co., New York; 1949.

38. A. P. Smith and F. S. Grimaldi; "The Fluorimetric Determination of Uranium in Nonsaline and Saline Waters, Collected Papers on Methods of Analysis for Uranium and Thorium"; Geological Survey Bulletin 1006; U. S. Government Printing Office, Washington, D. C.; 1954.

39. A. E. Greendale and M. Honma; "Glove Box and Associated Equipment for the Removal of Radioactive Fallout from Hexcell Collectors"; USNRDL-TR-157, May 1957; U. S. Naval Radiological Defense Laboratory, San Francisco 24, California; Unclassified.

40. M. Honma and A. E. Greendale; "Correction for Hexcell Background in Fallout Samples"; Unpublished data; U. S. Naval Radiological Defense Laboratory, San Francisco 24, California.

41. R. C. Bolles and N. E. Ballou; "Calculated Activities and Abundances of U^{235} Fission Products"; USNRDL-456, August 1956; U. S. Naval Radiological Defense Laboratory, San Francisco 24, California; Unclassified.

42. C. F. Miller; "Response Curves for USNRDL 4-Pi Ionization Chamber"; USNRDL-TR-155, May 1957; U. S. Naval Radiological Defense Laboratory, San Francisco 24, California; Unclassified.

43. P. D. LaRiviere; "Response of Two Low-Geometry Scintillation Counters to Fission and Other Products"; USNRDL-TR-303, February 1959; U. S. Naval Radiological Defense Laboratory, San Francisco 24, California; Unclassified.

44. C. F. Miller; "Proposed Decay Schemes for Some Fission-Product and Other Radionuclides"; USNRDL-TR-160, 17 May 1957; U. S. Naval Radiological Defense Laboratory, San Francisco 24, California; Unclassified.

45. C. F. Miller; "Analysis of Fallout Data. Part III; The Correlation of Some Castle Fallout Data from Shots 1, 2, and 3"; USNRDL-TR-222, May 1958; U. S. Naval Radiological Defense Laboratory, San Francisco 24, California; Secret Restricted Data.

46. V. A. J. VanLint; "Gamma Rays from Plane and Volume Source Distributions"; Program 2, Operation Redwing, ITR-1345, September 1956; Weapons Effects Tests, Field Command, Armed Forces Special Weapons Project, Sandia Base, Albuquerque, New Mexico; Confidential Restricted Data.

47. "The Effects of Nuclear Weapons"; U. S. Atomic Energy Commission, Washington, D. C., June 1957; Unclassified.

48. L. E. Glendenin; "Determination of Strontium and Barium Activities in Fission"; NNES IV, 9, Paper 236, 1951.

49. D. N. Hume; "Determination of Zirconium Activity by the Barium Fluozirconate Method"; NNES IV, 9, Paper 245, 1951.

50. E. M. Scadden; "Improved Molybdenum Separation Procedure"; Nucleonics 15, 102, 1957.

51. L. E. Glendenin; "Improved Determination of Tellurium Activity in Fission"; NNES IV, 9, Paper 274, 1951.

52. E. Mizzan; "Phosphotungstate Precipitation Method of Analysis of Radioactive Cesium in Solutions of Long-Lived Fission Products"; AECL Report PDB-128, July 1954.

53. L. E. Glendenin and others; "Radiochemical Determination of Cerium in Fission"; Anal. Chem. 27, 59, 1955.

54. L. Wish and M. Rowell; "Sequential Analysis of Tracer Amounts of Np, U, and Pu in Fission-Product Mixtures by Anion Exchange"; USNRDL-TR-117, 11 October 1956; U. S. Naval Radiological Defense Laboratory, San Francisco 24, California; Unclassified.

55. "Salted Weapons (C)"; AFSWP SWPDV-11-942.6, May 1957; Secret Restricted Data.

56. J. O. Blomeke; "Nuclear Properties of U^{235} Fission Products"; ORNL-1783, November 1955; Oak Ridge National Laboratory, Oak Ridge, Tennessee; Unclassified.

57. W. E. Thompson; "Spectrometric Analysis of Gamma Radiation from Fallout from Operation Redwing"; USNRDL-TR-146, 29 April 1957: U. S. Naval Radiological Defense Laboratory, San Francisco 24, California; Confidential Restricted Data.

58. "The Effects of Atomic Weapons"; U. S. Atomic Energy Commission, Washington, D. C., Revised September 1950; Unclassified.

59. K. Way and E. P. Wigner; "The Rate of Decay of Fission Products"; MDDC 1194, August 1947; Unclassified; also Phys. Rev. 73, 1318, 1948.

60. H. F. Hunter and N. E. Ballou; "Simultaneous Slow Neutron Fission of U^{235} Atoms. Individual Total Rates of Decay of the Fission Products"; USNRDL ADC-65, April 1949; U. S. Naval Radiological Defense Laboratory, San Francisco 24, California; Unclassified.

61. C. F. Miller; "Gamma Decay of Fission Products from the Slow-Neutron Fission of U^{235}"; USNRDL-TR-187, 11 July 1957; U. S. Naval Radiological Defense Laboratory, San Francisco 24, California; Unclassified.

62. "Radiological Recovery of Fixed Military Installations"; Navy, Bureau of Yards and Docks, NavDocks TPPL-13; Army Chemical Corps TM 3-225, interim revision, April 1958; Unclassified.

63. E. R. Tompkins and L. B. Werner; "Chemical, Physical, and Radiochemical Characteristics of the Contaminant"; Project 2.6a, Operation Castle, WT-917, September 1955; U. S. Naval Radiological Defense Laboratory, San Francisco 24, California; Secret Restricted Data.

64. H. V. Sverdrup, M. W. Johnson, and R. H. Fleming; "The Oceans, Their Physics, Chemistry, and General Biology"; Prentice-Hall, New York, 1942.

65. K. O. Emery, J. L. Tracey, Jr., and H. S. Ladd; "Geology of Bikini and Nearby Atolls. Bikini and Nearby Atolls: Part 1, Geology"; Geological Survey Professional Paper 260-A, U. S. Government Printing Office, Washington, D. C., 1954.

66. S. C. Foti; "Construction and Calibration of a Low Geometry Scintillation Counter"; Un-

published data, U. S. Naval Radiological Defense Laboratory, San Francisco 24, California.

67. E. A. Schuert; "A Fallout Forecasting Technique with Results Obtained at the Eniwetok Proving Ground"; USNRDL-TR-139, 3 April 1957; U. S. Naval Radiological Defense Laboratory, San Francisco 24, California; Unclassified.

68. E. A. Schuert; "A Fallout Plotting Device"; USNRDL-TR-127, February 1957; U. S. Naval Radiological Defense Laboratory, San Francisco 24, California; Unclassified.

69. L. Fussell, Jr.; "Cloud Photography"; Project 9.1a, Operation Redwing, ITR-1343, March 1957; Edgerton, Germeshausen and Grier, Inc., Boston, Massachusetts; Secret Formerly Restricted Data.

70. Meteorological Report on Operation Redwing; Part I, "Meteorological Data," Volumes 1, 2, and 11 and Part II, "Meteorological Analyses," Volumes 1, 2, and 3; Joint Task Force 7; JTFMC TP-1, 1956; Unclassified.

71. D. F. Rex; "Vertical Atmospheric Motions in the Equatorial Central Pacific"; Joint Task Force 7 Meteorological Center, Pearl Harbor, T. H.; Unclassified.

72. J. C. Kurtyka; "Precipitation Measurements Study"; State of Illinois Water Survey Division, Report of Investigation No. 20, 1953.

73. L. E. Egeberg and T. H. Shirasawa; "Standard Platform Sampling Bias Studies, Part I, Preliminary Studies of Airflow"; USNRDL-TM-70, 25 February 1957; U. S. Naval Radiological Defense Laboratory, San Francisco 24, California; Unclassified.

74. H. K. Chan; "Analysis of Standard Platform Wind Bias to Fallout Collection at Operation Redwing"; USNRDL-TR-363, September 1959; U. S. Naval Radiological Defense Laboratory, San Francisco 24, California; Unclassified.

75. W. W. Perkins and G. Pence; "Standard Platform Sampling Bias Studies, Part II, Rainfall Bias Studies"; USNRDL Technical Memorandum (in publication); U. S. Naval Radiological Defense Laboratory, San Francisco 24, California; Unclassified.

76. P. Brown and others; "Gamma Exposure versus Distance"; Project 2.1, Operation Redwing, WT-1310, 20 February 1960; U. S. Army Signal Engineering Laboratories, Fort Monmouth, New Jersey; Secret Restricted Data.

Appendix B
MEASUREMENTS

B.1 BUILDUP DATA

TABLE B.1 OBSERVED IONIZATION RATE, BY TIME-INTENSITY RECORDER

Station and Shot	
YAG 40-B, No. 9 ZU	
H + hr	mr/hr
3.37	2.28
3.57	16.8
3.73	44.2
4.07	129
4.37	470
5.07	1,480
6.07	3,340
7.07	1,660
8.07	1,360
9.07	1,240
11.1	966
14.1	754
18.1	588
22.1	478
26.1	404
30.1	340
42.1	233
54.1	181
66.1	129
78.1	105

YAG 40, No. 13 (Deck) ZU	
H + hr	r/hr
3.53	0.0165
3.63	0.0318
3.70	0.0386
3.77	0.0722
3.85	0.0847
3.97	0.128
4.05	0.165
4.17	0.249
4.32	0.480
4.57	0.957
4.77	1.31
4.95	1.92
5.08	2.37
5.25	3.25
5.40	4.06
5.57	4.58
5.73	5.67
5.90	5.76
6.07	6.20
6.32	6.75
6.57	7.57
6.82	7.57
7.07	7.29
7.32	7.20
7.57	6.94
7.82	6.66
8.07	6.30
8.32	6.20
8.57	6.02
8.82	5.76
9.07	5.67

Station and Shot	
YAG 40, No. 13 (Deck) ZU	
H + hr	r/hr
9.32	5.49
9.57	5.31
9.82	5.13
10.1	5.13
10.6	4.68
11.1	4.41
11.6	4.14
12.1	3.97
12.6	3.97
13.1	3.70
13.6	3.61
14.1	3.34
14.6	3.43
15.1	3.25
15.6	3.07
16.1	3.07
16.6	2.98
17.1	2.90
17.6	2.81
18.1	2.72
19.1	2.62
20.1	2.45
21.1	2.36
22.1	2.28
24.1	2.10
26.1	1.92
28.1	1.75
30.1	1.66
34.1	1.49
38.1	1.31
42.1	1.17
46.1	1.11
50.1	0.940
54.1	0.844
58.1	0.740
62.1	0.679
66.1	0.635
72.1	0.583
78.1	0.539
80.1	0.495

YAG 39-C, No. 9 ZU	
H + hr	mr/hr
12.7	0.559
13.1	0.706
13.6	0.765
14.1	0.926
15.1	1.47
16.1	2.96
17.1	4.29
18.1	6.54
19.1	8.36
20.1	9.42
21.1	10.2
22.1	10.2
23.1	10.8

Station and Shot	
YAG 39-C, No. 9 ZU	
H + hr	mr/hr
24.1	11.1
25.1	11.4
27.1	11.8
29.1	11.3
30.1	11.3
32.1	10.5
34.1	10.2
36.1	8.96
38.1	8.51
40.1	8.21
42.1	7.74
46.1	6.54
50.1	6.25
54.1	5.64
58.1	5.19
62.1	4.89
66.1	4.60
70.1	4.29
74.1	4.14
78 1	4.00
80.5	3.85

YAG 39, No. 13 (Deck) ZU	
H + hr	mr/hr
13.0	3.24
14.0	4.86
15.0	6.66
16.0	13.1
17.0	17.2
18.0	25.4
19.0	31.8
20.0	34.2
21.0	34.9
24.0	37.4
25.0	37.6
29.0	36.3
30.0	36.2
31.0	34.6
32.2	33.5
42.0	26.3
48.0	21.8
49.0	20.8
50.0	19.9
52.0	19.8
66.0	15.8
68.0	15.4
69.0	14.9
70.0	14.6
72.0	14.2

Station and Shot	
YFNB 13-E, ZU	
H + min	r/hr
20	0.0016
21	0.007
22	0.009
23	0.016
24	0.068
27	0.31
28	0.55
29	0.72
55	2.89
180	1.83
195	1.69
210	1.5
300	0.96
420	0.66
600	0.43
1,015	0.22
1,495	0.16
1,975	0.078
3,415	0.041

How F, ZU	
H + min	r/hr
23	0.0055
24	0.0086
26	0.013
27	0.051
28	0.092
28+	0.37
30	0.47
32	0.66
33	0.68
34	0.73
41	0.87
46	1.09
49	1.61
54	2.13
59	2.57
62	2.87
64	2.87
68	2.74
70	2.57
74	2.74
80	2.61
87	2.57
97	2.48
106	2.48
112	2.39
120	2.17
130	2.00
151	1.70
200	1.17
400	0.54

TABLE B.1 CONTINUED

YFNB 29-G ZU

H+min	r/hr
10	0.0005
20	0.03
26	0.26
27	0.54
28	0.83
29	0.99
31	1.32
33	3.10
35	4.0
36	4.94
43	9.21
49	9.64
94	7.05
124	5.64
139	4.7
184	3.06
274	2.12
424	1.36
484	0.99
544	0.80
574	0.78
649	0.70
799	0.55
1,624	0.31
2,524	0.19
3,424	0.15

YAG 40-B, No. 9 FL

H + hr	mr/hr
6.00	0.050
8.00	0.550
9.00	5.10
10.0	17.4
11.0	48.0
12.0	71.1
15.0	71.1
16.0	81.5
17.0	81.5
18.0	81.5
19.0	71.1
20.0	71.1
21.0	69.7
22.0	59.4
23.0	58.2
25.0	53.0
30.0	39.0
35.0	35.2
40.0	30.0
45.0	27.6
50.0	16.2
55.0	14.9
58.0	13.7
63.0	12.4
70.0	11.1
75.0	10.4
79.0	9.20

YAG 40, No. 13 (Deck) FL

H+hr	mr/hr
6.00	0
8.00	1.93
8.57	8.18
9.00	17.4
9.57	38.0
10.0	61.9
11.0	142
12.0	225
13.0	248
14.0	237
15.0	237
16.0	248
17.0	259
18.0	248
19.0	237
20.0	231
21.0	225
22.0	214
23.0	197
24.0	180
30.0	145
35.0	125
40.0	109
45.0	88.4
50.0	56.8
55.0	52.3
58.0	46.6
63.0	44.4
70.0	39.9
75.0	37.6
79.0	22.1

YAG 39-C, No. 9 FL

H + hr	mr/hr
4.12	0.061
4.37	0.417
4.53	0.646
4.78	1.01
4.95	1.88
5.10	3.30
5.38	6.19
5.68	8.23
6.05	10.7
6.27	12.3
6.52	15.4
6.72	19.4
7.02	21.9
7.28	21.9
7.50	23.7
7.75	26.1
8.02	28.6
8.28	29.9
8.57	29.9
8.77	32.3
9.19	32.9
9.60	31.7

YAG 39-C, No. 9 FL

H + hr	mr/hr
10.1	32.3
10.5	35.5
11.0	33.4
11.6	37.2
12.1	36.0
12.6	34.6
13.1	33.4
13.6	32.3
14.1	31.0
15.1	29.2
16.0	27.3
17.0	26.1
18.0	24.9
19.0	23.7
20.0	22.5
21.0	21.3
22.0	19.4
23.0	19.4
24.0	17.7
26.0	16.3
28.0	14.6
30.0	13.4
32.0	12.4
34.0	11.6
36.0	11.0
38.0	10.4
40.0	9.80
45.0	8.71
50.0	6.55
55.0	5.77
60.0	5.04
64.9	4.68
70.1	4.33
75.0	4.15
80.0	3.50

YAG 39, No. 13 (Deck) FL

H + hr	mr/hr
4.62	3.34
5.23	21.8
5.57	42.9
6.57	45.6
7.07	78.4
7.57	87.8
8.57	121
9.00	121
10.0	121
11.0	141
12.0	131
13.0	121
15.0	102
18.0	83.0
22.0	69.0
26.0	55.0
30.0	46.5
36.0	39.2

YAG 39, No. 13 (Deck) FL

H+hr	mr/hr
42.0	33.7
47.0	28.2
48.0	21.8
54.0	15.4
66.0	10.8
75.0	9.27
76.0	6.30
80.0	6.04

LST 611-D, No. 1 FL

H + hr	mr/hr
6.57	0.14
7.32	0.67
7.57	2.2
7.90	15.3
8.40	32
8.73	57
8.90	76
9.07	99
9.23	88
9.40	83
9.57	80
10.1	78
10.9	71
12.1	65
13.1	60
14.1	55
15.6	48
17.6	44
19.6	38
21.6	35
23.6	32

YFNB 13-E FL

H + min	r/hr
21	0.0016
24	0.0054
26	0.0048
30	0.030
32	0.56
35	2.26
37	6.82
77	21.8
137	11.5
257	5.5
377	2.5
437	1.9
497	1.6
557	1.5
617	1.2
617	1.4

TABLE B.1 CONTINUED

Station and Shot		Station and Shot		Station and Shot		Station and Shot	
YFNB 29 H FL		YAG 40-B, No. 9 NA		YAG 40, No. 13 (Deck) NA		YAG 40, No. 13 (Deck) NA	
H + min	r/hr	H + hr	mr/hr	H + hr	mr/hr	H + hr	mr/hr
35	0.004	11.0	45.7	7.18	6.64	50.2	9.15
36	0.0046	11.3	49.3	7.30	10.0	52.1	7.84
38	0.011	11.6	51.2	7.47	11.4	54.0	7.62
40	0.018	11.9	52.7	7.63	12.4	56.0	4.79
42	0.042	12.1	52.7	7.80	13.7	57.9	4.46
44	0.075	12.3	55.3	7.95	14.3	60.1	4.35
45	0.10	12.5	55.3	8.10	13.1	64.0	4.08
51	0.27	12.7	57.8	8.33	13.0	68.1	3.81
53	0.38	12.9	55.3	8.48	13.5	72.0	3.48
54	0.49	14.0	55.3	8.62	16.0	74.9	3.32
56	0.57	15.0	55.3	8.75	18.6		
58	0.63	16.0	55.3	8.85	27.4	YAG 39-C, No. 9 NA	
77	0.96	17.0	55.3	9.02	38.2	H + hr	mr/hr
91	0.98	17.6	51.4	9.27	51.4	1.97	0.161
100	0.94	18.0	50.2	9.47	56.5	2.22	4.00
175	0.55	19.0	48.8	9.67	63.9	2.38	14.4
250	0.33	20.0	46.3	9.98	74.5	2.47	21.4
470	0.14	21.0	25.9	10.3	80.2	2.55	33.5
630	0.077	22.0	21.0	10.6	92.0	2.65	48.2
850	0.055	23.0	18.4	11.0	103	3.00	68.3
1,100	0.043	24.0	17.7	11.3	120	3.30	88.2
1,500	0.024	25.0	16.6	11.6	122	3.50	95.7
1,800	0.0198	26.0	16.2	12.0	125	3.70	144
		27.0	14.3	12.2	129	3.87	207
YAG 40-B, No. 9 NA		28.0	13.9	12.3	126	4.18	372
H + hr	mr/hr	29.0	13.1	12.5	129	4.42	431
5.07	0.146	30.0	12.5	12.7	120	4.62	481
6.02	0.120	32.0	11.8	13.0	116	4.85	485
6.23	0.175	34.0	10.8	13.5	113	5.17	498
6.38	0.260	36.0	10.3	14.0	113	5.33	525
6.62	0.370	38.0	9.80	15.0	105	5.48	507
6.87	0.590	40.0	9.20	15.9	103	5.67	516
6.98	0.800	42.0	9.40	16.9	101	5.85	516
7.09	1.44	44.0	9.10	18.0	91.4	6.02	512
7.14	1.30	46.0	8.20	18.9	87.0	6.37	481
7.18	1.88	48.0	7.70	20.0	82.5	6.57	471
7.26	2.31	51.0	7.40	20.2	70.1	6.77	445
7.36	3.61	54.0	6.05	20.4	36.2	7.18	422
7.52	3.55	55.0	6.55	21.0	27.4	7.40	400
7.73	4.30	56.0	6.30	22.0	24.1	7.63	386
7.93	4.80	58.0	6.18	23.0	21.3	8.10	361
8.10	5.55	59.0	5.55	24.0	21.9	8.37	347
8.45	7.05	60.0	5.49	25.0	20.8	8.62	329
8.69	9.30	62.0	5.30	26.0	19.7	9.18	304
8.90	13.1	65.0	4.93	27.0	17.0	9.48	289
9.12	19.0	69.0	4.68	28.0	16.4	9.78	267
9.27	22.2	75.0	4.18	29.0	15.4	10.2	259
9.42	24.1			30.0	14.9	10.5	246
9.55	26.0	YAG 40, No. 13 (Deck) NA		32.0	14.3	10.9	232
9.70	28.3	H + hr	mr/hr	34.0	13.4	11.3	222
9.90	31.0	4.83	0.200	36.0	12.9	11.6	207
10.1	33.6	5.57	0.556	38.0	12.0	12.1	203
10.3	34.8	6.12	0.808	40.0	11.7	12.6	193
10.5	38.7	6.65	1.80	42.0	11.1	13.0	184
10.8	42.5	6.97	3.15	44.0	10.6	14.1	168
				46.0	10.2		
				48.0	9.58		

TABLE B.1 CONTINUED

Station and Shot		Station and Shot		Station and Shot		Station and Shot	
YAG 39-C, No. 9 NA		YAG 39, No. 13 (Deck) NA		LST 611-D, No. 1 NA		How F NA	
H+hr	mr/hr	H + hr	mr/hr	H + hr	r/hr	H + min	r/hr
15.2	149	6.57	1,130	2.2	0.00042	6	0.0010
16.0	80.0	6.82	900	2.4	0.00045	33	0.0011
17.0	60.7	7.00	773	2.7	0.00051	45	0.0019
18.0	58.1	7.32	728	2.9	0.00087	48	0.0056
19.0	56.9	7.57	671	3.1	0.0015	53	0.048
20.0	53.1	7.82	624	3.2	0.0029	54	0.069
21.0	45.8	8.32	603	3.4	0.0044	55	0.083
22.0	36.1	8.82	557	3.7	0.0085	59	0.11
23.0	34.7	9.32	502	3.8	0.013	66	0.145
24.0	32.4	9.82	468	4.0	0.015	76	0.137
26.0	29.9	10.3	434	4.1	0.017	93	0.13
27.0	25.0	10.8	412	4.4	0.010	100	0.135
28.0	22.6	11.6	378	4.6	0.008	110	0.14
30.0	22.0	12.0	344	4.7	0.011	120	0.148
32.0	21.4	12.6	332	4.80	0.0109	125	0.146
34.0	19.6	13.0	305	4.9	0.012	134	0.148
36.0	18.4	13.6	288	4.97	0.012	140	0.150
38.0	17.8	14.1	277	5.07	0.016	Malfunction	
40.0	17.2	14.6	266	5.6	0.042		
42.0	16.0	15.0	243	6.1	0.043	YFNB 29-H, NA	
44.0	15.3	15.6	221	7.1	0.034	H + min	r/hr
46.0	14.6	15.7	132	10.1	0.020	11	0.0011
48.0	13.9	16.0	110	14.1	0.012	40	0.0012
50.0	13.2	16.6	108	16.1	0.0081	45	0.0026
55.0	11.7	17.0	106	18.1	0.0067	47	0.0091
59.0	10.6	18.0	98.7	24.1	0.0044	50	0.033
60.0	11.7	19.0	92.1	27.0	0.0039	51	0.062
64.0	10.1	20.0	88.9			52	0.075
70.1	9.15	21.0	76.7	YFNB 13-E NA		53	0.079
73.9	8.43	22.0	69.1	H + min	r/hr	54	0.083
		23.0	65.8	10	0.0047	60	0.084
YAG 39, No. 13 (Deck) NA		24.0	63.8	18	0.037	72	0.10
H + hr	mr/hr	25.0	61.3	27	0.60	80	0.116
1.82	0.78	26.0	59.1	29	4.04	104	0.108
2.30	11.0	27.0	53.6	38	8.5	180	0.087
2.37	18.7	28.0	51.4	46	7.0	205	0.080
2.43	36.1	30.0	48.1	58	4.6	255	0.066
2.50	73.3	32.0	44.8	72	3.4	330	0.047
2.68	110	34.0	42.8	91	2.75	400	0.035
2.78	101	36.0	41.0	118	2.3	420	0.030
3.00	143	38.0	39.3	121	2.1	480	0.026
3.12	177	40.0	37.5	136	1.8	610	0.018
3.40	221	42.0	35.8	219	1.0	780	0.013
3.65	310	44.0	34.5	301	0.67	920	0.011
3.90	558	47.0	31.8	406	0.41	1,000	0.0078
4.12	900	50.0	29.1	631	0.20	1,005	0.0054
4.32	1,240	53.0	25.4	1,006	0.08	1,150	0.0050
4.57	1,070	56.0	23.6	1,066	0.059	1,250	0.0040
4.82	900	59.0	23.6	1,306	0.042	1,300	0.0034
5.00	900	64.0	21.8	1,546	0.036	1,600	0.0028
5.32	1,010	66.0	20.8	1,666	0.033	1,900	0.0023
5.57	1,130	74.0	18.1	1,786	0.031	2,400	0.0020
5.82	1,130			1,906	0.046	2,700	0.0014
6.00	1,490			2,026	0.056		
6.32	1,240			2,146	0.056		
				2,266	0.041		
				2,626	0.032		
				3,106	0.02		
				3,466	0.015		

TABLE B.1 CONTINUED

Station and Shot		Station and Shot		Station and Shot		Station and Shot	
YAG 40-B, No. 9 TE		YAG 40-B, No. 9 TE		YAG 40, No. 13 (Deck) TE		YAG 39-C, No. 9 TE	
H + hr	r/hr	H + hr	r/hr	H + hr	r/hr	H + hr	r/hr
4.35	0.0017	44.2	0.262	24.0	2.74	3.32	1.70
4.60	0.0057	46.2	0.207	25.0	2.64	3.37	1.88
4.73	0.0134	48.2	0.193	26.0	2.52	3.42	2.05
4.95	0.127	50.2	0.191	26.6	2.08	3.45	2.05
5.20	0.598	52.2	0.179	27.0	1.47	3.50	2.33
5.43	1.08	54.2	0.173	28.0	1.42	3.53	2.51
5.58	1.33	56.2	0.167	29.0	1.42	3.57	2.51
5.88	1.76	58.2	0.159	30.0	1.36	3.62	2.69
6.10	1.86	60.2	0.152	31.0	1.35	3.63	2.69
6.38	1.90	62.2	0.139	32.0	1.30	3.67	3.05
6.62	1.98	64.2	0.133	33.0	1.25	3.70	3.14
6.85	2.13	66.2	0.129	34.0	1.22	3.73	3.14
7.10	2.23	68.2	0.127	35.0	1.19	3.85	3.59
7.28	2.24	70.2	0.126	36.0	1.14	3.93	4.96
7.70	2.21	72.2	0.118	37.0	1.08	3.95	5.43
8.23	2.03	75.2	0.113	38.0	0.730	4.00	5.89
8.75	1.94			39.0	0.660	4.03	6.34
9.25	2.09	YAG 40, No. 13 (Deck) TE		40.0	0.588	4.10	6.72
9.75	1.89	H + hr	r/hr	41.0	0.572	4.13	7.28
10.3	1.85	4.48	0.0040	42.0	0.566	4.15	7.55
10.8	1.79	4.62	0.0097	43.0	0.512	4.20	7.55
11.2	1.80	4.75	0.0252	44.0	0.478	4.22	8.20
11.7	1.56	4.90	0.111	45.0	0.470	4.25	8.67
12.2	1.60	4.97	0.233	46.0	0.260	4.28	8.20
12.8	1.57	5.07	0.793	48.0	0.243	4.30	8.67
13.2	1.48	5.15	1.20	50.0	0.215	4.31	9.15
13.8	1.40	5.32	2.41	52.0	0.203	4.32	8.67
14.2	1.35	5.48	3.52	54.0	0.172	4.35	9.15
14.7	1.32	5.73	5.08	55.0	0.181	4.42	10.1
15.2	1.25	6.00	6.31	57.0	0.172	4.47	11.0
15.8	1.21	6.23	6.76	59.0	0.154	4.52	11.0
16.2	1.15	6.73	7.22	61.0	0.154	4.58	11.5
16.7	1.13	7.00	7.22	63.0	0.152	4.62	11.0
17.2	1.09	7.23	7.43	65.0	0.140	4.73	9.15
17.8	1.05	7.73	6.65	68.0	0.132	5.07	8.20
18.2	1.01	8.00	6.19	72.0	0.123	5.15	8.20
19.2	0.992	8.23	5.97	75.0	0.115	5.23	7.55
20.2	0.927	8.57	5.97			6.15	5.43
21.2	0.881	9.00	6.54	YAG 39-C, No. 9 TE		7.15	4.52
22.2	0.832	9.23	6.65	H + hr	r/hr	8.15	4.06
23.2	0.784	10.0	6.65	2.00	0.0017	9.15	3.59
24.2	0.770	11.0	6.65	2.20	0.0175	10.2	2.96
25.2	0.702	11.6	6.65	2.23	0.0308	11.2	2.70
26.2	0.670	12.0	6.54	2.28	0.0467	12.2	2.33
27.3	0.608	13.0	5.64	2.30	0.0591	13.2	2.15
28.2	0.596	14.0	5.42	2.33	0.0714	14.2	1.88
29.3	0.576	15.0	4.29	2.35	0.0837	15.2	1.70
30.2	0.568	16.0	3.97	2.37	0.109	16.2	1.52
31.2	0.554	17.0	3.84	2.70	0.514	17.2	1.30
32.2	0.527	18.0	3.52	2.85	0.728	18.1	1.13
33.4	0.439	19.0	3.29	2.97	0.906	19.2	1.07
34.1	0.432	20.0	3.18	3.05	1.08	20.2	0.995
35.3	0.415	21.0	3.08	3.13	1.29	21.1	0.942
36.1	0.403	22.0	2.96	3.20	1.41	22.1	0.888
38.4	0.339	23.0	2.86	3.27	1.60	24.2	0.763
40.4	0.307					26.2	0.594
42.2	0.292					28.2	0.505

TABLE B.1 CONTINUED

YAG 39 C, No. 9 TE	
H+hr	r/hr
30.1	0.465
32.2	0.461
34.2	0.412
36.2	0.381
38.3	0.376
40.1	0.310
42.2	0.292
44.0	0.290
48.0	0.243
50.1	0.238
53.2	0.215
56.2	0.192
60.1	0.171
63.9	0.158
66.2	0.151
70.5	0.139
72.4	0.136
74.4	0.131
76.4	0.123
78.6	0.113
79.4	0.113

YAG 39, No. 13 (Deck) TE	
H + hr	r/hr
1.30	0.0002
2.10	0.0082
2.23	0.0479
2.32	0.138
2.35	0.172
2.38	0.263
2.57	0.691
2.73	1.55
3.00	2.81
3.23	4.41
3.32	5.31
3.57	8.02
4.00	13.6
4.07	14.5
4.32	18.4
4.57	19.3
5.00	20.2
5.57	18.7
6.00	16.9
6.57	15.5
7.00	14.5
7.57	13.4
8.57	12.7
9.00	11.7
9.57	10.8
10.0	9.83
10.6	8.96
11.0	8.96
12.0	8.49
13.0	7.12
14.0	6.19
15.0	5.84
16.0	5.84
17.0	5.13
18.0	4.85

YAG 39, No. 13 (Deck) TE	
H+hr	r/hr
20.0	3.88
21.0	3.61
22.0	3.52
23.0	3.52
24.0	3.07
25.0	2.98
26.0	2.90
27.0	2.36
28.0	2.28
29.1	2.19
30.1	2.10
31.0	2.10
32.1	1.92
33.1	1.84
34.0	1.75
35.0	1.49
36.0	1.44
37.1	1.36
38.1	1.37
39.0	1.09
40.0	1.04
41.0	1.00
42.0	0.972
42.9	0.955
45.0	0.894
47.2	0.886
49.0	0.825
51.0	0.799
53.0	0.772
55.0	0.711
57.0	0.659
59.0	0.642
61.0	0.616
63.1	0.564
64.9	0.555
66.0	0.529
67.0	0.516
69.0	0.499
71.0	0.485
73.0	0.459
75.0	0.451
77.0	0.424
79.0	0.376
80.2	0.374

LST 611-D, No. 1 TE	
H + hr	r/hr
7.18	0.002
7.23	0.0033
7.73	0.024
8.23	0.019
8.65	0.027
8.95	0.048
9.28	0.082
9.51	0.10
9.78	0.12
10.0	0.12
10.28	0.13
10.48	0.17

LST 611-D, No. 1 TE	
H+hr	r/hr
10.73	0.24
10.98	0.18
11.23	0.182
11.73	0.187
12.23	0.198
12.35	0.205
12.98	0.224
13.56	0.256
14.23	0.247
14.85	0.236
15.48	0.215
21.11	0.146
24.23	0.112
31.73	0.085
34.48	0.066
38.48	0.054
40.48	0.051

YFNB 13-E TE	
H+min	r/hr
18	0.0056
26	0.013
30	0.021
32	0.022
35	0.020
36	0.025
37	0.019
40	0.018
43	0.020
46	0.022
50	0.030
61	0.090
71	0.20
81	0.52
91	1.11
101	1.87
111	2.13
114	2.34
116	2.5
118	2.34
123	2.21
177	2.25
204	1.9
309	1.0
429	0.7
909	0.30
1,269	0.15
1,500	0.12
2,109	0.076
3,069	0.042
3,309	0.016
3,549	0.009
3,789	0.0085
4,029	0.0081
4,509	0.0072

How F TE	
H+min	r/hr
101	0.0069
107	0.016
109	0.024
112	0.032
113	0.036
115	0.041
116	0.044
117	0.051
118	0.060
119	0.064
128	0.101
142	0.15
149	0.19
152	0.20
173	0.22
195	0.21
221	0.19
251	0.173
341	0.11
401	0.092
599	0.061
749	0.051
899	0.042
1,289	0.029
1,589	0.024
1,889	0.021

YFNB 29-H TE	
H+min	r/hr
1	0.00056
3	0.00046
14	0.0016
16	0.015
20	0.047
22	0.30
24	0.60
25	0.80
26	0.90
28	2.0
34	3.8
38	7.4
44	10.0
49	13.2
490	9.9
670	7.1
730	6.9
850	6.3
920	5.9
970	5.3
1,300	3.5
2,000	1.9
3,000	1.14
3,200	0.72

TABLE B.2 INCREMENTAL COLLECTOR DATA

Tray Number	Exposure Began (Mike Time) 28 May 56	Midpoint of Exposure TSD		γ Activity	γ Activity per Unit Time
		hr	min	counts/min	counts/min²
Designator: YAG 40-A-1 ZU Counting Time: Corrected to H+12 hours Nominal Exposure Interval: Variable					
337	0915	3.4		36,330	2,400
330	0930	3.7		307,800	30,800
331	0940	3.8		298,900	29,890
332	0950	4.1		1,392,000	69,600
333	1010	4.3		2,378,000	237,800
334	1020	4.5		2,149,000	214,900
335	1030	4.7		1,219,000	121,900
336	1040	4.8		1,808,000	180,800
324	1050	5.0		4,023,000	402,300
325	1100	5.2		4,741,000	474,000
326	1110	5.3		4,687,000	468,700
327, 328	1120	5.7		16,423,000	547,400
329	1150	6.0		5,140,000	514,000
318, 319	1200	6.3		12,628,000	451,000
320	1228	6.7		5,044,000	229,300
321, 322	1250	7.1		4,065,000	176,700
323	1313	7.4		291,900	36,480
308	1321	7.5		349,200	23,280
309	1336	7.8		541,300	36,090
310	1351	8.1		316,500	16,660
311	1410	8.4		701,500	35,070
312	1430	8.7		189,540	9,480
313	1450	9.1		320,000	16,000
314	1510	9.4		309,500	15,480
End of run	1530				
Designator: YAG 40-B-7 ZU Counting Time: H+55.1 to H+62.9 hours Nominal Exposure Interval: 15 minutes					
401	0918	3.5		233,400	15,560
402	0932.7	3.7		349,300	23,287
403	0947.4	4.0		368,500	24,567
404	1002.1	4.2		1,225,000	81,667
405	1017.1	4.5		2,089,000	139,267
406	1031.8	4.7		2,091,000	139,400
407	1047	5.0		2,626,000	175,067
408	1102	5.2		4,299,000	286,600
409	1117.4	5.5		4,146,000	276,400
410	1132.6	5.7		4,928,000	328,533
411	1147.8	6.0		3,916,000	261,067
412	1203	6.3		1,469,000	97,933
413	1218.2	6.5		908,600	60,573
414	1233.4	6.7		1,074,000	71,600
415	1248.6	7.0		1,001,000	66,733
416	1303.8	7.2		141,100	9,407
417	1319	7.5		110,200	7,347
418	1334.2	7.8		53,340	3,556
419	1349.4	8.0		26,830	1.789
420	1404.6	8.3		60,730	4,049

TABLE B.2 CONTINUED

Tray Number	Exposure Began (Mike Time) 28 May 56	Midpoint of Exposure TSD		γ Activity	γ Activity per Unit Time
		hr	min	counts/min	counts/min²
421	1419.8	8.5		84,300	5,620
422	1435.0	8.8		116,000	7,733
423	1450.2	9.0		148,600	9,907
424	1505.4	9.3		179,200	11,946
425	1520.6	9.5		114,300	7,620
426	1535.8	9.8		95,720	6,380
427	1551.0	10.1		113,900	7,593
428	1606.2	10.3		53,230	3,549
429	1621.4	10.6		63,720	4,248
430	1636.6	10.8		87,920	5,861
431	1651.8	11.0		57,860	3,857
432	1707	11.3		63,490	4,233
433	1722.2	11.6		42,370	2,825
434	1737.4	11.8		32,260	2,151
435	1752.6	12.1		32,390	2,159
436	1807.8	12.3		18,430	1,229
437	1823	12.6		14,260	951
438	1838.2	12.8		15,610	1,041
439	1853.4	13.1		15,790	1,053
440	1908.6	13.3		10,150	677
441	1923.8	13.6		20,150	1,343
442	1939	13.9		16,950	1,130
443	1954.2	14.1		17,210	1,147
444	2009.4	14.4		12,960	864
445	2024.6	14.6		12,150	810
446	2039.8	14.8		12,460	831
447	2055	15.1		12,280	819
448	2110.2	15.4		4,462	297
449	2125.4	15.6		10,600	707
450	2140.1	16.1		111,600	3,434
451	2212.6	—		719,900	47,993
End of run	End of fallout				
Designator: YAG 39-C-20 ZU					
Counting Time: H+66 to H+70 hours					
Nominal Exposure Interval: 15 minutes					
229	1805	12.3		1,929	128
230	1820	12.5		1,690	112
231	1835	12.8		4,440	296
232	1850	13.0		1,474	98
233	1905	13.3		8,880	591
234	1920	13.5		2,540	169
235	1935	13.8		452	30
236	1950	14.0		1,093	73
237	2005	14.3		1,389	93
238	2020	14.5		2,412	161
239	2035	14.8		1,663	111
240	2050	15.0		3,552	236
241	2105	15.3		6,532	435
242	2120	15.5		12,860	859
243	2135	15.8		10,670	711
244	2150	16.0		6,076	405
245	2205	16.3		7,651	510
246	2220	16.7		14,880	425
247	2255	17.1		14,190	992
248	2309.3	19.0		131,900	570
249	0300	21.2		18,400	1,330
250	0314.2	21.4		9,236	615
251	0329.2	21.7		2,767	192
252	0344.2	21.9		2,647	177
253	0359.2	22.2		5,074	338
254	0414.2	22.4		8,143	541
255	0429.2	22.7		7,990	519

TABLE B.2 CONTINUED

Tray Number	Exposure Began (Mike Time) 28 May 56	Midpoint of Exposure TSD		γ Activity	γ Activity per Unit Time
		hr	min	counts/min	counts/min²
256	0444.2	22.9		6,497	433
257	0459.2	23.2		6,872	458
258	0514.2	23.4		6,776	452
259	0529.2	23.7		5,337	356
260	0544.2	23.9		8,816	588
261	0559.2	24.2		8,378	559
262	0614.2	24.4		4,577	303
263	0629.2	24.7		3,479	232
264	0644.2	24.9		4,396	292
265	0659.2	25.2		4,047	269
266	0714.2	25.4		4,546	303
267	0729.2	25.7		5,055	336
268	0744.2	25.9		4,137	276
269	0759.2	26.2		3,497	233
270	0814.2	26.4		3,400	226
271	0829.2	26.7		5,780	385
272	0844.2	26.9		4,195	279
273	0859.2	27.2		5,464	364
274	0914.2	27.4		3,076	205
275	0929.2	27.7		4,774	318
276	0944.2	27.9		4,608	307
277	0959.2	28.2		3,303	220
278	1014.2	28.4		149,800	9,970
279	1029.2	28.7		3,005	200
280	1044.2	28.9		2,610	176
281	1059.2	29.2		1,814	121
282	1114.2	29.4		3,230	216
283	1129.2	29.7		2,849	190
284	1144.2	29.9		3,372	225
End of run	1159.2				
Designator: YFNB 13-E-57 ZU					
Counting Time: H+39.3 to H+42.8 hours					
Nominal Exposure Interval: 15 minutes					
1200	0556	0.1	6	521	35
1201	0611	0.4	24	752,200	501,040
1202	0626	0.6	36	2,726,000	181,733
1203	0641	0.9	54	5,819,000	387,933
1204	0656	1.1	66	7,034,000	468,933
1205	0711	1.4	84	3,870,000	258,000
1206	0726	1.6	96	2,752,000	183,467
1207	0741	1.9	114	1,248,000	83,200
1208	0756	2.1	126	445,900	29,727
1209	0811	2.4	144	173,700	10,247
1210	0826	2.6	156	157,300	10,486
1211	0841	2.9	174	39,860	2,657
1212	0856	3.1	186	7,098	473
1213	0911	3.4	204	28,790	1,919
1214	0926	3.6	216	19,318	1,288
1215	0941	3.9	234	6,211	414
1216	0956	4.1	246	5,363	358
1217	1011	4.4	264	4,474	298
1218	1026	4.6	276	3,699	247
1219	1041	4.9	294	1,267	84
1220	1056	5.1	306	1,113	74
1221	1111	5.4	324	1,034	69
1222	1126	5.6	336	1,629	109
1223	1141	5.9	354	2,148	145
1224	1156	6.1	366	8,504	567

TABLE B.2 CONTINUED

Tray Number	Exposure Began (Mike Time) 28 May 56	Midpoint of Exposure TSD		γ Activity	γ Activity per Unit Time
		hr	min	counts/min	counts/min²
1225	1211	6.4	384	800	53
1226	1226	6.6	396	850	57
1227	1241	6.9	414	1,036	69
1228	1256	7.1	426	536	36
1229	1311	7.4	444	1,249	83
1230	1326	7.6	456	586	39
1231	1341	7.9	474	5,734	382
1232	1356	8.1	486	21,079	1,405
1233	1411	8.4	504	12,420	828
1234	1426	8.6	516	568	38
1235	1441	8.9	534	1,818	121
1236	1456	9.1	546	12,490	833
1237	1511	9.4	564	—	—
1238	1526	9.6	576	1,066	71
1239	1541	9.9	594	684	46
1240	1556	10.1	606	480	32
1241	1611	10.4	624	126	8
1242	1626	10.6	636	404	27
1243	1641	10.9	654	574	38
1244	1656	11.1	666	820	55
1245	1711	11.4	684	613	41
1246	1726	11.6	696	1,164	78
1247	1741	11.9	714	—	—
1248	1756	12.1	726	Background	
1249				Background	
1250 to 1253				Background	
1254	1941	13.8	828	Background	
Designator: How F-64 ZU					
Counting Time: H+20.2 to H+22.8 hours					
Nominal Exposure Interval: 15 minutes					
858	0556	0.1	6	19	1
859	0611	0.4	24	2,996	199
860	0626	0.6	36	2,082,000	138,800
861	0641	0.9	54	1,113,000	74,200
862	0656	1.1	66	710,200	46,747
863	0711	1.4	84	754,700	50,313
864	0726	1.6	96	907,800	60,520
865	0741	1.9	114	216,700	14,447
866	0756	2.1	126	74,300	4,953
867	0811	2.4	144	134,800	8,987
868	0826	2.6	156	50	3
869	0841	2.9	174	15	1
870	0856	3.1	186	46	3
871	0911	3.4	204	124	8
872	0926	3.6	216	15	1
873	0941	3.9	234	79	5
874	0956	4.1	246	64	4
875	1011	4.4	264	742	50
876	1026	4.6	276	47	3
877 to 899				Background	
End of run	1641	10.7		Background	

TABLE B.2 CONTINUED

Tray Number	Exposure Began (Mike Time) 28 May 56	Midpoint of Exposure TSD		γ Activity	γ Activity per Unit Time
		hr	min	counts/min	counts/min²
Designator: YFNB 29-G-71 ZU Counting Time: H+29.6 to H+35.4 hours Nominal Exposure Interval: 2 minutes					
1257	0558.2		3	274	137
1258	0600		5	1,059	530
1259	0602		7	34	17
1260	0603.8		9	−4	−2
1261	0605.6		10	−2	−1
1262	0607.3		12	−3	−2
1263	0609.2		14	85	42
1264	0611		16	38	19
1265	0612.8		18	47	24
1266	0615		20	43	22
1267	0617		22	39	20
1268	0618.8		23	44	22
1269	0621		26	203	102
1270	0622.7		28	212	206
1271	0624.6		30	375	172
1272	0626.4		31	97,120	48,560
1273	0628.4		33	7,320	3,660
1274	0630.3		35	768,900	384,450
1275	0632.1		37	289,100	144,500
1276	0634.1		39	1,569,000	784,500
1277	0636.2		41	58,000	29,000
1278	0638.3		43	35,200	17,600
1279	0640.5		46	1,321,000	660,500
1280	0642.7		48	670,700	335,350
1281	0644.8		50	337,700	168,850
1282	0646.8		52	138,000	69,000
1283	0648.7		54	1,666,000	833,000
1284	0650.8		56	451,600	225,800
1285	0652.8		58	382,200	191,100
1286	0654.3		59	1,534,000	767,000
1287	0656.5		62	2,581,000	1,290,500
1288	0658.8		64	1,466,000	733,000
1289	0700.8		66	377,900	188,950
1290	0702.9		68	1,499,000	749,500
1291	0705		70	1,089,000	544,500
1292	0707		72	1,635,000	817,500
1293	0709.1		74	1,048,000	524,000
1294	0711.2		76	321,700	160,850
1295	0713		78	623,000	311,500
1296	0715		80	1,386,000	693,000
1297	0716.7		82	531,600	265,800
1298	0718.5		83	711,400	355,700
1299	0720.7		85	610,200	305,100
1300	0722.4		87	1,032,000	516,000
1301	0724.5		90	429,700	214,850
1302	0726.7		92	1,159,000	579,500
1303	0728.8		94	334,600	167,300
1304	0730.8		96	725,000	362,500
1305	0733		98	416,900	208,450
1306	0735.1		100	172,400	86,200
1307	0737		102	270,400	135,200
1308	0739.1		104	188,300	94,150
1309	0741.2		106	239,100	119,550
1310	0743.3		108	360,300	180,150
1311	0745.5		110	1,032,000	516,000
End of run	0747.2				

TABLE B.2 CONTINUED

Tray Number	Exposure Began (Mike Time) 12-13 June 56	Midpoint of Exposure TSD		γ Activity	γ Activity per Unit Time
		hr	min	counts/min	counts/min²
Designator: YAG 40-A-1 FL					
Counting Time: Corrected to H+12 hours					
Nominal Exposure Interval: Variable					
3815	1145	5. 9		434	5. 8
2690	1300	7. 1		405	6. 8
3814	1400	7. 8		15,453	515
2689	1430	8. 3		393	13. 1
3813	1500	8. 8		15,370	512
2688	1530	9. 3		22,130	738
3812	1600	9. 8		76,380	2,546
2687	1630	10. 3		24,670	822
3811	1700	10. 8		114,400	3,813
2686	1730	11. 3		52,230	1,741
3810	1800	11. 8		45,700	1,523
2685	1830	12. 3		4,495	150
3809	1900	13. 1		192	3
2684	2000	13. 8		175	6
3808	2030	14. 3		22,170	739
2683	2100	14. 8		13,470	449
3807	2130	15. 3		55,500	1,850
2682	2200	15. 8		79,590	2,653
3806	2230	16. 3		29,380	979
2681	2300	16. 8		75,600	2,520
3805	2330	17. 3		11,530	384
2680	2400	17. 8		15,950	532
3804	0030	18. 3		23,920	797
2679	0100	18. 8		84	3
3803	0130	19. 3		18,520	617
2678	0200	19. 8		64	2
3802	0230	20. 3		89	3
2677	0300	20. 8		6,609	220
3801	0330	21. 3		27,860	929
2676	0400	21. 8		9,400	313
3800	0430	22. 3		202,000	6,733
2675	0500	22. 8		16,070	537
3799	0530	23. 3		73	2
2674	0600	23. 8		147	5
3798	0630	24. 3		29	1
2673	0700	24. 8		196	6
3797	0730	25. 3		126	4
2669	0800	25. 8		356	11. 9
3796	0830	26. 2		275	13. 7
2671	0850	26. 7		3,801	95
End of run	0930	27. 1			
Designator: YAG 40-B-7 FL					
Counting Time: Corrected to H+12 hours					
Nominal Exposure Interval: 15 minutes					
	12 June 56				
2638	1235	6. 3		1,273	84. 8
3764	1250	6. 5		1,301	86. 7
2637	1305	6. 8		714	47. 6
3763	1320	7. 0		414	27. 6
2636	1335	7. 3		392	26. 1
3762	1350	7. 5		3,347	223
2635	1405	7. 8		146	9. 7
3761	1420	8. 0		1,525	102

TABLE B.2 CONTINUED

Tray Number	Exposure Began (Mike Time) 12 June 56	Midpoint of Exposure TSD		γ Activity	γ Activity per Unit Time
		hr	min	counts/min	counts/min²
2634	1435	8.3		520	34.7
3760	1450	8.5		1,876	125
2633	1505	8.8		5,733	382
3759	1520	9.0		17,379	1,159
2632	1535	9.3		5,602	373
3758	1550	9.5		36,505	2,434
2631	1605	9.8		271	18.1
3759	1620	10.0		50,997	3,400
2630	1635	10.3		28,380	1,892
3756	1650	10.5		163,700	10,910
2629	1705	10.8		9,928	662
3755	1720	11.0		17,720	1,181
2628	1735	11.3		11,990	799
3754	1750	11.5		3,799	253
2627	1805	11.8		8,997	600
3753	1820	12.0		45,806	3,054
2626	1835	12.3		210	14
3752	1850	12.5		32,833	2,189
2625	1905	12.8		7,223	482
3751	1920	13.0		960	64
2624	1935	13.3		293	19.5
3750	1950	13.5		804	53.6
2623	2005	13.8		290	19.3
3749	2020	14.0		717	47.8
2622	2035	14.3		41	3
3748	2050	14.5		807	53.8
2621	2105	14.8		118	7.9
3747	2120	15.0		22,809	1,521
2620	2135	15.3		4,565	304
3746	2150	15.5		193	12.9
2619	2205	15.8		176	11.7
3745	2220	16.0		17,653	1,177
2618	2234	16.3		326	21.7
3744	2249	16.5		2,627	175
2617	2304	16.8		1,360	90.6
3743	2319	17.0		1,877	125
2616	2334	17.3		283	18.9
3742	2349	17.5		8,805	587
2615	0004	17.8		374	24.9
3741	0019	18.0		21,188	1,412
2614	0034	18.3		7,158	477
3740	0049	18.5		625	41.7
2613	0104	18.8		644	42.9
3739	0119	19.0		675	45.0
2612	0133	19.3		1,948	130
3738	0148	19.5		843	56.2
2611	0203	19.8		1,974	132
End of run	0218	19.9			
Designator: YAG 39-C-20 FL Counting Time: Corrected to H+12 hours Nominal Exposure Interval: 15 minutes					
2176	1050	4.5		948	63.2
3318	1104.6	4.8		16,210	1,081
2177	1119.6	5.0		870	58.0
3319	1134.6	5.3		65,930	4,395
2178	1149.6	5.5		35,540	2,369
3320	1205.5	5.8		371,000	24,730
2179	1220.8	6.0		463	30.9

TABLE B.2 CONTINUED

Tray Number	Exposure Began (Mike Time) 12 June 56	Midpoint of Exposure TSD		γ Activity	γ Activity per Unit Time
		hr	min	counts/min	counts/min²
3321	1236.1	6.3		994	66.3
2180	1251.2	6.5		213	14.2
3322	1306.2	6.8		13,220	881
2181	1321.5	7.1		23	1
3323	1326.9	7.3		852	56.8
2182	1352.2	7.6		12,960	864
3324	1407.5	7.8		2,218	148
2183	1422.9	8.1		275	18.3
3325	1437.9	8.3		1,301	86.7
2184	1452.9	8.6		1,054	70.3
3326	1508.3	8.8		1,463	97.5
2185	1523.5	9.1		474	31.6
3327	1538.8	9.3		8,106	540
2186	1554.1	9.6		211	14.1
3328	1609.3	9.9		904	60.3
2187	1624.4	10.1		1,275	85
3329	1639.4	10.4		26,870	1,791
2188	1654.7	10.6		26,920	1,795
3330	1710.0	10.8		30,140	2,009
2189	1725	11.1		904	60.3
3331	1740	11.4		1,765	118
2190	1755	11.6		167	11.1
3332	1810.3	11.9		1,345	89.6
2191	1825.5	12.1		18,880	1,259
3333	1840.5	12.4		7,738	516
2192	1855.8	12.6		298	199
3334	1911.2	12.9		484	32.3
2193	1926.2	13.1		172	11.5
3335	1941.2	13.4		19,360	1,291
2194	1956.5	13.6		616	41.1
3336	2011.8	13.9		782	521
2195	2027.1	14.2		1,120	74.4
3337	2042.1	14.4		2,243	150
2196	2057.3	14.7		12,925	862
3338	2112.4	14.9		1,567	104
2197	2127.4	15.2		506	33.7
3339	2142.4	15.4		653	43.5
2198	2157.4	15.6		578	38.5
3340	2212.7	15.9		1,535	102
2199	2228.0	16.2		249	16.6
3341	2243	16.4		887	59.1
2200	2258.3	16.7		619	41.3
3342	2313.6	16.9		1,250	83.3
2201	2328.6	17.2		536	35.7
3343	2343.9	17.4		495	33.0
2202	2358.9	17.7		308	20.5
3344	0013.9	17.9		1,125	75.0
2203	0028.9	18.2		460	30.6
End of run	0042.2				
Designator: LST 611-D-50 FL Counting Time: Corrected to H+12 hours Nominal Exposure Interval: 15 minutes					
2667	1327	7.2		426	28.4
3792	1342.3	7.4		1,079	72
2666	1357.5	7.7		28,757	1,915
3791	1412.7	7.9		622	41.5
2665	1427.9	8.1		18,747	1,250

TABLE B. 2 CONTINUED

Tray Number	Exposure Began (Mike Time) 12 June 56	Midpoint of Exposure TSD		γ Activity	γ Activity per Unit Time
		hr	min	counts/min	counts/min²
3790	1443. 2	8. 4		1, 891	126
2664	1458. 4	8. 7		69, 250	4, 620
3789	1513. 6	8. 9		31, 126	2, 070
2663	1528. 8	9. 2		6, 348	422
3788	1544	9. 4		785	52. 4
2662	1559. 2	9. 7		216	14. 4
3787	1614. 4	9. 9		348	23. 2
2661	1629. 6	10. 2		477	31. 8
3786	1644. 8	10. 4		398	26. 5
2660	1700	10. 7		472	31. 5
3785	1715. 2	10. 9		743	49. 5
2659	1730. 4	11. 2		218	14. 5
3784	1745. 6	11. 4		1, 088	72. 5
2658	1800. 8	11. 7		83	5. 5
3783	1816	12. 0		1, 922	128
2657	1831. 2	12. 2		840	56
3782	1846. 4	12. 5		1, 239	82. 6
2656	1901. 6	12. 7		63	4
3781	1916. 8	13. 0		626	41. 7
2655	1932	13. 2		425	28. 3
3780	1947. 2	13. 5		425	28. 3
2654	2002. 6	13. 7		432	29. 8
3779	2017. 8	14. 0		2, 482	165
2653	2033	14. 2		93	6. 2
3778	2048. 1	14. 5		11, 269	751
2652	2103. 3	14. 8		194	12. 9
3777	2118. 5	15. 0		965	64. 3
2651	2133. 7	15. 3		697	46. 5
3776	2148. 9	15. 5		536	35. 7
2650	2204. 1	15. 8		161	10. 7
3775	2219. 3	16. 0		402	26. 8
2649	2234. 5	16. 3		663	44. 2
3774	2250	16. 5		1, 481	98. 7
2648	2305. 2	16. 8		140	9. 3
3773	2320. 4	17. 0		402	26. 8
2647	2435. 6	17. 3		536	35. 7
3772	2550. 8	17. 5		187	12. 5
2646	0006	17. 8		1, 219	81. 3
3771	0021. 2	18. 1		1, 189	79. 3
2645	0036. 4	18. 3		375	25. 0
3770	0051. 6	18. 5		1, 658	110
2644	0106. 8	18. 8		4, 037	269
3769	0122	19. 1		1, 735	116
2643	0137. 2	19. 3		519	34. 6
3768	0152. 4	19. 6		409	27. 3
2642	0207. 6	19. 8		1, 209	80. 6
3767	0222. 8	20. 1		1, 112	74. 1
2641	0238	20. 3		2, 184	145. 0
3766	0253. 2	20. 6		988	65. 9
2640	0308. 4	20. 8		583	38. 9
End of run	0323. 6				

TABLE B.2 CONTINUED

Tray Number	Exposure Began (Mike Time) 12 June 56	Midpoint of Exposure TSD		γ Activity	γ Activity per Unit Time
		hr	min	counts/min	counts/min²
Designator: YFNB 29-H-78 FL Counting Time: Corrected to H + 12 hours Nominal Exposure Interval: 15 minutes					
3067	0626	0.1	6	912	60.8
1917	0641	0.4	24	1,426	95.0
3068	0656	0.6	36	3,404	227
1918	0711	0.9	54	3,295	220
3069	0726	1.1	66	2,239,000	149,300
1919	0741	1.4	84	967,100	64,470
3070	0756	1.6	96	619,300	41,290
1920	0811	1.9	114	Background	—
3071	0826 to 0841	2.1	126	Background	—
to	ea. 15 min			Background	—
1922	0911	2.9	174	Background	—
3073	0926	3.1	186	1,003	66.9
1923	0941	3.4	204	4,297	286
3074	0956	3.6	216	5,459	364
1924	1011 to 1026	3.9	234	Background	—
to	ea. 15 min			Background	—
1926	1111	4.9	294	Background	—
3077	1126	5.1	306	1,635	109
1927	1141	5.4	324	Background	—
3078	1156	5.6	336	Background	106
1928	1211	5.9	354	Background	—
3079	1226	6.1	366	Background	76.3
1929	1241	6.4	384	Background	—
3080	1256	6.6	396	Background	—
1930	1311	6.9	414	6,248	416
3081	1326	7.1	426	3,719	248
1931	1341 to 1356	7.4	444	Background	—
to	ea. 15 min			Background	—
1933	1441	8.4	504	Background	—
3084	1456	8.6	516	6,312	421
1934	1511 to 1526	8.9	534	Background	—
to	ea. 15 min			Background	—
3091	1826	12.1	726	Background	—
End of run	1835				
Designator: YAG 40-A-1 NA Counting Time: Corrected to H + 12 hours Nominal Exposure Interval: Variable					
	11-12 July 56				
1863	0700	1.6		Background	—
3016	0745	2.1		Background	—
1864	0815	2.6		Background	—
3017	0900	3.6		Background	—
1865	1003	4.5		Background	—
3018	1046	5.1		Background	—
1866	1115	5.6		Background	—
3019	1145	6.1		Background	—
1867	1222	6.9		12,290	232
3020	1315	7.6		10,360	345
1868	1345	8.1		6,036	183
3021	1418	8.6		30,350	1,084
1869	1446	9.1		99,110	3,418
3022	1515	9.6		89,020	2,967
1870	1545	10.1		93,970	3,132

TABLE B.2 CONTINUED

Tray Number	Exposure Began (Mike Time) 11-12 July 56	Midpoint of Exposure TSD		γ Activity	γ Activity per Unit Time
		hr	min	counts/min	counts/min²
3023	1615	10.6		72,090	2,403
1871	1645	11.1		27,380	913
3024	1715	11.6		50,380	1,679
1872	1745	12.1		50,340	1,678
3025	1815	12.6		48,960	1,632
1873	1845	13.1		28,440	948
3026	1915	13.6		40,240	1,298
1874	1946	14.1		45,210	1,559
3027	2015	14.6		21,420	714
1875	2045	14.9		8,650	577
3028	2100	15.3		12,410	414
1876	2130	15.8		21,720	603
3029	2206	16.4		18,880	787
1877	2230	16.8		1,795	56
3030	2302	17.3		803	29
1878	2330	17.8		1,142	38
3031	2400	18.3		1,403	45
1879	0031	18.8		65	2
End of run	0100	19.1			

Designator: YAG 40-B-7 NA
Counting Time: Corrected to H+12 hours
Nominal Exposure Interval: 15 minutes

	11 July 56				
3290	0717	1.5		431	29
2148	0732.7	1.7		794	53
3291	0747.8	2.0		625	42
2149	0802.9	2.2		0	—
3292	0818	2.5		188	12
2150	0833.1	2.7		79	5
3293	0848.2	3.0		804	54
2151	0903.3	3.2		0	—
3294	0918.4	3.5		5,975	398
2152	0933.5	3.7		14	1
3295	0948.6	4.0		476	32
2153	1003.7	4.2		2,987	199
3296	1018.8	4.5		218	14
2154	1033.9	4.7		938	62
3297	1049.0	5.0		2,590	173
2155	1104.1	5.2		287	19
3298	1119.2	5.5		71	5
2156	1134.3	5.7		2,015	135
3299	1149.4	6.0		147	10
2157	1204.5	6.2		1,233	82
3300	1219.6	6.5		228	15
2158	1234.7	6.7		314	21
3301	1249.8	7.0		1,350	90
2159	1304.9	7.2		12,562	837
3302	1320.0	7.5		14,150	943
2160	1335.1	7.7		12,110	807
3303	1350.2	8.0		75,320	5,021
2161	1405.3	8.2		751	50
3304	1420.4	8.5		355	24
2162	1435.5	8.7		35,170	2,345
3305	1450.6	9.0		675	45
2163	1505.7	9.2		44,760	2,984
3306	1520.8	9.5		44,490	2,966

TABLE B.2 CONTINUED

Tray Number	Exposure Began (Mike Time) 11 July 56	Midpoint of Exposure TSD		γ Activity	γ Activity per Unit Time
		hr	min	counts/min	counts/min²
2164	1535.9	9.7		6,659	444
3307	1551.0	10.0		36,910	2,461
2165	1606.1	10.2		223	15
3308	1621.2	10.5		51,410	3,427
2166	1636.3	10.7		7,156	447
3309	1651.4	11.0		5,568	3,709
2167	1706.5	11.2		2,553	170
3310	1721.6	11.5		25,350	1,690
2168	1736.7	11.7		649	43
3311	1751.8	12.0		15,744	1,050
2169	1806.9	12.2		22,710	1,514
3312	1822	12.5		4,844	323
2170	1837.1	12.7		5,514	368
3313	1852.5	13.1		24,940	1,663
2171	1907.6	13.3		13,990	933
3314	1922.7	13.6		2,190	146
2172	1937.8	13.8		17,990	1,200
3315	1952.9	14.1		2,633	176
2173	2008	14.3		11,540	769
3316	2023.1	14.6		824	55
2174	2038.2	14.8		11,081	739
3317	2053.3	15.1		1,067	71
2175	2108.4	15.3		19,981	1,332
End of run	2123.5	15.5			
Designator: YAG 39-C-20 NA Counting Time: Corrected to H+12 hours Nominal Exposure Interval: 15 minutes					
1312	0800	2.2		105	7
1313	0815	2.4		118,320	7,888
1314	0830	2.7		21,020	1,401
1315	0845	2.9		44,430	2,962
1316	0900	3.2		49,500	3,300
1317	0915	3.4		46	3
1318	0930	3.7		111,060	7,404
1319	0945	3.9		143,380	9,559
1320	1000	4.2		365,370	24,360
1321	1015	4.4		128,200	8,547
1322	1030	4.7		101,500	6,767
1323	1045	4.9		75,770	5,051
1324	1100	5.2		147,700	9,850
1325	1115	5.4		23,030	1,535
1326	1130	5.7		47,730	3,182
1327	1145	5.9		15,450	1,030
1328	1200	6.2		89,620	5,975
1329	1215	6.4		0	—
1330	1230	6.7		6,823	455
1331	1245	6.9		172	11
1332	1300	7.2		2,386	159
1333	1315	7.4		6,483	432
1334	1330	7.7		164	11
1335	1345	7.9		1,896	126
1336	1400	8.2		43,180	288
1337	1415	8.4		4,945	330
1338	1430	8.7		3,978	262
1339	1445	8.9		85	6
1340	1500	9.2		72	5

TABLE B.2 CONTINUED

Tray Number	Exposure Began (Mike Time) 11 July 56	Midpoint of Exposure TSD		γ Activity	γ Activity per Unit Time
		hr	min	counts/min	counts/min²
1341	1516	9.4		3,483	232
1342	1531	9.7		1,239	86
1343	1546	9.9		147	10
1344	1601	10.2		3,144	210
1345	1616	10.4		4,528	302
1346	1630	10.7		1,271	85
1347	1646	10.9		6,906	460
1348	1701	11.2		5,309	354
1349	1716	11.4		7,442	496
1350	1731	11.7		4,778	318
1351	1746	11.9		139	9
1352	1801	12.2		2,655	177
1353	1816	12.4		0	—
1354	1831	12.7		3,118	208
1355	1845	12.9		6,136	409
1356	1901	13.2		13,890	926
1357	1916	13.4		4,381	292
1358	1931	13.7		252	17
1359	1946	13.9		535	36
1360	2001	14.2		15,940	1,063
1361	2016	14.4		436	29
1362	2031	14.7		1,137	76
1363	2046	14.9		1,243	83
1364	2101	15.2		22,240	1,483
1365	2116	15.4		22,142	1,476
1366	2131	15.7		91,205	6,080
1367	2146	15.9		8,506	567
End of run	2201	16.1			
Designator: LST 611-D-41 NA Counting Time: Corrected to H+12 hours Nominal Exposure Interval: 12 minutes					
2898	0904	3.2		933	78
1742	0916	3.4		185	16
2899	0927.8	3.6		Background	—
1743	0939.7	3.8		Background	—
2900	0951.8	4.0		261	22
1744	1003.7	4.2		223	19
2901	1015.5	4.4		67	5.5
1745	1027.7	4.6		634	53
2902	1040.0	4.8		406	34
1746	1052.2	5.0		3,822	318
2903	1104.0	5.2		30,480	2,540
1747	1116.1	5.4		15,060	1,255
2904	1127.9	5.6		4,232	353
1748	1139.8	5.8		Background	—
2905	1151.7	6.0		8,637	718
1749	1203.6	6.2		Bkg	—
2906	1215.4	6.4		1,085	90
1750	1227.3	6.6		1,201	100
2907	1239.2	6.8		247	21
1751	1251.0	7.0		288	24
2908	1302.8	7.2		1,598	133
1752	1314.7	7.4		1,802	150
2909	1326.6	7.6		2,201	183
1753	1338.5	7.8		Background	—
2910	1350.3	8.0		453	38

TABLE B. 2 CONTINUED

Tray Number	Exposure Began (Mike Time) 11 July 56	Midpoint of Exposure TSD		γ Activity	γ Activity per Unit Time
		hr	min	counts/min	counts/min²
1754	1402. 3	8. 2		417	35
2911	1414. 2	8. 4		323	27
1755	1426. 3	8. 6		579	48
2912	1438. 3	8. 8		222	18
1756	1450. 1	9. 0		163	14
2913	1502. 0	9. 2		97	8
1757	1513. 8	9. 4		129	11
2914	1525. 7	9. 6		125	10
1758	1537. 6	9. 8		191	16
2915	1549. 4	10. 0		191	16
1759	1601. 2	10. 2		145	12
2916	1613. 1	10. 4		Background	—
1760	1624. 9	10. 6		211	18
2917	1636. 8	10. 8		111	9
1761	1648. 8	11. 0		199	17
2918	1700. 7	11. 2		288	24
1762	1712. 7	11. 4		122	10
2919	1724. 5	11. 6		222	18
1763	1736. 5	11. 8		159	13
2920	1748. 4	12. 0		69	6
1764	1800. 2	12. 2		214	18
2921	1812. 2	12. 4		203	17
1765	1824. 1	12. 6		145	12
2922	1835. 8	12. 8		277	23
1766	1847. 8	13. 0		127	11
2923	1859. 6	13. 2		672	48
1767	1911. 5	13. 4		567	47
2924	1923. 3	13. 6		940	78
1768	1935. 2	13. 8		123	10
2925 End of run	1947. 2 to 1959	14. 0		284	24
Designator: YFNB 13-E-57 NA Counting Time: Corrected to H + 12 hours Nominal Exposure Interval: 15 minutes					
2351	0556	0. 1	6	56, 590	3, 773
3487	0611	0. 4	24	1, 743, 300	116, 200
2352	0626	0. 6	36	918, 500	61, 230
3488	0641	0. 9	54	931, 600	62, 100
2353	0656	1. 1	66	194, 600	12, 970
3489	0711	1. 4	84	146, 400	9, 760
2354	0726	1. 6	96	100, 000	6, 666
3490	0741	1. 9	114	57, 400	3, 827
2355	0756	2. 1	126	69, 600	4, 640
3491	0811	2. 4	144	82, 110	5, 473
2356	0826	2. 6	156	10, 580	705
3492	0841	2. 9	174	10, 300	687
2357	0856	3. 1	186	1, 595	106
3493	0911	3. 4	204	1, 028	69
2358	0926	3. 6	216	4, 496	300
3494	0941	3. 9	234	2, 365	158
2359	0956	4. 1	246	5, 278	352
3495	1011	4. 4	264	495	33
2360	1026	4. 6	276	616	41
3496	1041	4. 9	294	420	28
2361	1056	5. 1	306	573	38

TABLE B.2 CONTINUED

Tray Number	Exposure Began (Mike Time) 11 July 56	Midpoint of Exposure TSD		γ Activity	γ Activity per Unit Time
		hr	min	counts/min	counts/min²
3497	1111	5.4	324	552	37
2362	1126	5.6	336	878	58
3498	1141	5.9	354	1,103	74
2363	1156	6.1	366	2,548	170
3499	1211	6.4	384	828	55
2364	1226	6.6	396	1,536	102
3500	1241	6.9	414	567	38
2365	1256	7.1	426	557	37
3501	1311	7.4	444	482	32
2366	1326	7.6	456	520	35
3502	1341	7.9	474	492	33
2367	1356	8.1	486	617	41
3503	1411	8.4	509	648	43
2368	1426	8.6	516	742	49
3504	1441	8.9	534	35,000*	2,333
End of run	1456	10.0	600		
Designator: How F-64 NA					
Counting Time: Corrected to H+12 hours					
Nominal Exposure Interval: 15 minutes					
3543	0550	—	—	Background	—
2410	0605	—	—	Background	—
3544	0620	—	—	Background	—
2411	0635	0.75	45	127	8.5
3545	0650	1.0	60	24,410	1,627
2412	0705	—	75	Background	—
3546	0720	—	1	Background	—
2413	0735	—	—	Background	—
3547	0750	—	—	Background	—
2414	0805	—	135	Background	—
3548	0820	2.5	150	250	17
2415	0835	2.8	168	11,020	736
3549	0850	3.0	180	372	25
2416	0905	3.3	198	Background	—
3550	0920	3.5	210	573	38
2417	0935	3.8	228	2,450	163
3551	0950	4.0	240	Background	—
2418	1005	4.3	258	16,670	1,111
3552	1020	4.5	270	242	16
2419	1035	4.8	288	129	9
3553	1050	5.0	300	122	8
2420	1105	5.3	318	Background	—
3554	1120	5.5	330	133	9
2421	1135	5.8	348	Background	—
3555	1150	6.0	360	Background	—
2422	1205	6.3	378	Background	—
3556	1220	6.5	390	602	40
2423	1235	6.8	408	5,739	383
End of run	1250				
Designator: YFNB 29-H-78 NA					
Counting Time: Corrected to H+12 hours					
Nominal Exposure Interval: 15 minutes					
914	—	—	—	Background	—
915	0556	0.1	6	Background	—
916	0611	0.4	24	892	59
917	0626	0.6	36	740	49

TABLE B.2 CONTINUED

Tray Number	Exposure Began (Mike Time) 11 July 56	Midpoint of Exposure TSD		γ Activity	γ Activity per Unit Time
		hr	min	counts/min	counts/min²
918	0641	0.9	54	78,010	5,201
919	0656	1.1	66	179,514	11,970
920	0711	1.4	84	Background	—
921	0726	1.6	96	Background	—
922	0741	1.9	114	Background	—
923	0756	2.1	126	Background	—
924	0811	2.4	144	Background	—
925	0826	2.6	156	Background	—
926	0841	2.9	174	26,850	1,790
927	0856	3.1	186	8,913	594
928	0911	3.4	204	703	47
929	0926	3.6	216	Background	—
930	0941	3.9	234	4,887	326
931	0956	4.1	246	Background	—
932	1011 to 1026	4.4	264	Background	—
to	ea. 15 min			Background	—
969	1926	13.6	816	Background	—
End of run	1941	13.8	828		

Designator: YAG 40-A-1 TE
Counting Time: Corrected to H+12 hours
Nominal Exposure Interval: Variable

1850	0810	2.7	35	—
2994	0951	4.4	147,748	3,890
1839	1029	4.9	607,100	40,470
P-2999	1044	5.1	537,776	48,890
1842	1055	5.3	3,761,285	188,060
3000	1115	5.7	11,624,936	465,000
1856	1140	6.1	17,325,405	866,300
P-2993	1200	6.4	3,116,723	207,780
1834	1215	6.6	6,376,846	425,100
2986	1230	6.9	5,266,514	309,790
1844	1247	7.1	7,439,262	572,300
P-2991	1300	7.4	1,608,283	100,517
1838	1316	7.6	5,194,303	346,300
2992	1331	7.9	3,440,155	172,007
1837	1351	8.3	10,462,893	373,700
P-2997	1419	8.8	2,885,754	96,190
1832	1449	9.3	11,137,524	484,200
2988	1512	9.6	776,442	51,760
1855	1527	9.9	5,835,239	291,800
P-3005	1547	10.2	767,586	38,380
1843	1607	10.5	3,709,095	185,400
2990	1627	10.9	2,940,929	117,637
1852	1652	11.4	2,911,091	80,863
P-2989	1728	12.0	1,123,353	35,104
1836	1800	12.5	1,859,306	58,110
3004	1832	13.0	482,186	17,220
1841	1900	13.5	354,591	11,440
P-2995	1931	14.0	43,616	1,504
1849	2000	14.5	43,530	1,451
3002	2030	15.0	5,831	188
1840	2101	15.5	1,356,448	46,770
P-2987	2130	16.0	4,611	140
1835	2203	16.5	833	25
3006	2236	16.9	4,888	444
1848	2247	17.2	1,287	46
P-3003	2315	17.5	—	—
1851	2316	17.7	1,031	34
3008	2346	18.0	—	—
1833	2347	18.2	803	26
End of run	2413			

TABLE B.2 CONTINUED

Instrument	Tray Number	Exposure Began (Mike Time) 21 July 56	Midpoint of Exposure TSD		γ Activity	γ Activity per Unit Time
			hr	min	counts/min	counts/min²
Designator: YAG-40-A-1, 2 TE Counting Time: Corrected to H+12 hours Nominal Exposure Interval: Variable						
Grease Trays only from each instrument						
A-1	1850	0810 to 0951	2. 7		~35	0. 315
A-1	1839	1029 to 1044	4. 9		607,100	40,470
A-1	1842	1055 to 1115	5. 3		4,455,285	405,020
A-2	2142	1115 to 1140	5. 7		18,777,802	1,252,000
A-1	1856	1140 to 1200	6. 1		17,325,405	866,300
A-2	2145	1200 to 1215	6. 4		9,013,823	600,921
A-1	1834	1215 to 1230	6. 6		6,376,846	425,100
A-2	2144	1230 to 1247	6. 9		8,920,405	524,700
A-1	1844	1247 to 1300	7. 1		7,439,262	572,300
A-2	2125	1300 to 1316	7. 4		7,289,977	449,400
A-1	1838	1316 to 1331	7. 6		5,194,303	346,300
A-2	2129	1331 to 1351	7. 9		6,666,000	333,300
A-1	1837	1351 to 1419	8. 3		10,462,893	373,700
A-2	2132	1419 to 1449	8. 8		18,810,709	627,000
A-1	1832	1449 to 1512	9. 3		11,137,524	484,200
A-2	2131	1512 to 1527	9. 6		2,518,337	167,900
A-1	1855	1527 to 1547	9. 9		5,835,239	291,800
A-2	2133	1547 to 1607	10. 2		4,602,232	230,110
A-1	1843	1607 to 1627	10. 5		3,709,095	185,400
A-2	2137	1627 to 1652	10. 9		4,649,959	186,000
A-1	1852	1652 to 1728	11. 4		2,911,091	80,863
A-2	2136	1728 to 1800	12. 0		5,283,346	165,100
A-1	1836	1800 to 1832	12. 5		1,859,306	58,110
A-2	2139	1832 to 1900	13. 0		633,986	22,640
A-1	1841	1900 to 1931	13. 5		354,591	11,440
A-2	2138	1931 to 2000	14. 0		66,707	2,300
A-1	1849	2000 to 2030	14. 5		43,530	1,451
A-1	1840	2101 to 2130	15. 5		1,356,448	46,770
A-1	1835	2203 to 2236	16. 5		833	25
Designator: YAG 40-B-7 TE Counting Time: Corrected to H+12 hours Nominal Exposure Interval: 15 minutes						
	3094	1002	4. 4		790	53
	1945	1017	4. 6		13,193	879
	3095	1032	4. 9		83,782	5,591
	1946	1047	5. 1		1,526,080	101,740
	3096	1102	5. 4		481,080	32,072
	1947	1117	5. 6		3,543,120	236,200
	3097	1132	5. 9		747,536	49,840
	1948	1147	6. 1		3,064,320	204,290
	3098	1202	6. 4		528,960	35,260
	1949	1217	6. 6		2,190,320	146,020
	3099	1232	6. 9		908,048	60,536
	1950	1247	7. 1		3,155,520	210,370
	3100	1302	7. 4		946,960	63,130
	1951	1317	7. 6		2,745,120	183,008
	3101	1332	7. 9		535,040	35,670
	1952	1347	8. 1		1,551,920	103,460
	3102	1402	8. 4		843,600	56,240

TABLE B.2 CONTINUED

Tray Number	Exposure Began (Mike Time) 21 July 56.	Midpoint of Exposure TSD		γ Activity	γ Activity per Unit Time
		hr	min	counts/min	counts/min^2
1953	1417	8.6		1,749,520	116,630
3103	1432	8.9		513,760	34,250
1954	1447	9.1		3,302,960	220,200
3104	1502	9.4		826,880	55,130
1955	1517	9.6		1,744,960	116,300
3105	1532	9.9		568,480	37,890
1956	1547	10.1		1,130,880	75,390
3106	1602	10.4		607,544	40,500
1957	1617	10.6		669,864	44,660
3107	1632	10.9		298,224	19,880
1958	1647	11.1		922,792	61,520
3108	1702	11.4		218,272	14,550
1959	1717	11.6		322,088	21,470
3109	1732	11.9		36,328	2,421
1960	1747	12.1		140,448	9,363
3110	1802	12.4		112,875	7,525
1961	1817	12.6		322,088	21,470
3111	1832	12.9		56,118	3,741
1962	1847	13.1		88,524	5,901
3112	1902	13.4		31,692	2,112
1963	1917	13.6		35,902	2,393
3113	1932	13.9		4,985	332
1964	1947	14.1		14,029	935
3114	2002	14.4		18,057	1,203
1965	2017	14.6		32,132	2,142
3115	2032	14.9		5,563	370
1966	2047	15.1		37,240	2,482
3116	2102	15.4		19,912	1,327
1967	2117	15.6		44,323	2,954
3117	2132	15.9		2,553	170
1968	2147	16.1		7,174	478
3118	2202	16.4		1,398	93
1969	2217	16.6		56,513	3,767
3119	2232	16.9		10,396	693
1970	2247	17.1		54,476	3,631
3120	2302	17.4		19,456	1,297
1971	2317	17.6		43,502	2,900
3121	2332	17.9		668	44
1972	2347	18.1		322,513	21,510
End of run	0002	18.3			
Designator: YAG 39-C-20 TE					
Counting Time: H + 36.4 to H + 40.8 hours					
Nominal Exposure Interval: 15 minutes					
2813	0747	2.1		63,740	4,249
3933	0802	2.4		143,380	9,558
2812	0817	2.6		1,132,000	75,430
3932	0832	2.9		1,148,000	76,560
2811	0847	3.1		4,362,000	290,780
3931	0902	3.4		2,458,000	163,900
2810	0917	3.6		8,359,000	557,200
3930	0932	3.9		4,875,000	325,000
2809	0947	4.1		18,570,000	1,238,000
3929	1002	4.4		9,457,000	630,400
2808	1017	4.6		19,780,000	1,318,000
3928	1032	4.9		1,074,000	71,580
2807	1047	5.1		1,868,000	124,600

TABLE B.2 CONTINUED

Tray Number	Exposure Began (Mike Time) 21 July 56	Midpoint of Exposure TSD		γ Activity	γ Activity per Unit Time
		hr	min	counts/min	counts/min²
3927	1102	5.4		916,700	61,110
2806	1117	5.6		507,400	33,820
3926	1132	5.9		105,700	6,607
2805	1148	6.1		731,100	48,740
3925	1203	6.4		193,300	12,880
2804	1218	6.6		188,900	12,590
3924	1233	6.9		291,200	19,410
2803	1248	7.1		1,869,000	124,600
3923	1303	7.4		553,600	36,910
2802	1318	7.6		674,900	44,990
3922	1333	7.9		139,400	9,293
2801	1348	8.1		374,000	24,940
3921	1403	8.4		130,800	8,721
2800	1418	8.6		379,400	25,290
3920	1433	8.9		21,900	1,459
2799	1448	9.1		57,380	3,825
3919	1503	9.4		76,740	5,116
2798	1518	9.6		57,040	3,802
3918	1533	9.9		20,660	1,377
2797	1548	10.1		100,400	6,695
3917	1603	10.4		20,820	1,388
2796	1618	10,6		39,890	2,659
3916	1633	10.9		4,680	312
2795	1648	11.1		13,260	884
3915	1703	11.4		13,650	909
2794	1718	11.6		58,060	3,870
3914	1733	11.9		7,248	483
2793	1748	12.1		6,096	406
3913	1803	12.4		6,096	406
2792	1818	12.6		14,670	978
3912	1833	12.9		57,940	3,862
2791	1848	13.1		56,020	3,734
3911	1903	13.4		46,260	3,084
2790	1918	13.6		136,800	9,118
3910	1933	13.9		27,860	1,857
2789	1948	14.1		8,144	543
3909	2003	14.4		1,616	108
2788	2018	14.6		8,656	577
3908	2033	14.9		9,296	619
2787	2048	15.1		89,810	5,987
3907	2103	15.4		12,530	835
2786	2118	15.6		726,900	48,458*
End of run	2133	15.8			
Designator: LST 611-D-41 TE Counting Time: H + 321 to H + 297 hours Nominal Exposure Interval: 12 minutes					
2262	1303	7.4		5,416	451
3401	1315	7.6		3,606	301
2261	1327	7.8		6,272	523
3400	1339	8.0		1,448	121
2260	1351	8.2		2,286	190
3399	1403	8.4		1,130	94
2259	1415	8.6		3,516	293
3398	1427	8.8		3,800	317
2258	1439	9.0		7,370	614
3397	1451	9.2		6,196	516

TABLE B. 2 CONTINUED

Tray Number	Exposure Began (Mike Time) 21 July 56	Midpoint of Exposure TSD		γ Activity	γ Activity per Unit Time
		hr	min	counts/min	counts/min²
2257	1503	9. 4		11,660	971
3396	1515	9. 6		9,432	786
2256	1527	9. 8		18,920	1,576
3395	1539	10. 0		6,984	582
2255	1551	10. 2		24,090	2,007
3394	1603	10. 4		11,690	974
2254	1615	10. 6		79,410	6,620
3393	1627	10. 8		20,380	1,698
2253	1639	11. 0		36,000	3,000
3392	1651	11. 2		9,464	789
2252	1703	11. 4		17,260	1,438
3391	1715	11. 6		7,680	640
2251	1727	11. 8		12,000	1,000
3390	1739	12. 0		2,978	248
2250	1751	12. 2		10,360	863
3389	1803	12. 4		5,664	472
2249	1815	12. 6		9,900	825
3388	1827	12. 8		7,626	636
2248	1839	13. 0		8,192	683
3387	1851	13. 2		10,580	882
2247	1903	13. 4		35,800	2,984
3386	1915	13. 6		12,620	1,052
2246	1927	13. 8		8,488	707
3385	1939	14. 0		2,400	200
2245	1951	14. 2		3,468	289
3384	2003	14. 4		3,480	290
2244	2015	14. 6		3,648	304
3383	2027	14. 8		2,144	179
2243	2039	15. 0		3,774	314
3382	2051	15. 2		946	79
2242	2103	15. 4		406	34
3381	2115	15. 6		510	42
2241	2127 to 2139	15. 8		214	18
to	ea. 12 min			Background	—
2235	2351	18. 2		Background	—
End of run	0003	18. 3			
Designator: YFNB 13-E-57 TE					
Counting Time: H + 17. 4 to H + 17. 8 hours					
Nominal Exposure Interval: 15 minutes					
1974	0546		7	20,608	1,375
3123	0601		22	22,530	1,472
1975	0616		37	291,600	19,420
3124	0631		52	2,351,000	156,700
1976	0646		67	1,603,000	106,800
3125	0707		82	1,483,000	98,900
1977	0716		97	13,780,000	917,500
3126	0731		112	3,032,000	200,000
End of run	0746		120		

TABLE B. 2 CONTINUED

Tray Number	Exposure Began (Mike Time) 21 July 56	Midpoint of Exposure TSD		γ Activity	γ Activity per Unit Time
		hr	min	counts/min	counts/min²
Designator: How-F-64 TE					
Counting Time: H + 19. 2 to H + 20. 4 hours					
Nominal Exposure Interval: 15 minutes					
2206	0546	0. 1	6	784	52
3347	0601	0. 4	24	0	0
2207	0616	0. 6	36	1,040	69
3348	0631	0. 9	54	784	52
2208	0646	1. 1	66	1,424	95
3349	0701	1. 4	84	0	0
2209	0716	1. 6	96	784	52
3350	0731	1. 9	114	0	0
2210	0746	2. 1	126	880	59
3351	0801	2. 4	144	188,500	12,560
2211	0816	2. 6	156	260,100	17,300
3352	0831	2. 9	174	194,900	13,000
2212	0846	3. 1	186	320,800	21,400
3353	0901	3. 4	204	16	1
2213	0916	3. 6	216	0	0
3354	0931	3. 9	234	1,040	69
2214	0946	4. 1	246	14,480	965
3355	1001	4. 4	264	16	1
2215	1016	4. 6	276	400	27
3356	1031	4. 9	294	656	44
2216	1046	5. 1	306	1,040	69
3357	1101	5. 4	324	0	0
2217	1116	5. 6	336	528	35
3358	1131	5. 9	354	7,688	512
2218	1146	6. 1	366	400	27
3359	1201	6. 4	384	0	0
2219	1216	6. 6	396	144	9
3360	1231	6. 9	414	2,318	155
2220	1246	7. 1	426	17,170	1,142
3361	1301	7. 4	444	2,192	146
2221	1316	7. 6	456	2,064	138
3362	1331	7. 9	474	3,216	212
2222	1346	8. 1	486	3,348	223
End of run	1357	8. 2	492		
Designator: YFNB-29-H-78 TE					
Counting Time: H + 79. 2 to H + 81. 6 hours					
Nominal Exposure Interval: 15 minutes					
1371	0546	0. 1	6	2,016	134
1372	0601	0. 4	24	9,184	610
1373	0616	0. 6	36	2,379,000	162,000
1374	0631	0. 9	54	4,874,000	325,000
1375	0646	1. 1	66	7,905,000	525,000
1376	0701	1. 4	84	7,930,000	527,000
1377	0716	1. 6	96	9,919,000	612,000
1378	0731	1. 9	114	7,897,000	525,000
1379	0746	2. 1	126	6,577,000	438,000
1380	0801	2. 4	144	8,594,000	570,000
1381	0816	2. 6	156	2,962,000	198,000
1382	0831	2. 9	174	9,229,000	615,000
1383	0845. 5	3. 1	186	10,560,000	700,000
1384	0900	3. 4	204	15,715,000	1,040,000
1385	0915	3. 6	216	9,448,000	630,000

TABLE B. 2 CONTINUED.

Tray Number	Exposure Began (Mike Time) 21 July 56	Midpoint of Exposure TSD		γ Activity	γ Activity per Unit Time
		hr	min	counts/min	counts/min²
1386	0930	3. 9	234	6,331,000	422,000
1387	0945	4. 1	246	3,128,000	209,000
1388	1000	4. 4	264	1,944,000	129,000
1389	1015	4. 6	276	2,067,000	138,000
1390	1030	4. 9	294	841,900	56,100
1391	1045	5. 1	306	370,600	24,600
1392	1100	5. 4	324	311,200	20,800
1393	1115	5. 6	336	58,530	3,900
1394	1130	5. 9	354	8,740	580
1395	1145	6. 1	366	1,316	87
1396	1200	6. 4	384	15,650	1,040
1397	1215	6. 6	396	2,340	150
1398	1230	6. 9	414	2,852	190
1399	1245	7. 1	426	4,900	326
1400	1300	7. 4	444	17,840	1,180
1401	1315	7. 6	456	46,880	3,120
1402	1330	7. 9	474	8,484	565
1403	1345	8. 1	486	2,596	173
1404	1400	8. 4	504	5,924	400
1405	1415	8. 6	516	23,300	1,550
1406	1430	8. 9	534	35,750	2,300
1407	1445	9. 1	546	78,240	5,200
1408	1500	9. 4	564	12,200	800
1409	1515	9. 6	576	5,540	370
1410	1530	9. 9	594	4,004	268
1411	1545	10. 1	606	14,120	920
1412	1600	10. 4	624	9,892	655
1413	1615	10. 6	636	33,570	2,200
1414	1630	10. 9	654	45,600	3,000
1415	1645	11. 1	666	76,320	5,000
1416	1700	11. 4	684	28,070	1,870
1417	1715	11. 6	696	83,600	5,550
1418	1730	11. 9	714	8,868	590
1419	1745	12. 1	726	34,340	2,300
1420	1800	12. 4	744	35,880	2,360
1421	1815	12. 6	756	21,170	1,410
1422	1830	12. 9	774	16,800	1,120
1423	1845	13. 1	786	114,980	7,600
1424	1900	13. 4	804	131,360	8,700
1425	1915	13. 6	816	292,500*	19,400
End of run	1945	14. 0	840		

*Probably cross-contaminated in transport.

TABLE B.3 MEASURED RATE OF PARTICLE DEPOSITION, SHOTS ZUNI AND TEWA

Station	Mean Collection Time (TSD)	Number of Particles/ft²/hr/micron-interval Mean Particle Size, microns																		
	hr	62.5	72.5	92.5	112.5	132.5	155	195	235	275	315	365	485	605	725	845	1,000	1,400	1,800	2,200	2,600
Shot Zuni																					
YAG 40-B-7 ZU	3.98	2,139	609	310	168	72	42	46	67	42	20	27	3	0.02							
	4.98	9,229	3,042	2,507	1,641	1,292	807	399	244	163	89	14	0.01								
	4.99	2,434	3,342	2,198	1,308	920	428	297	129	43	7										
	7.00	7,330	1,584	952	599	344	278	127	65	16	10	13	0.01								
	8.02	756	224	82	49	22	6														
	9.03	2,839	634	362	221	120	39	36	1	3											
	10.04	1,180	280	109	92	67	32	15	15	1	0.4	0.5									
	11.06	1,059	219	127	63	66	13	1	1	0.4											
	12.07	529	237	92	33	9	2	0.4	0.4												
	13.08	741	201	106	63	28	40	8	0.4	2											
	14.09	786	246	149	61	22	7	2			1										
	15.11	105	201	147	56	15	0.1	7	0.1												
YAG 39-C-20 ZU	13.03	918	322	161	26	38	8	5		1											
	15.03	183	125	89	25	12	1	4													
	17.10	562	127	72	93	32	37	6					0.7								
	19.14	3,637	617	162	55	16	19	5	3	3	0.2				0.2	0.01					
	21.16	361	126	181	79	63	36	8	0.1				0.7								
	23.16	306	110	52	27	1	4	0.6	0.1												
	25.16	260	59	32	22	4	5	0.3		2											
	27.16	796	273	133	31	14	11	13	3	0.6											
	29.16	61	70	10	16	0.9	7	5													
YFNB 29-G-71 ZU	0.12	5,607	909	626	431	61	59	48	7		0.3	6									
	0.23	11,623	1,620	959	235	177	133	91	17	16	17	13	4	0.01							
	0.43	3,058	815	305	432	97	163	28	69	1	11	1	1								
	0.68	5,700	1,100	399	133	102	126	56	12			3	0.1								
	0.90	9,208	2,450	1,149	1,072	659	484	615	207	295	293	133	74	52	20	24	7	0.2	0.04	0.9	
	1.11	4,713	1,015	404	141	162	117	21	2	33	2	5	12	6	4	4	1	0.4			
	1.27	3,441	1,898	429	270	51	10	36		10	10	20	15	3	5	0.01					
	1.49	8,318	1,760	1,057	257	143	68	15	71	45	13	14	30	9	15	0.01					
	1.67	10,770	3,764	1,113	454	374	129	205	10	30	57	8	9	10	3	0.1	0.3	0.3			
YFNB 13-E-67 ZU	0.63	688	299	179	82	79	54	29	17	32	14	6	3	5	0.6	1	0.6	1	0.01		
	2.13	857	235	170	55	50	19	5	14	9	5	6	3	3	2	0.04					
	3.63	1,439	420	271	163	124	53	22	15	3	0.3	1									
	5.38	352	69	45	29	10	0.4	0.4	2												
	6.63	306	63	41	8	5	6	7	8	2	0.4	0.3									
	8.13	428	68	64	23	20	80		2												
	9.63	183	73	17	12	11	2	2	1												
	11.38	561	101	45	44	15	5	5	0.2	2											
	12.88	1,546	447	181	86	52	45	4	4	0.6	1	0.2	0.1	0.1		1		0.2			
How F-64 ZU	0.38	673	242	13:	41	29	30	7	4	0.1	1										
	1.38	443	254	88	38	7	10	6	9	2	7	4	1	5	0.5	0.1	0.01				
	2.38	352	171	118	35	3	10	1	0.3		1	3	0.4	0.1	0.4						
	3.38	597	284	112	22	18	6	0.7	1	1		0.5	0.02								
	4.13	4,074	1,184	495	339	171	154	72	43	23	13	7	0.9	1							
	5.34	168	92	53	14	14	4														
	6.38	642	153	88	27	29	7	3	1	1	4										
	7.38	2,173	764	374	235	72	42	20	14	15	1	3	0.2	0.1							
	8.13	1,010	428	161	67	24	28	10	1			0.5	0.02								
	9.38	964	384	109	71	24	11	3	1	0.3		0.1	0.7								
	10.38	30	258	615	370	168	74	52	15	11	4	0.9	0.6	0.02	0.4						

TABLE B.3 CONTINUED

Station	Mean Collection Time (TSD)	Number of Particles/ft³/hr/micron-interval — Mean Particle Size, microns																			
	hr	52.5	72.5	92.5	112.5	132.5	155	195	235	275	315	365	485	605	725	845	1,000	1,400	1,800	2,200	2,600
Shot Tewa																					
YAG 40-	4.64	1,267	271	139	119	35	10	3	1	1											
B-7 TE	6.14	2,161	1,230	822	309	135	62	59	21	12		1	0.4								
	7.64	1,607	711	558	395	265	175	80	33	10	0.05		1	0.02							
	9.14	737	130	495	296	164	121	43	19	2	1										
	10.64	1,104	484	272	194	144	46	41	1	1	1										
	12.14	392	151	85	29	10	1	5	1				0.5	0.02							
	13.64	470	241	79	52	7	1	3		1			0.2								
	15.14	958	49	64	25	11	16	2			1										
	16.64	571	180	121	72	33	45	3													
YAG-39-	3.64	3,952	885	459	126	71	110	154	195	128	86	42	3	0.01							
C-20 TE	5.64	424	508	202	70	36	16	12	10	4											
	6.66	1,882	268	126	55	9	21	11	5												
	8.16	684	835	513	171	79	36	12	1	5	2	2	0.02								
	9.66	476	124	67	15	12	2	4	4												
	11.16	971	190	94	25	32	7	2	2	1	1										
	12.66	579	139	39	28	6	2	3				0.6									
	14.16	1,371	178	58	40	16	21			1		0.1	0.1								
	15.16	863	286	114	69	24	20	9	2	6	0.6	0.8	0.6								
LST 611-	6.18	76	189	278	132	79	30	12		1											
D-41 TE	8.98	342	244	264	147	106	29	25	2												
	10.18	764	272	201	122	87	50	19													
	10.98	157	602	412	156	128	37	19	1												
	12.18	114	214	245	42	63	53	10	3												
	12.98	385	100	134	112	61	66	3													
	14.18	290	102	61	40	17	2	2													
	14.98	429	266	122	34	19	10					0.03	0.03								
	16.18	511	127	87	64	12	11	5	5	1		1									
	16.98	77	166	184	92	24	9	6	1						0.05						
YFNB 13-	0.13	1,334	565	725	538	352	94	31	15	7	2	0.2			0.4	0.6		0.1			
E-57 TE	0.63	1,198	375	265	166	147	69	77	24	7	1	0.05	0.8	0.1							
	1.13	552	837	591	612	333	120	43	13	23	6	6	0.5		0.7						
	1.63	976	928	652	302	155	125	52	23	22	28	25	13	1	0.4	0.2					
YFNB 29-	0.13	536	2,196	1,134	275	148	72	43	27	8	2	4	0.4	0.6	2	0.1	0.09				
H-76 TE	1.38	310	1,120	990	491	360	153	146	101	85	41	30	42	26	7	0.04					
	2.87	135	809	481	229	151	79	43	45	150	125	142	47	0.5	5	0.02					
	4.37	322	183	206	65	51	46	73	68	72	21	3									
	5.87	256	68	48	10		16	2	2												
	7.37	113	97	50	13		9	1	2												
	8.87	512	99	47	9			1	3	1											
	10.37	188	247	70	25		4		1												
	11.87	514	268	106	31	18	7	4		2											
	13.37	200	278	114	12	33	9	4	2	1		0.8									
How F-	0.13	840	361	128	94	38	29	11	5												
64 TE	1.13	941	289	112	85	21	24	1	1												
	2.13	164	199	102	90	75	20	12	1	4	1	0.3									
	3.13	157	79	121	48	25	13	8		2											
	4.13	462	301	162	97	70	62	16				0.02	0.4								
	5.13	208	205	98	34	13		9	8			0.1	0.1								
	6.13	220	163	86	36	4	32	4	1	0.	0.3										
	7.13	2,189	518	151	104	72	54	7		1											
	8.13	842	404	145	60	32	19	1	2	4	2	1	0.02	0.4							

TABLE B.4 CALCULATED RATE OF MASS DEPOSITION, SHOTS ZUNI AND TEWA

Station	Mean Collection Time (TSD)	Microgram/ft²/hr/micron-interval — Mean Particle Size, microns																			μg/ft²-hr
		52.5	72.5	92.5	112.5	132.5	155	195	235	275	315	365	485	605	725	845	1,000	1,400	1,800	2,200	2,600	(52.5 to 2,600 μ)
	hr																					
Shot Zuni																						
YAG 40-B-7 ZU	3.98	383	287	303	296	208	197	426	1,078	1,088	808	1,631	534	5								384,855
	4.98	1,652	1,433	2,450	2,867	3,716	3,713	3,657	3,927	4,213	3,471	893	2									1,051,060
	5.99	4,358	1,574	2,148	2,301	2,646	1,856	2,727	2,070	1,124	275	22										523,970
	7.00	1,312	746	901	1,054	991	1,282	1,169	1,046	416	396	804	2									319,725
	8.02	138	106	80	88	66	32															9,680
	9.03	507	299	384	390	346	183	338	31	92												59,520
	10.04	211	132	107	162	250	149	143	250	48												35,715
	11.06	190	103	134	147	190	63	11	22	10	16	31	21									23,703
	12.07	95	112	91	42	26	11	4	6													7,975
	13.08	133	95	104	112	62	187	77	7	52												20,790
	14.09	141	116	146	90	66	36	21														12,315
	15.11	19	95	145	99	44	1	64	2	2	52											12,080
YAG 39-C-20 ZU	13.03	164	192	156	47	110	36	48	1	36												16,360
	15.03	33	59	87	45	37	6	36	1													7,295
	17.10	101	60	71	164	92	173	59					100									23,990
	19.14	651	244	158	98	48	89	53	40	89	11				140	11						69,120
	21.16	65	59	178	140	181	167	60	2				103	1								28,870
	23.16	58	52	51	49	5	19	8	22													6,015
	25.16	47	28	32	39	13	25	3	52													5,210
	27.18	142	129	131	56	41	51	124	60	22												19,890
	29.18	11	33	11	29	3	34	58	1													5,160
YFNB 29-G-71 ZU	0.12	1,004	426	614	760	176	273	446	115		15	403										121,620
	0.23	2,081	763	930	416	511	613	839	274	471	678	790	625	3								341,395
	0.43	548	384	298	760	281	750	257	1,113	33	440	75	160									184,070
	0.68	1,020	516	391	235	294	564	533	204			227	22									122,090
	0.90	1,648	1,184	1,122	1,887	1,982	2,231	6,634	3,324	7,600	11,328	7,999	10,436	14,481	9,421	18,075	9,541	975	336	12,888		16,159,845
	1.11	844	478	395	250	468	539	198	47	852	90	357	1,725	1,823	2,321	3,605	1,396	189				1,917,700
	1.27	816	894	419	477	148	46	357	1	289	412	1,234	2,184	1,003	3,603	11						853,960
	1.49	1,489	829	1,033	482	413	467	142	1,143	1,164	528	879	4,250	2,599	7,517	13						1,856,015
	1.67	1,928	1,773	1,068	799	1,077	594	1,868	172	787	2,215	524	1,386	2,840	1,669	127	437	1,084				2,054,285
YFNB 13-E-67 ZU	0.63	123	141	176	145	229	252	273	277	826	568	409	464	1,555	317	814	1,004	3,432	76			2,038,090
	2.13	163	111	167	97	146	86	49	233	247	214	371	490	993	1,412	304						425,380
	3.63	256	196	268	287	359	245	208	244	89	14	102	10									63,355
	5.38	63	33	44	52	36	2	4	33													5,670
	6.63	55	30	40	16	16	28	73	131	89	17	16										16,870
	8.13	77	32	63	42	60	41		33													6,400
	9.63	33	35	17	22	34	9	26	21													4,890
	11.38	104	48	44	76	43	27	49	3	70	4											10,505
	12.88	277	211	178	152	160	208	44	65	21	54	18	19	37	2	1,013	5	690	4			329,360
How F-64 ZU	0.38	121	114	128	73	86	139	66	78	4	53											21,190
	1.38	78	120	87	68	23	46	63	156	62	307	255	247	1,440	277	759	20					375,050
	2.38	63	91	116	62	9	49	17	6	2	76	197	66	45	215							69,430
	3.38	107	134	110	40	52	28	7	23	35		32	3									17,305
	4.13	729	856	448	596	484	716	661	701	603	536	436	134	296								256,965
	5.38	30	44	53	25	41	22															4,285
	6.38	115	72	86	48	85	32	32	22	33	156	1										17,515
	7.38	389	356	366	414	208	196	190	226	391	54	195	42	37								103,190
	8.13	181	202	158	118	71	133	98	28	2		32	3									27,045
	9.38	173	181	107	126	72	82	31	30	10		11	103									25,485
	10.38	8	120	601	651	486	342	483	243	301	180	49	93	7	218							135,485

TABLE B.4 CONTINUED

Station	Mean Collection Time (TSD) hr	Microgram/ft³/hr/micron-interval Mean Particle Size, microns 52.5	72.5	92.5	112.5	132.5	155	195	235	275	315	365	485	605	725	845	1,000	1,400	1,800	2,200	2,600	μg/ft²-hr (52.5 to 2,600 μ)
Shot Tewa																						
YAG 40-B-7 TE	4.64	227	128	136	210	102	47	36	22	33												20,310
	6.14	381	580	803	844	383	201	543	350	332	26	60	66	6								135,560
	7.64	286	335	546	696	762	805	733	535	272	2		221	6								160,745
	9.14	133	344	484	522	474	561	402	300	57	63	3										69,050
	10.64	198	228	267	342	414	214	360	21	49	16											86,860
	12.14	70	71	83	51	32	21	54	22				75	7								22,085
	13.64	84	114	78	93	21	6	35	1	34		17	37									20,320
	15.14	172	23	63	44	32	75	22	13	20	75	9	16									17,865
	16.64	102	85	118	127	95	209	30	12	20												20,840
YAG 39-C-20 TE	3.64	708	417	449	222	205	509	1,416	3,140	3,308	3,359	4,289	3,660	113								793,650
	5.64	76	240	196	124	111	74	113	168	113	3											37,868
	8.66	337	128	124	97	37	99	199	98	3												29,940
	8.16	123	384	603	361	226	176	111	20	134	109	134	3									63,635
	9.66	85	59	66	27	35	13	43	73													9,335
	11.16	174	90	92	44	92	35	25	39	32	50											15,625
	12.66	104	66	39	50	18	9	34				49										10,335
	14.16	246	84	57	72	48	98	3	1	34		145	131									18,020
	15.16	155	136	113	123	70	96	90	42	144	21	843	641	3								42,065
LST 611-D-41 TE	0.16	14	89	272	233	229	142	111	1	47	65											31,225
	0.66	61	115	256	259	505	127	231	36	13												35,500
	10.16	137	128	197	216	250	231	183														32,700
	10.66	28	284	462	279	368	172	186	3													40,080
	12.16	21	101	239	110	154	244	94	46													24,505
	12.66	69	48	131	197	177	300	31	1													22,905
	14.16	52	48	60	71	49	13	23														8,105
	14.66	77	125	119	61	56	47	2				23	49									24,810
	16.16	92	60	85	114	35	54	54	92	43	3	63										21,665
	16.66	14	78	181	163	71	43	55	17						270	20						53,560
YFNB 13-E-67 TE	0.13	239	267	709	948	1,014	436	288	250	196	115	15			198	495	2	484	46			429,220
	0.63	214	177	258	293	424	326	707	387	185	53	3	119	32								114,155
	1.13	99	396	678	1,078	957	556	399	210	607	240	6,956	496		732	168						285,440
	1.63	175	437	637	532	447	578	478	376	570	1,098	1,846	1,872	418	198							622,925
YFNB 29-H-78 TE	0.13	96	1,035	1,106	485	430	333	401	434	231	99	253	63	196	1,114	107	118					349,010
	1.38	56	531	967	868	1,036	708	1,340	1,626	2,193	1,594	1,836	8,965	7,287	3,364	33						2,594,356
	2.87	24	381	471	404	435	366	402	722	3,879	4,879	6,688	6,636	1,408	249	18						2,268,935
	4.37	58	87	202	116	147	216	677	1,103	1,874	844	19										197,675
	5.87	46	32	48	18	3	76	20	42													8,665
	7.37	20	46	50	24	1	46	13	34													5,685
	8.87	92	47	47	16			14	51	32												7,265
	10.37	34	116	69	46		19	6	22	2												7,790
	11.87	92	127	104	56	53	33	44		69												12,775
	13.37	36	131	118	22	96	48	44	31	36		51										18,085
How F-64 TE	0.13	150	170	126	166	113	137	103	93													23,130
	1.13	169	130	110	130	63	113	9	50	11	16											16,675
	2.13	29	94	101	159	217	96	111	22	119	67	281										31,945
	3.13	28	35	119	86	74	61	77	2	89												15,495
	4.13	83	142	159	173	203	289	153	5			1	66									37,580
	5.13	37	97	96	61	39	3	84	133	13	17	10	20									22,275
	6.13	40	77	85	64	13	15	38	19	23	15		37	61								37,000
	7.13	392	244	148	184	207	252	66		36	3											34,575
	8.13	151	191	143	106	94	89	18	48	111	88	74	4	132								49,370

TABLE B.5 MEASURED RATE OF PARTICLE DEPOSITION, SUPPLEMENTARY DATA, SHOTS ZUNI AND TEWA

Station	Mean Collection Time (TSD)	Number of Particles/ft²/hr/micron-interval, Mean Particle Size, microns																		
	hr	52.5	72.5	92.5	112.5	132.5	155	195	235	275	315	365	485	605	725	845	1,000	1,400	1,800	2,200	2,600
Shot Zuni																					
YAG 40-	3.49	5,933	817	317	96	47	16	14	3	22	2	0.8	0.8								
B-7 ZU	3.74	702	142	70	17	28	10	29	20	11	4	5	4	0.1	0.6						
	4.47	2,560	719	361	266	229	216	295	260	239	141	62	2								
	5.23	13,014	5,721	3,903	2,251	1,463	1,274	617	547	246	90	20	0.5	0.4							
	5.48	12,143	3,741	2,742	1,920	1,199	1,015	479	189	134	22	7									
	5.74	26,027	5,739	2,784	1,914	1,343	524	624	145	92	36	2									
	6.24	25,940	2,933	1,794	737	469	180	162	68	2	8	0.02									
	6.75	11,973	1,454	1,322	724	568	365	144	64	27	17	3									
	7.25	1,165	356	215	108	68	26	22	6	6	1										
	7.76	423	212	128	63	41	9	3	1												
	8.27	771	233	165	68	59	24	7	10												
	8.52	242	350	156	145	53	36	13	6												
	8.78	2,390	229	153	100	44	31	15	1												
	9.28	4,115	531	329	134	33	30	11		2		0.02	0.4								
	9.53	1,255	389	339	202	123	84	25	8	2	0.4										
	9.79	1,074	328	205	135	110	67	35	12	6	1	4	0.02								
	10.55	892	223	145	107	41	32	15	1		4	0.06	1	1							
	10.80	771	270	140	136	47	25	8	7	1	0.6										
	11.31	559	215	134	102	72	42	19	14	3	0.4	0.8									
	11.56	514	180	74	34	14	6	2		4											
	11.81	1,074	166	141	60	32	9	4													
	12.32	984	156	81	16	11	2	1	1												
	12.58	378	168	107	71	33	45	1	2												
	12.83	696	97	101	52	44	27	8	4			0.5	0.02								
	13.33	726	173	109	62	47	10	22	2												
	13.59	741	161	65	24	11	8														
	13.84	847	95	60	25	10	6	1	1		0.9	0.2									
	14.35	1,089	119	46	39	8	1	3													
	14.60	801	166	67	12	10	2	1	1	1		0.8									
	14.88	1,664	148	120	53	16	6	1	3	2											
	15.36	968	78	46	55	9	3	5													
	15.61	720	172	152	41	42	32	4	1		4	0.02	0.4								
YAG 39-	12.53	367	94	39	21	10	13														
C-20 ZU	14.03	1,224	220	75	10	4	3	1				0.1	1	0.02							
	14.28	428	253	147	70	16	21	4													
	15.28	91	57	11	17	10	9	3	1												
	15.78	551	151	85	33	16	3	5			0.5	0.04	0.4								
	16.03	153	123	79	31	14	6														
	16.28	398	65	64	30	14	1														
	22.18	91	62	70	9	14	4		0.4		0.4										
	24.17	260	148	48	53	10	1	2	0.5	0.4											
	26.18	76	67	37	8	2		2													
	29.93	995	288	70	56	10	11	2				0.5	0.1								
YFNB 13-	0.13	1,699	416	271	131	70	38	21	7	2	0.4										
E-57 ZU	0.88	4,088	982	665	468	355	399	155	104	69	27	11	16	16	2	1	3	0.07			
	1.13	16,492	1,638	997	661	389	269	306	94	124	71	55	28	9	10	3	0.04				
	1.63	6,031	1,904	973	526	326	189	143	64	62	74	31	16	7	3	0.2	0.09				
	1.88	2,939	843	576	278	125	126	94	21	19	13	16	18	5	4	1	0.2				
	2.63	1,729	555	312	68	22	15	7	1	3	4	4	2	0.8							
	3.38	1,071	288	168	99	19	50	38	20	7	0.1	0.4	0.04	0.4							
	4.63	1,117	81	27	11	10	5														
	5.13	336	181	62	23	23	2	4													
	5.88	362	113	16	17	6		4													
	6.38	620	86	45	34	19	5	6	4												
	6.88	672	190	56	42	3	2	1													
	7.38	1,209	372	228	69	50	50	12	0.8	0.4	2										
	7.88	1,874	272	120	41	14	19	7	2	1											
	8.63	841	286	182	84	51	7	6													
	9.13	678	196	80	31	4	5		0	1	0.09										

TABLE B.5 CONTINUED

Station	Mean Collection Time (TSD) hr	Number of Particles/ft³/hr/micron-interval, Mean Particle Size, microns: 52.5	72.5	92.5	112.5	132.5	155	195	235	275	315	365	425	605	725	845	1,000	1,400	1,800	2,200	2,600
Shot Zuni																					
	9.88	851	126	68	27	6	4		2												
	10.38	352	90	3	5	5	1														
	11.88	949	152	53	14	13	11	10													
	12.13	780	109	27	27	15	8		0.4	0.4		0.5	0.02								
	12.38	719	214	114	33	23	7	5	7	.1											
	12.63	1,056	333	177	39	35	7	3	3												
YFNB 29-	0.20	21,899	2,193	915	580	360	154	111	20												
Q-71 ZU	0.40	6,394	1,450	1,143	315	429	92	63	35		3	0.1									
	0.59	728	141	94	35	18	15	33	3	0.2	2	0.07	0.08	0.2							
	0.80	14,251	1,102	589	271	133	155	18	7	2			1	7	3	3	1	1	0.04		
	0.99	4,950	3,581	1,561	1,006	720	253	237	104	49	21	53	42	40	3	0.01	3	1	0.04		
	1.20	8,112	2,524	728	316	205	89	67	32	0.6	22	6	26	7	18	4	0.03	0.02			
	1.24	15,421	2,393	788	767	248	222	145	76	9	0.04	29	72	56	14	6	1	8	0.04		
	1.36	12,745	1,734	720	464	412	97	59	122	64	39	65	33	13	2						
	1.60	20,626	753	678	313	109	90	34	54	29	17	47	15	10	0.01						
	1.67	10,770	3,764	1,113	454	374	129	205	10	30	57	8	9	10	3	0.1	0.3	0.3			
	1.78	6,029	1,337	1,135	436	176	56	81	44	2	23	33	8	4	0.9						
	1.84	52,072	30,301	17,978	9,110	3,663	2,261	1,188	593	207	182	83	80	14	9	6					
Shot Tewa																					
YAG 40-	5.14	292	1,179	448	219	133	65	46	16	14	0.1										
B-7 TE	5.64	1,073	1,846	981	386	224	199	109	33	22	1	0.8									
	6.64	984	752	551	356	168	104	65	36	13	4										
	7.14	1,141	1,094	660	339	218	112	71	25	16	2										
	8.14	1,004	518	317	243	108	79	34	14												
	8.64	230	572	526	353	218	107	35	25	1	7	1	0.1								
	9.64	1,715	838	404	225	169	105	38	6	1											
	10.14	1,108	564	290	157	90	43	18	7	1	1										
	11.14	1,078	240	145	68	52	11	13	2		1										
	11.64	310	263	196	99	83	34	10	10	3											
	12.64	441	316	174	166	79	56	13	3	1	0.1	0.7	0.4								
	13.14	616	218	111	34	8	8			1	1										
	14.14	837	230	94	21	18	16														
	14.64	312	256	93	98	30	11	1													
	15.64	292	124	113	90	13	10	2		1					0.4	0.02					
	16.14	220	128	43	37	4	3														
	17.14	518	225	114	58	6	9	3		6	0.9										
	17.64	514	244	130	28	24	9	2	2	1											
YAG 39-	3.14	1,904	528	324	165	86	49	57	21	90	61	20	4	0.6							
C-20 TE	4.14	6,405	2,623	1,857	1,148	1,165	793	550	375	225	123	13	1								
	4.64	716	1,909	1,574	968	900	580	468	247	142	47	4	0.01	0.7	0.03						
	6.16	1,280	314	151	96	66	31	11	21	1	3										
LST 611-	11.78	364	611	266	56	44	7	7													
D-41 TE	15.78	267	95	50			1														
	16.58	210	49	34	10																
	17.38	58	126	93	36		5	1													
	17.78	77	180	107	32	43	30	2													
YFNB 29-	1.88	1,236	940	453	219	145	455	92	49	58	54	64	25	10	1	1					
H-78 TE	3.88	2,927	343	251	128	72	74	66	86	123	87	62	45	7	0.03						
	4.12	450	187	81	7	38	44	88	83	67	15	1	0.04	0.8							

TABLE B.6 CALCULATED RATE OF MASS DEPOSITION, SUPPLEMENTARY DATA, SHOTS ZUNI AND TEWA

Station	Mean Collection Time (TBD)	Number of Particles/ft²/hr/micron-interval — Mean Particle Size, microns																			μg/ft²-hr
		52.5	72.5	92.5	112.5	132.5	155	195	235	275	315	365	435	605	725	845	1,000	1,400	1,800	2,200	2,600	(52.5 to 2,600 μ)
	hr																					
Shot Zuni																						
YAQ 40-B-7 ZU	3.49	1,062	385	310	169	136	78	138	62	589	86	49	124									82,645
	3.74	126	67	69	31	83	46	272	321	290	186	360	568	36	326	1						172,285
	4.47	456	329	364	466	660	995	2,709	4,016	6,167	5,462	3,744	332									1,181,535
	5.23	2,330	2,695	3,014	3,960	4,264	5,861	6,303	6,786	6,330	3,491	1,251	72	116								1,677,820
	5.48	2,174	1,762	2,679	3,378	3,448	4,671	4,392	3,040	2,450	873	455										934,718
	5.74	4,659	2,704	2,721	3,367	3,065	2,414	5,723	3,334	2,367	1,393	161	1									894,778
	6.24	4,643	1,382	1,788	1,298	1,361	629	1,495	1,411	141	335	24										309,070
	6.75	2,143	779	1,292	1,275	1,628	1,686	1,506	1,035	710	690	206										348,695
	7.23	209	168	211	191	290	121	206	102	161	76	6										47,510
	7.76	76	106	125	111	119	48	84	32													14,605
	8.27	138	110	162	166	172	111	72	173	10												26,130
	8.82	43	165	163	255	153	166	134	99	2												31,295
	8.78	428	108	150	176	128	148	141	27	23	16											28,860
	9.28	737	251	322	237	96	179	103	11	62		1	64									45,085
	9.53	228	184	332	357	386	387	232	130	71	19											61,075
	9.79	192	155	200	239	317	311	323	205	164	66	296	3									85,905
	10.55	160	105	142	168	119	150	139	30	2	167	4	19	37								42,425
	10.80	138	128	138	239	136	118	74	121	36	2											27,540
	11.31	106	101	131	186	209	198	177	232	98	19	50										46,870
	11.56	82	85	73	60	42	32	32	1	124	3											13,113
	11.81	192	79	138	106	82	43	45														14,985
	12.32	176	74	79	29	33	12	16	20	1												8,423
	12.58	68	95	105	126	96	210	15	32	10												19,060
	12.83	125	46	89	93	127	125	55	76	2		31	3									21,830
	13.33	130	82	107	109	136	47	204	35													20,705
	13.59	133	76	64	43	33	37															7,430
	13.84	152	45	59	44	30	20	17	20	10	36	18										11,940
	14.35	105	56	46	70	24	6	26	1													7,390
	14.60	144	78	66	22	30	11	10	31	32	80											12,505
	14.86	290	70	110	93	47	31	16	51	71	2											16,700
	15.36	173	37	43	96	26	17	40														7,700
	15.61	129	81	149	73	122	147	44	30	13	16	1	63									25,315
YAQ 39-C-26 ZU	12.63	66	46	36	37	29	61	3														5,415
	14.03	219	104	73	19	13	14	11				11	196	5								32,190
	14.28	77	119	144	124	46	90	46	1													15,995
	15.28	16	27	13	31	30	43	36	19													5,325
	15.78	89	71	63	59	45	15	52	5			32	6	135								27,225
	16.03	27	86	77	86	43	29															6,165
	16.28	71	40	63	6	43	1	15														3,635
	22.18	16	30	65	16	42	19	4	7													5,085
	24.18	47	70	48	94	30	6	37	0	11	16											9,380
	26.16	14	32	36	16	7		15	1													2,435
	29.93	178	136	68	99	29	53	22				32	3									16,395
YFNB 13-E-87 ZU	0.13	304	196	266	232	202	177	194	117	71	15											44,245
	0.88	732	463	650	825	1,021	1,030	1,420	1,673	1,787	1,071	679	2,231	4,568	1,300	1,293	3,892	348				2,733,730
	1.13	2,952	780	955	1,164	1,120	1,240	2,000	1,610	3,204	2,772	3,343	3,968	2,646	8,022	2,550	52					2,425,800
	1.63	1,080	897	961	946	939	873	1,319	1,033	1,668	2,891	1,881	2,216	2,100	1,673	159	118					1,346,650
	1.88	526	398	562	488	360	590	566	341	489	230	975	2,677	1,489	1,960	1,362	255					1,171,840
	2.63	316	262	305	150	65	69	67	30	92	176	245	310	223								149,035
	3.38	192	135	164	178	86	234	368	329	182	5		64	13	215							88,055
	4.63	200	38	27	21	30	24															4,390
	5.13	60	71	62	41	67	13	42														7,340
	5.88	63	53	16	31	28		46	1													4,960
	6.38	93	40	44	61	57	24	63	78	3												10,320
	6.88	121	90	86	76	10	11	11														6,705
	7.38	216	176	224	122	148	96	116	0	11	79	6										27,725

TABLE B.6 CONTINUED

Station	Mean Collective Time (TSD)	Number of Particles/ft²/hr/micron-interval — Mean Particle Size, microns: 52.5	72.5	92.5	112.5	132.5	155	195	235	275	315	365	435	505	725	845	1,000	1,400	1,800	2,200	2,600	μg/ft²-h. (52.5 to 2,600 μ)
	hr																					
Shot Zuni																						
	1.86	282	129	117	74	42	30	69	42	34												16,648
	6.63	151	135	126	60	90	35	33	1													12,935
	9.13	121	66	35	30	15	14	3	40	35	2				320	1						35,320
	9.88	153	57	67	48	10	22		33													7,160
	10.38	63	43	4	10	14	6	4														2,730
	11.88	170	72	62	26	30	52	66														10,135
	12.13	140	52	27	40	45	30	7	7	11		32	3									12,205
	12.38	120	101	112	50	60	26	47	123	3												15,600
	12.63	160	157	176	80	93	32	30	60													15,750
YFNB 29-G-71 ZU	0.20	3,020	1,033	895	1,030	1,057	708	1,016	333	1												187,810
	0.40	1,145	662	1,217	858	1,236	424	602	564	184		214	21									183,685
	0.58	130	64	93	63	36	70	31	48	6	91	4	11	60								25,265
	0.80	2,351	819	576	478	384	715	166	116	75			20	1,068	1,439	2,404	2,194	4,900	343			4,634,915
	0.98	866	1,867	1,536	1,176	2,071	1,168	2,176	1,671	1,279	813	3,236	5,843	11,187	1,618	9	4,724	4,200	311			6,801,870
	1.20	1,452	1,782	712	861	682	488	622	817	22	861	401	3,673	2,184	8,676	3,438	400	893				3,025,355
	1.36	2,766	1,127	771	1,330	714	1,021	1,236	1,226	242	5	1,765	10,196	4,069	2,867	1,191	10,328	158				5,605,705
	1.38	2,391	817	704	817	1,185	446	643	1,971	1,656	1,527	3,911	4,764	3,586	1,121							2,906,905
	1.60	3,092	366	663	851	313	418	318	686	148	694	2,030	3,139	2,028	6							938,955
	1.67	1,928	1,773	1,666	786	1,077	594	1,988	172	167	2,215	524	1,366	2,946	1,668	127	427	1,084				2,054,283
	1.78	1,979	630	1,109	771	606	261	766	707	76	604	2,011	1,226	2,209	447							791,200
	1.86	9,321	14,272	17,868	16,025	16,528	10,401	10,699	8,616	8,241	7,047	4,869	11,278	3,801	6,230	6,776						6,417,163
Shot Tewa																						
YAG 40-B-7 TE	5.14	33	555	438	386	383	300	424	266	383	5											92,670
	5.64	182	870	959	681	647	818	1,008	546	575	68	49										166,290
	6.64	176	354	530	928	463	488	588	569	85	200	5.64										126,420
	7.14	204	516	646	597	638	617	634	416	432	85											135,416
	8.14	100	242	310	420	319	366	326	227	3												62,460
	8.64	61	270	513	655	627	494	471	408	81	284	117	19									119,320
	9.64	307	394	395	307	486	484	384	98	32												73,890
	10.14	196	266	283	276	260	196	174	122	47	73											48,085
	11.14	193	113	142	121	151	62	126	27	10	59											24,660
	11.64	50	124	152	174	268	186	161	174	99												11,641
	12.64	79	150	178	227	227	256	120	55	51	4	46	30									47,540
	13.14	110	103	109	61	25	61	55	2	3	45											14,665
	14.14	150	108	93	36	52	71	1														10,570
	14.64	66	121	81	174	89	65	16	31													13,395
	15.64	52	58	111	159	38	48	30	6	50					205	15						43,170
	16.14	39	80	42	66	13	15	6														6,170
	17.14	93	106	111	104	18	44	28	5	173	36											18,750
	17.64	82	116	128	51	70	46	29	35	32	2											14,000
YAG 39-C-20 TE	3.14	341	249	317	291	249	239	527	347	1,892	2,862	1,202	693	177	1							485,420
	6.14	1,141	1,235	1,818	2,021	3,350	3,648	5,043	6,017	5,787	4,143	787	21									1,241,625
	6.64	126	900	1,838	1,705	2,589	2,672	4,252	3,961	2,684	1,829	297	1	209	17							819,066
	8.16	229	148	148	136	192	143	166	338	36	143	1										48,950
LST 611-D-61 TE	11.78	65	288	261	98	128	31	72	1													20,635
	15.78	48	45	48	1		9	1														3,095
	16.58	38	23	33	18																	2,065
	17.38	18	60	92	64	2	23	17														5,785
	17.78	14	65	108	57	124	142	31														13,898
YFNB 29-H-78 TE	1.88	221	443	443	388	417	209	848	799	1,500	2,118	3,881	3,650	2,977	577	102						1,565,215
	3.98	524	162	245	228	209	341	613	1,383	2,178	3,394	6,464	1,824	18								1,841,675
	6.12	61	88	78	14	113	206	616	1,344	1,737	609	71	6	245								223,660

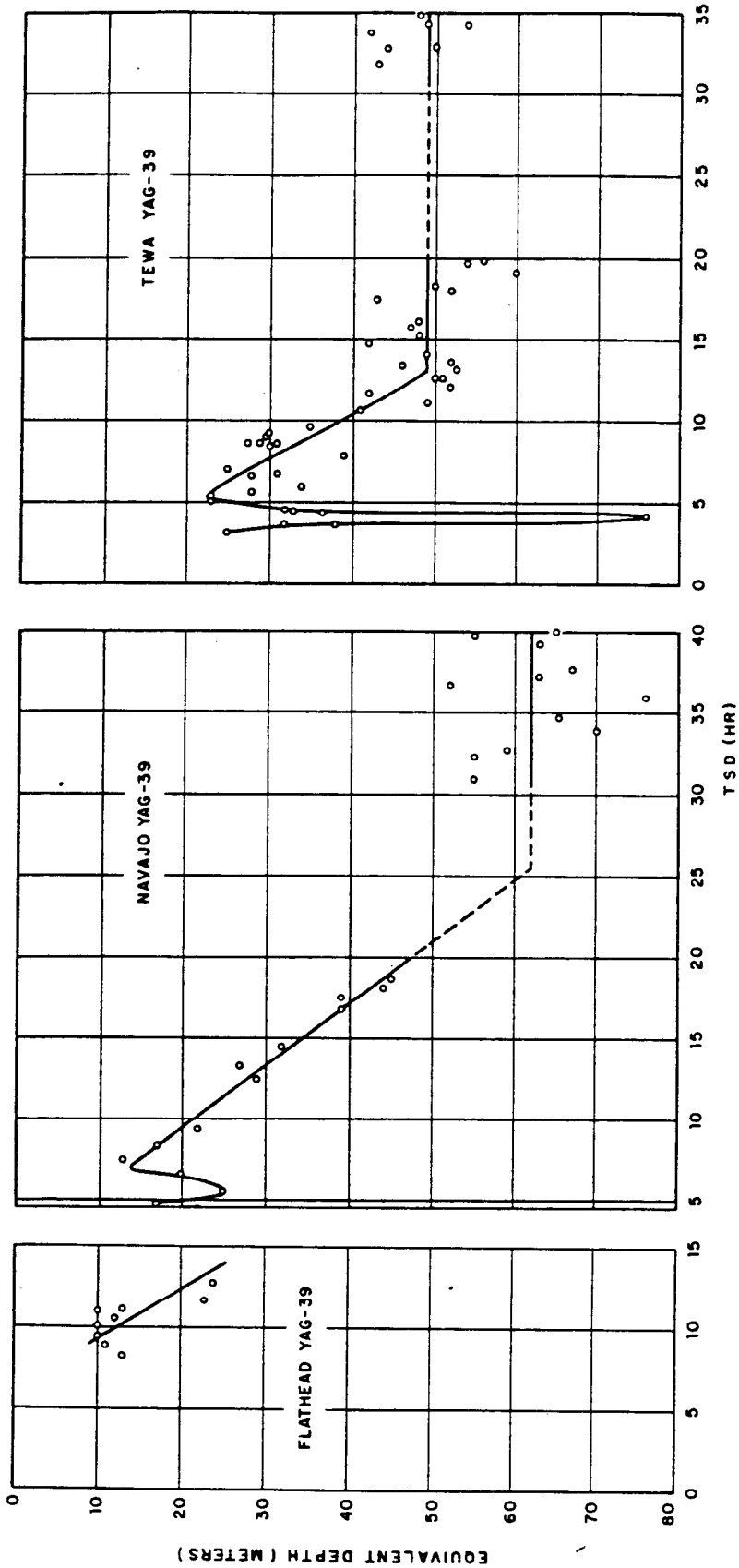

Figure B.1 Ocean-penetration rates, Shots Flathead, Navajo, and Tewa.

B.2 PHYSICAL, CHEMICAL, AND RADIOLOGICAL DATA

TABLE B.8 WEIGHT, ACTIVITY, AND FISSION VALUES FOR SIZED FRACTIONS FROM WHIM SAMPLE YFNB 29 ZU

Size Range	Weight		CIC Assay *			Fissions	
	Grams	Percent of Total	Value at H + 262 hr	Percent of Total	Specific Activity	Total	Per Gram
microns			10^{-5} ma		10^{-5} ma/gm	10^{14}	10^{14}
1,000	37.70	41.8	1.08	15.8	0.0286	21.	0.56
500 to 1,000	41.91	46.4	3.14	46.0	0.0749	60.	1.4
250 to 500	4.97	5.5	1.35	19.8	0.272	26.	5.2
100 to 250	3.51	3.9	0.734	10.7	0.209	14.	4.0
50 to 100	0.80	0.9	0.155	2.3	0.194	3.0	3.8
50	1.38	1.5	0.371	5.4	0.269	7.1	5.1
Total	90.27		6.83		0.0757	131.	1.5

* Response to 100 μg of Ra = 588 × 10^{-8} ma

PAGE 208 DELETED

TABLE B. 9 REQUENCIES AND ACTIVITY CHARACTERISTICS OF PARTICLE SIZE AND PARTICLE TYPE GROUPS, SHOTS ZUNI AND TEWA

Size Group	Composite				Angular		Spherical		Agglomerates	
	Number of Particles	Activity			Frequency	Median Activity	Frequency	Median Activity	Frequency	Median Activity
		Minimum	Maximum	Median						
microns		well counts/min				well counts/min		well counts/min		well counts/min
YAG 40, Shot Zuni (nonrandom sample)										
Activities in well counts/min at H+12 hours										
31 to 42	8	78	11,354	835	6	1,255	2	387	0	—
43 to 60	20	33	833,600	6,985	13	6,797	5	6,631	2	423,448
61 to 84	37	58	459,321	12,213	27	11,871	10	17,450	0	—
85 to 102	6	4,460	50,608	32,434	6	32,434	0	—	0	—
103 to 120	42	69	525,449	41,412	24	25,083	12	87,795	6	56,728
121 to 145	13	19,063	683,362	77,622	4	24,771	8	304,282	1	58,585
146 to 170	34	3,686	771,326	113,209	12	65,067	15	259,931	7	114,803
171 to 200	24	3,816	1,675,122	166,982	13	92,070	11	457,315	0	—
201 to 240	27	25,565	1,310,318	168,795	22	152,710	2	420,669	3	221,828
241 to 260	25	32,178	726,969	145,494	22	131,935	0	—	3	217,674
261 to 315	9	53,105	493,500	223,424	6	181,658	0	—	3	365,685
316 to 382	1	—	—	1,774,146	1	1,774,146	0	—	0	—

Size Group	Composite					Angular			Spherical			Agglomerates		
	Number of Particles	Activity			Group	Frequency	Activity		Frequency	Activity		Frequency	Activity	
		Minimum	Maximum	Median			Median	Group		Median	Group		Median	Group
microns		well counts/min					well counts/min			well counts/min			well counts/min	
YAG 40, Shot Tewa														
Activities in well counts/min at H+300 hours														
11 to 33	5	0	3,222	372	4,209	4	218	987	1	3,222	3,222	0	—	—
34 to 66	28	0	80,483	1,596	191,972	17	1,860	169,221	3	3,424	9,532	8	1,125	13,219
67 to 99	49	0	47,181	7,103	519,360	24	8,293	241,291	11	14,776	194,762	14	4,111	83,307
100 to 132	61	0	48,757	15,129	998,547	38	16,889	685,795	8	8,932	66,648	15	13,504	246,104
133 to 165	78	4	53,806	17,243	1,564,034	40	15,247	678,500	8	10,827	88,475	30	26,224	797,059
166 to 198	46	0	387,697	25,877	1,628,637	30	24,503	803,776	4	3,757	30,261	12	37,363	794,600
199 to 231	19	19	99,094	34,435	693,709	12	34,078	402,758	0	—	—	7	34,591	290,951
232 to 264	16	94	136,203	49,444	849,701	4	34,571	125,221	0	—	—	12	53,599	724,480
265 to 297	10	8	122,553	55,708	599,034	2	43,855	87,709	1	8	8	7	72,695	511,317
298 to 330	14	19	155,625	55,282	926,556	2	63,499	126,985	0	—	—	12	55,282	799,571
331 to 363	1	—	—	64,086	64,086	0	—	—	0	—	—	1	64,086	64,086
364 to 396	2	3,176	138,856	71,016	142,032	0	—	—	1	3,176	3,176	1	138,856	138,856
397 to 429	0	—	—	—	—	—	—	—	—	—	—	-	—	—
430 to 462	3	1,267	39,308	10,997	51,572	2	6,132	12,264	1	39,308	39,308	0	—	—
463 to 495	0	—	—	—	—	—	—	—	—	—	—	-	—	—
496 to 528	2	92,668	197,740	145,214	290,428	0	—	—	0	—	—	2	145,214	290,428
Total	334				8,523,877	175		3,334,507	38		435,392	121		4,753,978
Contribution, pct						52.4		39.1	11.4		5.1	36.2		55.8

TABLE B.9 CONTINUED

Size Group	Composite						Angular			Spherical			Agglomerates		
	Number of Particles	Frequency with Zero Activity	Activity				Frequency	Activity		Frequency	Activity		Frequency	Activity	
			Minimum	Maximum	Median	Group		Median	Group		Median	Group		Median	Group
microns			well counts/min					well counts/min			well counts/min			well counts/min	
YAG 39, Shot Tewa Activities in well counts/min at H+300 hours															
10 to 21	20	7	0	232	18	1,161	5	0	57	15	61	1,104	0	—	—
22 to 30	51	19	0	477	14	3,115	34	11	1,532	16	68	1,583	1	0	0
31 to 42	59	27	0	872	16	5,263	45	9	3,554	3	0	307	11	22	1,402
43 to 60	63	17	0	5,451	54	12,481	31	64	1,335	3	469	9,913	29	27	1,233
61 to 84	49	8	0	2,180	64	11,992	29	61	5,666	0	—	—	20	64	6,326
85 to 120	41	4	0	8,994	317	80,647	25	543	48,395	1	739	739	15	98	31,513
121 to 170	9	1	0	15,755	494	32,430	6	676	16,170	1	494	494	2	7,883	15,766
171 to 240	5	0	1,958	27,120	16,402	80,525	2	10,757	21,514	1	27,120	27,120	2	15,946	31,891
241 to 340	3	0	5,658	76,906	34,344	166,908	3	34,344	116,908	0	—	—	0	—	—
341 to 480	0	—	—	—	—	—	—	—	—	—	—	—	—	—	—
481 to 680	0	—	—	—	—	—	—	—	—	—	—	—	—	—	—
Total	300					344,522	180		215,131	40		41,260	80		88,131
Contribution, pct							60.0		62.4	13.4		12.0	26.7		25.6
LST 611, Shot Tewa Activities in well counts/min at H+300 hours															
10 to 21	39	18	0	161	19	1,897	22	13	1,017	17	19	880	0	—	—
22 to 30	23	10	0	212	11	939	22	24	929	1	10	10	0	—	—
31 to 42	32	12	0	343	41	2,269	27	44	1,820	3	29	106	2	172	343
43 to 60	26	13	0	1,112	10	2,436	20	19	2,261	4	0	118	2	29	57
61 to 84	12	2	0	7,909	108	14,161	7	198	9,598	1	128	128	4	53	4,435
85 to 120	14	3	0	11,941	1,994	47,417	8	4,201	35,755	1	3,282	3,282	5	0	8,380
121 to 170	20	3	0	17,640	8,699	176,014	14	11,323	150,672	0	—	—	6	883	25,342
171 to 240	6	1	0	39,681	11,438	82,752	5	8,798	68,472	0	—	—	1	14,280	14,280
241 to 340	0	—	—	—	—	—	—	—	—	—	—	—	—	—	—
341 to 480	0	—	—	—	—	—	—	—	—	—	—	—	—	—	—
481 to 680	0	—	—	—	—	—	—	—	—	—	—	—	—	—	—
Total	172					327,885	125		270,524	27		4,524	20		52,837
Contribution, pct							72.7		82.5	15.7		1.4	11.6		16.1

TABLE B.9 CONTINUED

Size Group	Number of Particles	Frequency with Zero Activity	Composite Activity Minimum	Composite Activity Maximum	Composite Activity Median	Composite Activity Group	Angular Frequency	Angular Activity Median	Angular Activity Group	Spherical Frequency	Spherical Activity Median	Spherical Activity Group	Agglomerates Frequency	Agglomerates Activity Median	Agglomerates Activity Group
microns			well counts/min					well counts/min			well counts/min			well counts/min	
YFNB 13, Shot Tewa **Activities in well counts/min at H+300 hours**															
10 to 21	27	8	0	250	33	1,488	19	35	868	8	29	620	0	—	—
22 to 30	54	22	0	399	25	3,014	38	24	1,933	16	38	1,081	0	—	—
31 to 42	28	7	0	356	87	2,820	25	91	2,775	2	23	45	1	0	0
43 to 60	19	3	0	1,225	74	2,707	15	74	2,345	0	—	—	4	87	362
61 to 84	8	2	0	1,166	83	1,612	6	83	446	0	—	—	2	583	1,166
85 to 120	11	4	0	2,424	125	5,618	6	135	963	1	0	0	4	1,116	4,655
121 to 170	2	0	78	7,126	3,602	7,204	1	78	78	0	—	—	1	7,126	7,126
171 to 240	1	1	—	—	0	0	0	—	—	0	—	—	1	0	0
241 to 340	0	—	—	—	—	—	—	—	—	—	—	—	—	—	—
341 to 480	2	0	792,378	984,805	888,592	1,777,183	2	888,592	1,777,183	0	—	—	0	—	—
481 to 680	1	1	—	—	0	0	0	—	—	1	0	0	0	—	—
Total	153					1,801,646	114		1,786,591	27		1,746	12		13,309
Contribution, pct							74.5		99.2	17.6		0.1	7.8		0.7
YFNB 29, Shot Tewa **Activities in well counts/min at H+300 hours**															
10 to 21	33	6	0	506	48	2,514	20	44	1,683	13	70	841	0	—	—
22 to 30	18	9	0	610	13	1,299	15	0	1,107	3	60	192	0	—	—
31 to 42	19	5	0	534	62	1,853	16	53	1,487	0	—	—	3	84	366
43 to 60	22	4	0	395,842	490	408,345	15	167	404,211	1	9	9	6	848	4,125
61 to 84	12	2	0	5,554	272	11,149	8	272	8,493	1	927	927	3	88	1,729
85 to 120	16	0	90	7,801	926	37,525	7	785	20,133	4	554	4,472	5	1,625	12,920
121 to 170	12	1	0	83,316	2,029	118,296	6	1,433	93,965	0	—	—	6	2,421	24 331
171 to 240	8	1	0	21,240	6,186	55,882	3	6,590	19,723	1	21,240	21,240	4	2,728	14,919
241 to 340	9	0	3,614	619,448	61,653	1,445,691	6	112,640	720,292	1	61,653	61,653	2	331,873	663,746
341 to 480	13	0	6,204	1,698,631	71,445	3,265,945	9	142,176	2,918,445	3	71,446	341,296	1	6,204	6,204
481 to 680	7	0	50,641	489,310	184,800	1,610,536	5	184,800	1,086,799	0	—	—	2	261,869	523,737
Total	169					6,959,045	110		5,276,338	27		430,630	32		1,252,077
Contribution, pct							65.1		78.8	16.0		6.0	18.9		18.0

TABLE B. 10 SURVEY OF SHOT TEWA REAGENT FILMS FOR SLURRY PARTICLE TRACES *

Station and Instrument	Number of Reagent Film Examined †	Serial Number of Tray Having Slurry Particles	Number of Slurry Particles	
			Definite	Doubtful
YAG 40-A-1	10	—	0	0
YAG 40-A-2	7	3006		4
		2988		2
YAG 40-B-7	28	—	0	0
YAG 39-C-20	27	3930	5	
		3931	3	
		3927	1	
		3924		‡
YAG 39-C-24	27	3721		2
		3727		4
YAG 39-C-33	27	3828		‡
		3829		‡
LST 611-D-37	27	3211		1
		3224		1
		3231		1
LST 611-D-41	27	3394	1	
		3393	1	
		3401		1
LST 611-D-50	12	—	0	0
YFNB 29-G-71	5	3433		~57§
YFNB 29-H-78	0	—	—	—
YFNB 13-E-57	5	—	0	0
How F-64	17	—	0	0
Totals	219	17	11	73

* Private communication from N. H. Farlow.
† Every reagent film in each IC examined.
‡ Covered with contaminated rain.
§ Primarily splashes.

TABLE B.11 TOTAL ACTIVITY AND MASS OF SLURRY FALLOUT

Collecting Station	Shot Flathead			Shot Navajo		
	Total Activity * (counts/min)/ft^2 × 10^8	Total Mass NaCl μg/ft^2	Total Number Droplets number/ft^2	Total Activity * (counts/min)/ft^2 × 10^8	Total Mass NaCl μg/ft^2	Total Number Droplets number/ft^2
YFNB 13-E-57	†	—	—	51.0	125,000	16,000
YFNB 29-H-78	45.9	10,700	178,000	3.6	9,000	1,150
YAG 39-C-20	8.4	300	714	21.2	13,200	1,740
YAG 39-C-24	1.6	57	135	†	—	—
LST 611-D-37	19.6	690	1,640	†	—	—
LST 611-D-50	2.6	92	219	†	—	—
YAG 40-A-1	13.1	460	489	9.2	4,400	15,000
YAG 40-A-2	11.5	410	436	†	—	—
YAG 40-B-7	6.5	230	460	†	—	—

* Photon count in well counter at H + 12 hours.

† Values unavailable due to instrument malfunction or incomplete sampling run.

TABLE B.12 GAMMA ACTIVITY AND FISSION CONTENT OF OCC AND AOC_1 COLLECTORS BY Mo^{99} ANALYSIS (AREA = 2.60 ft^2)

The activities listed are for the unopened, covered collector on the floor of the doghouse counter. Fission values determined by radiochemical analysis are underlined; corresponding total fissions are corrected for recovery loss. All other fission values are computed from the derived ratio fission/doghouse counts/min at 100 hr (see Table B.13). In most cases the observed ratio for a given platform is used for the other collectors on that platform. For the YFNB 29, the ratio used is based on the average of the two independent fission values reported. How F Flathead is computed from the average ratio obtained from all other Flathead platforms.

Collector Designator	Shot Zuni			Shot Flathead		
	Doghouse Activity at 100 hrs	Recovered Number of Fissions	Total Fissions	Doghouse Activity at 100 hrs	Recovered Number of Fissions	Total Fissions
	counts/min			counts/min		
YAG 40-B- 4	433,600 *	—	7.38×10^{13}	421,500	5.29×10^{13}	7.56×10^{13}
- 5	4,538,900	—	7.73×10^{14}	84,480	—	1.52×10^{13}
- 6	7,458,800	1.27×10^{15}	1.27×10^{15}	35,200	—	6.31×10^{12}
-17	5,868,700	—	9.99×10^{14}	34,140	—	6.12×10^{12}
-18	2,833,200	—	4.82×10^{14}	101,900	—	1.83×10^{13}
-19	4,047,400	—	6.89×10^{14}	439,650	—	7.89×10^{13}
YAG 39-C-21	87,300	8.26×10^{12}	8.26×10^{12}	82,100	1.27×10^{13}	1.37×10^{13}
-22	35,560	—	3.36×10^{12}	31,400	—	5.24×10^{12}
-23	35,560	—	3.36×10^{12}	17,820	—	2.97×10^{12}
-34	34,400	—	3.25×10^{12}	50,270	—	8.39×10^{12}
-35	64,180	—	6.07×10^{12}	92,430	—	1.54×10^{13}
-36	132,120	—	1.25×10^{13}	106,130	—	1.77×10^{13}
LST 611-D-38				73,120	—	1.74×10^{13}
-39				13,576	—	3.22×10^{12}
-40	NO FALLOUT; COLLECTORS NOT EXPOSED			11,580 *	2.09×10^{12}	2.75×10^{12}
-51				21,840 *	—	5.19×10^{12}
-52				136,490	—	3.24×10^{13}
-53				241,150 *	—	5.73×10^{13}
YFNB 13-E-54	2,805,200	7.95×10^{14}	7.95×10^{14}	4,962,300	9.52×10^{14}	1.05×10^{15}
-55	3,305,800	—	9.37×10^{14}	5,596,600	—	1.18×10^{15}
-56	4,656,000	—	1.32×10^{15}	6,890,600	—	1.46×10^{15}
-58	1,780,900 *	—	5.05×10^{14}	5,880,700	—	1.24×10^{15}
-59	3,073,000	—	8.71×10^{14}	7,364,000	—	1.56×10^{15}
-60	4,004,200	—	1.13×10^{15}	4,978,600	—	1.05×10^{15}
How F-61	2,081,000	5.01×10^{14}	5.01×10^{14}	666	—	1.26×10^{11}
-62	2,361,000	—	5.68×10^{14}	1,107	—	2.10×10^{11}
-63	2,877,000	—	6.92×10^{14}	1,443	—	2.74×10^{11}
-65	2,229,000	—	5.37×10^{14}	603	—	1.14×10^{11}
-66	2,064,000	—	4.97×10^{14}	604	—	1.15×10^{11}
-67	1,776,000	—	4.27×10^{14}	620	—	1.18×10^{11}
YFNB 29-G-68	4,320,000	1.19×10^{15}	1.19×10^{15}	219,800	3.47×10^{13}	3.81×10^{13}
-69	4,419,600	—	1.20×10^{15}	266,900	—	4.84×10^{13}
-70	5,881,700	—	1.60×10^{15}	303,550	—	5.50×10^{13}
-72	5,283,600	—	1.44×10^{15}	272,450	—	4.94×10^{13}
-73	4,054,000	—	1.10×10^{15}	233,760	—	4.24×10^{13}
-74	4,884,800	—	1.33×10^{15} †	230,400	—	4.17×10^{13}
YFNB 29-H-75	5,732,200	1.39×10^{15}	1.54×10^{15}	316,600	4.79×10^{13}	5.99×10^{13}
-76	7,476,800	—	2.03×10^{15}	271,700	—	4.93×10^{13}
-77	8,889,000	—	2.42×10^{15}	302,880	—	5.49×10^{13}
-79	7,476,800	—	2.03×10^{15}	298,560	—	5.41×10^{13}
-80	6,180,800	—	1.68×10^{15}	309,500	—	5.61×10^{13}
-81	5,615,900	—	1.53×10^{15}	247,680	—	4.49×10^{13}
Standard cloud	83,000	—	9.84×10^{12}	164,000	—	2.79×10^{13}

TABLE B.12 CONTINUED

Collector Designator	Shot Navajo			Shot Tewa	
	Doghouse Activity at 100 hrs	Recovered Number of Fissions	Total Fissions	Doghouse Activity at 100 hrs	Total Fissions ‡
	counts/min			counts/min	
YAG 40-B- 4	85,800	1.72×10^{13}	1.91×10^{13}	13,383,300	1.95×10^{15}
- 5	67,080	—	1.49×10^{13}	4,504,700	6.56×10^{14}
- 6	52,260	—	1.16×10^{13}	3,743,200	5.45×10^{14}
-17	54,990	—	1.22×10^{13}	4,958,600	7.22×10^{14}
-18	69,615	—	1.55×10^{13}	3,846,800	5.60×10^{14}
-19	80,145	—	1.78×10^{13}	13,879,700	2.02×10^{15}
YAG 39-C-21	191,760	3.90×10^{13}	4.48×10^{13}	23,623,200	4.54×10^{15}
-22	149,600	—	3.49×10^{13}	5,754,700	1.11×10^{15}
-23	117,640	—	2.75×10^{13}	6,306,500	1.21×10^{15}
-34	129,200	—	3.02×10^{13}	6,192,200	1.19×10^{15}
-35	176,700	—	4.13×10^{13}	9,091,900	1.75×10^{15}
-36	205,360	—	4.80×10^{13}	27,328,300	5.25×10^{15}
LST 611-D-38	16,860	3.03×10^{12}	3.74×10^{12}	1,337,000	2.44×10^{14}
-39	18,130	—	4.02×10^{12}	810,900	1.48×10^{14}
-40	9,016	—	2.00×10^{12}	962,800	1.76×10^{14}
-51	8,722	—	1.93×10^{12}	1,259,000	2.30×10^{14}
-52	17,836	—	3.96×10^{12}	1,336,500	2.44×10^{14}
-53	19,600	—	4.35×10^{12}	1,830,400	3.34×10^{14}
YFNB 13-E-54	727,600	—	1.46×10^{14}	2,584,300	5.95×10^{14}
-55	476,000	—	9.58×10^{13}	3,616,300	8.32×10^{14}
-56	804,640	1.30×10^{14}	1.62×10^{14}	5,740,900	1.32×10^{15}
-58	806,070	—	1.62×10^{14}	4,180,400	9.62×10^{14}
-59	714,000	—	1.44×10^{14}	2,149,100	4.95×10^{14}
-60	675,240	—	1.36×10^{14}	2,447,800	5.63×10^{14}
How F-61	16,110	3.04×10^{12}	3.62×10^{12}	255,940	6.56×10^{13}
-62	18,820	—	4.23×10^{12}	275,000	7.05×10^{13}
-63	18,980	—	4.26×10^{12}	331,570	8.5×10^{13}
-65	18,440	—	4.14×10^{12}	251,790	6.45×10^{13}
-66	15,890	—	3.57×10^{12}	214,470	5.50×10^{13}
-67	15,130	—	3.40×10^{12}	238,140	6.10×10^{13}
YFNB 29-G-68	8,330	—	2.06×10^{12}	17,914,700	3.61×10^{15}
-69	9,500	—	2.35×10^{12}	§	—
-70	11,370	—	2.81×10^{12}	32,654,400	6.26×10^{15}
-72	10,880	—	2.69×10^{12}	37,489,100	7.18×10^{15}
-73	5,292 *	—	1.31×10^{12}	18,895,700	3.62×10^{15}
-74	10,090	—	2.50×10^{12}	18,678,100	3.58×10^{15} ¶
YFNB 29-H-75	13,130	2.60×10^{12}	3.10×10^{12}	37,371,900	6.79×10^{15}
-76	7,546 *	—	1.87×10^{12}	46,094,000	9.41×10^{15}
-77	14,110	3.10×10^{12}	3.65×10^{12}	64,372,000	1.23×10^{16}
-79	16,660	—	4.12×10^{12}	61,366,400	1.18×10^{16}
-80	17,050	—	4.22×10^{12}	45,756,700	8.77×10^{15}
-81	11,560	—	2.86×10^{12}	37,853,100	7.25×10^{15}
Standard Cloud	16,900	—	3.46×10^{12}	315,000	4.71×10^{13}

* Imperfect collection for quantity/area; hexcell and/or liner lost.
† Independent value by UCRL: 1.38×10^{15}
‡ All recoveries > 96 percent. No correction made.
§ Absurd value excluded.
¶ Independent value by UCRL: 4.15×10^{15}

TABLE B. 13 OBSERVED DOGHOUSE GAMMA ACTIVITY-FISSION CONTENT RELATIONSHIP

Collector Designator	Fissions (Mo^{99})/Doghouse counts/min at 100 hour x 10^6			
	Zuni	Flathead	Navajo	Tewa
YAG 40-B-4	—	1. 794	2. 226	1. 457
-6	1. 703	—	—	—
YAG 39-C-21	0. 946	1. 669	2. 336	1. 922
LST 611-D-38	—	—	2. 218	1. 825
-40	—	2. 375	—	—
YFNB 13-E-54	2. 834	2. 116	—	2. 302
-56	—	—	2. 013	—
How F-61	2. 407	—	2. 247	2. 563
YFNB 29-G-68	2. 755 } 2. 721	1. 733 } 1. 812	—	2. 015 } 1. 916
H-75	2. 687 }	1. 892 }	2. 361 } 2. 474	1. 817 }
-77	—	—	2. 587 }	—
Standard Cloud *	1. 186	1. 701	2. 047	1. 495
Mean and σ (pct)	2. 07 ± 37. 9	1. 90 ± 13. 7	2. 25 ± 8. 07	1. 92 ± 19. 5

* This sample was a point source. To compare with extended sources, cloud sample activities should be decreased ~7 percent, raising the reported ratio a corresponding amount.

TABLE B. 14 DIP-COUNTER ACTIVITY AND FISSION CONTENT OF AOC_2 COLLECTORS (AREA = 0. 244 ft^2)
I. SHOTS FLATHEAD AND NAVAJO

The fallout samples from each of these events were relatively unfractionated allowing activities of all samples from Flathead and Navajo to be converted directly to fissions by a constant factor; 1.01×10^6 and 1.24×10^6 fission/dip counts/min at 100 hr, respectively. Details may be found in Table B. 15. The AOC_2 collections (complete sample or aliquot thereof) were made up to a standard volume of 2 liters for counting.

Collector Location	Shot Flathead		Shot Navajo	
	Dip Activity at 100 hr	Total Fissions	Dip Activity at 100 hr	Total Fissions
	counts/min		counts/min	
Skiff AA	1.36×10^7 *	1.37×10^{13}	1.65×10^6	2.05×10^{12}
BB	2.21×10^7	2.23×10^{13}	1.12×10^6	1.39×10^{12}
CC	4.81×10^6	4.86×10^{12}	6.28×10^5	7.79×10^{11}
DD	6.08×10^4	6.14×10^{10}	7.55×10^5	9.36×10^{11}
EE	4.81×10^3	4.86×10^9	4.99×10^5	6.19×10^{11}
FF	7.07×10^4	7.14×10^{10}	2.11×10^5	2.62×10^{11}
HH	1.27×10^7	1.28×10^{13}	4.98×10^6	6.18×10^{12}
KK	9.10×10^4 †	9.19×10^{10}	2.87×10^6	3.56×10^{12}
LL	7.95×10^4	8.03×10^{10}	6.12×10^5	7.59×10^{11}
MM	‡		2.89×10^6	3.58×10^{12}
PP	3.20×10^6	3.23×10^{12}	1.74×10^7	2.16×10^{13}
RR	1.78×10^5	1.80×10^{11}	1.54×10^6	1.91×10^{12}
SS	3.77×10^4	3.81×10^{10}	—	—
TT	1.00×10^3	1.01×10^9	5.95×10^5	7.38×10^{11}
UU	6.03×10^4	6.09×10^{10}	—	—
Raft 1-P-85	1.09×10^4	1.10×10^{10}	1.78×10^5	2.21×10^{11}
2-R-86	6.41×10^6	6.47×10^{12}	9.23×10^5	1.14×10^{12}
3-S-87	1.33×10^6	1.34×10^{12}	9.04×10^5	1.12×10^{12}
How K-82	5.22×10^3	5.27×10^9	5.26×10^4	6.52×10^{10}
George L-83	5.16×10^7	5.21×10^{13}	1.26×10^7 §	1.56×10^{13}
William M-84	8.74×10^3	8.83×10^9	—	—
Charlie M-84	—	—	9.70×10^6	1.20×10^{13}

TABLE B.14 CONTINUED

II. SHOTS ZUNI AND TEWA.

Because of fractionation in each of these events, the dip activity observed at 100 hours was first converted to doghouse activity at 100 hours (a constant relation for any sample as shown in Table B.15) in order to utilize the fission relations of Table B.13. Values of the latter relation for locations other than shown were estimated by proximity in location and/or time of arrival.

Collector Location	Shot Zuni					Shot Tewa				
	Dip Activity at 100 hr	Doghouse Activity / Dip Activity at 100 hr	Equivalent Doghouse Activity at 100 hr	Fission Doghouse counts/min at 100 hr	Total Fissions	Dip Activity at 100 hr	Doghouse Activity / Dip Activity at 100 hr	Equivalent Doghouse Activity at 100 hr	Fissions Doghouse counts/min at 100 hr	Total Fissions
	counts/min		counts/min	$\times 10^8$		counts/min		counts/min	$\times 10^8$	
Skiff AA	‡	5.568×10^{-3}			—	1.91×10^7 *	5.568×10^{-3}	1.09×10^5	1.46	1.59×10^{13}
BB	3.74×10^7 †		2.08×10^6	1.64	3.41×10^{13}	7.32×10^7		4.08×10^5	1.92	7.83×10^{13}
CC	4.28×10^6 †		2.38×10^4	1.75	4.17×10^{12}	7.59×10^6		4.23×10^4	1.92	8.12×10^{12}
DD	1.72×10^7		9.58×10^4	1.79	1.71×10^{13}	1.68×10^5		9.35×10^2	2.43	2.27×10^{11}
EE	3.38×10^6		1.88×10^4	1.65	3.10×10^{12}	2.58×10^4		1.44×10^2	2.43	3.50×10^{10}
FF	2.00×10^3 *		1.11×10^1	1.43	1.59×10^9	8.90×10^3		4.96×10^1	2.43	1.21×10^{10}
GG	2.02×10^7 *		1.12×10^5	1.91	2.14×10^{13}	9.64×10^7		5.37×10^5	1.92	1.03×10^{14}
HH	2.46×10^6 †		1.37×10^4	1.95	2.67×10^{12}	8.06×10^7		4.49×10^5	1.92	8.62×10^{13}
KK	2.24×10^6 *		1.25×10^4	1.91	2.39×10^{12}	8.80×10^4		4.90×10^2	2.43	1.19×10^{11}
LL	1.09×10^5		6.07×10^2	1.58	9.59×10^{10}	1.99×10^4		1.11×10^2	2.43	2.70×10^{10}
MM	8.82×10^5 †		4.91×10^3	1.77	8.69×10^{11}	1.89×10^6		1.05×10^6	1.46	1.54×10^{14}
PP	—		—	—	—	9.33×10^7		5.19×10^5	1.92	9.96×10^{13}
RR	3.84×10^5 †		2.14×10^3	1.97	4.22×10^{11}	8.50×10^6		4.73×10^3	2.43	1.15×10^{12}
SS	1.60×10^5 *		8.91×10^2	1.65	1.47×10^{11}	—		—	—	—
TT	3.71×10^5		2.07×10^3	1.40	2.90×10^{11}	6.58×10^4		3.66×10^2	2.43	8.89×10^{10}
UU	1.40×10^3 †		7.80×10^2	1.75	1.37×10^{11}	—		—	—	—
WW	—		—	—	—	2.96×10^6		1.65×10^6	1.92	3.17×10^{14}
XX	—		—	—	—	8.26×10^7		4.60×10^5	1.46	6.72×10^{13}
YY	—		—	—	—	6.35×10^7		3.54×10^5	1.46	5.17×10^{13}
Raft 1-P-85	5.58×10^7		3.11×10^5	2.67	8.30×10^{13}	1.68×10^7		9.35×10^4	2.43	2.27×10^{13}
2-R-86	1.21×10^8		6.74×10^5	2.67	1.80×10^{14}	1.35×10^7		7.52×10^5	2.43	1.83×10^{14}
3-S-87	7.67×10^7		4.27×10^5	2.67	1.14×10^{14}	2.39×10^8		1.33×10^6	1.92	2.55×10^{14}
How K-82	3.07×10^7		1.71×10^5	2.67	4.57×10^{13}	2.78×10^6		1.54×10^4	2.43	3.74×10^{12}
George L-83	8.17×10^7		4.55×10^5	2.67	1.21×10^{14}	1.84×10^8		1.02×10^6	2.43	2.48×10^{14}
William M-84	3.63×10^7		2.02×10^5	2.67	5.39×10^{13}	—		—	—	—
Charlie M-84	—		—	—	—	1.33×10^8		7.41×10^5	1.92	1.42×10^{14}

* Funnel and hexcell lost. † Hexcell lost. ‡ Skiff or collector lost. § Collector tilted slightly by blast.

TABLE B. 15 DIP PROBE AND DOGHOUSE-COUNTER CORRELATION WITH FISSION CONTENT

The listed dip-counter activities were observed on aliquots of OCC samples and are corrected to an equivalent dip count for the total recovered number of fissions (see Table B. 12).

Sample	Recovered Number of Fissions*	Time of Dip Count	Dip Activity Corrected to H+100 hr	Fissions / Dip counts/min at 100 hr	Fissions† / Doghouse counts/min at 100 hr	Doghouse Act. at 100 hr / Dip Act. at 100 hr
		H+hr	counts/min	$\times 10^{6}$	$\times 10^{6}$	$\times 10^{-3}$
YAG 40-B-6 ZU	1.27×10^{15}	1,559.4	12.5×10^{6}	1.02	1.703	5.88
YAG 39-C-21 FL	1.27×10^{13}	217.4	13.7×10^{6}	0.927	1.669	5.56
	1.27×10^{13}	241.6	13.4×10^{6}	0.947	1.669	5.68
	1.27×10^{13}	388.1	13.2×10^{6}	0.962	1.669	5.77
YFNB 13-E-54 FL	9.52×10^{14}	268.2	86.2×10^{7}	1.10	2.116	5.20
	9.52×10^{14}	335.4	91.4×10^{7}	1.04	2.116	4.92
	9.52×10^{14}	387.8	90.4×10^{7}	1.05	2.116	4.96
	9.52×10^{14}	722.7	82.0×10^{7}	1.16	2.116	5.48
YFNB 29-G-68 FL	3.47×10^{13}	263.8	37.5×10^{6}	0.925	1.733	5.34
	3.47×10^{13}	388.0	35.2×10^{6}	0.985	1.733	5.69
	3.47×10^{13}	723.2	33.1×10^{6}	1.05	1.733	6.06
YAG 39-C-21 NA	3.90×10^{13}	194.7	30.3×10^{6}	1.29	2.336	5.52
	3.90×10^{13}	239.4	30.4×10^{6}	1.28	2.336	5.48
YFNB 13-E-56 NA	1.30×10^{14}	194.8	11.1×10^{7}	1.17	2.013	5.81
	1.30×10^{14}	239.5	11.6×10^{7}	1.12	2.013	5.56
	1.30×10^{14}	364.4	10.2×10^{7}	1.27	2.013	6.31
YAG 39-C-21 TE	4.54×10^{15}	287.9	44.4×10^{6}	1.02	1.922	5.31
	4.54×10^{15}	340.3	44.4×10^{6}	1.02	1.922	5.31
	4.54×10^{15}	412.2	41.9×10^{6}	1.08	1.922	5.62
YFNB 13-E-54 TE	5.95×10^{14}	340.1	43.9×10^{7}	1.36	2.302	5.91
	5.95×10^{14}	412.0	40.5×10^{7}	1.47	2.302	6.39
Mean and σ						5.608 ± 6.69 pct‡

* From Table B. 12

† From Table B. 13

‡ The mean reported in Table B. 14 was originally calculated in error. Since the correction amounts to less than 1 pct it was not made.

TABLE B.16 ELEMENTAL ANALYSIS OF DEVICE ENVIRONMENT

The sea water analysis is after Sverdrup (Reference 64), except U which was determined from a Bikini lagoon water sample taken just prior to Tewa. The remaining analyses were made at NRDL for Project 2.6a, Operation Castle (Reference 63), except the Ca and Mg reef values which were estimated from Reference 65.

Element	Fraction by weight				Observed Operational Backgrounds (mg/2.6 ft^2)	
	Sea water	Surface Coral (Zu and Fl)	Reef and Lagoon Floor (Tewa)	Avg. Surface and Lagoon Floor (Na)	Sea Stations	How Island
Ca	0.00040	0.340	0.368	0.354	2.16 ± 0.92	4.15 ± 2.27
Na	0.01056	0.0033	0.0069	0.0051	2.49 ± 0.86	4.12 ± 0.97
K	0.00038	0.00001	0.0003	0.00016	0.42 ± 0.09	0.51 ± 0.11
Cl	0.01898	0.0023	0.0017	0.0020	1.31 ± 0.39	2.67 ± (?)
Mg	0.00127	0.0260	0.0110	0.0185	1.63 ± 0.33	2.50 ± 1.07
Fe	2×10^{-6}	4.2×10^{-5}	0.0002	0.000121	0.86 ± 0.14	0.65 ± 0.15
U	3×10^{-9}	*	*	*	†	†
Pb	4×10^{-9}	*	*	*	0.96 ± 0.05	0.96 ± 0.05
Cu	8×10^{-8}	1.6×10^{-6}	1.6×10^{-6}	1.6×10^{-6}	0.30 ± 0.09	0.26 ± 0.07

* Not available. † Not detectable.

Pages 222 thru 231 Deleted.

TABLE B.19 AIR-IONIZATION RATES OF INDUCED PRODUCTS FOR 10^4 FISSIONS/FT^3, PRODUCT/FISSION RATIO OF UNITY (SC)

Product half life is given directly below the nuclide symbol. Values are in r/hr and the number in parentheses indicates the number of zeros between the decimal point and the first significant figure.

Age		Na^{24}	Cr^{51}	Mn^{54}	Mn^{56}	Fe^{59}	Co^{57}	Co^{58}	Co^{60}	Cu^{64}	Sb^{122}
	hr	15h	27.2d	304d	2.58h	45.2d	270d	72d	5.27y	12.8h	2.75d
45.8 minutes	0.763	(8)250	(12)539	(11)118	(8)547	(10)119	(12)218	(11)598	(12)575	(9)174	(10)740
1.12 hours	1.12	(8)246	(12)539	(11)118	(8)496	(10)119	(12)218	(11)598	(12)575	(9)171	(10)737
1.64	1.64	(8)240	(12)539	(11)118	(8)432	(10)118	(12)218	(11)598	(12)575	(9)166	(10)735
2.40	2.40	(8)232	(12)538	(11)118	(8)352	(10)118	(12)218	(11)598	(12)575	(9)160	(10)727
3.52	3.52	(8)220	(12)538	(11)118	(8)261	(10)118	(12)218	(11)597	(12)575	(9)150	(10)719
5.16	5.16	(8)204	(12)537	(11)118	(8)167	(10)118	(12)218	(11)597	(12)575	(9)137	(10)707
7.56	7.56	(8)182	(12)535	(11)118	(9)878	(10)118	(12)218	(11)597	(12)575	(9)121	(10)689
11.1	11.1	(8)155	(12)533	(11)118	(9)341	(10)118	(12)218	(11)596	(12)575	(10)997	(10)666
16.2	16.2	(8)123	(12)531	(11)118	(10)865	(10)117	(12)218	(11)594	(12)575	(10)756	(10)630
23.8	23.8	(9)887	(12)526	(11)118	(10)112	(10)117	(12)218	(11)592	(12)575	(10)502	(10)581
1.45 days	34.8	(9)524	(12)520	(11)118	(12)583	(10)116	(12)217	(11)590	(12)575	(10)277	(10)517
2.13	51.1	(9)244	(12)511	(11)118	(14)751	(10)115	(12)217	(11)586	(12)575	(10)115	(10)438
3.12	74.9	(10)823	(12)498	(11)118	(16)126	(10)113	(12)217	(11)580	(12)575	(11)319	(10)340
4.57	109.7	(10)166	(12)480	(11)117		(10)111	(12)216	(11)572	(12)574	(12)488	(10)236
6.70	160.8	(11)156	(12)455	(11)117		(10)107	(12)215	(11)561	(12)574	(13)309	(10)138
9.82	235.7	(13)478	(12)420	(11)116		(10)102	(12)213	(11)545	(12)573	(15)554	(11)630
14.4	345.6	(15)321	(12)374	(11)115		(11)951	(12)210	(11)521	(12)572	(17)138	(11)198
21.1	506.4		(12)315	(11)113		(11)858	(12)207	(11)488	(12)571		(12)366
30.9	741.6		(12)246	(11)110		(11)738	(12)202	(11)444	(12)569		(13)310
45.3	1,087		(12)170	(11)107		(11)592	(12)194	(11)387	(12)566		(15)837
66.4	1,594		(13)994	(11)102		(11)428	(12)184	(11)315	(12)562		(17)399
97.3	2,335		(13)452	(12)949		(11)267	(12)170	(11)235	(12)556		
143	3,432		(13)141	(12)855		(11)132	(12)151	(11)151	(12)547		
208	4,992		(14)272	(12)738		(12)488	(12)128	(12)808	(12)534		
301	7,224		(15)252	(12)596		(12)117	(12)101	(12)330	(12)516		

TABLE B.19 CONTINUED

Age		Sb^{124}	Ta^{180}	Ta^{182}	Au^{198}	Pb^{203}	U^{237}	U^{239}	Np^{239}	Np^{240}
	hr	60d	8.15h	114d	2.7d	52h	6.75d	23.5m	56h	7.3m
45.8 minutes	0.763	(10)133	(10)703	(11)513	(10)711	(10)501	(10)126	(9)507	(10)258	(9)290
1.12 hours	1.12	(10)133	(10)684	(11)513	(10)709	(10)500	(10)125	(9)270	(10)300	(9)287
1.64	1.64	(10)133	(10)652	(11)513	(10)704	(10)496	(10)125	(9)107	(10)326	(9)281
2.40	2.40	(10)133	(10)614	(11)513	(10)699	(10)490	(10)125	(10)280	(10)338	(9)270
3.52	3.52	(10)133	(10)557	(11)513	(10)689	(10)484	(10)124	(11)386	(10)337	(9)256
5.16	5.16	(10)132	(10)484	(11)513	(10)677	(10)474	(10)123	(12)212	(10)332	(9)236
7.56	7.56	(10)132	(10)394	(11)513	(10)660	(10)459	(10)122	(14)301	(10)321	(9)210
11.1	11.1	(10)132	(10)292	(11)512	(10)636	(10)437	(10)120	(17)577	(10)308	(9)176
16.2	16.2	(10)132	(10)190	(11)511	(10)603	(10)408	(10)118		(10)289	(9)137
23.8	23.8	(10)131	(11)992	(11)510	(10)554	(10)370	(10)113		(10)263	(10)944
1.45 days	34.8	(10)131	(11)388	(11)509	(10)494	(10)319	(10)108		(10)230	(10)550
2.13	51.1	(10)130	(12)973	(11)507	(10)415	(10)256	(10)101		(10)188	(10)248
3.12	74.9	(10)128	(12)129	(11)504	(10)321	(10)186	(11)914		(10)140	(11)767
4.57	109.7	(10)126	(14)668	(11)499	(10)221	(10)118	(11)789		(11)909	(11)139
6.70	160.8	(10)123	(16)872	(11)493	(10)128	(11)595	(11)634		(11)482	(12)113
9.82	235.7	(10)119	(18)149	(11)484	(11)576	(11)219	(11)458		(11)191	(14)290
14.4	345.6	(10)112		(11)470	(11)178	(12)507	(11)287		(12)491	(16)126
21.1	506.4	(10)104		(11)452	(12)318	(13)594	(11)143		(13)670	
30.9	741.6	(11)929		(11)426	(13)258	(14)259	(12)529		(14)364	
45.3	1,087	(11)786		(11)390	(15)643	(16)256	(12)121		(16)509	
66.4	1,594	(11)616		(11)343	(17)277	(19)304	(13)137		(19)954	
97.3	2,335	(11)431		(11)284	(21)995		(15)578			
143	3,432	(11)254		(11)215			(17)520			
208	4,992	(11)120		(11)145			(20)742			
301	7,224	(12)410		(12)825						

TABLE B.21 GAMMA-RAY PROPERTIES OF CLOUD AND FALLOUT SAMPLES BASED ON GAMMA-RAY SPECTROMETRY (NRB)

Cloud samples are particulate collections in small pieces of filter paper. All fallout samples are aliquots of OCC sample solutions except those indicated as solid, which are aliquoted undissolved, by weight.

Sample Designation	Age	Number of Fissions	Average Energy $\bar{E}$	mr/hr at 3 ft, (SC), for N_f fissions/ft²			Total Photons per sec	Photons/sec 10^6 fission
				By Line E	By $\bar{E}$	Error Using $\bar{E}$		
	hr	N_f	kev			pct	$\times 10^6$	
Shot Cherokee								
Standard cloud sample								
1	53	8.82×10^{12}	294	20.64	21.15	2.47	11.62	1.317
2	74		299	17.18	17.66	2.79	9.65	1.094
3	98		310	11.94	12.15	1.76	6.53	0.740
4	166		337	7.88	8.36	6.09	4.04	0.458
5	191		379	6.36	6.87	8.02	2.91	0.330
6	215		391	5.82	6.24	7.22	2.59	0.294
7	242		417	5.00	5.40	8.00	2.10	0.238
8	262.5		446	4.44	4.81	8.33	1.75	0.198
9	335		490	3.46	3.81	10.12	1.26	0.143
10	405.5		509	2.85	3.10	8.77	0.99	0.112
11	597.5		626	1.82	1.98	8.79	0.52	0.059
Shot Zuni								
Standand cloud sample								
1	53	9.84×10^{12}	477	62.47	67.36	7.83	22.98	2.335
2	69		413	49.92	52.89	5.95	20.82	2.116
3	93		422	37.90	39.64	4.59	15.28	1.553
4	117		433	28.45	30.12	5.87	11.31	1.149
5	192		437	16.71	17.78	6.40	6.62	0.673
6	242		485	13.05	14.03	7.51	4.71	0.479
7	454		589	6.28	6.84	8.92	1.90	0.193
8	790		624	3.29	3.52	6.99	0.93	0.095
9	1,295		559	1.56	1.65	6.45	0.48	0.049
How F-61								
1	240	1.00×10^{13}	210	1.72	1.73	0.58	1.34	0.134
2	460		247	0.64	0.65	1.56	0.43	0.043
YAG 40-B-19								
2	266	3.71×10^{14}	419	181.18	193.33	6.71	74.98	0.202
3	362	(solid)	480	110.18	119.14	8.13	40.4	0.109
4	459		508	105.62	113.95	7.89	36.29	0.098
5	790		606	51.07	54.87	7.44	14.83	0.040
6	983		731	53.46	56.63	5.93	12.87	0.035
6'	987		706	49.24	51.89	5.38	12.21	0.033
7	1,298		710	38.09	40.91	7.40	9.58	0.026
8	1,728.5		706	28.41	30.05	5.77	7.07	0.019
9	2,568.5		711	18.85	19.60	3.98	4.60	0.012
10	2,810		731	14.50	16.02	10.48	3.65	0.010
How F-67								
1	359	7.29×10^{13}	318	10.66	11.38	6.75	5.82	0.080
2	460.5	(solid)	385	8.31	8.73	5.05	3.69	0.051
3	981		610	4.38	4.53	3.42	1.20	0.016
4	1,606		646	3.54	3.64	2.82	0.93	0.013
YAG 40-B-6								
1	383	5.08×10^{13}	444.76	12.92	13.79	6.73	5.05	0.10
2	458		457.16	9.43	10.07	6.79	3.58	0.070
3	982		656.58	4.49	4.76	6.01	1.2	0.024
4	1,605		695.12	3.47	3.60	3.75	0.86	0.017

pgs 235 thru 236 Deleted

TABLE B. 21 CONTINUED

Sample Designation	Age	Number of Fissions	Average Energy $\bar{E}$	mr/hr at 3 ft, (SC), for N_f fissions/ft^2			Total Photons per sec	Photons/sec / 10^6 fissions
				By Line E	By $\bar{E}$	Error Using $\bar{E}$		
	hr	N_f	kev			pct	$\times 10^6$	
Shot Flathead								
Standard cloud sample								
2	96.5	2.79×10^{13}	335.88	61.12	62.88	2.88	30.49	1.093
3	195	↓	402.04	27.94	29.18	4.44	11.82	0.424
4	262		489.13	18.94	20.36	7.50	6.44	0.231
5	334		535.96	16.31	17.73	8.39	5.39	0.193
6	435		573.61	11.06	12.01	8.59	3.43	0.123
7	718		661.49	6.08	6.56	7.89	1.64	0.059
8	1,031		708.63	3.16	3.42	8.23	0.80	0.029
9	1,558		678.61	2.08	2.21	6.25	0.54	0.019
YAG 39-C-36								
1	119.5	1.06×10^{13} *	306.28	14.77	15.20	2.91	8.08	0.762
2	598	(solid)	532.08	1.99	2.17	9.05	0.65	0.061
YFNB 13-E-56								
1	337	4.44×10^{12}	515.74	13.38	14.52	8.52	4.58	0.103
2	722	(solid)	659.93	5.96	6.38	7.05	1.60	0.036
3	1,032	↓	681.15	3.71	3.95	6.47	0.96	0.022
4	1,538		699.09	1.77	1.85	4.52	0.44	0.010
YFNB 13-E-54								
1	357	3.81×10^{13}	389.11	12.41	13.52	8.94	5.66	0.149
2	720	↓	549.26	5.08	5.51	8.46	1.64	0.043
3	1,034.5		672.88	3.55	3.73	5.07	0.92	0.024
4	1,538.5		662.90	1.94	2.00	3.09	0.50	0.013
Shot Navajo								
Standard cloud sample								
1	51.5	3.46×10^{12}	567.68	20.50	22.97	12.05	6.62	1.913
2	69	↓	483.11	13.32	14.65	9.98	4.94	1.428
3	141		396.37	5.00	5.31	6.70	2.18	0.630
4	191		482.27	4.84	5.18	7.02	1.75	0.506
5	315		604.29	2.13	2.32	8.92	0.63	0.182
6	645.5		585.68	0.72	0.78	8.33	0.22	0.064
YFNB 13-E-54								
1	197	2.40×10^{13}	496.15	9.34	9.96	6.63	3.27	0.136
3	311	(solid)	658.79	8.15	8.74	7.24	2.19	0.091
4	360	↓	710.86	8.36	8.92	6.70	2.09	0.087
5	551		818.31	5.69	6.01	5.62	1.24	0.052
YAG 39-C-36								
1	216	—	436.11	1.92	2.05	6.77	0.76	—
2	260	—	549.03	0.99	1.04	5.05	0.31	—
YFNB 13-E-66								
1	237.5	6.50×10^{12}	518.87	4.40	4.75	7.95	1.49	0.229
2	359	↓	676.86	2.98	3.21	7.72	0.78	0.120
3	551		688.41	1.58	1.70	7.59	0.41	0.063
YAG 39-C-21	309.5	3.90×10^{12}	604.65	1.96	2.10	7.14	0.57	0.146

TABLE B. 21 CONTINUED

Sample Designation	Age	Number of Fissions	Average Energy $\bar{E}$	mr/hr at 3 ft, (SC), for N_f fissions/ft^2			Total Photons per sec	Photons/sec / 10^6 fission
				By Line E	By $\bar{E}$	Error Using $\bar{E}$		
	hr	N_f	kev			pct	$\times 10^6$	
Shot Tewa								
Standard cloud sample								
1	71.5	4.71×10^{13}	401.33	127.1	131.64	3.57	53.42	1.134
2	93.5		378.45	94.25	97.60	3.55	42.00	0.892
3	117.0		377.50	75.64	79.29	4.83	34.21	0.726
4	165.0		373.02	62.27	65.71	5.52	28.69	0.609
5	240.5		460.73	44.21	47.38	7.17	16.75	0.356
6	333.5		489.33	24.88	27.01	8.56	8.99	0.191
7	429.0		548.48	18.47	20.16	9.15	6.00	0.127
8	578.5		629.64	12.70	13.83	8.90	3.62	0.077
9	765.5		664.50	10.40	11.18	7.50	2.78	0.059
10	1,269.0		646.80	4.94	5.21	5.47	1.33	0.028
11	1,511.0		656.33	4.13	4.33	4.84	1.09	0.023
YAG 39-C-36								
1	173.0	1.77×10^{13}	345.84	16.78	17.41	3.75	8.2	0.463
2	237.0	(solid)	355.39	12.27	12.81	4.40	5.87	0.332
3	312.0		397.60	7.99	8.42	5.38	3.45	0.195
4	407.0		416.92	5.69	6.04	6.15	2.36	0.133
5	576.0		571.65	3.95	4.22	6.84	1.21	0.068
YFNB 13-E-56								
1	238	3.40×10^{13}	270.06	11.84	12.24	3.38	7.38	0.217
2	335	(solid)	295.56	7.16	7.46	4.19	4.11	0.121
3	413		327.78	4.85	5.07	4.54	2.52	0.074
4	578		434.03	3.82	4.00	4.71	1.50	0.044
5	1,270		542.00	1.64	1.67	1.83	0.50	0.015
6	1,512		563.09	1.16	1.17	0.86	0.34	0.010
Y3-T-1C-D	243	—	360.31	1.01	1.06	4.95	0.48	—
YFNB 13-E-54								
1	263	2.38×10^{13}	306.39	6.87	7.21	4.95	3.83	0.161
2	316		330.48	4.61	4.85	5.21	2.39	0.100
3	408.5		373.45	3.49	3.71	6.30	1.62	0.068
4	624.0		484.14	1.76	1.90	7.95	0.64	0.027
YAG 39-C-21								
1	287	1.82×10^{14}	427.26	68.72	73.34	6.72	27.96	0.154
3	411		465.32	40.67	43.65	7.33	15.28	0.084
4	626		564.53	23.70	25.53	7.72	7.40	0.041
5	767		605.21	17.33	18.66	7.67	5.07	0.028
6	1,271		672.61	9.75	10.18	4.21	2.51	0.014
7	1,513		669.95	7.83	8.08	3.19	2.00	0.011

TABLE B.22 COMPUTED DOGHOUSE DECAY RATES OF FALLOUT AND CLOUD SAMPLES

Activities are computed in units of (counts/sec)/10^4 fissions for a point source in a covered OCC tray on the floor of the counter. The product/fission ratio for the induced product activities (IP) appears directly below the nuclide symbol. Induced activities are summed and added to the fission product activity (FP) for the total computed count rate. Numbers in parentheses denote the number of zeros between the decimal point and the first significant figure, e.g., (3)291 = 0.000291.

Age		Na^{24}	Cr^{51}	Mn^{54}	Mn^{56}	Fe^{59}	Co^{57}	Co^{58}	Co^{60}	Cu^{64}	Sb^{122}	Sb^{124}
	hr	0.0109	0.00173	0.011	0.011 *	0.00041	0.0031	0.0036	0.00264	0.0090	0.0252 †	0.0084
Shot Zuni, Average Lagoon-Area Composition:												
45.8 min	0.763	(6)119	(10)419	(9)175	(6)544	(10)401	(10)921	(9)319	(10)111	(7)356	(7)335	(8)123
1.12 hrs	1.12	(6)117	(10)419	(9)175	(6)494	(10)401	(10)921	(9)319	(10)111	(7)347	(7)335	(8)123
1.64 hrs	1.64	(6)114	(10)419	(9)175	(6)430	(10)401	(10)920	(9)319	(10)111	(7)338	(7)333	(8)123
2.40 hrs	2.40	(6)110	(10)419	(9)175	(6)351	(10)400	(10)920	(9)319	(10)111	(7)326	(7)330	(8)123
3.52 hrs	3.52	(6)105	(10)419	(9)175	(6)260	(10)400	(10)920	(9)318	(10)111	(7)306	(7)328	(8)123
5.16 hrs	5.16	(7)970	(10)417	(9)175	(6)166	(10)400	(10)920	(9)318	(10)111	(7)280	(7)320	(8)123
7.56 hrs	7.56	(7)868	(10)415	(9)175	(7)874	(10)399	(10)920	(9)318	(10)111	(7)246	(7)312	(8)122
11.1 hrs	11.1	(7)738	(10)415	(9)175	(7)340	(10)398	(10)919	(9)318	(10)111	(7)203	(7)302	(8)122
16.2 hrs	16.2	(7)583	(10)412	(9)175	(8)861	(10)397	(10)919	(9)317	(10)111	(7)154	(7)285	(8)122
23.8 hrs	23.8	(7)409	(10)408	(9)175	(8)112	(10)395	(10)919	(9)316	(10)111	(7)103	(7)265	(8)121
1.45 days	34.8	(7)249	(10)405	(9)175	(10)581	(10)392	(10)917	(9)314	(10)111	(8)564	(7)235	(8)121
2.13 days	51.1	(7)117	(10)398	(9)175	(12)748	(10)388	(10)916	(9)312	(10)111	(8)234	(7)199	(8)120
3.12 days	74.9	(8)391	(10)388	(9)174		(10)382	(10)913	(9)309	(10)111	(9)651	(7)154	(8)118
4.57 days	109.7	(9)787	(10)374	(9)174		(10)374	(10)910	(9)305	(10)111	(10)936	(7)107	(8)116
6.70 days	160.8	(10)743	(10)353	(9)173		(10)362	(10)905	(9)299	(10)110	(11)629	(8)625	(8)113
9.82 days	235.7	(11)228	(10)327	(9)172		(10)345	(10)898	(9)290	(10)110	(12)112	(8)285	(8)109
14.4 days	345.6		(10)291	(9)169		(10)321	(10)887	(9)278	(10)110		(9)897	(8)104
21.1 days	506.4		(10)246	(9)167		(10)290	(10)872	(9)260	(10)110		(9)166	(9)958
30.9 days	741.6		(10)190	(9)164		(10)250	(10)851	(9)237	(10)109		(10)141	(9)857
45.3 days	1,087		(10)132	(9)158		(10)200	(10)820	(9)206	(10)109		(12)381	(9)727
66.4 days	1,594		(11)772	(9)151		(10)145	(10)777	(9)168	(10)108			(9)569
97.3 days	2,335		(11)351	(9)141		(11)902	(10)717	(9)125	(10)107			(9)398
143 days	3,432		(11)110	(9)126		(11)447	(10)638	(10)803	(10)105			(9)235
208 days	4,992		(12)211	(9)109		(11)165	(10)540	(10)432	(10)102			(9)111
301 days	7,224		(13)195	(10)882		(12)398	(10)425	(10)176	(11)990			(10)379

TABLE B.22 CONTINUED

Age	hr	Ta^{180} 0.0691‡	Ta^{182} 0.0326	Pb^{203} 0.050	Sum of FP
Shot Zuni, Average Lagoon-Area Composition					
45.8 min	0.763	(6)871	(8)355	(6)170	(4)6034
1.12 hrs	1.12	(6)850	(8)355	(6)170	(4)3946
1.64 hrs	1.64	(6)808	(8)355	(6)168	(4)2429
2.40 hrs	2.40	(6)760	(8)355	(6)167	(4)1469
3.52 hrs	3.52	(6)690	(8)355	(6)164	(5)8828
5.16 hrs	5.16	(6)599	(8)355	(6)161	(5)5243
7.56 hrs	7.56	(6)489	(8)355	(6)156	(5)3248
11.1 hrs	11.1	(6)362	(8)355	(6)148	(5)2210
16.2 hrs	16.2	(6)235	(8)355	(6)139	(5)1519
23.8 hrs	23.8	(6)123	(8)352	(6)126	(6)9903
1.45 days	34.8	(7)481	(8)352	(6)108	(6)5959
2.13 days	51.1	(7)121	(8)352	(7)870	(6)3336
3.12 days	74.9	(8)160	(8)349	(7)635	(6)1879
4.57 days	109.7	(10)829	(8)346	(7)400	(6)1133
6.70 days	160.8	(11)108	(8)342	(7)202	(7)6834
9.82 days	235.7		(8)336	(8)745	(7)4159
14.4 days	345.6		(8)326	(8)172	(7)2598
21.1 days	506.4		(8)313	(9)202	(7)1749
30.9 days	741.6		(8)295	(11)880	(7)1249
45.3 days	1,087		(8)270	(13)850	(8)9022
66.4 days	1,594		(8)238		(8)6424
97.3 days	2,335		(8)197		(8)4413
143 days	3,432		(8)149		(8)2726
208 days	4,992		(8)100		(8)1401
301 days	7,224		(9)570		(9)5868

TABLE B. 22 CONTINUED

Age		Na^{24}	Cr^{51}	Mn^{54}	Mn^{56}	Fe^{59}	Co^{57}	Co^{58}	Co^{60}	Cu^{64}	Sb^{122}	Sb^{124}
	hr	0. 0109	0. 00173	0. 011	0. 011*	0. 00041	0. 0031	0. 0036	0. 00264	0. 0090	0. 219	0. 073
Shot Zuni, Cloud Composition:												
45. 8 min	0. 763	(6)119	(10)419	(9)175	(6)544	(10)401	(10)921	(9)319	(10)111	(7)356	(6)291	(7)107
1. 12 hrs	1. 12	(6)117	(10)419	(9)175	(6)494	(10)401	(10)921	(9)319	(10)111	(7)347	(6)291	(7)107
1. 64 hrs	1. 64	(6)114	(10)419	(9)175	(6)430	(10)401	(10)920	(9)319	(10)111	(7)338	(6)289	(7)107
2. 40 hrs	2. 40	(6)110	(10)419	(9)175	(6)351	(10)400	(10)920	(9)319	(10)111	(7)326	(6)287	(7)107
3. 52 hrs	3. 52	(6)105	(10)419	(9)175	(6)260	(10)400	(10)920	(9)318	(10)111	(7)306	(6)285	(7)107
5. 16 hrs	5. 16	(7)970	(10)417	(9)175	(6)166	(10)400	(10)920	(9)318	(10)111	(7)280	(6)278	(7)107
7. 56 hrs	7. 56	(7)868	(10)415	(9)175	(7)874	(10)399	(10)920	(9)318	(10)111	(7)246	(6)272	(7)106
11. 1 hrs	11. 1	(7)738	(10)415	(9)175	(7)340	(10)398	(10)919	(9)318	(10)111	(7)203	(6)263	(7)106
16. 2 hrs	16. 2	(7)583	(10)412	(9)175	(8)861	(10)397	(10)919	(9)317	(10)111	(7)154	(6)247	(7)106
23. 8 hrs	23. 8	(7)409	(10)408	(9)175	(8)112	(10)395	(10)919	(9)316	(10)111	(7)103	(6)230	(7)105
1. 45 days	34. 8	(7)249	(10)405	(9)175	(10)581	(10)392	(10)917	(9)314	(10)111	(8)564	(6)204	(7)105
2. 13 days	51. 1	(7)117	(10)398	(9)175	(12)748	(10)388	(10)916	(9)312	(10)111	(8)234	(6)173	(7)104
3. 12 days	74. 9	(8)391	(10)388	(9)174		(10)382	(10)913	(9)309	(10)111	(9)651	(6)134	(7)103
4. 57 days	109. 7	(9)787	(10)374	(9)174		(10)374	(10)910	(9)305	(10)111	(10)936	(7)931	(7)101
6. 70 days	160. 8	(10)743	(10)353	(9)173		(10)362	(10)905	(9)299	(10)110	(11)629	(7)543	(8)985
9. 82 days	235. 7	(11)228	(10)327	(9)172		(10)345	(10)898	(9)290	(10)110	(12)112	(7)247	(8)949
14. 4 days	345. 6		(10)291	(9)169		(10)321	(10)887	(9)278	(10)110		(8)780	(8)905
21. 1 days	506. 4		(10)246	(9)167		(10)290	(10)872	(9)260	(10)110		(8)144	(8)832
30. 9 days	741. 6		(10)190	(9)164		(10)250	(10)851	(9)237	(10)109		(9)122	(8)745
45. 3 days	1, 087		(10)132	(9)158		(10)200	(10)820	(9)206	(10)109		(11)331	(8)631
66. 4 days	1, 594		(11)772	(9)151		(10)145	(10)777	(9)168	(10)108		(13)162	(8)494
97. 3 days	2, 335		(11)351	(9)141		(11)902	(10)717	(9)125	(10)107			(8)346
143 days	3, 432		(11)110	(9)126		(11)447	(10)638	(10)803	(10)105			(8)204
208 days	4, 992		(12)211	(9)109		(11)165	(10)540	(10)432	(10)102			(9)964
301 days	7, 224		(13)195	(10)882		(12)396	(10)425	(10)176	(11)990			(9)329

TABLE B.22 CONTINUED

Age		Ta^{180}	Ta^{182}	Pb^{203}	Sum of FP
hr		0.0411	0.0194	0.050	
Shot Zuni, Cloud Composition:					
45.8	min	0.763	(6)518	(8)211	(6)170	(3)1658
1.12	hrs	1.12	(6)506	(8)211	(6)170	(3)1068
1.64	hrs	1.64	(6)481	(8)211	(6)168	(4)6723
2.40	hrs	2.40	(6)452	(8)211	(6)167	(4)4223
3.52	hrs	3.52	(6)411	(8)211	(6)164	(4)2706
5.16	hrs	5.16	(6)356	(8)211	(6)161	(4)1788
7.56	hrs	7.56	(6)291	(8)211	(6)156	(4)1221
11.1	hrs	11.1	(6)215	(8)211	(6)148	(5)8454
16.2	hrs	16.2	(6)140	(8)211	(6)139	(5)5677
23.8	hrs	23.8	(7)732	(8)210	(6)126	(5)3650
1.45	days	34.8	(7)286	(8)210	(6)108	(5)2302
2.13	days	51.1	(8)719	(8)210	(7)870	(5)1428
3.12	days	74.9	(9)949	(8)208	(7)635	(6)8938
4.57	days	109.7	(10)493	(8)206	(7)400	(6)5891
6.70	days	160.8	(12)641	(8)204	(7)202	(6)3971
9.82	days	235.7		(8)200	(8)745	(6)2667
14.4	days	345.6		(8)194	(8)172	(6)1728
21.1	days	506.4		(8)186	(9)202	(6)1073
30.9	days	741.6		(8)175	(11)880	(7)6306
45.3	days	1,087		(8)161	(13)850	(7)3421
66.4	days	1,594		(8)141		(7)1734
97.3	days	2,335		(8)117		(8)9067
143	days	3,432		(9)889		(8)1954
208	days	4,992		(9)596		(8)2502
301	days	7,224		(9)340		(8)1114

TABLE B.22 CONTINUED

Age		Na^{24}	Cr^{51}	Nm^{54}	Nm^{56}	Fe^{59}	Co^{57}	Co^{58}	Co^{60}	Cu^{64}	Ta^{180}
	hr	0.0314	0.0120	0.10	0.094	0.0033	0.00224	0.00193	0.0087	0.0278	0.038 ¶
Shot Navajo, Average Fallout Composition:											
45.8	min	0.763	(6)342	(9)290	(8)159	(5)465	(9)322	(10)665	(9)171	(10)364	(6)110	(6)479
1.12	hrs	1.12	(6)336	(9)290	(8)159	(5)422	(9)322	(10)665	(9)171	(10)364	(6)107	(6)467
1.64	hrs	1.64	(6)330	(9)290	(8)159	(5)368	(9)322	(10)665	(9)171	(10)364	(6)104	(6)445
2.40	hrs	2.40	(6)317	(9)290	(8)159	(5)300	(9)322	(10)665	(9)171	(10)364	(6)101	(6)418
3.52	hrs	3.52	(6)301	(9)290	(8)159	(5)222	(9)322	(10)665	(9)171	(10)364	(7)945	(6)380
5.16	hrs	5.16	(6)279	(9)289	(8)159	(5)142	(9)322	(10)665	(9)171	(10)364	(7)865	(6)329
7.56	hrs	7.56	(6)250	(9)288	(8)159	(6)747	(9)321	(10)665	(9)170	(10)364	(7)759	(6)269
11.1	hrs	11.1	(6)213	(9)288	(8)159	(6)290	(9)320	(10)664	(9)170	(10)364	(7)628	(6)199
16.2	hrs	16.2	(6)168	(9)286	(8)159	(7)736	(9)319	(10)664	(9)170	(10)364	(7)475	(6)129
23.8	hrs	23.8	(6)118	(9)283	(8)159	(8)959	(9)318	(10)664	(9)169	(10)364	(7)317	(7)676
1.45	days	34.8	(7)716	(9)281	(8)159	(9)496	(9)316	(10)663	(9)168	(10)364	(7)174	(7)264
2.13	days	51.1	(7)336	(9)276	(8)159	(11)639	(9)313	(10)662	(9)167	(10)364	(8)723	(8)665
3.12	days	74.9	(7)113	(9)269	(8)158		(9)308	(10)660	(9)166	(10)364	(8)201	(9)878
4.57	days	109.7	(8)227	(9)259	(8)158		(9)301	(10)658	(9)163	(10)364	(9)289	(10)456
6.70	days	160.8	(9)214	(9)245	(8)157		(9)291	(10)654	(9)160	(10)363	(10)194	(12)593
9.82	days	235.7	(11)656	(9)227	(8)156		(9)278	(10)649	(9)156	(10)363	(12)348	
14.4	days	345.6		(9)202	(8)154		(9)259	(10)641	(9)149	(10)362		
21.1	days	506.4		(9)170	(8)152		(9)233	(10)630	(9)140	(10)361		
30.9	days	741.6		(9)132	(8)149		(9)201	(10)615	(9)127	(10)360		
45.3	days	1,087		(10)918	(8)144		(9)161	(10)592	(9)111	(10)358		
66.4	days	1,594		(10)535	(8)137		(9)116	(10)561	(10)901	(10)355		
97.3	days	2,335		(10)244	(8)128		(10)726	(10)518	(10)670	(10)351		
143	days	3,432		(11)760	(8)115		(10)360	(10)461	(10)430	(10)345		
208	days	4,992		(11)146	(9)992		(10)133	(10)390	(10)232	(10)338		
301	days	7,224		(12)136	(9)802		(11)319	(10)307	(11)942	(10)326		

TABLE B.22 CONTINUED

Age		Ta^{182}	Pb^{203}	Sum of FP
	hr	0.038	0.0993	
Shot Navajo, Average Fallout Composition:				
45.8	min	0.763	(8)414	(6)644	(3)1171
1.12	hrs	1.12	(8)414	(6)642	(4)7727
1.64	hrs	1.64	(8)414	(6)636	(4)4870
2.40	hrs	2.40	(8)414	(6)631	(4)3015
3.52	hrs	3.52	(8)414	(6)621	(4)1868
5.16	hrs	5.16	(8)414	(6)608	(4)1175
7.56	hrs	7.56	(8)414	(6)598	(5)7600
11.1	hrs	11.1	(8)414	(6)560	(5)5065
16.2	hrs	16.2	(8)414	(6)524	(5)3337
23.8	hrs	23.8	(8)410	(6)475	(5)2124
1.45	days	34.8	(8)410	(6)408	(5)1326
2.13	days	51.1	(8)410	(6)329	(6)8054
3.12	days	74.9	(8)407	(6)239	(6)4914
4.57	days	109.7	(8)403	(6)151	(6)3154
6.70	days	160.8	(8)399	(7)762	(6)2061
9.82	days	235.7	(8)391	(7)281	(6)1353
14.4	days	345.6	(8)380	(8)652	(7)8691
21.1	days	506.4	(8)365	(9)762	(7)5473
30.9	days	741.6	(8)344	(10)332	(7)3355
45.3	days	1,087	(8)315		(7)1968
66.4	days	1,594	(8)277		(7)1126
97.3	days	2,335	(8)229		(8)6652
143	days	3,432	(8)174		(8)3877
208	days	4,992	(8)117		(8)1989
301	days	7,224	(9)665		(9)8710

TABLE B. 22 CONTINUED

Age		Na^{24}	Cu^{64}	Co^{57}	Co^{58}	Sum of F?
	hr	0. 00145	0. 00217	0. 0036	0. 0053	
Shot Flathead, Average Fallout Composition:						
45. 8 min	0. 763	(7)158	(8)857	(9)107	(9)470	(3)1171
1. 12 hrs	1. 12	(7)155	(8)838	(9)107	(9)470	(4)7727
1. 64 hrs	1. 64	(7)152	(8)814	(9)107	(9)469	(4)4870
2. 40 hrs	2. 40	(7)146	(8)786	(9)107	(9)469	(4)3015
3. 52 hrs	3. 52	(7)139	(8)738	(9)107	(9)469	(4)1868
5. 16 hrs	5. 16	(7)129	(8)675	(9)107	(9)469	(4)1175
7. 56 hrs	7. 56	(7)115	(8)592	(9)107	(9)468	(5)7600
11. 1 hrs	11. 1	(8)982	(8)490	(9)107	(9)467	(5)5065
16. 2 hrs	16. 2	(8)776	(8)371	(9)107	(9)466	(5)3337
23. 8 hrs	23. 8	(8)544	(8)247	(9)107	(9)465	(5)2124
1. 45 days	34. 8	(8)331	(8)136	(9)107	(9)463	(5)1326
2. 13 days	51. 1	(8)155	(9)564	(9)106	(9)460	(6)8054
3. 12 days	74. 9	(9)521	(9)157	(9)106	(9)455	(6)4914
4. 57 days	109. 7	(9)105	(10)226	(9)106	(9)449	(6)3154
6. 70 days	160. 8	(11)989	(11)152	(9)105	(9)440	(6)2061
9. 82 days	235. 7	(12)303	(13)271	(9)104	(9)427	(6)1353
14. 4 days	345. 6			(9)103	(9)409	(7)8691
21. 1 days	506. 4			(9)101	(9)383	(7)5473
30. 9 days	741. 6			(10)988	(9)349	(7)3355
45. 3 days	1, 087			(10)952	(9)304	(7)1968
66. 4 days	1, 594			(10)902	(9)248	(7)1126
97. 3 days	2, 335			(10)833	(9)184	(8)6652
143 days	3, 432			(10)741	(9)118	(8)3877
208 days	4, 992			(10)627	(10)636	(8)1989
301 days	7, 224			(10)494	(10)259	(9)8710

TABLE B.22 CONTINUED

Age		Na^{24}	Cr^{51}	Mn^{54}	Fe^{59}	Co^{57}	Co^{58}	Co^{60}	Cu^{64}	Ta^{182}
	hr	(2)284	(3)297	(3)53	(3)167	(3)182	(3)289	(3)81	(2)228	(2)6
Shot Tewa, Average Lagoon-Area Composition:										
45.8 min	0.763	(7)310	(11)719	(11)843	(10)163	(11)541	(10)256	(11)339	(8)901	(9)654
1.12 hrs	1.12	(7)304	(11)719	(11)843	(10)163	(11)541	(10)256	(11)339	(8)880	(9)654
1.64 hrs	1.64	(7)298	(11)719	(11)843	(10)163	(11)540	(10)256	(11)339	(8)855	(9)654
2.40 hrs	2.40	(7)287	(11)719	(11)843	(10)163	(11)540	(10)256	(11)339	(8)825	(9)654
3.52 hrs	3.52	(7)273	(11)719	(11)843	(10)163	(11)540	(10)255	(11)339	(8)775	(9)654
5.16 hrs	5.16	(7)253	(11)716	(11)843	(10)163	(11)540	(10)255	(11)339	(8)709	(9)654
7.56 hrs	7.56	(7)226	(11)713	(11)843	(10)162	(11)540	(10)255	(11)339	(8)622	(9)654
11.1 hrs	11.1	(7)192	(11)713	(11)843	(10)162	(11)540	(10)255	(11)339	(8)515	(9)654
16.2 hrs	16.2	(7)152	(11)707	(11)843	(10)162	(11)540	(10)254	(11)339	(8)390	(9)654
23.8 hrs	23.8	(7)106	(11)701	(11)843	(10)161	(11)539	(10)253	(11)339	(8)260	(9)648
1.45 days	34.8	(8)648	(11)695	(11)843	(10)160	(11)539	(10)252	(11)339	(8)143	(9)648
2.13 days	51.1	(8)304	(11)683	(11)843	(10)158	(11)538	(10)251	(11)339	(9)593	(9)648
3.12 days	74.9	(8)102	(11)665	(11)837	(10)156	(11)536	(10)248	(11)339	(9)165	(9)642
4.57 days	109.7	(9)205	(11)642	(11)837	(10)152	(11)534	(10)245	(11)339	(10)237	(9)636
6.70 days	160.8	(10)194	(11)606	(11)832	(10)147	(11)531	(10)240	(11)338	(11)159	(9)630
9.82 days	235.7	(12)594	(11)561	(11)827	(10)140	(11)527	(10)233	(11)338	(13)285	(9)618
14.4 days	345.6		(11)499	(11)816	(10)131	(11)521	(10)223	(11)337		(9)600
21.1 days	506.4		(11)422	(11)806	(10)118	(11)512	(10)209	(11)336		(9)576
30.9 days	741.6		(11)327	(11)790	(10)102	(11)499	(10)190	(11)335		(9)542
45.3 days	1,087		(11)227	(11)763	(11)815	(11)481	(10)166	(11)333		(9)497
66.4 days	1,594		(11)132	(11)726	(11)590	(11)456	(10)135	(11)330		(9)437
97.3 days	2,335		(12)603	(11)678	(11)367	(11)421	(10)100	(11)327		(9)362
143 days	3,432		(12)188	(11)610	(11)182	(11)374	(11)644	(11)322		(9)275
208 days	4,992		(13)362	(11)526	(12)673	(11)317	(11)347	(11)314		(9)184
301 days	7,224		(14)336	(11)425	(12)161	(11)250	(11)141	(11)304		(9)105

TABLE B.22 CONTINUED

Age		hr	Pb^{203} (4)178	Sum of FP
Shot Tewa, Average Lagoon-Area Composition:				
45.8	min	0.763	(10)607	(4)6035
1.12	hrs	1.12	(10)605	(4)3947
1.64	hrs	1.64	(10)600	(4)2430
2.40	hrs	2.40	(10)594	(4)1470
3.52	hrs	3.52	(10)586	(5)8831
5.16	hrs	5.16	(10)573	(5)5246
7.56	hrs	7.56	(10)555	(5)3252
11.1	hrs	11.1	(10)529	(5)2214
16.2	hrs	16.2	(10)495	(5)1524
23.8	hrs	23.8	(10)449	(6)9968
1.45	days	34.8	(10)386	(6)6037
2.13	days	51.1	(10)310	(6)3427
3.12	days	74.9	(10)226	(6)1983
4.57	days	109.7	(10)142	(6)1243
6.70	days	160.8	(11)719	(7)7919
9.82	days	235.7	(11)265	(7)5126
14.4	days	345.6	(12)614	(7)3366
21.1	days	506.4	(13)719	(7)2287
30.9	days	741.6	(14)313	(7)1566
45.3	days	1,087		(7)1048
66.4	days	1,594		(8)6888
97.3	days	2,335		(8)4499
143	days	3,432		(8)2734
208	days	4,992		(8)1401
301	days	7,224		(9)5868

TABLE B.22 CONTINUED

Age	hr	Na^{24} (2)284	Cr^{51} (3)297	Mn^{54} (3)53	Fe^{59} (3)167	Co^{57} (3)182	Co^{58} (3)289	Co^{60} (3)81	Cu^{64} (2)228	Ta^{182} 0.01
Shot Tewa, Average Cloud and Outer Fallout Area Composition:										
45.8 min	0.763	(7)310	(11)719	(11)843	(10)163	(11)541	(10)256	(11)339	(8)901	(8)109
1.12 hrs	1.12	(7)304	(11)719	(11)843	(10)163	(11)541	(10)256	(11)339	(8)880	(8)109
1.64 hrs	1.64	(7)298	(11)719	(11)843	(10)163	(11)540	(10)256	(11)339	(8)855	(8)109
2.40 hrs	2.40	(7)287	(11)719	(11)843	(10)163	(11)540	(10)256	(11)339	(8)825	(8)109
3.52 hrs	3.52	(7)273	(11)719	(11)843	(10)163	(11)540	(10)255	(11)339	(8)775	(8)109
5.16 hrs	5.16	(7)253	(11)716	(11)843	(10)163	(11)540	(10)255	(11)339	(8)709	(8)109
7.56 hrs	7.56	(7)226	(11)713	(11)843	(10)162	(11)540	(10)255	(11)339	(8)622	(8)109
11.1 hrs	11.1	(7)192	(11)713	(11)843	(10)162	(11)540	(10)255	(11)339	(8)515	(8)109
16.2 hrs	16.2	(7)152	(11)707	(11)843	(10)162	(11)540	(10)254	(11)339	(8)390	(8)109
23.8 hrs	23.8	(7)106	(11)701	(11)843	(10)161	(11)539	(10)253	(11)339	(8)260	(8)108
1.45 hrs	34.8	(8)648	(11)695	(11)843	(10)160	(11)539	(10)252	(11)339	(8)143	(8)108
2.13 days	51.1	(8)304	(11)683	(11)843	(10)158	(11)538	(10)251	(11)339	(9)593	(8)108
3.12 days	74.9	(8)102	(11)665	(11)837	(10)156	(11)536	(10)248	(11)339	(9)165	(8)107
4.57 days	109.7	(9)205	(11)642	(11)837	(10)152	(11)534	(10)245	(11)339	(10)237	(8)106
6.70 days	160.8	(10)194	(11)606	(11)832	(10)147	(11)531	(10)240	(11)338	(11)159	(8)105
9.82 days	235.7	(12)594	(11)561	(11)827	(10)140	(11)527	(10)233	(11)338	(13)285	(8)103
14.4 days	345.6		(11)499	(11)816	(10)131	(11)521	(10)223	(11)337		(8)100
21.1 days	506.4		(11)422	(11)806	(10)118	(11)512	(10)209	(11)336		(9)960
30.9 days	741.6		(11)327	(11)790	(10)102	(11)499	(10)190	(11)335		(9)904
45.3 days	1,087		(11)227	(11)763	(11)815	(11)481	(10)166	(11)333		(9)828
66.4 days	1,594		(11)132	(11)726	(11)590	(11)456	(10)135	(11)330		(9)729
97.3 days	2,335		(12)603	(11)678	(11)367	(11)421	(10)100	(11)327		(9)603
143 days	3,432		(12)188	(11)610	(11)182	(11)374	(11)644	(11)322		(9)458
208 days	4,992		(13)362	(11)526	(12)673	(11)317	(11)347	(11)314		(9)307
301 days	7,224		(14)336	(11)425	(12)161	(11)250	(11)141	(11)304		(9)175

TABLE B.22 CONTINUED

Age		Pb^{203}	Sum of FP
	hr	(4)178	
Shot Tewa, Average Cloud and Outer Fallout Area Composition:			
45.8	min	0.763	(10)607	(3)1171
1.12	hrs	1.12	(10)605	(4)7727
1.64	hrs	1.64	(10)600	(4)4870
2.40	hrs	2.40	(10)594	(4)3015
3.52	hrs	3.52	(10)586	(4)1868
5.16	hrs	5.16	(10)573	(4)1175
7.56	hrs	7.56	(10)555	(5)7600
11.1	hrs	11.1	(10)529	(5)5065
16.2	hrs	16.2	(10)495	(5)3337
23.8	hrs	23.8	(10)449	(5)2124
1.45	days	34.8	(10)386	(6)1326
2.13	days	51.1	(10)310	(6)8054
3.12	days	74.9	(10)226	(6)4914
4.57	days	109.7	(10)142	(6)3154
6.70	days	160.8	(11)719	(6)2061
9.82	days	235.7	(11)265	(6)1353
14.4	days	345.6	(12)614	(7)8691
21.1	days	506.4	(13)719	(7)5473
30.9	days	741.6	(14)313	(7)3355
45.3	days	1,087		(7)1968
66.4	days	1,594		(7)1126
97.3	days	2,335		(8)6652
143	days	3,432		(8)3877
208	days	4,992		(8)1989
301	days	7,224		(9)8710

* Assumed same as Mn^{54} from ratio observed at Navajo.

† Based on ratio Sb^{122}/Sb^{124} for cloud sample.

‡ Based on ratio Ta^{180}/Ta^{182} for cloud sample.

§ Based on ratios U^{240}/U^{239} and U^{240}/U^{237} for cloud sample.

¶ Assumed same as Ta^{182}.

TABLE B.23 OBSERVED DOGHOUSE DECAY RATES OF FALLOUT AND CLOUD SAMPLES

Fallout samples listed are total undisturbed OCC trays, counted with aluminum covers in place on the floor of the counter, ~36 inches from a 1 inch NaI(Tl) crystal. The standard cloud samples are essentially point sources of filter paper in lusteroid tubes, placed in a clean OCC tray, and similarly covered and counted. The extended sources, or fallout samples, have been corrected to a point source equivalent by increasing the observed counting rate by 7 percent (Reference 66). Their fission contents appear under Total Fissions in Table B.12.

Counting Time	Observed Activity	
H + hr	counts/min	counts/sec / 10^4 fissions
	YAG 39-C-23 ZU	
192.2	14,930	7.93×10^{-7}
383.1	4,647	2.46×10^{-7}
598.3	2,073	1.13×10^{-7}
771.5	1,416	7.51×10^{-8}
1,538	509	2.71×10^{-8}
	YFNB 13-E-55 ZU	
97.6	3,518,106	6.69×10^{-7}
191	1,415,754	2.69×10^{-7}
383	411,888	7.84×10^{-8}
771	119,308	2.27×10^{-8}
1,538	48,315	9.19×10^{-9}
1,970	39,819	7.58×10^{-9}
2,403	33,252	6.33×10^{-9}
	YFNB 13-E-58 ZU	
70.3	2,544,603	8.99×10^{-7}
95.7	1,909,529	6.74×10^{-7}
191	769,170	2.72×10^{-7}
383	223,190	7.88×10^{-8}
771	63,691	2.25×10^{-8}
1,539	26,463	9.34×10^{-9}
	How F-B-5 ZU	
76.8	3,577,190	9.68×10^{-7}
95.6	2,865,850	7.76×10^{-7}
190.9	1,232,290	3.34×10^{-7}
383.1	322,064	8.72×10^{-8}
771	96,753	2.62×10^{-8}
1,539	44,244	1.20×10^{-8}
1,971	36,563	9.89×10^{-9}
2,422	31,178	8.44×10^{-9}
	YAG 40-B-17 FL	
166.3	19,453	5.67×10^{-7}
383.1	5,138	1.50×10^{-7}
743.6	1,620	4.72×10^{-8}
1,534.7	495	1.44×10^{-8}
	YAG 39-C-22 FL	
70.4	42,589	1.45×10^{-6}
167.6	16,251	5.53×10^{-7}
384.3	4,150	1.41×10^{-7}
742.8	1,220	4.15×10^{-8}
1,534	390	1.33×10^{-8}

Counting Time	Observed Activity	
H + hr	counts/min	counts/sec / 10^4 fissions
	How F-B-12 ZU	
76.9	2,945,620	9.97×10^{-7}
98.3	2,242,750	7.59×10^{-7}
190.8	930,350	3.15×10^{-7}
382.1	266,730	9.03×10^{-8}
771.4	78,557	2.66×10^{-8}
1,539	35,970	1.22×10^{-8}
	How F-63 ZU	
76.7	3,935,480	1.01×10^{-6}
95.6	3,015,700	7.77×10^{-7}
191.0	1,194,420	3.08×10^{-7}
382.2	336,322	8.67×10^{-8}
771.4	94,770	2.44×10^{-8}
1,539	40,136	1.03×10^{-8}
	ZU Standard Cloud	
52.1	144,652	2.450×10^{-6}
70.8	113,582	1.923×10^{-6}
94.2	87,319	1.478×10^{-6}
123.3	65,194	1.104×10^{-6}
170.2	44,193	7.489×10^{-7}
189.6	38,414	6.504×10^{-7}
237.6	27,537	4.664×10^{-7}
285.9	20,138	3.414×10^{-7}
406.4	11,154	1.890×10^{-7}
525.6	7,420	1.260×10^{-7}
770.6	3,943	6.676×10^{-8}
1,538	1,200	2.032×10^{-8}
	YFNB 13-E-58 FL	
220.0	2,360,643	3.39×10^{-7}
382.8	944,495	1.36×10^{-7}
742.6	284,202	4.09×10^{-8}
1,534.9	85,797	1.23×10^{-8}
	YFNB 29-H-79 FL	
94.7	312,141	1.03×10^{-6}
167.8	158,986	5.24×10^{-7}
384.1	40,390	1.33×10^{-7}
1,535.5	3,722	1.23×10^{-8}

TABLE B.23 CONTINUED

Counting Time	Observed Activity	
H + hr	counts/min	counts/sec / 10^{4} fissions
	YAG 39-C-23 FL	
69.9	24,407	1.47×10^{-6}
167.9	9,480	5.69×10^{-7}
382.6	2,344	1.41×10^{-7}
743.8	708	4.25×10^{-8}
1,534.4	225	1.35×10^{-8}
	LST 611-D-53 FL	
166.1	149,251	4.65×10^{-7}
384.2	35,315	1.10×10^{-7}
742.7	10,828	3.37×10^{-8}
1,534.8	3,098	9.64×10^{-9}
1,845.7	2,409	7.50×10^{-9}
2,209	1,960	6.10×10^{-9}
2,900	1,363	4.24×10^{-9}
	YFNB 13-E-55 FL	
219.6	2,235,884	3.38×10^{-7}
382.9	865,062	1.31×10^{-7}
743.4	270,865	4.09×10^{-8}
1,535.4	81,183	1.19×10^{-8}
2,209	52,372	7.92×10^{-9}
2,900	36,557	5.52×10^{-9}
	YAG 39-C-22 NA	
74.2	200,434	1.02×10^{-6}
144.3	92,195	4.71×10^{-7}
219.5	49,082	2.51×10^{-7}
359.5	21,233	1.08×10^{-7}
746.9	6,983	3.57×10^{-8}
915.7	5,460	2.80×10^{-8}
1,080.7	4,413	2.25×10^{-8}
1,366.1	3,409	1.74×10^{-8}
1,490.0	2,959	1.51×10^{-8}
1,870.5	2,479	1.27×10^{-8}
2,205.6	2,059	1.05×10^{-8}
2,837.9	1,577	8.06×10^{-9}
	YAG 39-C-23 NA	
69.7	172,144	1.12×10^{-6}
143.7	73,853	4.79×10^{-7}
218.9	39,141	2.54×10^{-7}
358.8	16,750	1.08×10^{-7}
747.0	5,611	3.64×10^{-8}
1,080.3	3,469	2.25×10^{-8}
1,365.6	2,822	1.83×10^{-8}
1,490.8	2,462	1.59×10^{-8}
	LST 611-D-53 NA	
74.6	28,098	1.15×10^{-6}
143.6	12,919	5.30×10^{-7}
219.6	7,899	3.24×10^{-7}
358.6	2,892	1.19×10^{-7}
746.6	974	3.99×10^{-8}
1,082.2	581	2.38×10^{-8}
1,348.0	465	1.90×10^{-8}
1,515.7	396	1.62×10^{-8}

Counting Time	Observed Activity	
H + hr	counts/min	counts/sec / 10^{4} fissions
	FL Standard Cloud	
52.4	287,838	1.72×10^{-6}
69.1	230,228	1.38×10^{-6}
94.0	175,925	1.05×10^{-6}
165.3	92,377	5.52×10^{-7}
237.3	53,830	3.22×10^{-7}
381.8	24,750	1.48×10^{-7}
742.4	7,872	4.70×10^{-8}
1,534	2,220	1.33×10^{-8}
	YAG 40-B-17 NA	
166.6	28,016	3.92×10^{-7}
219.6	18,249	2.67×10^{-7}
358.5	7,642	1.12×10^{-7}
746.4	2,649	3.87×10^{-8}
1,344.1	1,281	1.87×10^{-8}
1,514.9	1,107	1.62×10^{-8}
	YFNB 13-E-60 NA	
69.8	999,232	1.31×10^{-6}
143.5	429,456	5.63×10^{-7}
219.7	232,011	3.04×10^{-7}
359.4	102,949	1.34×10^{-7}
747.0	36,000	4.72×10^{-8}
915.6	27,495	3.60×10^{-8}
1,082.2	22,014	2.89×10^{-8}
1,344.3	16,757	2.20×10^{-8}
1,513.9	14,601	1.91×10^{-8}
1,870.4	11,469	1.50×10^{-8}
2,205.1	9,718	1.27×10^{-8}
2,773.6	7,277	9.54×10^{-9}
	How F-63 NA	
70.4	28,717	1.20×10^{-6}
143.8	12,278	5.14×10^{-7}
219.1	6,454	2.70×10^{-7}
359.0	2,880	1.21×10^{-7}
746.1	924	3.86×10^{-8}
1,365	466	1.95×10^{-8}
1,517	415	1.74×10^{-8}
	YFNB 29-H-79 NA	
71.4	23,959	1.04×10^{-6}
145.9	10,530	4.56×10^{-7}
218.8	5,730	2.48×10^{-7}
358.9	2,702	1.17×10^{-7}
746.4	1,050	4.54×10^{-8}
1,366.0	561	2.43×10^{-8}
1,515.9	516	2.23×10^{-8}

TABLE B.23 CONTINUED

Counting Time	Observed Activity		Counting Time	Observed Activity	
H + hr	counts/min	counts/sec / 10^4 fissions	H + hr	counts/min	counts/sec / 10^4 fissions
	YFNB 13-E-55 NA		1,102.7	6,500	2.300×10^{-6}
74.5	664,981	1.24×10^{-6}	1,515.0	3,938	1.394×10^{-6}
144.4	297,774	5.54×10^{-7}	1,850.0	2,819	9.974×10^{-9}
219.0	153,938	2.86×10^{-7}	2,184.0	2,286	8.089×10^{-9}
358.7	60,274	1.12×10^{-7}	2.856.0	1,520	5.380×10^{-9}
746.8	20,954	4.40×10^{-8}		**NA Standard Cloud**	
1,081.9	14,486	2.70×10^{-8}	49.8	35,258	1.698×10^{-6}
1,365.8	11,729	2.18×10^{-8}	71.9	24,185	1.164×10^{-6}
1,516.0	11,087	2.06×10^{-8}	142.9	10,784	5.194×10^{-7}
	YAG 40-B-17 TE		218.6	5,724	2.757×10^{-7}
166.2	2,574,369	6.35×10^{-7}	357.6	2,438	1.174×10^{-7}
240.6	1,416,545	3.49×10^{-7}	814.0	736	3.543×10^{-8}
407.8	532,469	1.32×10^{-7}	1,083.0	513	2.471×10^{-8}
674.6	239,457	5.91×10^{-8}	1,342.0	397	1.910×10^{-8}
766.7	171,997	4.25×10^{-8}	1,512.0	339	1.632×10^{-8}
910.8	142,537	3.52×10^{-8}		**LST 611-D-53 TE**	
1,125.6	102,048	2.52×10^{-8}	166.1	956,332	5.11×10^{-7}
1,299.7	81,898	2.02×10^{-8}	240.5	519,659	2.77×10^{-7}
1,494.7	67,541	1.67×10^{-8}	408.3	199,818	1.07×10^{-7}
	YAG 39-C-23 TE		674.9	87,570	4.67×10^{-8}
240.1	1,665,239	2.45×10^{-7}	766.8	70,485	3.76×10^{-8}
408.2	630,800	9.30×10^{-8}	911.0	52,294	2.79×10^{-8}
675.9	266,401	3.92×10^{-8}	1,108.6	38,524	2.06×10^{-8}
766.7	218,954	3.22×10^{-8}	1,318.9	30,370	1.62×10^{-8}
910.8	163,349	2.40×10^{-8}	1,514.6	24,862	1.33×10^{-8}
1,126.4	117,404	1.73×10^{-8}	1,850	19,289	1.03×10^{-8}
1,300.6	93,898	1.38×10^{-8}	2,184.0	16,056	8.57×10^{-9}
1,493.4	78,074	1.15×10^{-8}	2,855.0	11,593	6.19×10^{-9}
	YAG 39-C-35 TE			**YFNB 13-E-55 TE**	
240.4	2,404,826	2.45×10^{-7}	120.1	2,537,344	5.44×10^{-7}
408.0	888,580	9.05×10^{-8}	239.9	851,909	1.83×10^{-7}
675.1	398,518	4.06×10^{-8}	408.9	300,596	6.44×10^{-8}
767.0	318,530	3.24×10^{-8}	675.2	127,629	2.73×10^{-8}
910.8	237,960	2.42×10^{-8}	766.5	100,361	2.15×10^{-8}
1,125.6	172,678	1.76×10^{-8}	910.9	74,229	1.59×10^{-8}
1,299.6	138,005	1.41×10^{-8}	1,108.4	54,743	1.17×10^{-8}
1,495.1	113,942	1.16×10^{-8}	1,318.0	43,799	9.39×10^{-9}
1,831.0	88,350	9.00×10^{-9}	1,514.0	36,798	7.89×10^{-9}
2,165.0	72,540	7.39×10^{-9}		**YFNB 13-E-60 TE**	
2,856.0	53,454	5.45×10^{-9}	119.9	1,865,482	5.91×10^{-7}
	How F-63 TE		242.4	553,803	1.75×10^{-7}
120.2	259,094	5.44×10^{-7}	408.4	202,933	6.43×10^{-8}
240.4	86,299	1.81×10^{-7}	675.0	84,477	2.68×10^{-8}
407.6	29,213	6.13×10^{-8}	766.9	66,939	2.12×10^{-8}
675.2	12,115	2.54×10^{-8}	910.7	49,105	1.56×10^{-8}
766.6	9,691	2.03×10^{-8}	1,108.5	36,503	1.16×10^{-8}
1,125	5,393	1.13×10^{-8}	1,318.0	29,958	9.49×10^{-9}
1,318	4,305	9.03×10^{-9}	1,514.0	25,118	7.96×10^{-9}
1,514	3,727	7.82×10^{-9}		**YFNB 29-H-79 TE**	
	TE Standard Cloud		675.1	2,211,658	3.34×10^{-8}
71.5	441,580	1.562×10^{-6}	766.3	1,684,270	2.55×10^{-8}
119.8	246,649	8.728×10^{-7}	910.5	1,149,807	1.74×10^{-8}
144.0	212,310	7.512×10^{-7}	1,108.7	888,099	1.34×10^{-8}
239.0	98,678	3.492×10^{-7}	1,299.6	703,572	1.06×10^{-8}
406.5	38,975	1.379×10^{-7}	1,493.3	588,398	8.89×10^{-9}
909.8	9,202	3.256×10^{-8}			

TABLE B.24 COMPUTED BETA-DECAY RATES

Beta-emission rates for fission products (FP) and induced products (IP) are computed and summed for the total emission rate in units of (β/sec)/10^4 fissions. Product/fission ratios are listed directly under the nuclide symbol. Conversion to counting rates, (counts/sec)/10^4 fissions, for a weightless mount and (point) source is made in the last column by means of the shelf factor G_n for comparison with experimental results (Table B.25). Numbers in parentheses indicate the number of zeros between the decimal point and the first significant figure, e.g., (2)200 = 0.00200.

Age	Na^{24}	Co^{57}	Co^{58} *	Cu^{64} †	Sum of FP	counts/sec / 10^4 fissions (G_1 = 0.2628)
hr	0.00145	0.0036	0.0053	0.00217		
Shot Flathead, Average Fallout Composition:						
45.8 min	0.763	(3)180	No β	(6)756	(3)178	1.544	0.5274
1.12 hrs	1.12	(3)177		(6)756	(3)174	1.009	0.3324
1.64 hrs	1.64	(3)173		(6)755	(3)169	0.634	0.1969
2.40 hrs	2.40	(3)167		(6)755	(3)163	0.398	0.1166
3.52 hrs	3.52	(3)158		(6)754	(3)153	0.255	(1)7335
5.16 hrs	5.16	(3)146		(6)754	(3)140	0.166	(1)4893
7.56 hrs	7.56	(3)131		(6)754	(3)123	0.109	(1)3364
11.1 hrs	11.1	(3)111		(6)752	(3)102	(1)716	(1)2343
16.2 hrs	16.2	(4)880		(6)751	(4)773	(1)456	(1)1615
23.8 hrs	23.8	(4)618		(6)748	(4)513	(1)282	(1)1103
1.45 days	34.8	(4)376		(6)745	(4)283	(1)176	(2)7640
2.13 days	51.1	(4)175		(6)740	(4)117	(1)109	(2)5256
3.12 days	74.9	(5)590		(6)733	(5)327	(2)674	(2)3564
4.57 days	109.7	(5)119		(6)723	(6)498	(2)452	(2)2430
6.70 days	160.8	(6)112		(6)708	(7)315	(2)309	(2)1580
9.82 days	235.7	(8)344		(6)688	(9)566	(2)212	(3)9708
14.4 days	345.6	(10)230		(6)658	(11)141	(2)145	(3)5770
21.1 days	506.4			(6)617		(3)972	(3)3374
30.9 days	741.6			(6)561		(3)637	(3)1957
45.3 days	1,087			(6)489		(3)411	(3)1145
66.4 days	1,594			(6)398		(3)262	(4)6968
97.3 days	2,335			(6)296		(3)170	(4)4478
143 days	3,432			(6)191		(3)105	(4)2765
208 days	4,992			(6)102		(4)590	(4)1553
301 days	7,224			(7)417		(4)311	(5)8184

TABLE B.24 CONTINUED

Age	hr	Na^{24}	Mn^{56}	Fe^{59}	Co^{58} *	Co^{60}	Cu^{64} †	Ta^{180} §	Ta^{182}
		0.0314	0.094	0.0033	0.00193	0.0087	0.0278	0.038	0.038
Shot Navajo, Average Fallout Composition:									
45.8 min	0.763	(2)389	(1)572	(5)585	(6)275	(6)363	(2)228	(2)840	(4)267
1.12 hrs	1.12	(2)383	(1)519	(5)585	(6)275	(6)363	(2)223	(2)817	(4)267
1.64 hrs	1.64	(2)374	(1)451	(5)585	(6)275	(6)363	(2)217	(2)779	(4)267
2.40 hrs	2.40	(2)361	(1)368	(5)585	(6)275	(6)363	(2)209	(2)733	(4)267
3.52 hrs	3.52	(2)342	(1)273	(5)584	(6)275	(6)363	(2)197	(2)655	(4)267
5.16 hrs	5.16	(2)317	(1)175	(5)584	(6)275	(6)363	(2)180	(2)578	(4)267
7.56 hrs	7.56	(2)284	(2)918	(5)583	(6)274	(6)363	(2)158	(2)471	(4)267
11.1 hrs	11.1	(2)241	(2)356	(5)581	(6)274	(6)363	(2)131	(2)349	(4)267
16.2 hrs	16.2	(2)191	(3)904	(5)580	(6)273	(6)363	(3)991	(2)226	(4)266
23.8 hrs	23.8	(2)134	(3)118	(5)577	(6)272	(6)363	(3)658	(2)119	(4)266
1.45 days	34.8	(3)813	(5)610	(5)573	(6)271	(6)363	(3)363	(3)464	(4)265
2.13 days	51.1	(3)380	(7)785	(5)567	(6)270	(6)363	(3)150	(3)116	(4)264
3.12 days	74.9	(3)128	(9)132	(5)558	(6)267	(6)362	(4)418	(4)154	(4)262
4.57 days	109.7	(4)257		(5)546	(6)263	(6)362	(5)639	(6)798	(4)260
6.70 days	160.8	(5)243		(5)529	(6)258	(6)362	(6)404	(7)104	(4)256
9.82 days	235.7	(7)744		(5)504	(6)250	(6)361	(8)726	(10)178	(4)252
14.4 days	345.6	(9)499		(5)470	(6)240	(6)361	(10)181		(4)245
21.1 days	506.4			(5)424	(6)225	(6)360			(4)235
30.9 days	741.6			(5)365	(6)204	(6)359			(4)222
45.3 days	1,087			(5)292	(6)178	(6)357			(4)203
66.4 days	1,594			(5)212	(6)145	(6)354			(4)179
97.3 days	2,335			(5)132	(6)108	(6)350			(4)148
143 days	3,432			(6)653	(7)694	(6)345			(4)112
208 days	4,992			(6)241	(7)372	(6)337			(5)752
301 days	7,224			(7)579	(7)152	(6)325			(5)429

TABLE B. 24 CONTINUED

Age hr	Sum of FP	Counts/sec per 10^4 fissions ($G_3 = 0.0958$)
Shot Navajo, Average Fallout Composition:		
45.8 min 0.763	1.544	0.172
1.12 hrs 1.12	1.009	0.113
1.64 hrs 1.64	0.634	(1)714
2.40 hrs 2.40	0.398	(1)455
3.52 hrs 3.52	0.255	(1)300
5.16 hrs 5.16	0.166	(1)201
7.56 hrs 7.56	0.109	(1)136
11.1 hrs 11.1	(1)716	(2)913
16.2 hrs 16.2	(1)456	(2)599
23.8 hrs 23.8	(1)282	(2)382
1.45 days 34.8	(1)176	(2)242
2.13 days 51.1	(1)109	(2)149
3.12 days 74.9	(2)674	(3)912
4.57 days 109.7	(2)452	(3)592
6.70 days 160.8	(2)309	(3)388
9.82 days 235.7	(2)212	(3)252
14.4 days 345.6	(2)145	(3)162
21.1 days 506.4	(3)972	(3)103
30.9 days 741.6	(3)637	(4)663
45.3 days 1,087	(3)411	(4)422
66.4 days 1,594	(3)262	(4)271
97.3 days 2,335	(3)170	(4)179
143 days 3,432	(3)105	(4)112
208 days 4,992	(4)590	(5)643
301 days 7,224	(4)311	(5)343

* 0.57 β^+/dis. † 0.128 β^+/dis. ‡ 0.21 β^-/dis. § Product ratio assumed same as Ta^{182}.

TABLE B. 25 OBSERVED BETA-DECAY RATES

Beta counting samples, supported and covered by 0.80 mg/cm^2 of pliofilm, were prepared on the YAG 40 from aliquots of SIC tray stock solution. Measurements initiated there were usually continued on Site Elmer, and terminated at NRDL. When stock solution activity permitted, a portion was shipped to NRDL as soon as possible, allowing simultaneous field and NRDL decay measurements to be obtained. Nominally identical continuous-flow proportional detectors were installed at all three locations, and small response differences were normalized by Cs^{137} reference standards. No scattering or absorption corrections have been made to the observed counts.

Counter Location	Age	Activity	Counter Location	Age	Activity
	hr	counts/sec / 10^4 fissions		hr	counts/sec / 10^4 fissions
Shot Flathead, Sample 3473/β, 3.09 × 10^6 fission, Shelf 1					
YAG 40	16.4	127.4 × 10^{-4}	Site Elmer	112.3	22.83 × 10^{-4}
	19.5	109.3		123.8	20.07
	21.7	99.42		130.9	18.66
	24.0	89.42		136.6	17.84
	27.9	80.06		153.4	15.33
	31.1	72.70		161.5	14.69
	34.1	67.77		175.0	13.02
	36.6	63.35		194.2	11.49
	41.1	57.69		224.1	9.412
	45.0	53.26		247.8	8.339
	49.8	49.97	NRDL	194.8	11.49 × 10^{-4}
Site Elmer	54.1	44.22 × 10^{-4}		215	10.18
	57.9	40.97		261	7.718
	62.0	38.68		333	5.389
	65.6	36.47		429	3.586
	69.6	34.38		501	2.875
	73.8	34.21		598	2.226
	75.5	32.87		723	1.692
	78.8	30.66		891	1.226
	85.0	29.26		1,034	0.9812
	90.1	27.90		1,223	0.7773
	96.5	26.24		1,417	0.5916
	103.7	24.19		1,582	0.5194
Shot Navajo, Sample P-3753/β #2, 7.24 × 10^6 fission, Shelf 3.					
YAG 40	12.62	7.428 × 10^{-3}	NRDL	984	4.196 × 10^{-5}
	15.58	5.801		1,030	3.906
	18.24	4.933		1,080	3.731
	20.33	4.386		1,151	3.223
	23.76	3.701		1,198	3.269
	26.90	3.276		1,246	3.128
	29.78	2.950		1,342	2.620
	34.51	2.495		1,450	2.647
	38.0	2.262		1,485	2.477
	47.9	1.748		1,534	2.373
Site Elmer	67.8	1.157 × 10^{-3}		1,750	2.040
	74.6	1.027		1,850	1.883
	87.0	8.640 × 10^{-4}		2,014	1.710
	89.9	8.262		2,164	1.535
	99.0	7.363		2,374	1.425
YAG 40	122.9	5.691 × 10^{-4}		2,541	1.293
	150.0	4.446		2,666	1.252
	170.6	3.736		2,834	1.077
	226.1	2.597		3,266	9.346 × 10^{-6}
	278.5	1.973		3,500	8.678
NRDL	478	1.011 × 10^{-4}		3,914	7.413
	574	7.937 × 10^{-5}		4,320	6.308
	647	6.878		4,750	5.617
	693	6.436		5,330	4.857
	742	5.904		5,930	4.005
	814	5.359		6,580	3.752
	861	4.968		6,740	3.453
	912	4.733		8,230	3.039
				8,640	2.440

TABLE B.26 4-π GAMMA IONIZATION CHAMBER MEASUREMENTS

The fallout samples listed are all solutions of OCC samples. Because three instruments with varying responses were involved in measurements during Operation Redwing, observed values have been arbitrarily normalized linearly to a standard response of 700×10^{-9} ma for 100 μg of radium.

Sample		Number of Fissions	Age	Ion Current
Shot and Station	Volume			
	ml		hr	ma/fission × 10^{-21}
Shot Zuni				
YAG 40-B-6	10	5.08×10^{13}	387	8.096
			772	3.335
			1,540	1.499
How F-61 (1)	10	1.00×10^{13}	219	8.557
			243	7.284
			387	3.604
			772	1.645
			1,540	0.929
How F-61 (2)	10	1.00×10^{13}	239	7.143
How F-61 (3)	2	2.00×10^{12}	214	8.842
			429	3.053
Standard cloud	—	9.84×10^{12}	52.4	197.1
			190	51.49
			267	34.00
			526	13.64
			772	7.959
			1,540	2.751
			5,784	0.351
Shot Flathead				
YAG 39-C-21 (1)	10	5.08×10^{11}	220	18.60
			244	16.32
			266	14.33
			388	8.244
			746	3.334
			1,539	1.440
YFNB 13-E-54 (1)	10	3.81×10^{13}	267	11.86
			388	7.989
			746	3.099
YFNB 13-E-54 (2)	10	3.81×10^{13}	340	9.107
YFNB 29-G-68 (1)	10	1.39×10^{12}	220	19.20
			244	16.76
			266	14.80
			388	8.538
			747	3.457
			1,540	1.420
Standard cloud	—	2.79×10^{13}	73.6	80.90
			95.1	63.37
			166	34.11
			196	28.72
			387	12.30
			747	5.082
			1,539	1.663
Shot Navajo				
YAG 39-C-21 (1)	10	3.90×10^{12}	196	20.58
			244	15.58
			317	10.99
			387	8.441
			741	3.929
			915	2.884
			1,084	2.348
			1,347	1.843
			1,541	1.610

TABLE B.26 CONTINUED

Sample: Shot and Station	Sample: Volume	Number of Fissions	Age	Ion Current
	ml		hr	ma/fissions × 10^{-21}
Shot Navajo				
YAG 39-C-21 (2)	10	3.90×10^{12}	220	16.74
YFNB 13-E-56 (1)	10	6.50×10^{12}	196	23.44
			244	18.33
			317	12.13
			387	9.944
			746	4.572
			915	3.550
			1,084	2.866
			1,347	2.092
			1,540	2.009
YFNB 13-E-56 (2)	10	6.50×10^{12}	220	20.81
Standard cloud	—	3.46×10^{12}	52.5	143.44
			75.8	87.54
			148	37.83
			196	26.57
			387	11.06
			742	5.043
			915	3.928
			1,084	3.139
			1,344	2.434
			1,536	2.136
			6,960	0.380
Shot Tewa				
YAG 39-C-21 (1)	10	1.82×10^{14}	267	12.36
			292	10.92
			408	5.984
			580	3.589
			675	2.902
			773	2.632
			916	1.936
			1,108	1.680
			1,300	1.211
			1,517	1.056
			1,852	0.906
YAG 39-C-21 (2)	10	1.82×10^{14}	286	11.00
YFNB 13-E-54 (1)	10	2.38×10^{13}	292	6.345
			408	3.692
			580	2.134
			675	1.730
			773	1.458
			916	1.187
			1,108	0.964
			1,300	0.727
			1,517	0.653
YFNB 13-E-54 (2)	10	2.38×10^{13}	262	7.566
Standard cloud	—	4.71×10^{13}	77.0	88.74
			101.	69.07
			123	56.67
			172	39.83
			244	24.18
			408	12.15
			675	5.998
			773	4.904
			916	3.769
			1,108	2.726
			1,300	2.076
			1,517	1.664
			1,851	1.201

TABLE B. 27 GAMMA ACTIVITY AND MEAN FISSION CONTENT OF HOW F BURIED COLLECTORS (AREA = 2.60 FT^2)

The activities summarized in this table have been corrected for contributions from shots other than the one designated. Flathead produced no activity in these collectors resolvable from the Zuni background. The conversion to fissions was made by means of the How Island factors shown in Table B.13.

Collector Designator	Shot Cherokee * Doghouse Activity at 100 hr	Shot Zuni Doghouse Activity at 100 hr	Shot Navajo Doghouse Activity at 100 hr	Shot Tewa Doghouse Activity at 100 hr
	counts/min	counts/min	counts/min	counts/min
F-B1	79	2,154,000	20,809 ¶	262,800
-B2	87	2,261,000	14,145 ¶	250,860
-B3	548	2,022,000	13,870 ¶	203,380
-B4	598	1,963,000	9,088 ¶	246,760
-B5	2,560	2,737,000	19,443	206,940
-B6	897	1,504,000 †	30,650 †	303,820
-B7 ‡	80	3,448,000	26,454	329,970
-B8	96	2,295,000	7,688	138,500 †
-B9	30	2,168,000	8,163	208,640
-B10	174	2,463,000	18,550	200,450
-B11 §	240	1,287,000	6,176 ¶	39,370
-B12	1,056	2,189,000	17,654	216,810
Mean and σ :	537 ± 192 (35.8 pct)	2,250,200 ± 234,170 (10.41 pct)	14,300 ± 5,855 (40.94 pct)	233,384 ± 35,150 (15.06 pct)
Mean fissions/ collector		$5.42 \pm 0.57 \times 10^{14}$	$3.21 \pm 1.32 \times 10^{12}$	$5.98 \pm 0.90 \times 10^{13}$
Mean fissions/ ft^2		$2.08 \pm 0.22 \times 10^{14}$	$1.24 \pm 0.51 \times 10^{12}$	$2.30 \pm 0.35 \times 10^{13}$

* Values are pre-Redwing background activities.

† Collector in estimated platform shadow; omitted from mean value.

‡ Collector directly under platform; omitted from mean value.

§ Collector on sandbank slope; omitted from mean value.

¶ Water leakage during recovery; omitted from mean value.

TABLE B.28 HOW ISLAND SURVEYS, STATION F

I. OBSERVED IONIZATION RATES

"Closed Window" readings 3 feet above ground at points shown on station layout (Figure 2.8).

Survey Time (Mike)		Hours Since ZU	FL	NA	TE	Ionization Rate, mr/hr F-B1	F-B2	F-B3	F-B4	F-B5	F-B6	F-B7	F-B8	F-B9	F-B10	F-B11	F-B12	Mean and σ	Instrument Type and Serial
6 May	1200	—	—	—	—	0.20	0.20	0.20	0.20	0.40	0.40	0.20	0.20	0.20	0.20	0.20	0.20	0.23	T1B 2443
21	1615	—	—	—	—	0.05	0.05	0.10	0.05	0.50	0.20	0.10	0.10	0.10	0.10	0.20	0.30	0.15	MX-5 17539
22	1120	—	—	—	—	0.10	0.10	0.20	0.15	0.30	0.20	0.15	0.10	0.10	0.10	0.20	0.25	0.16	MX-5 65008
23	1040	—	—	—	—	0.20	0.20	0.20	0.20	0.40	0.40	0.20	0.20	0.20	0.20	0.20	0.20	0.32	T1B 2443
26	0930	—	—	—	—	0.10	0.10	0.20	0.20	0.30	0.20	0.15	0.10	0.10	0.10	0.15	0.20	0.28	MX-5 65008
28	1710	11.2	—	—	—	—	1400	—	1600	1800	—	—	—	1800	1800	1800	1800	1714 ± 157	Cutie Pie 5028
29	1216	30.3	—	—	—	590	580	600	570	580	530	560	580	550	580	450	560	561	Cutie Pie 5028
30	1025	52.5	—	—	—	300	300	310	300	310	320	290	240	250	340	240	300	292	Cutie Pie 5501
1 June	1032	100.6	—	—	—	150	160	160	160	140	160	140	100	110	160	110	160	142	Cutie Pie 0325
2	1008	124.2	—	—	—	100	110	110	100	110	120	100	84	88	110	86	100	101	Cutie Pie 5501
3	1053	149.0	—	—	—	89	88	94	89	88	99	85	68	68	90	63	88	84.1	Cutie Pie 5501
5	1135	197.6	—	—	—	60	61	65	59	60	73	57	44	46	59	44	64	57.7	Cutie Pie 5501
7	1230	246.6	—	—	—	45	46	48	46	48	62	40	28	30	40	32	38	41.9 ± 9.4	Cutie Pie 5516
12	1620	370.4	9.9	—	—	22	20	21	22	—	31	24	14	16	21	15	24	20.9	Cutie Pie 5507
13	1015	388.3	27.8	—	—	20	22	22	20	20	30	22	18	18	20	18	20	20.8 ± 3.2	Cutie Pie 5516
14	1023	412.4	51.9	—	—	20	19	20	20	19	23	21	12	15	19	14	16	18.2	Cutie Pie 5501
9 July	1600	1,018	658	—	—	10	9	9	8	8	9	14	4	6	7	8	7	8.25 ± 2.4	T1B 580
11	1300	1,063	703	7.1	—	—	80	—	80	—	—	—	—	80	—	80	80	80.0	T1B 2058
11	1628	1,066	706	10.5	—	55	51	53	53	56	54	55	50	49	50	47	52	52.1	Cutie Pie 5501
12	1050	1,085	725	28.9	—	16	20	16	15	14	19	18	12	14	16	14	14	15.7	Cutie Pie 5516
13	1400	1,112	752	56.1	—	15	14	14	12	13	14	16	10	11	11	10	10	12.5	Cutie Pie 5502
21	1418	1,304	944	248.	8.5	240	—	—	260	—	—	180	—	240	—	210	240	228 ± 29	T1B 7234
21	1622	1,306	946	250	10.6	220	210	220	190	180	210	200	160	190	180	140	220	193 ± 25	Cutie Pie 5503
22	1022	1,324	946	268	28.6	95	86	94	88	90	110	91	75	79	82	71	89	87.5 ± 10.2	Cutie Pie 5516
23	1100	1,349	989	293	53.2	36	36	38	36	34	30	30	30	30	32	28	32	32.7 ± 3.2	T1B 7826
25	0836	1,395	1,035	339	98.8	21	21	22	20	20	25	23	16	15	19	16	18	19.7 ± 3.0	Cutie Pie 5507

TABLE B.28 HOW ISLAND SURVEYS, STATION F
II. RESOLUTION OF IONIZATION RATES BY EVENT

The ionization rates for Shots Zuni, Navajo, and Tewa are shown; Shots Flathead and Dakota produced negligible amounts of fallout.

Hours Since				Ionization Rate, mr/hr					
						TE			
ZU	FL	NA	TE	ZU *	Na †	By Diff. ‡	By Relative Decay §	Mean Observed and σ	Residual Error
								pct	pct
11.2	—	—	—	1,714	—	—	—	1,714 ± 9.18	—
30.3	—	—	—	561	—	—	—	561	—
52.5	—	—	—	292	—	—	—	292	—
100.6	—	—	—	142	—	—	—	142	—
124.2	—	—	—	101	—	—	—	101	—
149.0	—	—	—	84.1	—	—	—	84.1	—
197.6	—	—	—	57.7	—	—	—	57.7	—
246.6	—	—	—	41.9	—	—	—	41.9 ± 22.5	—
370.4	9.9	—	—	20.9	—	—	—	20.9	—
388.3	27.8	—	—	20.8	—	—	—	20.8 ± 15.6	—
412.4	51.9	—	—	18.2	—	—	—	18.2	—
1,018	658	—	—	8.82	—	—	—	8.25 ± 29.3	—
1,063	703	7.1	—	8.60	71.4	—	—	80.0	—
1,066	706	10.5	—	8.60	43.5	—	—	52.1	—
1,085	725	28.9	—	8.46	7.24	—	—	15.7	—
1,112	752	56.1	—	8.32	4.18	—	—	12.5	—
1,304	944	248	8.5	7.55	0.463	220	199.2	228 ± 12.5	−9.45
1,306	946	250	10.6	7.55	0.456	185	161.7	193 ± 13.2	−12.6
1,324	964	268	28.6	7.48	0.410	79.6	64.3	87.5 ± 11.7	−19.2
1,349	989	293	53.2	7.48	0.364	24.9	34.5	32.7 ± 9.88	+38.5
1,395	1,035	339	98.8	7.34	0.293	12.1	15.3	19.7 ± 15.4	+26.4

* Computed from ZU + 1018 hr and later by 4-π gamma relative ionization decay of How F-64 ZU, Tray 856.

† Computed from difference, observed ZU, to NA + 56.1 hours; thereafter by 4-π gamma relative ionization decay of YAG 40-A-1, Tray P-3753.

‡ Computed from difference, observed (ZU + NA).

§ Computed from best fit of 4-π gamma relative ionization decay of YFNB 13-E-57, Tray 1973.

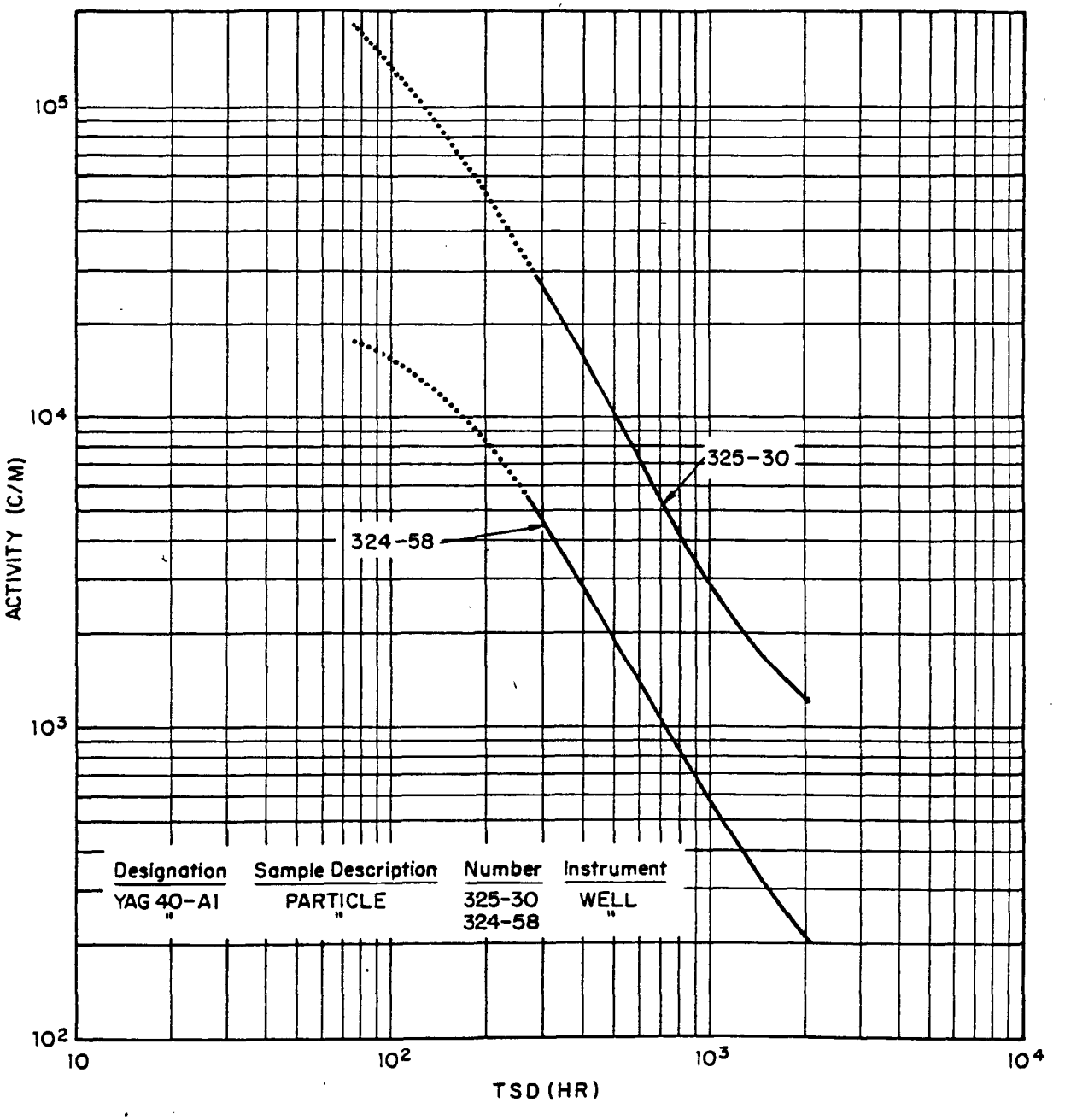

Figure B.2 Gamma decays of solid fallout particles, Shot Zuni.

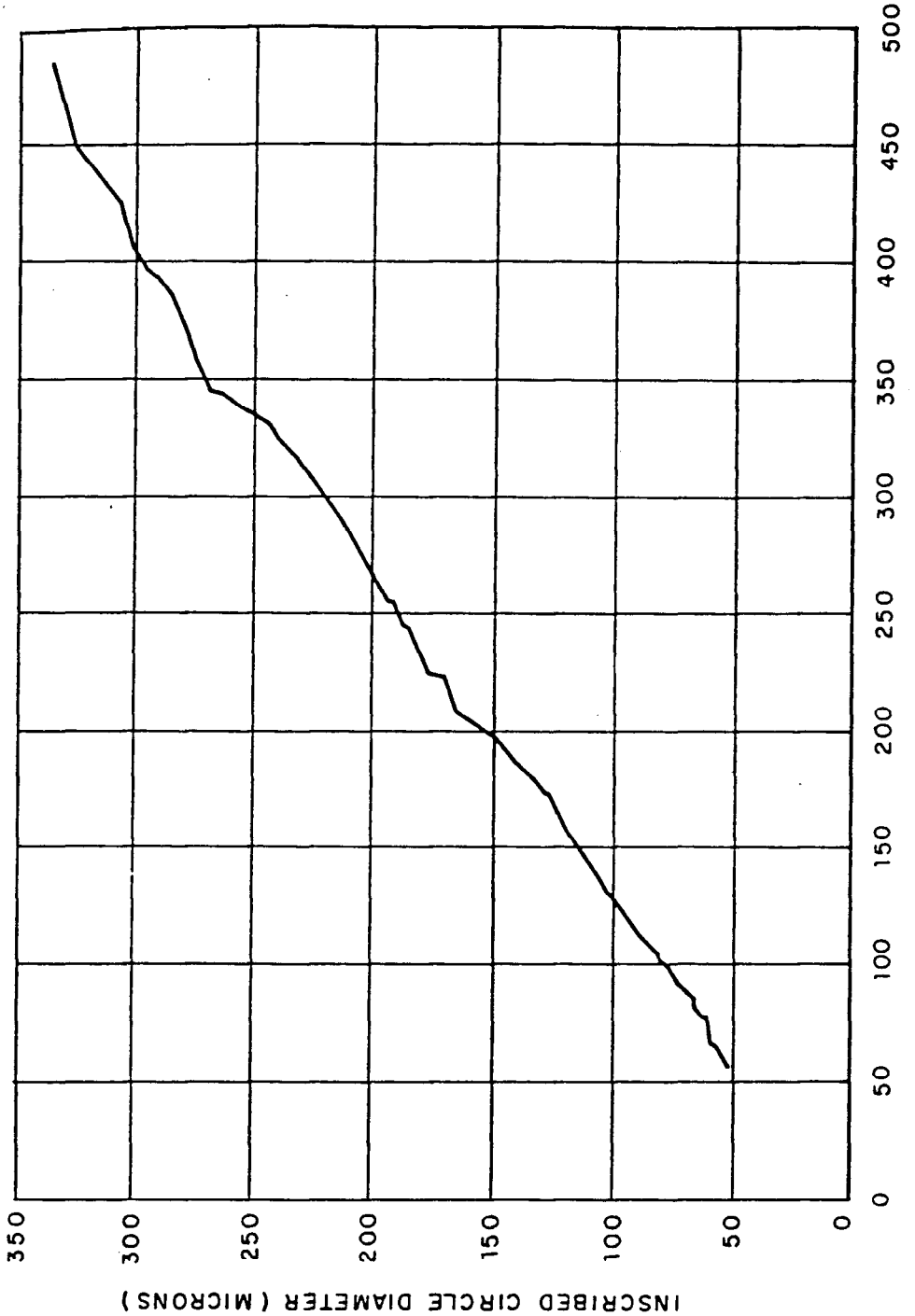

Figure B.5 Relation of inscribed to projected particle diameter.

pg 264 and 265 DELETED

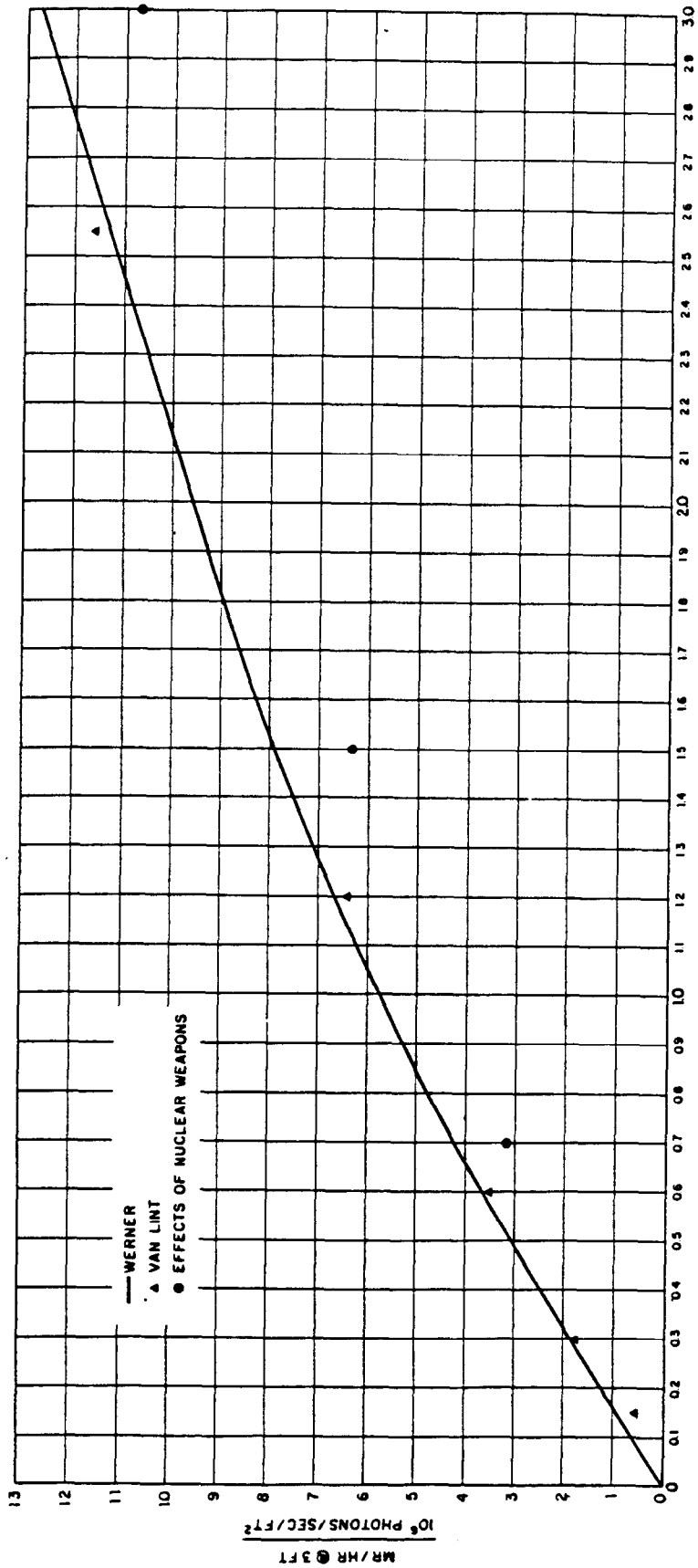

Figure B.6 Computed gamma-ionization rate above a uniformly contaminated smooth infinite plane.

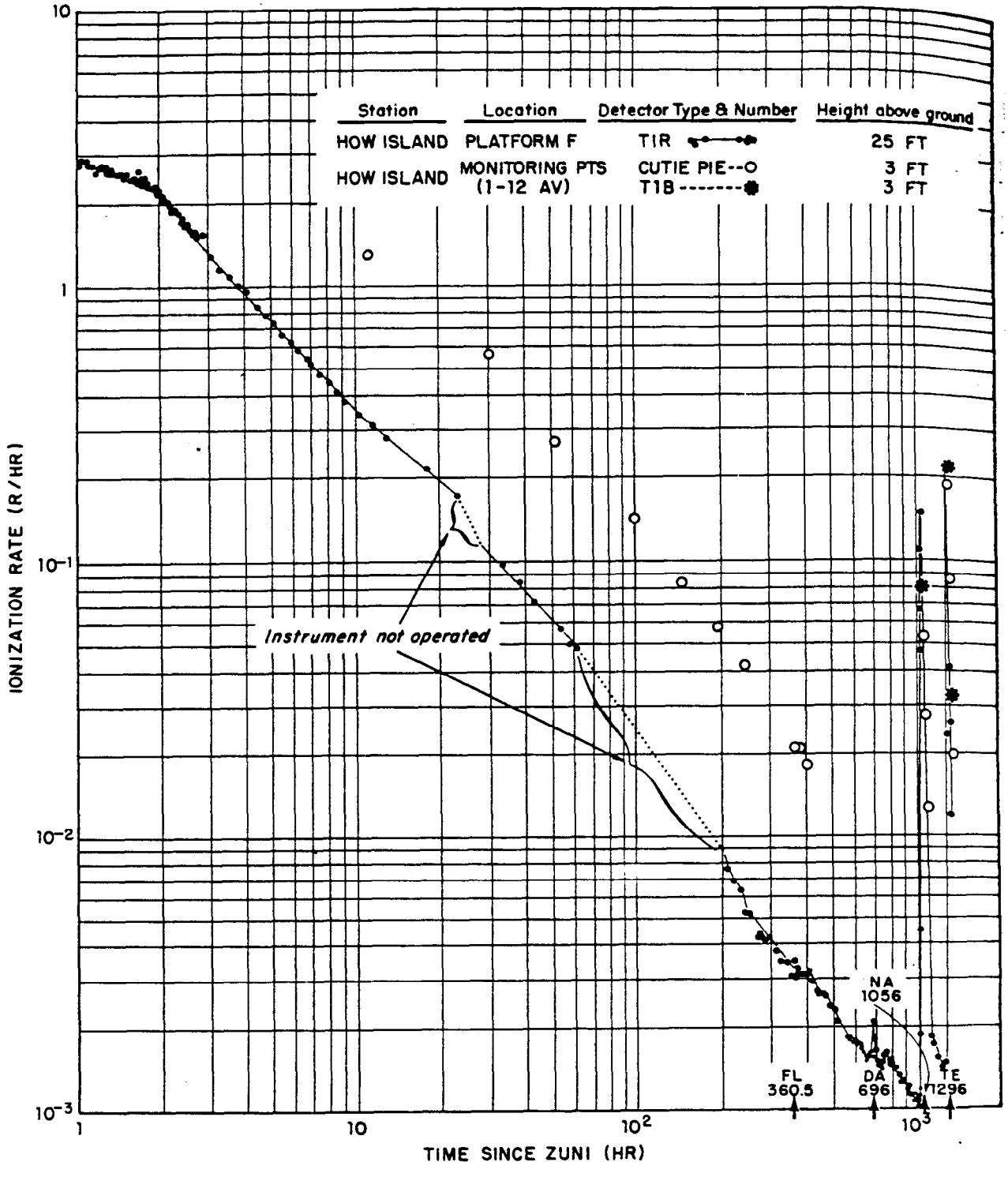

Figure B.7 Gamma-ionization-decay rate, Site How.